CHARACTERISING THE KINETICS OF HIGH TEMPERATURE BROWNING IN FOODS

A Thesis Presented In Partial Fulfilment Of The Requirements For The Degree Of Doctor Of Philosophy In Food And Bioprocess Engineering

At Massey University, Manawatū

New Zealand

SUREEWAN RAJCHASOM

2014

ABSTRACT

Kinetic models for describing the Maillard reaction have been developed extensively but a versatile model has not been obtained because this reaction is very complex. The objective of this research was to develop a kinetic model to describe and predict the Maillard browning reaction occurring at the surface of foods during high temperature cooking. Commercial frozen pastry dough and processed potato product were used as the model food in this study. The progress of brown colour development was determined using image analysis methods in the CIE colour space ($L^*a^*b^*$ scale). The lightness (L^*) was found to be the best parameter to represent the browning reaction in these products. The lightness-time curve followed first order kinetics.

The effects of temperature and moisture content on the Maillard browning reaction between amino acids and reducing sugars were studied. The effect of moisture content was investigated by baking pastry samples at five different initial moisture contents (44.55, 33.89, 22.92, 10.95 and 9.18 wt% of d.b.) on a hot temperature controlled pan at 160°C for 60 minutes. The lightness-time curve was fitted with a first order kinetic model by non linear regression using the recorded surface temperature history as an input to obtain the initial lightness (L^*_0), endpoint or final lightness (L^*_∞) and kinetic rate constants (k). Statistical analysis (ANOVA) was used to test the effect of moisture content on these parameters. The result showed that the moisture content had no significant effect on the browning kinetics of pastry at the 95% confidence level ($P<0.05$). The moisture content had the most influence on the initial lightness ($P<0.005$), whereas the final lightness was moderately affected ($P<0.05$). Consequently, the effect of moisture content on the lightness was not considered as a major factor for browning reaction and was not included in the model for this study. Moisture content

did however influence the time-temperature history at the food surface due to evaporation.

The effect of temperature was studied by baking pastry samples (44.55 %MC; wt% d.b.) at six different temperatures (120, 130, 140, 150, 160 and 170˚C) for 60 minutes. The temperature dependence of the Maillard browning reaction of pastry baking was found to follow the Arrhenius law. The kinetic parameters: the activation energy (E_a), the kinetic rate constant at 150ºC (k_{150}) and the initial and final lightness (L^*_0 and L^*_∞) were obtained from the model fitting. The parameters were fitted using both isothermal and non-isothermal methods. As the baking temperature conditions were controlled to a constant temperature so an isothermal model fitting was reasonable to use for a first approximation. The minimization of the residual sum of square errors by non-linear regression with the Levenberg-Marquardt algorithm function *lscurvefit* was applied for this fitting. The activation energy (E_a) and the kinetic rate constant at 150ºC (k_{150}) values were obtained at 65.93 kJ·mol^{-1} and 0.017 min^{-1}, respectively. The initial and final lightness (L^*_0 and L^*_∞) were estimated at 91.78 and 65.24, respectively. The goodness of this fit (R^2) was calculated as 0.91.

However, experimentally it was found that the temperature of the pastry surface was not absolutely constant, and hence isothermal fitting was probably not justified. Therefore, the experimental data for lightness change and time-temperature histories were re-fitted to estimate the kinetic parameters. The MATLAB® function *lsqnonlin* was used to optimise the kinetic parameters using a non-isothermal model. The activation energy (E_a) and the kinetic rate constant at 150ºC (k_{150}) values were estimated at 71.90 kJ/mol and 0.025 min^{-1}, respectively. The initial and final lightness (L^*_0 and L^*_∞) were obtained as 91.21 and 67.54, respectively. The goodness of this fit (R^2) was calculated as 0.92.

Experimental trials were carried out to validate the model using the kinetic parameters obtained from the non-isothermal model fitting. The time-temperature histories for non-isothermal baking conditions were generated using several different scenarios of pan and oven baking, which provided conductive and convective heat transfer. The validation results showed the model gave good predictions with absolute relative errors (e_{abs}), of 1.93% (n = 50) and 0.38% (n = 8) for pan and oven baking, respectively.

In addition, the developed model was shown to be applicable for use in another food type, processed potato products. The same method as the pastry baking was used for fitting the model for processed potato product baking. The kinetic parameters of E_a, k_{150}, L^*_0 and L^*_∞ were obtained as 55.99 kJ·mol^{-1}, 0.025 min^{-1}, 82.90 and 49.78, respectively. They were different to the kinetics of pastry baking because of the different composition of the processed potato product. The validation of the model against separate processed potato product baking experiments gave an absolute relative error (e_{abs}) of 1.95% (n = 20) which shows that the predictions were good.

The key to achieving good predictions of colour change was in basing the model on the experimentally recorded surface temperature history, rather than assuming the surface is at the cooking temperature as was done in many literature studies. The model could be accurately fitted if it were possible to measure both surface temperature and colour simultaneously during cooking. To achieve this, an oven was modified by installing a thermal camera and infrared (IR) window for observing the temperature and colour values at the same time during the cooking process.

It was found that the surface of the pastry rose up during the cooking process as water evaporation created a bubble inside the pastry. This causes some variation in colour between samples. Moreover, the kinetics of the browning reaction were affected by the cooking condition, which changed the mechanism of the reaction. More than one browning kinetic was found when the different cooking conditions were applied. From the results of this study, it was hypothesied that the heating rate of the cooking had an influence on the pathway of the reaction mechanism. The fission pathway appears to be dominant when the pastry sample was baked under high temperature conditions, which produced a fast rate of the browning reaction with higher brown colour intensity than the alternatives. A lower intensity of brown colour was found on the pastry sample when baked under a slower heating rate suggesting that many intermediate compounds, such as aroma and volatile compounds, were generated in the reductones mechanism pathway. Following this, it was suggested that to develop a powerful kinetic model, the real cooking conditions for each food need to be indentified and used to characterise the reaction rate.

ACKNOWLEDGEMENTS

Colour makes this world lively and beautiful from the artists' point of view. With colour, we tell the season whether to stop or go or if fruit is ripe. Without colour, life would be very different. There are many hidden meanings behind the shades of colour. Through my thesis topic, I have learnt a lot from colour change. This helped me understand that "it is the journey that matters, not the destination". There was not only the knowledge learnt but also the precious experience and friendships with the people here.

This thesis would not have been successful without the contributions of many people. I, therefore take this opportunity to express my sincerest gratitude to my chief supervisor, Professor John Bronlund and supervisor, Professor Tony Paterson for sparing their valuable time to give me useful guidance, suggestions, and constant encouragement throughout the study period. "With your constructive criticisms and professional attitudes, I have learnt a lot from you and these have inspired me to be a good teacher like you!" I am also thankful to my image supervisor, Associate Professor Donald Bailey for his advice on image techniques and his assistance in installing the lighting and image system. Thanks for guiding me and allowing me to use this fantastic method. "Thanks to everyone for being patient with me, believing in me and make me confident in my work. I am so happy to work with all of you and deeply appreciate and will always remember all your assistance".

I also wish to express my deepest appreciation to Dr. Colin Brown for his generous discussions, assistance, helpful suggestions, valuable knowledge and technical advice throughout my study.

My special gratitude is extended to the technicians and laboratory staff of the School of Engineering and Advanced technology (SEAT), Massey University, especially John Edwards, Anthony Wade, Bruce Collins, Clive Bardell, Kerry Grifiths and Colin Plaw for helping me to develop the deep fryer pan and installing the IR window into the oven for the use of the thermal camera. Nick Look for IT assistance and Ann-Marie Jackson for providing me with research facilities and timely laboratory equipment.

Moreover, I would like to thank all the staff of the School of Engineering and Advanced technology (SEAT), Massey University, Michelle Wagner, Linda Lowe, Fiona Falconer, Glenda Rosoman and Gayle Leader for looking after me very well and giving me a helping hand.

I wish to acknowledge Assistant Professor Montira Nopharatana, my master's supervisor who inspired me, improved all of my skills and gave me a good opportunity and experience while I was doing my master degree in Food Engineering, King Mongkut's University of Technology Thonburi (KMUTT), Thailand.

I would like to thank Rajamangkala University Technology of Lanna (RMUTL) for providing a doctoral scholarship. The College of Integrated Science and Technology, RMUTL for official grant support for me to be successful as a scholarship recipient and to complete this study.

Special thanks to Dr. Yoopayao Daroon and Professor Ian and Mrs. Blondie Warrington for introducing me to Massey University and for all their assistance.

Many thanks to my Thai friends in Palmy especially Lalida and her family for their kindness and inviting me to many lovely dinners at her house and for entertaining talk. I also thanks to Supornpan and her family, Dr. Tammarat, Dr. Pat, Piyamas, Parussaya, Rattanawan, Jantana, Chalida, Patcha, Janyawat, Pittiporn, Tiyaporn, Sireethorn and all of my friends whose names I have not mentioned including my PhD mates: Mazida, Eli, Gonzalo, George, Sadia and other in the postgrade room for being kind, and endorsing greatness of friendship while away from home. Thanks for sharing good time together.

I also thank my lovely friends in Thailand (Phon, Tal, Noon, Namkhing, Kun Mae Pla , Rachata and all of my KMUTT friends) for their encouragement and giving me support, especially Dr. Tassanee (P'Jum) for sending me Thai books and lovely songs and for all of her kindness, which always bring me happiness. Special thanks to P'Tum for always

being with me no matter what happened. I may not have got through the lonely times in NZ without you!

Last but not least, I am very grateful to my parents (Dad and Mum) and Rajchasom family and Na Jaw and N'Pie, for their unconditional love along with their endless encouragement and continuously support for me right through this journey. A million thanks goes to Dad and Mum for giving me a life and always taking very good care of me. Thanks for being patient with me and understanding about my physical absence for four years abroad. I appreciated your being there to see me through on my long journey.

แด่พ่อและแม่

ผู้ที่เป็นกำลังใจสำคัญที่สุดในชีวิต
ที่เล็งเห็นความสำคัญของการศึกษาและเป็นแรงบันดาลใจให้ลูกได้เดินทางมาถึงจุดนี้
สิ่งที่ลูกรับรู้มาตลอดชีวิต คือ พ่อกับแม่มักบอกเสมอว่าให้ตั้งใจเรียน เพราะท่านทั้งสองไม่มีโอกาสนี้
พ่อ เป็นบุคคลที่ถือได้ว่าเป็นผู้มีปัญญา
ทุกคำพูด ทุกคำสอนของพ่อ ไม่ได้มาจากความรู้หรือจากตำราเล่มไหนๆ
แต่ล้วนมาจากพื้นฐานของความดีที่มีอยู่ในตัวพ่อทั้งสิ้น
สิ่งเหล่านี้ทำให้ลูกคนนี้รักดี และดำรงตนอยู่ในทางที่ถูกเสมอมา
แม่ คือต้นแบบของความอดทนและความเข้มแข็ง
ถึงแม้ว่าลูกจะทำได้ไม่ถึงครึ่งของแม่
แต่ทุกครั้งที่ท้อถอยหรืออ่อนแอ คำพูดของแม่จะช่วยดึงให้ลูกลุกขึ้นสู้เสมอ
ขอบคุณทุกคำสอนของพ่อและแม่ที่บ่มเพาะให้เป็นอย่างทุกวันนี้
ลูกโชคดีมากที่ได้เกิดมาเป็นลูกพ่อกับแม่ค่ะ

CONTENTS

LIST OF TABLES

LIST OF FIGURES

LIST OF APPENDICES

Chapter 1

INTRODUCTION

1.1 Introduction

Appearance, flavour, texture and nutritional value are the main attributes considered by consumers in evaluating food quality when making food choices. Appearance may be influenced by a number of physical attributes of a food as well as a series of psychological perceptions. Appearance, which is significantly impacted by colour, is one of the first attributes considered in consumers' preference.

Colour in food may be influenced by naturally occurring pigments such as chlorophylls, carotenoids and anthocyanins, or by pigments resulting from both enzymatic and non-enzymatic browning reactions. Non enzymatic browning is an important chemical reaction occurring in food, which causes the colour to change to a golden brown. The reaction is very complex, and normally happens in food during high temperature processing. The Maillard reaction is the main reaction for non-enzymatic browning (Ames & Benjamin, 2003). It has been important to the food industry because the Maillard reaction impacts not only on the colour change, but also the aroma, taste and the nutritional values of foods, particularly in traditional processes such as the roasting of coffee, nuts and cocoa beans (Saklar *et al*., 2001; Demir *et al*., 2002; Kahyaoglu & Kaya, 2006 and Heyd *et al*., 2007), the baking of bakery products (Shibukawa *et al*., 1989; Zanoni *et al*., 1995; Broyart *et al*., 1998; Zhang & Datta, 2006; Purlis & Salvadori, 2007, 2009 and Purlis, 2010) and the cooking of meat products (Goňi & Salvadori, 2011 and Matsuda *et al*., 2013).

If controlled appropriately, non enzymatic browning is seen as being positive by consumers and is considered a good indicator of quality in food products. Specifically, colour changes into a golden colour are a pleasant characteristic occurring in optimal process conditions. But, then, on the other extreme, unpleasant burnt brown colours can form during overcooking (Labuza *et al*., 1994; Ilo & Berghofer, 1999; Demir *et al*., 2002; Nourian & Ramaswamy, 2003; Charissou *et al*., 2007 and Purlis & Salvadori, 2009). Therefore, monitoring and controlling the browning reaction is a key process for obtaining good product quality (Sakla *et al*., 2001).

Kinetic models describing the Maillard browning reaction have been developed for use to predict and control the process. The kinetics of the reaction must be characterised under a range of conditions. These include the chemical composition (type and availability of reactant), the pH, and water activity and processing factors such as temperature and time of heating (Ellis, 1959; Lopez & Pique, 1997; Ames, 1998; Fayle & Gerrard, 2002 and Ames & Benjamin, 2003). The reaction is also affected by metals, oxygen, and the presence of inhibitory agents, e.g., sulphite (Ames, 1990; deMan, 1999; Martins *et al*., 2001; Fayle & Gerrard, 2002). However, the key factors that highly affect the kinetics of the reaction are the combined effect of temperature and time of the cooking process (Maillard, 1912; Labuza *et al*., 1994; Lopez *et al*., 1997; Martins *et al*., 2001; Lee *et al*., 2007 and Ajandouz *et al*., 2008).

Most literature studies developed the browning kinetics by assuming isothermal conditions and by measuring the change of brown colour on the food surface. There are many methods for measuring the brownness on the surface of food. The newest technology of image analysis is the most popular and is generally used nowadays. The browning colour is generally measured and reported as an average value of the data for an area of the food sample. However, in real products such as crackers, cookies, biscuits or toasted bread, the extent of browning is not uniform. Browning is dependent on the temperature of the surface undergoing change. The distribution of colour on the food surface could be explained by different surface temperature histories across the surface of the product. Edges or blisters for example may heat more quickly than other parts of a product surface. Hence, assuming an average colour on the food surface as the browning index is unlikely to be useful.

Based on this it should be possible to explain the product colour distribution by coupling the local temperature and browning reaction through consideration of the product surface. In many cases it is difficult to measure the surface temperature during experimentation and most often, the surface is simply assumed to be at the cooking medium temperature. However, in food processes, phenomena such as water evaporation in baking or frying processes cause a thermal gradiant across the food surface. This makes using these systems unsuitable for isothermal studies of browning kinetics.

To evaluate the kinetics of browning, ideally the surface temperature would be constant (isothermal) throughout the experiment. This would result in an even colour distribution on the food surface. To ensure that the heat transfer on the food surface would be constant, a uniform shape and a smooth surface of the model food would be preferred. Therefore, a food and cooking system that resulted in uniform and constant conditions at the surface of the product should be developed so that accurate browning kinetics can be measured.

Consequently, the experimental conditions for the assumed conditions of the kinetic model will be achieved so the browning reaction in a range of foods can be explained. This model will provide a quantitative tool to predict high temperature browning which will be of benefit in food processing and product quality control.

1.2 Research aim

This research project aimed to study the kinetic reaction of Maillard browning that occurs during high temperature cooking including the effect of the water content of the sample, temperature and time of the cooking process on the reaction. This knowledge would lead to the development of an accurate mathematical model that could predict the reaction in a commercial food process.

1.3 Research objectives

To achieve the research aim, the specific objectives of this work were to:

1.3.1 Develop an appropriate model food, a cooking system design and a browning assessment method (an image analysis system) that would be applicable to use for

the study of the non-enzymatic browning reaction. These systems would provide reliable experimental data to be able to develop a kinetic model (Chapter 3).

1.3.2 Investigate the effects of the water activity of the food sample, the temperature and time of the cooking process on the kinetic rate of the non-enzymatic browning reaction (Chapter 4).

1.3.3 Develop a kinetic model for foods to predict non-enzymatic browning rates as a function of temperature and time (Chapters 4 and 5).

1.3.4 Combine the surface temperature and kinetic models to predict colour in browning processes and generalise the modelling methodology to be applicable for a range of foods (Chapters 6 and 7).

1.3.5 Design an experimental study and cooking conditions to investigate the best method for accurate estimation of the kinetic parameters for the model (Chapter 8).

Chapter 2

LITERATURE REVIEW

2.1 Introduction

For high temperature cooking of food, one of the most important reactions taking place is Maillard browning. This reaction is used to improve the appearance and taste of foods. The appearance of food, including colour, is normally used by consumers in evaluating the quality of cooked foods. With some foods, browning is needed for improving the colour, such as in bakery products, fried foods or in other high temperature food processes (Demir *et al*., 2002). The Maillard reaction is also related to aroma and the taste of food, in particularly in the roasting of coffee and cocoa beans, the baking of bread and cakes, the toasting of cereals and the cooking of meat. However, the browning reaction is also undesirable in some foods, for example in some dry foods because it can result in an off colour, off flavour, textural change and the production of toxins as well as losses in nutritional properties (Sapers *et al*., 1989; Martinez & Whitaker, 1995 and Manzocco *et al*., 2000).

The Maillard non-enzymatic browning reaction is a complex chemical reaction between amino acids and sugars involving many steps and pathways which change the initial substance colour to a melanoidin brown colour (Eskin & Shahidi, 2005 and Ames & Benjamin, 2003). Many studies have tried to elucidate the kinetic pathway of the Maillard reaction; however it is still a controversial issue. Trying to monitor and control this reaction using a kinetic model is a very important issue for food processors.

This chapter reviews the literature on the Maillard browning reaction to summarise the understanding of the chemistry of the Maillard reaction including its influence on food

properties, and the factors affecting the reaction such as temperature, time, moisture content and pH of the food involved. The methods for measuring the Maillard reaction in the food process are also discussed. In addition, the review covers the kinetic models for predicting the Maillard reaction.

2.2 Chemistry of the Maillard browning reaction

The Maillard reaction was first found in 1912 by the French scientist, Louis Camille Maillard, who investigated the reaction between reducing sugars and amino acid interactions, where a yellow-brown colour developed. This reaction is therefore called the "Maillard reaction" (Ellis, 1959; Labuza, 1990 and Ames & Benjamin, 2003).

The classical scheme of the Maillard reaction was first developed and presented by Hodge (1953) as shown in Figure 2.1. This is still used up to the present to describe the reaction. The condensation of the reducing sugar and amino compound, including many other carbohydrate and amine groups, is the beginning step of the Maillard reaction chemistry. Foods rich in reducing sugars and free amino acids are very reactive to the Maillard reaction. The reducing sugars in monosaccharide form include glucose, fructose, glyceraldehyde and galactose and in disaccharides include lactose and maltose (Ellis, 1959). Examples of reducing sugar sources are syrup and honey. Free amino acids such as lysine, glycine, cystine and leucine are mostly found in foods including milk, egg, nuts and cocoa and also fruits (Ellis, 1959; Danehy, 1986; Labuza, 1990; Davies & Labuza, 1997; deMan, 1999 and Fayle & Gerrard, 2002).

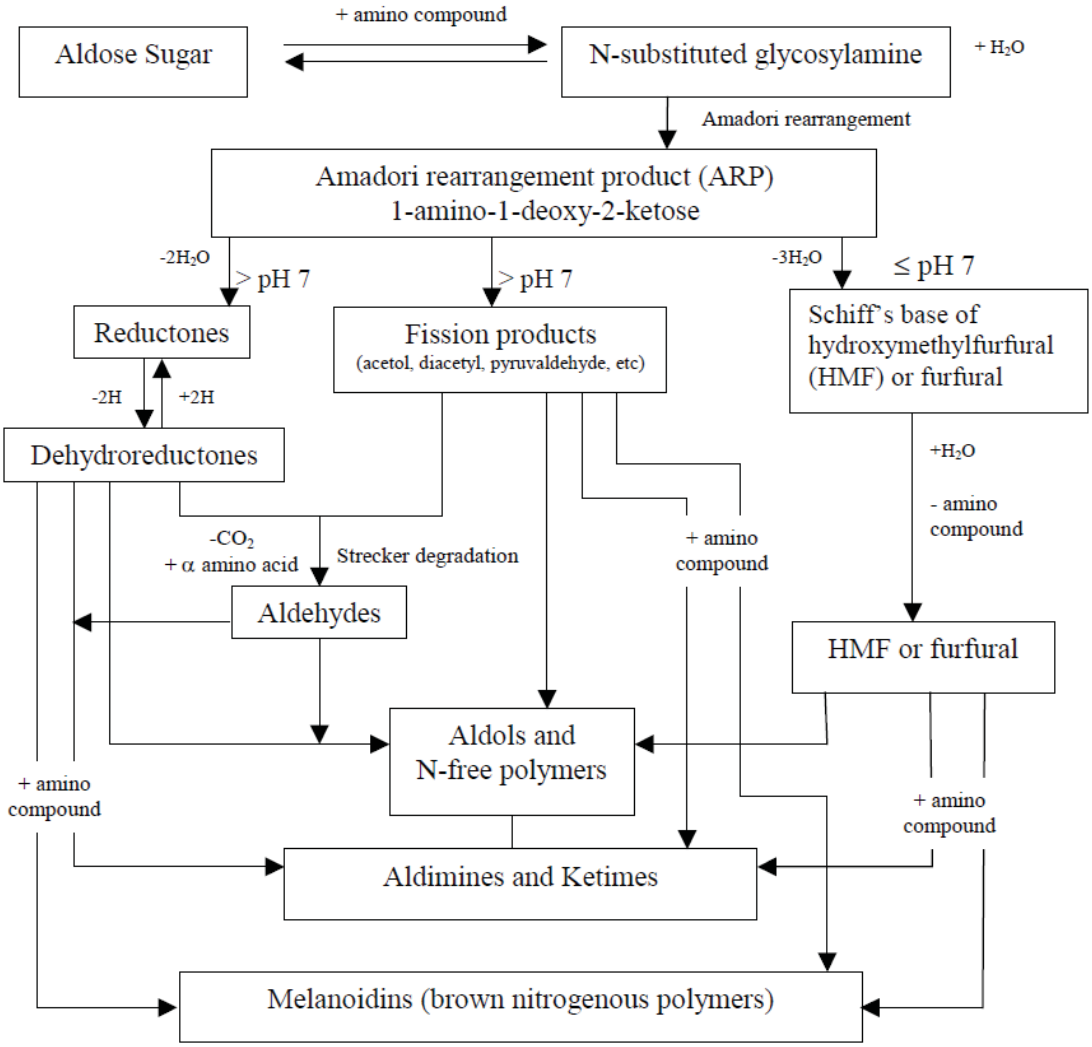

Figure 2.1 The mechanism of the Maillard reaction (Hodge, 1953).

The mechanism of the Maillard reaction as shown in Figure 2.1 is very complicated. However, scientists have tried to divide the reaction into three stages (Mauron, 1981; Davies & Labuza, 1997 and Van Boekel, 1998):

(1) The first stage consists of the condensation of a sugar and an amine in the Amadori rearrangement. It is known that no brown colour development occurs at this stage (Davies & Labuza, 1997). The carbonyl group of the aldose or ketose reacts with the free amino group of an amino acid. For this condensation mechanism the addition of the amino acid into the carbonyl group of the open chain form of the sugar is presented (deMan, 1999). Water is lost in this step, therefore the browning easily occurs in dried and concentrated foods and the equilibrium is highly dependent on the moisture level present (deMan, 1999).

One final product compound of this condensation reaction between aldose and amino acid is an N-substituted aldosylamine. In another case, N-substituted glycosylamines is determined as the final product of this condensation mechanism if the reaction takes place in the food sample which has ketose as a carbonyl group. However, this condensation product is extremely unstable and undergoes a series of rearrangements that are known as the Amadori and Heyns rearrangements. The rearrangement of the condensation product from the reaction between amino acid and aldose is called the Amadori whereas the Heyns is the name of the rearrangement of the condensation product from the amino acid and ketose. The Amadori product compound is 1-amino-1-deoxy-2-fructose, while the Heyns product compound is 1-amino-1-deoxy-2-ketose, they are the major intermediates for the browning reaction (Lea & Hannan, 1950; Kort, 1971; Ledl & Schleicher, 1990; Davies & Labuza, 1997 and Eskin & Shahidi, 2005).

(2) The second stage is the Strecker reaction which involves sugar dehydration and fragmentation and amino degradation. This reaction particularly happens at high temperatures (Davies & Labuza, 1997 and Eskin & Shahidi, 2005). Amino acids first react to form Schiff bases in a degradation reaction. The loss of one or more molecules of water in this process of degradation gives an amino or non amino compound (deMan, 1999). This is then followed by the hydrolysis of a new Schiff base to form an amine and aldehyde (Mauron, 1981). The forming of amine and aldehydes is important because these forms are supplementary flavour compounds and they also contribute to melanoidin formation (Hodge *et al*., 1972; Mauron, 1981 and Maga & Katz, 1982). The flavour formation is found as the product of the Strecker degradation in this stage leading to an off-flavour or a desirable flavour in some kinds of foods (Davies & Labuza, 1997).

(3) The third stage is the formation of heterocyclic nitrogen compounds by condensation or polymerization between the compounds from the Strecker reaction to form a brown pigment. The formation of brown pigment, tastes and also the processed flavour such as roasted and toasted aromas are characterized in this stage (Davies & Labuza, 1997 and deMan, 1999). The highly reactive intermediates in this stage are polymerized to the formation of N-,O-,S-heterocyclic compounds giving the brown colours known as melanoidins (Mauron, 1981 and Ames & Benjamin, 2003).

2.3 Factors affecting the Maillard reaction

There are many factors affecting the Maillard reaction rate in a food process. These include the type of reactants, the availability of reactants and the process factors of temperature, heating time, pH, and water activity (Ellis, 1959; Ames, 1998; Fayle & Gerrard, 2002 and Ames & Benjamin, 2003). The reaction is also affected by metals, oxygen, and the presence of inhibitory agents, such as sulphite (Ames, 1990 and Fayle & Gerrard, 2002).

2.3.1 Temperature

Maillard (1912) studied the influence of temperature and length of heating time on the reaction rate of browning. He found that the reaction rate increases with temperature. Many authors have confirmed this finding (Labuza *et al*., 1994; Lopez *et al*., 1997; Lee *et al*., 2007 and Ajandouz *et al*., 2008). An increase of temperature increases the reactivity between the sugar and amino group (Martins *et al*., 2001). The temperature dependence of a chemical reaction rate constant can be characterised with the Arrhenius equation and temperature coefficient (or Q_{10} value). The temperature coefficient (Q_{10}) is defined as the increase of rate of reaction when the temperature increases by 10°C. It was evident that Q_{10} values range from 2 to 8 (Ames, 1990).

It was reported that the temperature of the cooking system has not only an influence on the reaction rate, but also the pattern of reaction. The pathway of the Maillard reaction may change with different temperature conditions (Hodge, 1953). In addition, the composition of pigment formed is also affected by the process temperature. The intensity of colour pigment increases with increasing temperature (deMan, 1999). Several studies of model systems showed that an increase in temperature and/or time of heating resulted in increased colour development (Van Boekel, 1998; Martins *et al*., 2001; Purlis & Salvadori, 2007, 2009). More volatile compounds were also produced at increasing temperatures (Benzing-Purdie *et al*., 1985).

2.3.2 Moisture content and water activity (a_w)

Water is used as a part of the reaction and is also an intermediate product in the Maillard reaction; therefore the water content and water activity (a_w) have an influence on the browning reaction. The effect of moisture content is divided into two functions which are the pattern and rate of the browning reaction. If a large amount of water is present, caramelization is the main pattern of the browning, while the Maillard reaction is predominant at conditions of low water levels and at pH greater than 6 (Ames, 1990).

The water content has an influence on the rate of the Maillard reaction at very low and very high values of water content. In low water activity foods, the reactants are less mobile and this also slows down the reaction (Ames, 1990). In contrast, excessive moisture levels inhibit the reaction for moist food; the reaction is slowed because the reactants are diluted (Eichner & Karel, 1972). The practical optimum water activity (a_w) values for the Maillard reaction are in the range of 0.5-0.7 (Labuza, 1977; Rahman, 1995 and Eskin & Shahidi, 2005). This reinforces the study of Lea & Hannan, (1949; 1950) who showed the maximum loss of lysine paralleled the extent of browning at between water activities (a_w) of 0.6 and 0.7. Figure 2.2 shows the influence of moisture content and water activity (a_w) on chemical reactions of food.

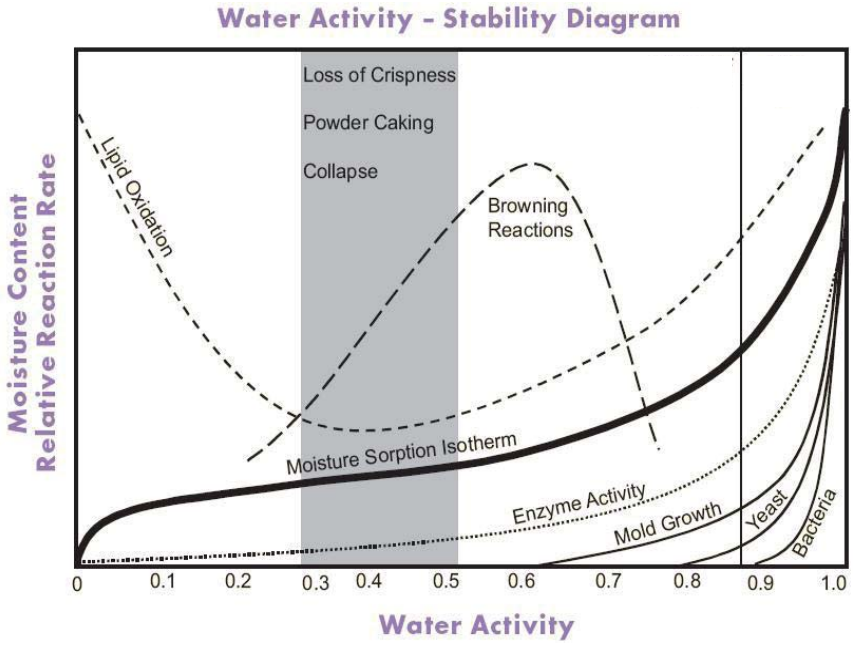

Figure 2.2 The influence of moisture content and water activity (a_w) on chemical reaction of food (adapted from Labuza, 1977).

The effect of moisture content was also studied by Dworschak & Carpenter (1980), who found that an increase in moisture content was the cause of an increase in the loss of lysine and tryptophan with the simultaneous increase in HMF formation and browning. In contrast, Danehy (1986) found that the browning reaction is favoured at an optimum moisture content corresponding to fairly low moisture levels. Therefore, the optimum range for the browning reaction cannot be confirmed because the effect may depend on the type of food and the conditions of the cooking system.

The effect of water activity (a_w) on browning reaction is also of concern in foods at low process temperatures (30-60˚C) such as dried food or food powder during storage (Lingnert, 1990) in order to prevent an undesired brown colour developing in the dried product. For the high temperature processes, the optimum range of water content is also important for the browning reaction. The influence of water content was found to relate with the activation energy as shown in Figure 2.3 (Lingnert, 1990). It can be observed from this diagram that the activation energy is high at low water content and shows a more constant trend between the water content of 10 and 40 wt%. High energies are required for the reaction to proceed at low water content.

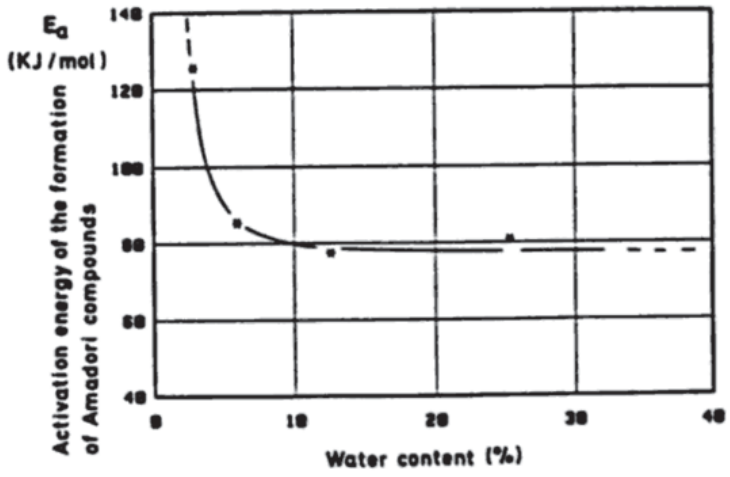

Figure 2.3 Relationship between the water content and the activation energy of formation of Amadori compounds in freeze-dried carrots at different temperatures (Echiner *et al.*, 1985 cited by Lingnert, 1990)

2.3.3 pH

The important role of pH on the Maillard reaction is its influence on the reaction pathway and the reaction rate (Ames, 1990 and Ames & Benjamin, 2003). Eskin & Shahidi (2005) explained that at low pH (below 7), the 1, 2-eneaminol pathway is favoured to form furfural, while the pathway involving the conversion of 2, 3-enediol to reductones and the subsequent fragmentation to furaneol and pyrones is favored at a high pH (above 7) (Figure 2.4). 3-deoxyosone and 1-methyl-2, 3-dicarbonyl are the intermediate compounds of the reaction of the 1, 2-eneaminol and 2, 3-enediol pathways, respectively.

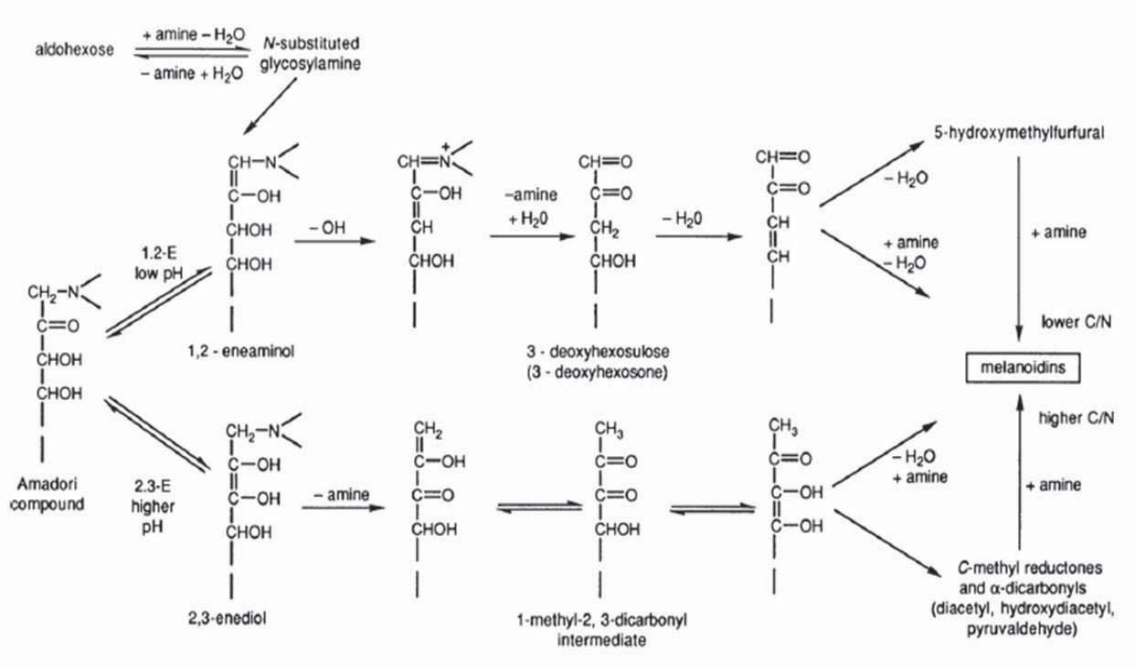

Figure 2.4 Maillard reaction: two major pathways from Amadori compounds to melanoidins (Nursten, 1986 cited by Eskin & Shahidi, 2005)

It can be explained in terms of the rate of reaction that the carbonylamino compounds in the Maillard reaction are favoured under alkaline conditions because the amine groups of the amino acids, peptides, and proteins are in the basic form. Low pH and high moisture levels assist hydrolysis of the glycosidic bond in sucrose, leading to an increase in the rate of Maillard reaction in protein-sucrose systems (Lee *et al.*, 1984).

In high pH conditions more of the hexoses are in the open chain or reducing form, which are easy to react (Burton & McWeeny, 1963). Several studies have reported an

increase in reaction rate as the pH increases (Eskin & Shahidi, 2005). Thus, less reaction is found in high acidity foods, for example pickles. An explanation for this in protein-sucrose systems, is sucrose, as a non reducing sugar, will only participate when the glycosidic bond is hydrolyzed and the reducing monosaccharide constituents are released. For this reason, the browning reaction is slowed down at low pH (Figure 2.5) (Lee *et al*., 1984 and Eskin & Shahidi, 2005).

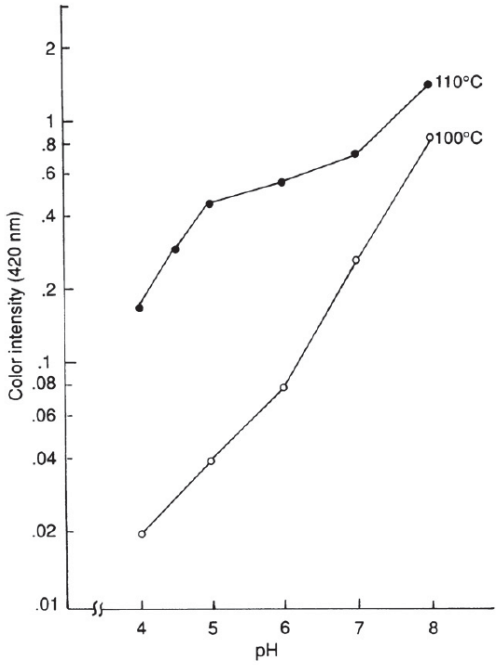

Figure 2.5 Changes in pigment formation as a function of pH (Lee *et al*., 1984).

2.3.4 The reactants (sugar and protein)

Reducing sugars are essential initial substances in the Maillard reaction because they provide the carbonyl groups for interaction with the free amino groups of amino acids, peptides and proteins (Eskin & Shahidi, 2005). Reactivity is related to their conformational stability or to the amount of open chain structure of sugar rings present in the reduced form in solution. The reactivity of pentoses is higher than hexoses, and hexose reactivity is higher than reducing disaccharides (Lea & Hannan, 1949; Ames, 1990; Davies & Labuza, 1997; deMan, 1999 and Fayle & Gerrard, 2002). Not only reducing disaccharides can react in the reaction but also the non reducing disaccharides are able to react after hydrolysis.

The type of amine also affects the rate of the Maillard reaction (Davies & Labuza, 1997). The smaller amino acids are more reactive. The order of reactivity is lysine > glycine > tryptophan > tyrosine (Davies & Labuza, 1997). Basic amino acids generally brown more easily than acidic amino acids in the following order: lysine>β-alanine > glutamine acid (Namiki, 1988). In general, the rate of browning decreases with the extension of chain length of the peptide (Davies & Labuza, 1997).

2.3.5 Metals

The Maillard reaction is inhibited by metals such as manganese and tin. These metals form a complex with amino acids to inhibit the browning reaction. In contrast, copper and iron catalyse the reaction to promote the rate (Ellis, 1959 and Bolin & Steels, 1987).

2.4 Measurement of the Maillard browning reaction

The method for determining the Maillard browning reaction can be divided into two main categories: direct and indirect methods. The direct method involves aiming to measure the chemical substances relating to the brown pigment formation or the consumption of the reactants. Conversely, the indirect method intends to measure the variation of colour produced by the Maillard reaction.

2.4.1 Direct or chemical method

Normally, the Maillard reaction is able to be measured by chemical analysis. Intermediate substances are employed as indicators for measuring the reaction kinetics in each of the three stages. In the early stage, after enzymatic breakdown of the protein, the Amadori product can be measured by amino acid analysis because the Amadori and Heyns product cannot be detected by UV absorption (Labuza, 1990 and Van Boekel, 1998). The Amadori product is hydrolysed in acid conditions giving an artificial amino acid which is furosine (Van Boekel, 1998). Furosine can also easily be monitored by reversed-phase high-performance liquid chromatography (HPLC) (Resmini *et al*., 1990) and ion-exchange chromatography (Hartkopf & Erbersdobler, 1993), in addition it is possible to apply capillary electrophoresis (Tirelli & Pellegrino, 1995). The gas chromatography-mass spectroscopy (GC-MS) method for measuring the lysine, furosine and carboxymethyllysine (CML) in cereal products is reported by Charissou *et al*. (2007). However, there is some problem with the furosine method because the content

of the Amadori is calculated from furosine content by using a conversion factor. This method possibly shows an error in calculation, since only 30-40% of the Amadori product is converted into furosine (Furth, 1988 and Labuza, 1990). Another method for estimating the amount of Amadori product is the application of HPLC to evaluate carboxymethyllysine (CML), which is oxidized by periodic acid and subsequent acid hydrolysis of the protein (Badoud *et al*., 1991 and Van Boekel, 1998).

The formation of hydroxymethyfurfural (HMF) from the Amadori compound in stage two is usually observed by UV spectrophotometer (Yeo & Shibamoto, 1991). This method is another indirect way to measure the Maillard reaction rate. HMF is also evaluated by the HPLC method (Van Boekel, 1998). Meydav *et al*. (1977) used spectroscopy in the visible wavelength range at 420 nm to evaluate HFM. However there were some drawbacks. The disadvantage for this method is that it is time consuming because this measurement requires filtration and centrifugation steps in the purification process. Such processes may influence the concentration of the pigments and cannot be used on-line (Amiot *et al*., 1992). Fluorescence spectroscopy was first used to assess the progress of browning in food by Adhikari & Tappel (1973). Since then there have been many studies in food research which have applied fluorescence to monitor the browning reaction, such as Matiacevich & Buera (2006) who focused on the kinetics of fluorescence and pigment development for the Maillard reaction in a liquid model system. Schamberger & Labuza (2006) and Zhu *et al*. (2009) applied fluorescence spectroscopy to assess the Maillard reaction in milk.

During the final stage of the Maillard reaction, the formation of brown colour pigments (melanoidins) from reactive compounds occurs, which can be monitored by the absorbance at a chosen wavelength: typically 420-460 nm (Van Boekel, 1998).

The chemical method is a conventional method, which has been generally used in liquid food systems such as apple juice concentrates during storage (Toribio *et al*., 1984), milk heating (Van Boekel, 1998), thermal treatment of apple puree (Ibarz *et al*., 2000), apple juice concentrate heating (Vaikousi *et al*., 2008), cashew apple juice (Damasceno *et al*., 2008), honey heating (Vaikousi *et al*., 2009) and blackberry juice heating (Jiménez *et al*., 2012). The application of the chemical method of measuring the browning reaction for some solid foods, such as dried skim milk (Franzen *et al*., 1990) and fried potato (Sahin, 2000) has also been used.

Some of the problems of the classical colour measurement method, including colouric observation at 420 or 490 nm, measurement of UV and IR (infared) spectrum analysis, are destructive of the sample, laborious and time consuming. Furthermore, these chemical methods are not so useful in following the history of colour development during the process (Purlis & Salvadori, 2007 and Puris, 2010).

2.4.2 Indirect or physical method

The obvious appearance of brown colour in the last stage can be measured by a colorimeter in tristimulus CIE *L*a*b** or Hunter *Lab* colour systems (Zhu *et al*., 2009). The application of a colorimeter has been widely used to identify the colour of food surfaces that have undergone the Maillard browning reaction for several kinds of food and cooking types.

Examples of the colorimeter method in food studies are cookie baking (Shibukawa *et al*., 1989), pea puree heating (Shin & Bhowmik, 1995), bread baking (Zanoni *et al*., 1995 and Mohd Jusoh *et al*., 2009), pastry baking in a microwave oven (Zuckerman & Miltz, 1997), maize grits in extrusion (Ilo & Berghofer, 1999), soy milk heating (Kwok *et al*., 1999), peach puree heating (Ávila & Silva, 1999), hazelnut roasting (Özdemir & Devres, 2000; Saklar *et al*., 2001; Demir *et al*., 2002 and Alamprese *et al*., 2009), kiwifruit drying (Maskan, 2001), potato frying (Krokida *et al*., 2001 and Nourian & Ramaswamy, 2003), cracker baking (Broyart & Trystram, 2002), wheat germ heating (Ibanoglu, 2002), tofu frying (Baik & Mittal., 2003), sesame seed roasting (Kahyaoglu & Kaya, 2006), *gulabjamun* indian dough ball frying (Jayendra Kumar *et al*., 2006), dehydrated potato (Acevedo *et al*., 2008), high temperature treatment of cashew apple (Lima *et al*., 2010) beef roasting (Goňi & Salvadori, 2011) and fish grilling (Matsuda *et al*., 2013).

However the main drawback of the reflectance measurement is that only a reduced section of the food or a small area of the surface material is analysed. The diameter of the measurement head of the spectrophotometer is normally between 6 to 8 mm. This is quite small compared with the area of the objective sample. Large surface correlations cannot be observed and the robustness of its applicability in non-homogeneous samples is obviously limited (Gökmen *et al*., 2008). For all the disadvantages of the chemical

and colorimeter methods, a new method of computer vision analysis system has been developed to apply in measuring the colour change of food during the browning process.

Computer vision system has been used in many research projects in the agriculture and food technology area (Wang & Sun, 2001). Computer vision analysis has important advantages over the classical colorimeter by analyzing the colour distribution over the whole surface and monitoring it during processing. It is cost effective, consistent and has high speed and accuracy (Locht *et al*., 1997; Brosnan & Sun, 2004; Yam & Papadakis, 2004 and Gökmen *et al*., 2008). Moreover, the computer vision does not come into contact with the sample during measurement and the images taken from this system can be saved to be re-analyzed at a later time (Purlis & Salvadori, 2007).

2.5 Image analysis method

Image analysis or computer vision (CV) is a technology for obtaining and analyzing an image of a real scene by computers to derive the information for quantifying, classifying and evaluating the quality of various materials (Wang & Sun, 2001; Brosnan & Sun, 2004 and Pedreschi *et al*., 2006). This technique presents many advantages; it is able to measure the distribution of colour on the surface and does not destroy the sample, and also verifies other physical characters such as image texture, morphological elements, and defects (Mendoza & Aguilera, 2004 and Pedreschi *et al*., 2006). Moreover, with the advantage of its greater speed, accuracy, cost effectiveness, consistency and recent advances in hardware and software, computer vision has attracted a significant amount of research aimed at replacing human inspection (Brosnan & Sun, 2004 and Mendoza & Aguilera, 2007). Computer vision systems have been increasingly applied in the agricultural and food industry for quality evaluation, detection of defects, identification, grading and sorting of fruit and vegetables, meat and fish, bakery products and prepared goods (Gerrard *et al*., 1996; Leemans *et al*., 1998; Segnini *et al*., 1999; Papadakis *et al*., 2000; Sun, 2000; Wang & Sun, 2001; Brosnan & Sun, 2004; Mendoza & Aguilera, 2004 and Pedreschi *et al*., 2006).

As the image analysis method is a relatively new technology it has been applied mostly to determining the colour of fruit or fresh products. However, food process technologists have been interested to apply this method to study browning kinetics.

Some examples of applying an image analysis system in browning kinetic studies are the studies of cheese baking (Wang & Sun, 2003), chocolate during storage (Briones & Aguilera, 2005), potato chips frying (Pedreschi *et al*., 2006, 2007 and Mendoza *et al*., 2007), bread baking (Purlis & Salvadori, 2007, 2009 and Purlis, 2010), coffee roasting (Hernández *et al*., 2008) and banana slices (Quevedo *et al*., 2009).

2.5.1 Image analysis system

Generally, an image analysis system consists of three basic components: a lighting unit for providing the illumination in the dark room, a camera for acquiring images and computer hardware and software for analyzing an image as shown in Figure 2.6 (Brosnan & Sun, 2004).

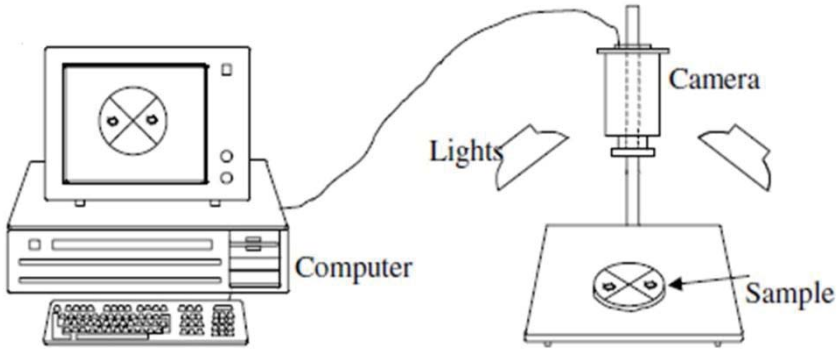

Figure 2.6 Components of a computer vision system (Brosnan & Sun, 2004).

One of the most important parts is the lighting system because the level and quality of illumination affects the vision analysis. The appearance of an object can be drastically changed with the object of interest being clarified or blurred by adjustment of the lighting (Brosnan & Sun, 2004). Therefore the quality of the image and the accuracy of the system depend on the performance of the illumination system (Brosnan & Sun, 2004). It was also stated that the image contrast can be enhanced by a well-designed illumination system. The design of illumination systems in a food industry application needs to consider location, lamp type and colour quality of the light. Some noise such as reflection and shadow can be reduced by setting good lighting and this helps to decrease processing time (Batchelor & Searcy, 1989).

Lighting can be placed both in front of and behind the objective, depending on the application (Gunasekaran, 2001). For example, if the objective is to measure a surface

feature such as defect detection in apples, carrots, mushroom and other fruit, or to measure the colour of food for both unprocessed and processed food, then front lighting (reflective illumination) is required (Davenel *et al*., 1988; Batchelor & Searcy, 1989; Yang, 1994; Heinemann *et al*., 1995; Leemans *et al*., 1998; Vízhányó & Felföldi, 2000 and Brosnan & Sun, 2004). In another way the lighting from behind (transmitted illumination) is used for determining the critical edge dimensioning or for sub-surface feature analysis as in the size inspection by making a shadow image (Hamey *et al*., 1993 and Brosnan & Sun, 2002). The elimination of natural light effects is important in image collection, so the image processing system needs to be set up in dark and closed rooms (Brosnan & Sun, 2004).

2.5.2 The process of image analysis

To study the kinetics of colour changing in food samples, an image analysis system has to measure representatively and accurately, the colour of the sample. The image processing steps involve acquisition, pre-processing, segmentation and statistic calculation (Batchelor & Searcy, 1989; Jain, 1989 and Gunasekaran, 2001).

2.5.2.1 Image acquisition

Images are captured using a colour digital camera. The colour digital camera is located vertically above the sample. Sample illuminators and the computer digital camera should be placed in a dark room in order to avoid light and reflection from the environment. Prior to operating the image system, the white balance needs to be set. The photographs of a colour standard are necessary to ensure the accuracy of the lighting system and digital camera (Batchelor & Searcy, 1989; Gunasekaran & Ding, 1994; Gunasekaran, 1996; Gunasekaran, 2001 and Brosnan & Sun, 2002).

2.5.2.2 Image pre-processing

Prior to analysis of the digital images, they can be pre-processed to improve their quality by manipulating the data for correction of geometric distortion, removal of noise, grey level correction and correction for blurring (Hamey *et al*., 1993 and Brosnan & Sun, 2004). The noise of the image can be removed and the contrast can be enhanced by using digital noise filtering. For example a linear Gaussian low pass filter or

averaging filter can be applied (Batchelor & Searcy, 1989; Jain, 1989; Brosnan & Sun, 2004; Abdullah *et al*., 2004 and Gonzalea & Woods, 2008).

2.5.2.3 Segmentation

The purpose of this step is to split the part of interest from the background by classifying disjoint regions of the image intensity. This segmented image is a binary image consisting only of black and white pixels, where '0' (black) and '1' (white) mean background and object, respectively (Jain, 1989; Gunasekaran & Ding, 1994 and Gunasekaran, 1996). Three techniques; thresholding, edge-based segmentation and region-based segmentation are mostly used in the segmentation step (Sun, 2000; Brosnan & Sun, 2004 and Sonka *et al*., 2008). Thresholding is commonly used because it is a simple and fast technique for characterising image regions based on constant reflectivity or light absorption of their surface. Edge-based segmentation detects discontinuities in grey level, colour or texture. Region segmentation groups the similar pixels together to be represented as a boundary or a region of interest (Brosnan & Sun, 2004).

2.5.2.4 Analysing and measuring

After the segmentation step, the objects of interest have been extracted and are ready to be analysed. For the study of browning kinetics in food, the colour space commonly used to describe the browning reaction is the *L*a*b** colour system because they are the standard colour parameters for agriculture and in the food area (Yam & Papadakis, 2004). In addition the *L*a*b** colour space is close to uniform, in that numerical changes in *L*a*b** are proportional to the perceived colour differences (León *et al*., 2006 and Hunt & Pointer, 2011). However, a digital image normally presents in the RGB colour model, which is the most often used model in capturing the intensity of the light in the red (*R*), green (*G*) or blue (*B*) spectrum, respectively.

The conversion of RGB into *L*a*b** units is therefore an important step when applying an image analysis method to agricultural or food products. The RGB-*L*a*b** conversion cannot be done directly using a standard formula like a conversion from centimetres to inches (Ilie & Welch, 2005 and León *et al*., 2006). The conversion can be

computationally approached using the mathematical transform model with known parameters (Segnini *et al*., 1999; Paschos, 2001; Mendoza & Aguilera, 2004).

The summary of the image analysis method step is shown in Figure 2.7.

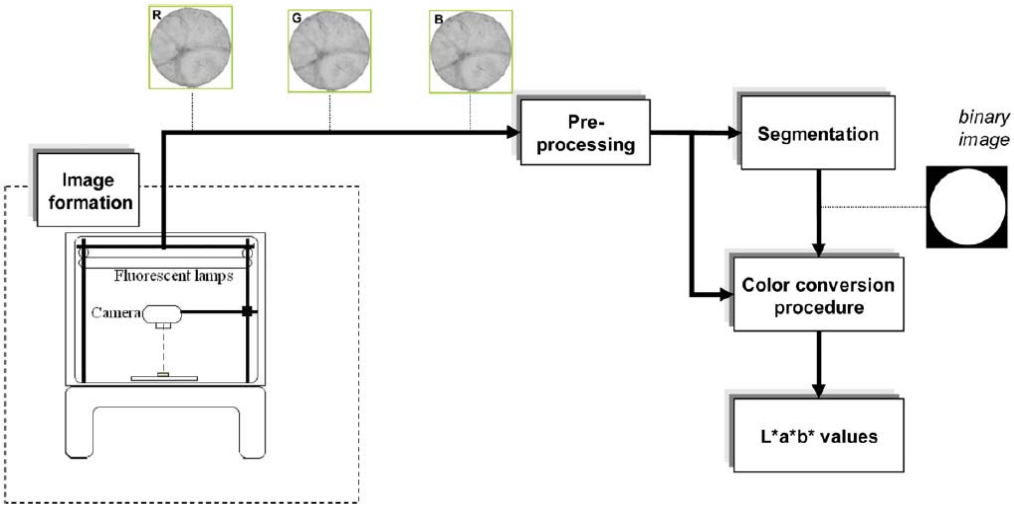

Figure 2.7 Schematic representation of the image analysis step (Pedreschi *et al*., 2006).

2.5.2.5 Colour system used in the browning kinetic study

The colour system generally found in the studies of browning kinetics is the *Lab* colour system. *Lab* is the shortened name of two different colour spaces, which are the Hunter *Lab* (Hunter *L, a, b*) and the other is CIE (CIE 1976 *L*a*b**). *Lab* is an informal short form of a colour-opponent space. Both spaces are absolute colour spaces and are derived based on nonlinear compression of the master space CIE 1931 XYZ colour space coordinates with the dimension *L* for lightness and *a* and *b* for the colour-opponent dimensions (Fairchild, 2005; Schanda, 2007 and Hunt & Pointer, 2011).

Hunter Lab Colour Space

The XYZ system has a drawback with respect to being a perceptually non-uniform colour scale and does not give a good indication of sample colour. So, the Hunter *Lab* colour scale was developed in 1966. The Hunter *Lab* colour scale is more visually uniform than the XYZ colour scale. In a uniform scale, the difference between points plotted in the colour space corresponds to visual differences between the colours plotted. The Hunter *Lab* colour space is organized in a cube form. The *L* axis runs from

top with the maximum value of 100 to 0 at the bottom. At the maximum of 100 is a perfect white and the minimum of 0 is an absolute black. The '*a*' and '*b*' axes have no specific numerical limits. Positive '*a*' is red; negative '*a*' is green. Positive '*b*' is yellow; negative '*b*' is blue. A diagram of the Hunter *Lab* colour space is shown in Figure 2.8 (Gilchrist *et al*., 1999).

Figure 2.8 The Hunter *Lab* colour space

CIE L, a*, b* Colour Space*

CIE *L*a*b** was invented in 1976 in order to solve the non-uniform scale problem in CIE XYZ colour space. CIE *L*a*b** (1976) is usually used to describe the colours visible to the human eye because it is a more uniform colour space and the most complete colour model (McLaren, 1976 and Schanda, 2007). It was developed by the International Commission on Illumination (McLaren, 1976). The * after *L*, *a* and *b* mean these value are derived from *L*, *a* and *b* in CIE colour space, therefore they present in the form of *L**, *a** and *b**. The meaning of three parameters (*L*a*b**) in the model represent the lightness, redness and yellowness of the colour, respectively. The value of the lightness is between 0 and 100 (*L** = 0 yields black and *L** = 100 indicates white), the redness (*a**) position between red and green (*a** is [-] negative values indicating green while [+] positive values indicate red) and the yellowness (*b**) position between yellow and blue (*b** is [-] negative values indicating blue and [+] positive values indicate yellow) (Gilchrist *et al*., 1999).

Different colour systems have been used in the studies of browning kinetic of foods. Some studies employed the Hunter *Lab* colour scale to model the browning kinetic such

as the study of bread baking (Zanoni *et al*., 1995), maize grits extrusion (Ilo & Berghofer, 1999), peach puree heating (Ávila & Silva, 1999), French fries in deep frying (Krokida *et al*., 2001) and sesame seeds roasting (Kahyaoglu & Kaya, 2006).

However, the CIE *L*a*b** scale has been more popular to apply in the browning kinetic study area than the Hunter *Lab* colour system. For example in the measurement of the kinetics of colour change using *L** for pea puree heating (Shin & Bhowmik, 1995), hazelnut drying (Lopez *et al*., 1997), cracker baking (Broyart *et al*., 1998), soy milk heating (Kwok *et al*., 1999), apple puree (Ibarz *et al*., 2000), tofu during frying (Baik & Mittal, 2003), potato cooking and frying (Nourian & Ramswamy, 2003), *gulabjamun* balls in deep frying (Jayendra Kumar *et al*., 2006), almond roasting (Lukac *et al*., 2007), and in bread baking (Purlis & Salvadori, 2007, 2009 and Purlis, 2010).

It was found from the review of the Hunter *Lab* colour space system, applications in the study of browning kinetics of food processes that most of the studies applied the conventional colorimeter as the measuring instrument in evaluating the browning reaction of food processes. Therefore, it can be mostly found that Hunter *Lab* colour space is used in colorimeter instruments. Conversely, the CIE colour system is applicable to use in the image processing method. This may be because the CIE colour system has advantages over the Hunter *Lab* colour system and it is a more recently developed colour system which has a more uniform evaluation method than the Hunter *Lab* colour system. Therefore the CIE colour system will be used in the image analysis method for this study.

2.6 The kinetic modelling of high temperature browning in food

The Maillard browning reaction is well known as an important feature affecting the food qualities such as colour, flavour, taste and aroma as well as the nutritional value of food. It has been necessary for food technologists to develop a mathematical model with the aim of predicting and therefore controlling the Maillard browning reaction during processing and storage. For this, kinetic modelling has been applied to foods to describe the Maillard reaction as a function of time and temperature.

The Maillard browning kinetics have been developed for many foods and many processes. For example browning kinetics have been studied in cookie baking (Shibukawa *et al*., 1989), bread baking (Zanoni *et al*., 1995; Zhang & Datta, 2006;

Purlis & Salvadori, 2007, 2009 and Purlis, 2010), pastry dough baking (Zuckerman & Miltz, 1997), cracker baking (Broyart *et al*., 1998), extrusion process (Ilo & Berghofer, 1999), wheat germ heating (İbanoğlu, 2002), deep fried potatoes (Sahin, 2000; Krokida *et al*., 2001; Moyano *et al*., 2002 and Nourian & Ramaswamy, 2003), *gulabjamum* indian dough ball frying (Jayendra Kumar *et al*., 2006), kiwifruit drying (Maskan, 2001), hazelnut roasting (Saklar *et al*., 2001 and Demir *et al*., 2002), sesame seed roasting (Kahyaoglu & Kaya, 2006), coffee bean roasting (Heyd *et al*., 2007), dehydrated potato (Acevedo *et al*., 2008), coffee roasting (Hernández *et al*., 2008),milk heating (Pagliarini *et al*., 1990), soy milk heating (Kwok *et al*., 1999), pea puree heating (Shine & Bhowmik, 1995), peach puree heating (Ávila & Silva, 1999), apple puree heating (Ibarz *et al*., 2000), apple juice concentrate heating (Vaikousi *et al*., 2008), honey and diluted honey heating (Vaikousi *et al*., 2009) and blackberry juice heating (Jiménez *et al*., 2012). It was found that the process parameters of temperature and time are the main factors affecting the Maillard reactions of food.

Generally, the generation or degradation of a component concentration in foods during thermal processing and storage has been described in terms of a kinetics model. Based on the general rate law, the disappearance of a compound in a closed system with only one compound reacting can be written in Equation 2.2 (Giannakourou & Taoukis, 2007).

$$-\frac{d[A]}{dt} = k[A]^n \tag{2.2}$$

where A is the concentration of the cooking component in the food ($J \cdot mol^{-1}$), k is the reaction rate constant ($mol \cdot min^{-1}$) and n is the reaction order (usually $0 \leq n \leq 2$). Typically, the reaction rate k follows an Arrhenius relationship with temperature (Equation 2.3).

$$k = k_0 \exp\left(-\frac{E_a}{RT}\right) \tag{2.3}$$

where k_0 is the Arrhenius constant (s^{-1}); E_a is the activation energy ($J \cdot mol^{-1}$); R is the universal gas constant (8.3145 $J \cdot mol^{-1} \cdot K^{-1}$) and T is absolute temperature (K).

At constant temperature, Equation (2.2) can be integrated for a chosen order with respect to time. The order of reaction is a parameter that gives a mathematical description of time and concentration dependence (Giannakourou & Taoukis, 2007).

After integration, a zero-order reaction is:

$$[A] = [A]_0 - kt \tag{2.4}$$

a first-order reaction is:

$$[A] = [A]_0 \exp(-kt) \text{`} \tag{2.5}$$

and a second-order reaction is:

$$\frac{1}{[A]} = \frac{1}{[A]_0} + kt \tag{2.6}$$

The Maillard browning reaction kinetics in food systems are generally considered to be zero or first order reactions. First order kinetics was found to be the most commonly used in literature, although zero and second order are also discussed.

Zero order kinetic models were used to describe the colour change due to browning reactions in many studies for example milk product heating (Franzen *et al*., 1990; Pagliarini *et al*., 1990 and Kwok *et al*., 1999), maize grits extrusion (Ilo & Berghofer, 1999), kiwifruits drying (Maskan, 2001), wheat germ heating (İbanoğlu, 2002), juice heating (Burdurlu & Karadeniz, 2003 and Vaikousi *et al*., 2008) and *gulabjamun* indian dough ball frying (Jayendra Kumar *et al*., 2006).

Pagliarini *et al*. (1990) investigated the kinetics of colour changes using the total colour difference (ΔE) and yellowness index (YI) in milk following heat treatment. The total colour difference (ΔE) and yellowness index (YI) were defined as:

$$\Delta E = \sqrt{\Delta a^2 + \Delta b^2 + \Delta L^2} \tag{2.7}$$

and

$$YI = 142.86 b / L \tag{2.8}$$

They found that both ΔE and YI increased at constant temperature following zero order kinetics.

Ilo & Berghofer (1999) and Jayendra Kumar *et al*. (2006) studied the kinetics of colour change of maize grits in extrusion and *gulabjamun* indian dough ball in frying using the CIE colour parameters (*L*a*b** scale). They found that all colour parameters changed

following zero order kinetics. In some reports, zero order kinetics were found to explain the change of *a* and *b* values due to heat treatment. Rhim *et al*. (1988) evaluated tristimulus Hunter *Lab* value of skim milk during heat treatment over the temperature range of 100-150°C and found that the *a* and *b* values of skim milk increased following zero order kinetics. This was in agreement with the finding of Kwok *et al*. (1999) who studied the kinetics of colour changes in soymilk heating and found that the *a** and *b** values increased following zero order kinetics. Maskan (2001) also applied zero order kinetics to describe the colour change in term of *a* value and total colour difference (ΔE) of kiwifruit during hot air and microwave drying. However, the *L* and *b* values in these studies were found to follow a first order kinetic model.

First order kinetics was frequently used for describing the browning reaction in terms of the colour change indicated by *Lab* in Hunter and *L*a*b** in CIE colour systems. In many kinds of food and cooking conditions such as pea puree (Shin & Bhowmik, 1993), bread baking (Zanoni *et al*., 1995; Broyart *et al*., 1998; Purlis & Salvadori, 2007, 2009 and Purlis, 2010), pastry dough baking (Zuckerman & Miltz, 1997), cracker baking (Broyart *et al*., 1998), peach puree heating (Ávila & Silva, 1999), apple puree heating (Ibarz *et al*., 2000), potato frying (Krokoda *et al*., 2001 and Nourian & Ramaswamy, 2003), hazelnut roasting (Demir *et al*., 2002), tofu frying (Baik & Mittal, 2003), sweet potato puree (Figueira *et al*., 2011), beef roasting (Goňi & Salvadori, 2011), blackberry juice heating (Jiménez *et al*., 2012) and fish grilling (Matsuda *et al*., 2013).

Other kinetic models have been used in the browning kinetic studies for example, a third-degree polynomial equation explained the kinetics of colour changes (*L, a, b* values) in wheat germ due to heat treatment (İbanoğlu, 2002), a cubic polynomials model described the effect of roasting time and temperature on the colour change of roasting sesame seeds (Kahyaoglu & Kaya, 2006) and an artificial neural network model was used to predict the quality of coffee roasting including the brightness (Hernández *et al*., 2008).

The temperature dependence of the reaction rate constant for Maillard browning is generally explained by the Arrhenius equation (Equation 2.3). To identify the kinetic parameters, isothermal and non-isothermal methods were used. In the study of Maillard reaction kinetics, an isothermal method is simpler and is generally used. Most of studies applied the isothermal method in the study of liquid food samples such as milk (Rhim *et*

al., 1988; Pagliarini *et al*., 1990; Narayanan *et al*., 1993 and Kwok *et al*., 1999) and fruit puree and juice (Shin & Bhowmik, 1993; Steet & Tong, 1996; Ávila & Silva, 1999; Ibarz *et al*., 2000; Selen Burdurlu & Karadeniz, 2003 and Vaikousi *et al*., 2008). The isothermal system is easy to implement in liquid food systems because the liquid food is homogeneous. However, some studies assumed a heating media as an isothermal system in some cooking systems such as pastry dough baking and fish grilling (Zuckerman & Miltz, 1997 and Matsuda *et al*., 2013), frying process (Sahin, 2000; Krokida *et al*., 2001; Baik & Mittal, 2003; Nourian & Ramaswamy, 2003 and Jayendra Kumar *et al*., 2006), baking and roasting process (Demir *et al*., 2002; Kahyaoglu & Kaya, 2006; Pulis & Salvadori, 2007 and Matsuda *et al*., 2013) and extrusion process (Ilo & Berghofer, 1999). In the study of Ilo & Berghofer (1999), the plate, oil, air and screw was assumed to be at a constant temperature and the food sample was assumed to be the same. Assuming isothermal conditions was also used in the kinetic models for the baking/ grilling, frying, baking and roasting systems described above. This may result in an error in kinetic parameter estimation because the Maillard reaction rate is highly affected by temperature but the temperature used in the kinetic model was not the real sample temperature. In addition, in food processes, phenomena such as water evaporation in baking or frying processes cause thermal gradients across the food surface.

The complication of using a non isothermal method means that there are only a few studies using this method in the Maillard reaction. For example cracker baking (Broyart *et al*., 1998) and bread baking (Purlis & Salvadori, 2009).

The reported range of the activation energy of the Maillard browning reaction was between 45.3 and 70.0 $kJ \cdot mol^{-1}$ for a baking process (Zanoni *et al*., 1995; Zuckerman & Miltz, 1997; Broyart *et al*., 1998 and Zhang & Datta, 2006), 28.66 and 165 $kJ \cdot mol^{-1}$ for a frying process (Krokida *et al*., 2001; Baik & Mittal, 2003; Nourian & Ramswamy, 2003 and Jayendra Kumar *et al*., 2006), 25 and 80.74 $kJ \cdot mol^{-1}$ for a roasting process (Demir *et al*., 2002; Kahyaoglu & Kaya, 2006 and Goňi & Salvadori, 2011), 28 and 140 $kJ \cdot mol^{-1}$ for a drying process (Rapusas & Driscoll, 1995 and Lopez *et al*., 1997), 31.5 and 50.7 $J \cdot mol^{-1}$ for a grilling process (Matsuda *et al*., 2013) and 67.9 and 117.5 $kJ \cdot mol^{-1}$ for liquid (milk and juice) food heating (Rhim *et al*., 1988; Pagliarini *et al*., 1990; Shin

& Bhowmik, 1995; Steet & Tong, 1996; Ávila & Silva, 1999; Kwok *et al*., 1999 and Ibarz *et al*., 2000).

2.7 Conclusion

The Maillard reaction is a complex reaction with many pathways involving several steps, which influence food appearance and qualities. Process conditions such as temperature and time are the most important factors affecting the reaction rate. The development of a mathematical kinetic model for the Maillard browning reaction is the best approach to predict and control the process and quality of the products. One of the problems to achieve the best kinetic model is the kinetic parameter estimation. This problem may be due to assuming isothermal conditions and developing the kinetics model using the temperature of the cooking medium rather than the temperature of the sample because it is so difficult to measure the real surface temperature during experimentation. However, using these assumptions for isothermal study of the browning kinetic was inappropriate because, in fact, a transient thermal gradient across the food surface was generally found in food processes due to water evaporation and edge effects in baking or frying processes. Therefore, a cooking system that provided an isothermal condition would be needed for this study.

Most studies used image analysis to investigate the average colour and represent the browning formation as it is affected by temperature histories. In fact the brown colour occurring in foods often shows an uneven colour on the surface, suggesting each area was affected by a different time-temperature history. There is a distribution of colour browning on the food surface as resulted by the differences in heat transfer distribution. This was because the surface of foods was not absolutely smooth, so some higher areas such as blisters or bumpy areas are heated quicker and resulted in more intensity of browning at that area. For these reasons, the average brown colour may not be truly reliable in estimating the temperature dependence and developing the kinetic model. Therefore a food and cooking system will be developed to achieve uniform and constant conditions at the surface of the product to measure the accurate browning kinetics for food cooking, in the next chapter.

Chapter 3

MODEL FOOD AND COOKING SYSTEM EVELOPMENT

3.1 Introduction

The literature review identified the potential to characterise the browning behaviour of food samples subjected to high temperature. It was generally commented that more browning is evident on edges or corners of products or where blisters form due to evaporation during cooking or a rough surface (Figures 3.1 and 3.2). Figure 3.1 shows an example of colour browning distribution in a macro scale at the edges and bubbling surface of the biscuit. More browning occurring at these areas is because the air flow affects higher convection heat transfer to the edges than that to other parts. In addition, the conduction heat transfer at the bubbling surface cannot conduct through the sample because there is a low conductivity of the air underneath the bubbling areas to slow down the heat transfer; therefore more heat accumulation at the bubbling areas result in more browning reaction.

Figure 3.1 The macro scale distribution of brown colour on the blister surface of a biscuit

Other evidence of the uneven brown colour due to uneven heat transfer or different temperature histories across the food surface was also explained in the micro scale, for

example, at the roughness surface of toast is shown in Figure 3.2. As can be seen from Figure 3.2 (a) that the distribution of brown colour is obviously seen in the overall view of the toast surface because a surface of bread is so rough, there are many bumpy peaks on its surface when examined at the micro scale (Figure 3.2 (b)). There is high exposed surface area to heat source that higher heat may transfer more quickly and then results in more browning at the peak areas compared to the trough parts which have lower exposed areas and a large mass to conduct heat into away from the hollows. In addition, there is the narrow pathway between the peaks for conduction away into the food, so lower browning reaction occurred at these areas.

(a) (b)

Figure 3.2 The micro scale distribution of brown colour on toast: (a) overall browning distribution on the toast's surface and (b) cross section of toast showing the dark brown colour at bumpy areas

In these cases the brown colour on the food's surface is observed some sort of average of a distribution of colour. But locally an area of appearance colour is actually a distribution of colour at both macro and micro scale. The distribution of colour at the macro or micro scale could be explained by different surface temperature histories across the surface of the product. Therefore assuming an average brown colour as the indicator of the browning reaction would be not absolutely correct for isothermal kinetic study.

Ideally, such a study requires the selection of a suitable food system to study the Maillard reaction kinetics under isothermal conditions. A suitable food system should provide a uniform brown colour on its surface, where the Maillard reaction is taking

place. A uniform brown colour on the sample surface can be characterised by a low value of standard deviation of colour value when measured by the image analysis system, so that the average value better represents the sample colour value. The homogeneous model food with a nice smooth surface would be preferred to avoid the problem of the macro and microscopic variation of the colour distribution. Hence, the model food developed can be extended to these other scenarios and to other foods.

To measure the kinetics, a method is needed to cook samples with known and well controlled temperature together with a robust method of measuring the colour of the sample. The cooking system would be developed to be close to an ideal isothermal cooking condition so that the constant heat transfer would be achieved to provide an even browning colour on the sample surface. To these aims, this chapter consists of three main sections; identifying the model food, developing the colour assessment method (image processing) and developing the cooking system to be used as the basis of the thesis.

3.2 Identifying the model food

High temperature browning occurs in many food systems but variations are likely due to compositional or surface differences. Therefore, a model food system that allows reproducible measurement was required. A number of potential model food samples were investigated for this purpose.

For the purpose of evaluating browning kinetics under isothermal conditions, a uniform colour is a preferred property to provide an uncomplicated colour evaluation. To achieve this, the surface of the sample should be smooth, remain flat and be in good contact with the heating surface. The composition of the model food should be homogeneous. The model food needs to have both reducing sugar and protein in its composition because they are the browning reactants.

Six different food systems were investigated to select the most appropriate model food for this study. These six food samples were almond nuts, shortbread, white chocolate, roux, gluten dough and pastry. The model food systems were studied using individual cooking process as appropriate for each type of food.

3.2.1 Almond nuts

Raw almond nuts supplies were selected as a potential model food because of their physical properties. They have an elliptical-flat shape. Therefore the browning on an almond nut surface is expected to be even if heat transfer to their surfaces can be made uniform. The almonds (70 g.) were roasted in a hot air oven at 150˚C for 60 minutes.

The browning behaviour on almond nuts was observed (Figure 3.3). It was seen that the intensity of brown colour of the almond nut's surface was uneven due to heat transfer across its complicated shape and un-smooth surface was not constant. In addition, shadows were observed behind the almond samples, which affect the image analysis process. It was concluded that an almond nut was not a good model food for studying the Maillard browning kinetics under isothermal conditions.

Figure 3.3 Almond roasted at 150˚C for 60 minutes

3.2.2 Shortbread

Shortbread is known to undergo Maillard type browning reactions because it has a low water content and high level of sugar, protein and fat. Shortbread was prepared using a recipe using 150 g of butter, 1 cup of plain flour, 1 cup of water, ½ cup of rice flour and ½ cup of sugar. All ingredients were well mixed in a large bowl and kneaded until they became a dough. Then the dough was rolled into a slab shape with a thickness of 15 mm. The shortbread dough was baked in a hot air oven at 160˚C for up to 50 minutes. During the baking process, a stainless steel tray was placed on the top of the short bread sample to provide better and more even heat transfer to the sample and help keep the sample surface flat.

After baking, images of the shortbread were taken and as shown in Figure 3.4. The browning was uneven because its surface was very rough. This is likely to have resulted from differences in the heat transfer between the peaks and troughs on the rough surface

of the shortbread. There were many bubbles on the surface due to evaporation of water inside the sample that could not move out because of the covering tray. The findings of uneven distribution of colour across the surface and the evaporation phenomenon lead to the conclusion that short bread was inappropriate for developing a simple kinetic model from isothermal conditions. Therefore, the shortbread could not be used as the model food sample for this study.

Figure 3.4 Shortbread baked at 160°C for 50 minutes

3.2.3 White chocolate

White chocolate was expected to be a good model food because it has a smooth surface and white colour. In addition white chocolate can provide a homogenous system, so heat could be transferred evenly. The white chocolate was put in a beaker and melted by indirect heating using hot water in a water bath at 80°C. The melted chocolate was then placed in an oven to bake at 150˚C for 15 minutes.

The baked chocolate is shown in Figure 3.5. It can be seen that the white chocolate was light brown after cooking and that the texture of the white chocolate was not homogeneous. During cooking, oil separated from the sample and the surface of the sample was very hard and rough. The brown colour was formed after 5 minutes, however the surface did not remain smooth. The surface of the white chocolate started to crack and became rougher as the process progressed, leading to fat separation and an uneven browning appearance on the sample surface. As a result, this model food system was unsuitable for the browning kinetic study.

Figure 3.5 White chocolate baked at 150°C for 15 minutes

3.2.4 Roux

Roux was also tested as a possible model food system because it is a homogenous food system. Roux is a paste and smooth at the surface. Roux was prepared as a mixture of 1 cup of wheat flour and ½ cup of oil cooked on a frying pan under high heat using domestic stove. After preparing, it was poured into a cookie mould tray. Then the tray was put in the oven for baking at 200˚C for 30 minutes.

Figure 3.6 shows an image of roux after baking at 200˚C for 30 minutes. The same result as in the white chocolate study was found in the roux study. After heating, the roux had a lot of bubbles because it was a paste and contained water. The bubbles were the result of liquid boiling during the cooking process. The high gloss from the oil also created reflections which make image analysis difficult. Therefore, roux is not a good model food system for studying of the browning reaction kinetics in an isothermal process.

Figure 3.6 Roux baked at 200°C for 30 minutes

3.2.5 Dough

Dough was made by mixing wheat flour and water. In this study, a sugar solution was used instead of water in order to provide a reducing sugar, which reacts with the protein in the flour for the browning reaction. The sugar solution was prepared with a ratio of 1 cup of white sugar and 1 cup of distilled water. The dough was prepared by mixing of 1 cup of plain flour and ½ cup of sugar solution. The dough was formed and the surface smoothed with a wooden roller. The dough was cut into small blocks with dimensions of 50×50 mm. The dough sample was baked in a hot air oven at 150˚C for 15 minutes.

The result of the dough baking study is shown in Figure 3.7. The surface of dough appeared to be very smooth and gave an even colour distribution of browning. Greater browning intensity occurred at the edges and corners of the samples because of the higher area for heat transfer at the corner and the edges. From this result, the browning reaction on the dough surface was satisfactory but the problem of edge effects was a concern.

Figure 3.7 Dough baked at 150°C for 15 minutes

It can be concluded from the results of all the samples, that the most satisfactory model food tested for use in this browning kinetic study was the dough. However, the preparation of dough was a problem since it has low stability and reproducibility. Thus frozen dough, for example a commercial frozen pastry, could be more practical. Circle shaped samples could be used to reduce the effect of the edge and corner browning.

3.2.6 Pastry

As described above, the preparation of consistent dough was a problem, due to the length of time required to make it and the inconsistent quality of the mixture. The quality of dough is a control factor since it may affect the browning kinetic study.

A commercial frozen savoury pastry ("Edmonds" brand) was selected for trial as the model food. The ingredients consisted of wheat flour, water, animal and vegetable fats and oils, salt, emulsifiers (soy lecithin, 471), colour (160a), acidity regulators (330, 500), antioxidant (320), flavour. The frozen pastry was left at room temperature for thawing and then cut into circular shapes of 50 mm diameter with a cookie cutter and then placed on the hot Teflon pan at 160˚C for 60 minutes.

The commercial savoury pastry baking presented an even brown colour on a macro scale on a smooth surface compared to the other food samples tested (Figure 3.8). The darker brown at the corner and edge was not found, thus the circular shape solved the problem of high heat transfer at the edge and corner. However, the brown colour on the surface was not absolutely uniform when considered on a micro scale. The uneven colour on the micro scale was caused by little bubbles due to water evaporation. Water evaporation occurring during the baking process, produces a high pressure under the sample, forming small bubbles which reduced the contact between the pan and the pastry. The bubble phenomenon under the pastry surface can be reduced by applying a weight to the top of the sample for creating more complete contact between the hot pan and the pastry sample, and more even colour was expected.

Figure 3.8 Pastry baked at 160°C for 60 minutes

Consequently, it can be concluded that the savoury pastry is an appropriate model food to use in the study of browning kinetics in high temperature processes since it meets the required qualities for the model food.

3.3 The image analysis processing development

From section 2.6 it was concluded that an image analysis system should be used for measuring the browning development on the pastry surface in this study. An image analysis system facilitates objective and non-destructive assessments of the visual quality characteristics of food products (Timmermans, 1998). This technique also provides low cost measurement with consistency and high accuracy (Locht *et al*., 1997; Brosnan & Sun, 2004 and Mendoza & Aguilera, 2007). This section gives detailed specifications of the image processing system and algorithms used to quantify the image for the colour change due to the Maillard browning reaction.

3.3.1 Equipment

An image processing system generally consists of three main items: a camera for image acquisition, a lighting source and software for analysis. The image system was set up in a dark room to avoid the variability caused by ambient light. The image analysis system consisted of:

1. A charge coupled device (CCD) camera (Sony DFW-SX900, with 1289×960 pixels of resolution).
2. A 12 mm, lens (FUJINON-TV Zoom Lens, H6x12.5R, 1:1.2/12.5-75).
3. Two light bulbs (OSRAM 100 W with a beam angle of 80˚, colour temperature of 2700 K, colour rendering index of 100).
4. A stand and a holder for the camera.
5. Stands for holding the lighting system.
6. A 197x197 mm white tile for calibration and background.
7. Computer (Pentium (R) IV CPU 3.00 GHz, 2.00 GB of RAM, NEC Computer Int'l).

3.3.2 Image acquisition system

The image acquisition system for this study includes a 12 mm lens and a charge coupled device (CCD) camera. The CCD camera was installed by holding it with a clamp holder and locating it vertically above the sample at a distance of 420 mm. The camera was

connected to the firewire port of a PC on which the VIPS (Visual Image Processing System, Massey University, New Zealand, Bailey & Hodgson, 1988) software was installed (see Figure 3.9).

To capture an image of the pastry, the sample was placed on a white tile. The tile provides a uniform consistent reference to set the white balance. Prior to operating the image system, the white balance was set by capturing an image of the tile. The images were taken at a resolution of 1280×960 pixels.

3.3.3 Lighting

A high quality image of the sample is important in image analysis, so even, consistent lighting are needed. The performance of the lighting system can greatly influence the quality of the image and plays an important role in the overall efficiency and accuracy of the system. Gunasekaran (1996) stated that the efficiency of the image analysis was improved by enhancing the image contrast with a well-designed lighting system. The lighting system, including location, lamp type and colour quality, is also concerned with factors that cause interference such as reflection and shadow (Bachelor, 1989 and Gonzalez & Woods 2008). For this study, two light bulbs (OSRAM 100 W with a beam angle of 80°, colour temperature of 2700 K, color rendering index of 100) were placed at an angle of 45° with respect to the camera. The distance between the light bulbs and the sample was of 300 mm (Figure 3.9). This provides even lighting while avoiding specular reflections from the pastry surface.

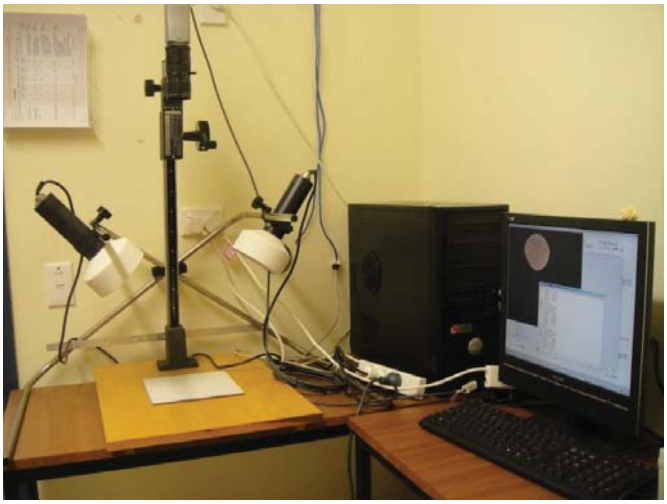

Figure 3.9 The system used for image acquisition of food samples

3.3.4 Image analysis software program

To process the images, the program VIPS was installed onto a computer. This software program was developed by Bailey & Hodgson (1988). All steps of image analysis were performed by the VIPS software including capturing the image of the sample, saving the file in BMP format, analysing the image and reporting the reading in the *L*a*b** colour space. The *L*a*b** colour space is the standard colour system used for food analysis. *L** refers to the lightness, which ranges from 0 to 100 (black to white) (Gilchrist *et al.*, 1999), *a** is the position between green (-) negative and red (+) positive values and *b** is the position between blue (-) negative and yellow (+) positive values. The algorithm used for this process is detailed in the next section and the VIPS code for the image analysis is shown in Appendix A1.1.

3.3.5 Image analysis algorithm

The VIPS code for processing the image performs the following steps. Firstly an image of the sample placed on a white tile was captured from firewire camera, and then the image resolution of 1280x960 pixels was reduced to 640x480 pixels, a more manageable size for display and processing. The captured image was displayed on the computer screen for the user to check the image. After the image was accepted, the images were white level normalised as follows. Thresholding and shrinking commands were used to remove the sample and select the background as a reference. As the tile base is white, this could be used. The white level was estimated by the average RGB (red, green, blue) values of this region. It is essential that no background pixels are saterated, as this would distort the colour value. The image was normalised linearly to set the white level of the tile to 212, scaling each of the RGB components. The level of 212 allowed sample points to be brighter than the tile. The uniformity of the background was also checked (to ensure that sample lighting was uniform) by ensuring that the standard deviation of all the RGB components was less than 10 grey levels. After that, a small image showing points that were overexposed was displayed and the details of the image e.g. the sample date and cooking conditions were obtained from the user and used for the image file name. The normalised image was saved for later reference.

The next step was to determine which pixels belonged to the object being imaged. The blue channel was used to create a mask to distinguish between sample and background

since the sample was significantly darker in the blue channel. To enable a global threshold to be used, the blue channel was divided by the maximum of the green and red channels for each sample. The background was removed and the masked image was displayed.

Finally the masked image was analysed by calculating the colour of the pastry sample in both RGB and *L*a*b** colour spaces. To convert RGB to *L*a*b** it was assumed that the camera provided pixels in linear RGB space. The RGB values were converted to XYZ using a D65 illuminant model, and then the XYZ values were converted to *L*a*b**. The mean value and standard deviation (S.D.) were calculated for the RGB and *L*a*b** colour data and saved to an Excel file for later analysis. All image algorithm steps are summarised and presented in Figure 3.10.

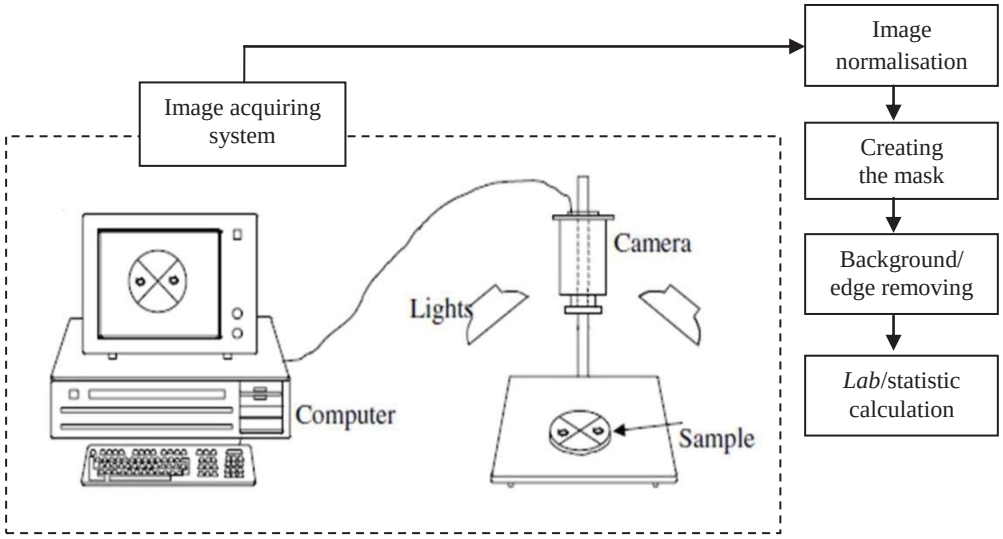

Figure 3.10 Schematic representation of the colour analysis algorithm step for image processing and calculation the *L* a* b** units (adapted from Brosnan & Sun, 2004)

3.3.6 Validation of image analysis setup

Before using image analysis for measuring the browning development on the sample surface in this study, the image system needed to be validated. This involved to measurement of the colour of the object using the image analysis system and comparing this with the standard colorimeter measurement method. In this case a spectrophotometer (CM-2600D, Konica Minolta, Osaka, Japan) was used for the validation. The spectrophotometer device was set up for the observer at 10° and

standard illumination source D65 with 8 mm for the measurement area value (MAV). The reflectance mode was used with specular component included (SCI). The calibration was done with a standard white tile (CM-A145, Konica Minolta, Osaka, Japan) prior to sample measurement.

Both methods of colour measurement (image and spectrophotometer) were applied to measure the colour of baked pastry samples. The pastry samples were baked using the pan baking system which is shown in section 3.4 and the baking methodology is demonstrated in section 5.2.1.

The values of lightness (L^*), redness (a^*) and yellowness (b^*) were obtained from both measurements and the values were plotted as shown in Figures 3.11, 3.12 and 3.13, respectively. It was seen from Figure 3.11 that the lightness values obtained from the image analysis system shows a linear relationship with the lightness values obtained from the spectrophotometer. Because of this linearity the image analysis can be used to measure the kinetics of colour change in the samples for the lightness value.

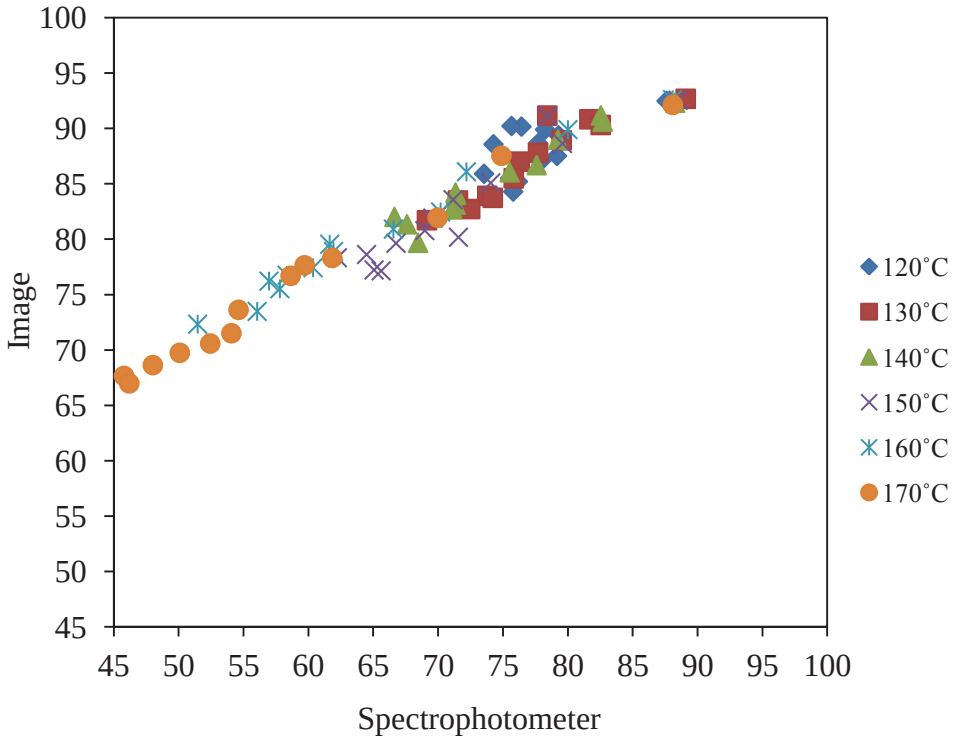

Figure 3.11 The comparison of average lightness (L^*) value measured using the image system and spectrophotometer

The data plot of average redness values of baked pastry obtained from the image analysis system and spectrophotometer colour measurement shows a nonlinear relationship (Figure 3.12). For this reason analysis of the kinetics for the change in *a** during browning may change, depending on which colour measurement is used. This is investigated later in Chapter 5.

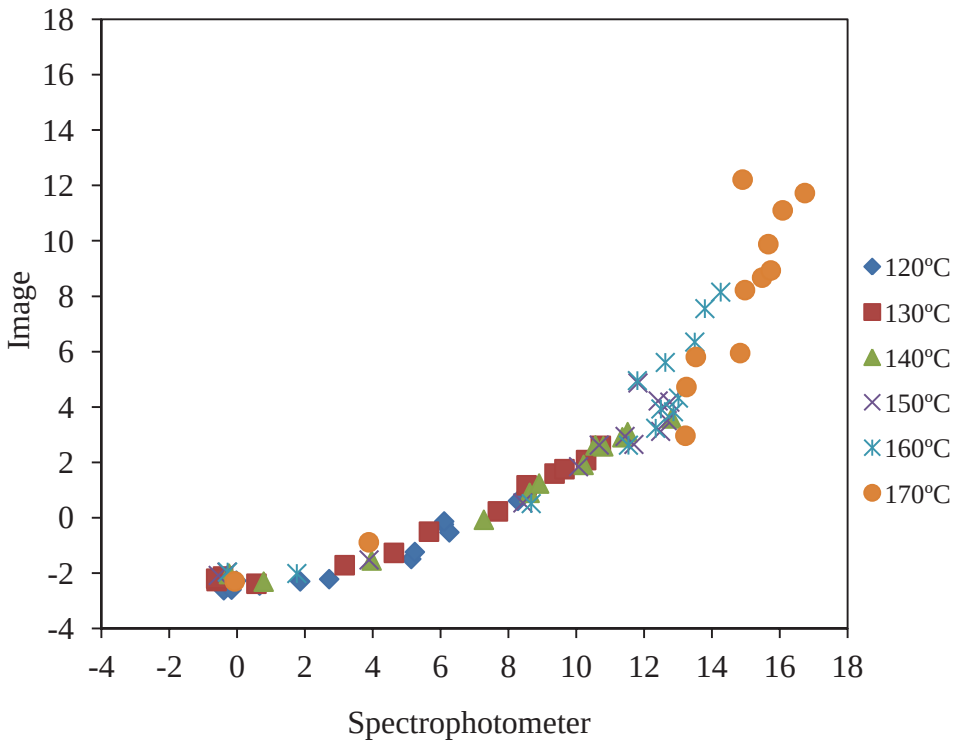

Figure 3.12 The comparison of average redness (*a**) value measured using the image system and spectrophotometer

The average yellowness values (*b**) measured using the image analysis and spectrophotometer was similarly presented and showed a linear but more scattered relationship. In subsequent experimental work it was found that the *b** value didn't follow any clear trends and was not used in kinetic analysis.

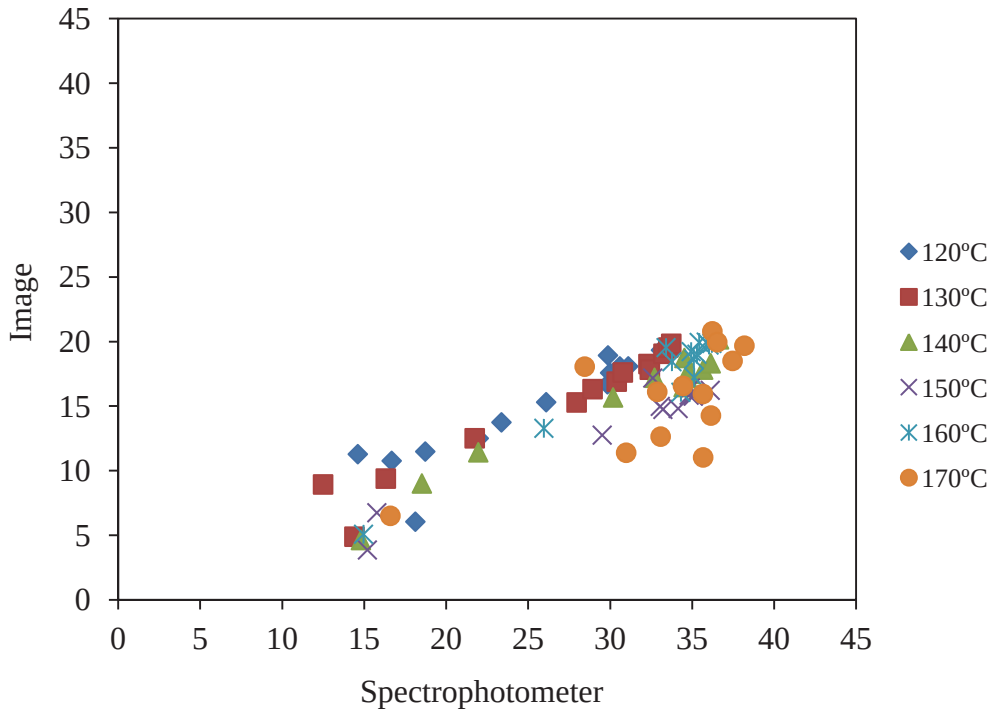

Figure 3.13 The comparison of average yellowness (*b**) value measured using the image system and spectrophotometer

3.4 Heating pan design

In the literature review, it was reported that the browning reaction is temperature and time dependent and can be explained by the Arrhenius equation (Zanoni *et al*., 1995; Zuckerman & Miltz, 1997; Broyart *et al*., 1998; Krokoda *et al*., 2001; Nourian & Ramaswamy, 2003; Purlis & Salvadori, 2007, 2009; Purlis, 2010; Goňi & Salvadori, 2011; Jiménez *et al*., 2012 and Matsuda *et al*., 2013). Isothermal conditions allow more simple kinetic parameter estimation. To achieve this constant temperature cooking conditions are required. Therefore a good control system was necessary.

A heating pan with a conductive heat transfer was selected as the heat source prototype for the pastry baking process. This was constructed using a deep fryer that was commercially available and the addition of a good oil temperature control (Figure 3.14).

3.4.1 Equipment

The baking pan system consisted of:

1. A deep fryer (ANViL model FFA 3001-TEU; Ganteng, South Africa)
2. A non stick teflon pan sheet
3. A heat transfer oil (REGAL R&O 46, CALTEX; Sydney, NSW, Australia)
4. A PID controller (CAL 3200, CAL Controls, Inc., Gurnee, IL)
5. The thermocouple probes (Type J: 20 gauge, accuracy ±0.5˚C, type K: chromel (+) and alumel (-), accuracy <250ºC ±1.5ºC and a surface self-adhesive thermocouple type J: SA1XL, OMEGA; Stamford, CT, USA)
6. A data logger (Measurement Computing^{TM}: USB DAQ data acquisition and Agilent 34970A Data Acquisition; California, USA)
7. A stirrer motor (STIRRERE DLS, VELP scientific F20100155, 50-60 Hz, 250 V, 60 Watt)
8. The stirrer blade (Oblique impeller blade stirrer, anchor stirrer, blade disc turbine stirrer, blade agitator impeller stirrer)
9. Computer (Pentium (R) IV CPU 3.00 GHz, 2.00 GB of RAM, NEC Computer Int'l).

3.4.2 Concept and prototype of heating pan

The heating pan for cooking pastry samples in the study was developed by adapting a deep frying cooker (Figure 3.14). The pan system consists of a deep fryer (ANViL model FFA 3001-TEU), a non stick teflon pan and a stirrer. The dimensions of the deep fryer pot were 258 mm wide, 317 mm long and 145 mm deep and the dimensions of the pan sheet were 210 mm wide and long and 34 mm deep. The deep fryer pot contained the oil which was used to heat the pan, it was heated by a 3000 watt heating coil and the oil's temperature was controlled by a PID controller (model CAL 3200). Oil was used as the heating medium because it has good heat transfer characteristic. A stirrer was applied to increase the heat transfer from the oil to the pan and to ensure the oil temperature was uniform.

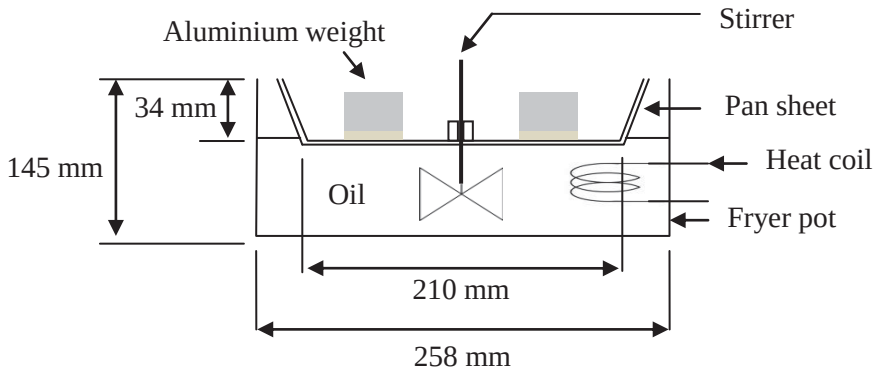

Figure 3.14 Conceptual sketch of oil bath with floating pan for cooking process

Figure 3.15 shows the prototype of the cooking system and demontrates that the system connected to a data logger (Measurement Computing^{TM}: USB DAQ data acquisition) and linked to a computer to collect the temperature data, which were measured using type K thermocouples (chromel (+) and alumel (-), accuracy <250ºC ±1.5ºC). These temperature data were important in developing the kinetic model for this study.

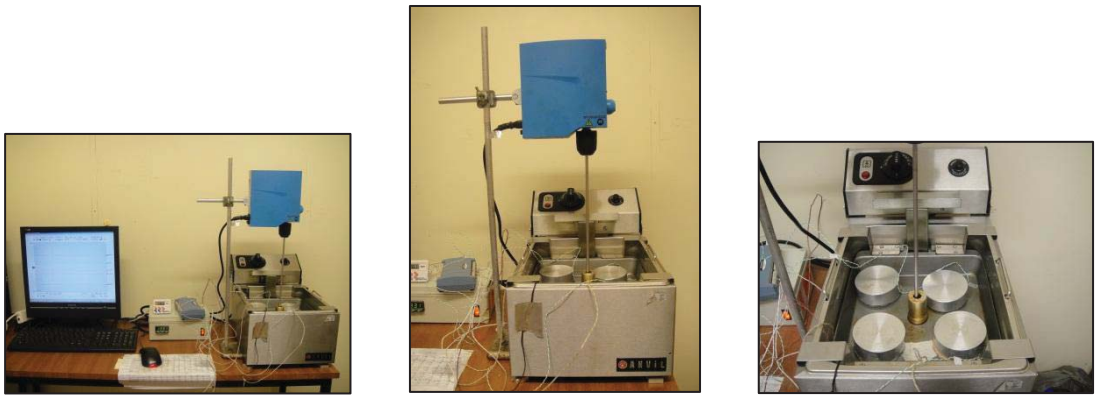

Figure 3.15 The prototype of the deep fryer cooking system

An important issue for this system was the heat transfer resistance between the oil and the non stick teflon pan sheet. In the development of a good isothermal cooking system, a minimum temperature difference and uniform heat transfer under the pan were required. Therefore the factors of the heating media, type and speed of the stirrer were studied to achieve the most isothermal sample cooking conditions possible.

3.4.3 The effect of stirrer speed on the heat transfer in the cooking system

Firstly, the designed pan system was tested to see the effect of the heat resistance on the heat transfer from the oil to the pan. A low heat resistance is an important factor for reducing the difference in temperature between the oil and the surface of pan. It was assumed that the movement of the oil would reduce the heat resistance, so the preliminary study of the deep fry pan cooking system investigated the different levels of stirrering speed. The results are shown in Figure 3.16. The effect of pastry baking on the drop of the pan temperature was also measured to see how quickly the temperature recovers after placing the pastry on the pan. The experimental study was divided into seven periods. The experimental design is detailed in the following:

1. The first period was run using a paddle type stirrer at 400 rpm for 35 minutes.
2. The same stirrer type was used but the speed was increased to 750 rpm for 10 minutes.
3. The speed was increased to 1000 rpm for 10 minutes.
4. The stirrer speed was increased to 1300 rpm and run for 10 minutes.
5. 10 minutes at 1600 rpm.
6. After the pan temperature was stable and the same speed of stirrer being used, a pastry sample was placed on the pan and left for 10 minutes after which the pastry was removed.
7. Finally the temperature drop effect was investigated again by placing another pastry sample at the last period of this experimental study. The pastry was cooked for 15 minutes during this period. The same speed of stirrer (1600 rpm) was still used.

The result of this study are shown in Figure 3.16 as a plot of the temperature profile of the oil compared with the the temperature of the pan's surface. It can be seen that there is a large temperature gap (5ºC) between the oil and pan's surface during the first period (35 minutes) because the rate of heat transfer from the oil to the pan was low. The low speed of the stirrer resulted in a low heat transfer rate.

However, the heat transfer rate was increased by increasing the stirrer speed, so the temperature difference between the oil and the pan surface was narrower (4ºC) during the second period when the speed was increased to 750 rpm. The temperature of the pan continously increased when higher speeds were applied during the third, fourth and fifth

periods. The temperature profile shows that the difference in temperature between the oil and the surface of the pan was reduced when increasing the speed of the stirrer from 400 to 1600 rpm. The temperature gap was narrowed from 5ºC to 4ºC. Thus, it can be concluded here that the stirrer speed has an influence on the heat transfer rate. More heat is transferred when the stirrer speed was increased.

During the sixth and seventh periods there were drops in the temperature of the pan's surface because cooler pastry samples were placed on the pan at these two points. After that the temperature increased to the same temperature as before. The recovery temperature time approximately took about 10 minutes. This does not correspond to isothermal conditions. In addition, the difference between the temperature of the oil and the pan's surface was still too large (4ºC). The system needed to be improved and the effects of the possible factors on the heat transfer in the cooking system are discussed in the following section.

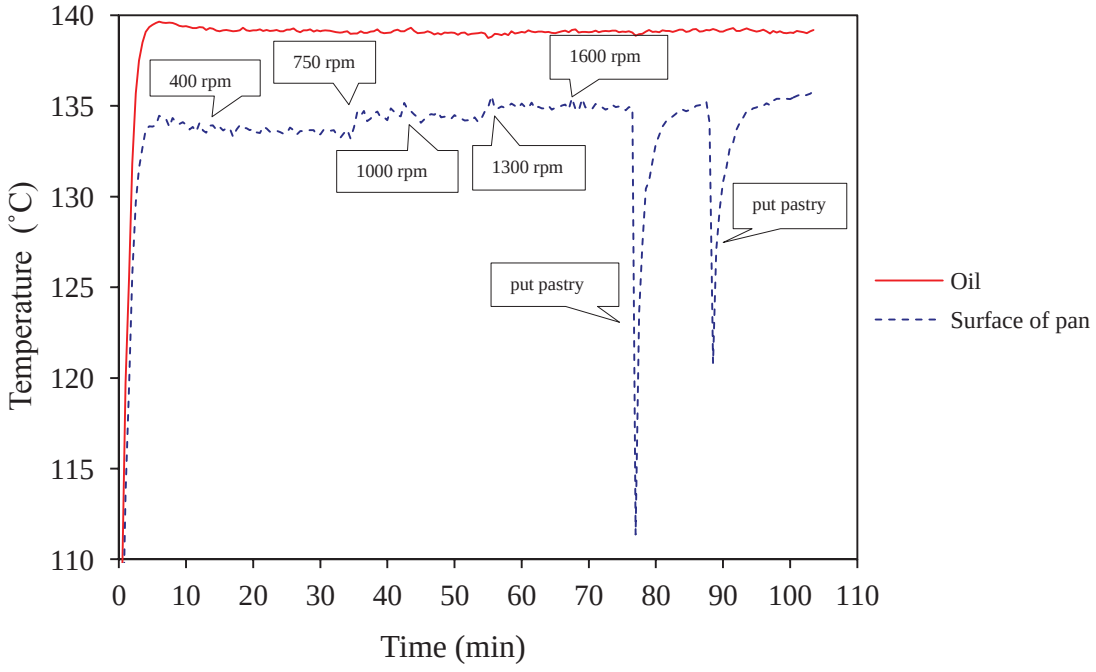

Figure 3.16 The temperature profile of oil and pan's surface when applying different stirrer speeds

3.4.4 The effect of heating media on the heat transfer of the cooking system

At the maximum speed of the stirrer the temperature gap between the oil and the pan surface was still too large. This was due to a low heat transfer rate between the oil and

the pan. To determine this effect, the feature of heat transfer in this cooking pan system was drawn and illustrated in Figure 3.17. The diagram displays the cross section of the pan sheet and the temperature of oil (θ_{oil}), surface of pan (θ_{si}) and a boundary layer (x_0) (Figure 3.17).

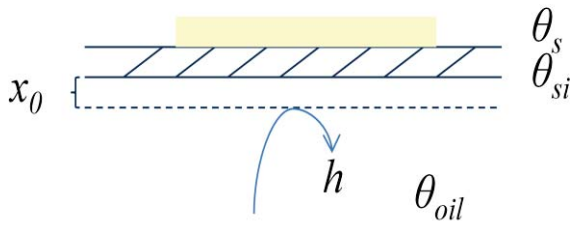

Figure 3.17 Consideration of resistances to heat transfer in pan cooking system

From the Figure 3.17, it can be seen that for a heat convection system a boundary layer normally occurs across the exchanger surface. A boundary layer is the layer of fluid in the immediate locality of a bounding surface where the velocity of the fluid becomes quiescient. A boundary layer interferes with heat transfer in a convection system. However if the boundary layer can be reduced then the heat transfer coefficient (h) can be increased (Equation 3.1). The heat transfer coefficient (h) has a relationship with the heat flux (ϕ) (Equation 3.2).

$$h = \frac{k}{x_0} \tag{3.1}$$

and

$$\phi = hA(\theta_{oil} - \theta_{si}) \tag{3.2}$$

where ϕ is heat transfer rate across the surface area of the pan ($J \cdot s^{-1}$ or W), h is heat transfer coefficient ($W \cdot m^{-2} \cdot K^{-1}$), A is heat exchange surface area (m^2), θ_{oil}, θ_{si} are the temperatures of the oil and surface of the pan (K), respectively, k is thermal conductivity ($W \cdot m^{-1} \cdot K^{-1}$) and x_0 is a boundary layer of unmoving fluid (m).

Equation 3.2 shows that the the heat transfer rate (ϕ) is a direct function of the heat transfer coefficeint (h) and heat exchanger surface area (A). According to Equation 3.2, increasing the heat exchange surface area (A) and the heat transfer coefficient (h) can reduce the temperature difference between the temperature of the oil and the temperature of the pan's surface. Increasing the heat exchange surface area (A) can be achived by adding fins. However, this method is costly and would only have a limited effect.

Considering Equation 3.1, a high value of the heat transfer coefficeint (h) is caused by a high thermal conductivity (k) and a low thickness of the boundary layer (x_0). The thermal conductivity (k) is a specific property of the heating media (oil). Consequently by manipulating conductivity it is possible to increase the heat flux. A comparison of the properties of heat transfer oil and cooking oil is shown in Table 3.1. The requirement properties such as a high thermal conductivity (k), high specific heat (c_p) and low viscosity (η) were determined as a criteria for selection.

Table 3.1 shows that cooking oil has marginally better thermophysical qualities than the heat transfer oil in terms of higher thermal conductivity (k), higher volumetric density (ρ) and lower viscosity (η). However, the heat transfer oil offers a greater stability for avoiding rancidity and polymerisation over long term use. In addition, the chemical and physical properties of the heat transfer oil vary less over the temperature range of interest compared with the cooking oil. Therefore, the heat transfer oil was chosen as the heating media.

Table 3.1 Specification of heat transfer and cooking oil

Key properties	**Thermal conductivity (k, W·m^{-1}·K^{-1})**	**Viscosity (η,cP)**	**Heat capacity (c_p,kJ·kg^{-1}·K^{-1})**	**Density (ρ, kg·m^{-3})**
Heat transfer oil[1]	0.142 at 38˚C 0.130 at 260˚C	43 at 40˚C 6.4 at 100˚C	1.90 at 38˚C 2.76 at 260˚C	0.85 at 38˚C 0.71 at 260˚C
Cooking oil[2]	0.16-0.22	30-40 at 40˚C 8 at 100˚C	1.67	0.9

Sources: [1]http://www.chevronlubricants.com 2/12/2010: 5:09pm; [2](Abramovi & Klofutar, 1998 and Demirbas, 2008)

The cooking system was run to test the effect of the heat transfer oil on the heat transfer rate across the heat exchanger area. The temperature profile of the oil, pan, and pastry were recorded and are presented in Figure 3.18.

The result shows that the oil temperature was very close to the set point of 140˚C after 10 minutes of processing and showed a stable profile throughout to the end of the

process (Figure 3.18). The temperature of all positions on the pan reached the steady state quickly (within 10 minutes) and they were close to the oil temperature at all points. It can be concluded that the heat transfer efficiency of this system was good for both the rate and uniformity of heat transfer. However the temperature difference between the oil and the pan was still large at around 4˚C.

A pastry sample was placed on the pan when the temperature was constant after 30 minutes. After placing the pastry on the pan, the temperature of the pastry quickly increased within 5 minutes, and came up to a temperature near that of the pan surface temperature but it took another 25 minutes to rise the last 5°C to match the surface temperature of the pan. The long time taken for the pastry to come up to the temperature of the pan means that non-isothermal conditions existed throughout the heating process, so increasing the temperature quicker is needed. The next step explored stirring options to achieve this result.

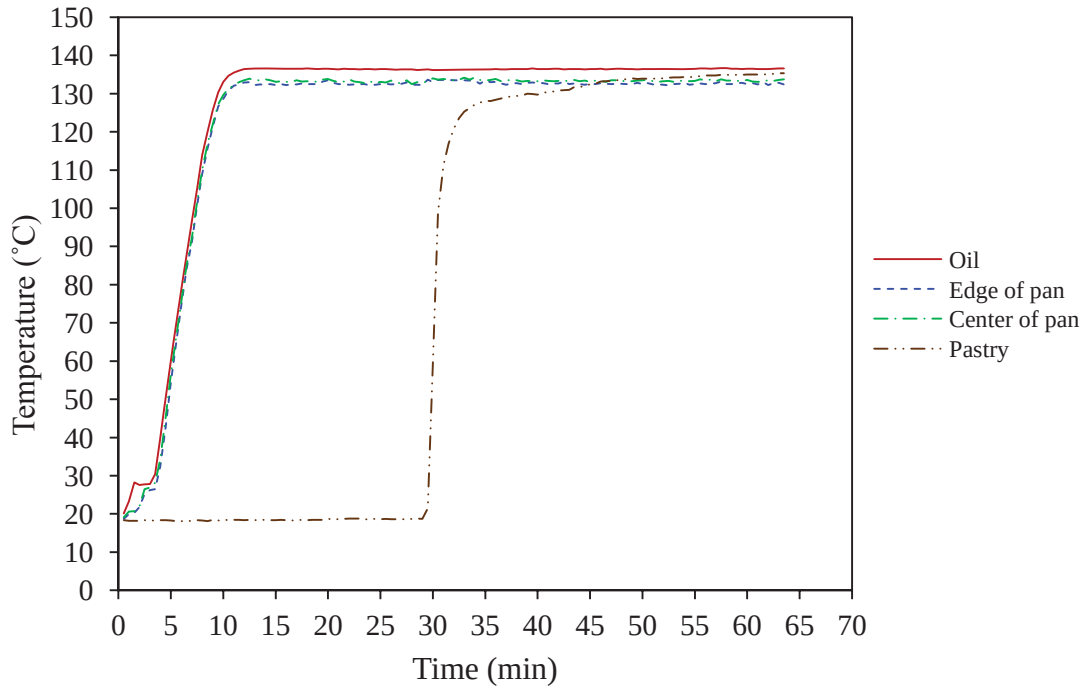

Figure 3.18 The temperature profile of oil and pan at different positions

3.4.5 The effect of stirrer type on the heat transfer of the cooking system

As was discussed, a high heat transfer rate is required for this cooking system to decrease the temperature difference between the oil and the surface temperature and to approach isothermal conditions at the pan surface. The thickness of the boundary layer

of unmoving fluid (x_0) can be decreased by turbulent mixing of the fluid (Equations 3.1 and 3.2). Different stirrer paddle designs for creating turbulent movement in the oil were explored and the types and the speed of the stirrers were investigated so that the most appropriate one could be selected. In a mixing system there are two types of mixing that the stirrer normally produces. These are axial and radial flow patterns, where the turbulent movement needs both patterns. Axial and radial flow patterns are shown in Figure 3.19.

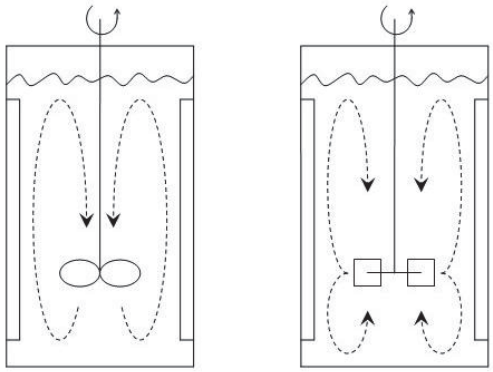

(a) (b)

Figure 3.19 The flow patterns in a mixing system: (a) axial flow and (b) radial flow

The flow pattern of the fluid system plays an important role on the energy transfer and it depends on the type of stirrer applied to the system. This study employed five different types of stirrer to create movement in the cooking system. The five different stirrer types are shown in Figure 3.20.

Each type of stirrer was applied to the cooking pan system at different speeds which were 300, 366, 1000, 1550 and 1180 rpm for stirrer type 1, 2, 3, 4 and 5 respectively. The different speeds were the maximum limit for each stirrer type. The experimental study was carried out by using each stirrer in the cooking system, when the system was turned on and the oil was heated up to the set point temperature of 140°C. After the temperature of the pan was constant at 140°C for 8 minutes, the pastry sample was placed on the pan and run for 35 minutes. During the experiment, the temperature of the oil and the surface of the pan were measured.

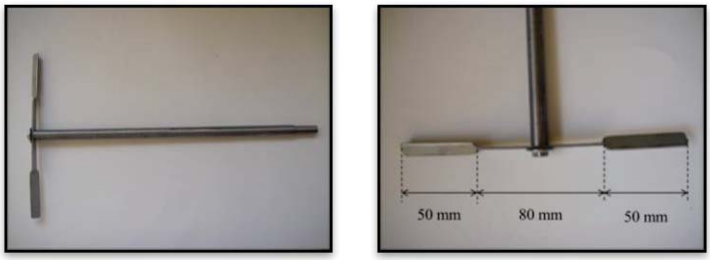

(a) stirrer type 1 (Oblique impeller blade stirrer)

(b) stirrer type 2(Anchor stirrer)

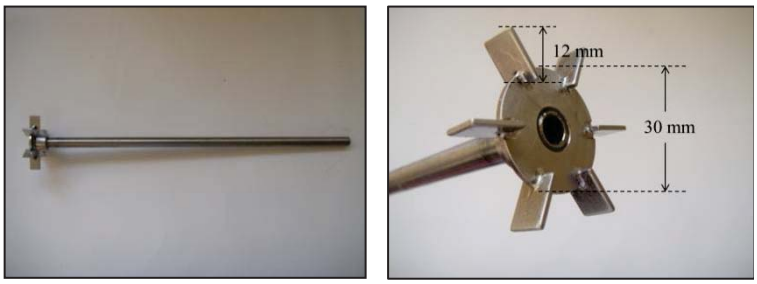

(c) stirrer type 3 (Blade disc turbine stirrer)

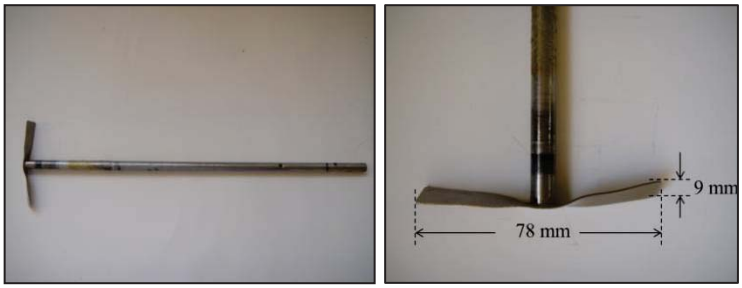

(d) stirrer type 4 (Blade agitator impeller stirrer)

(e) stirrer type 5

Figure 3.20 The stirrer types investigated to reduce thermal resistance between oil and pan surface

All observations for the system temperature and the pattern of oil fluid movement for each stirrer type were recorded. The temperature profiles of the cooking pan systems for the five different types of stirrer are shown in Figure 3.21.

The stirrer type 1 was applied with a maximum speed of 300 rpm. A vortex formed at the higher speeds (>500 rpm) which made the oil spread out from the oil bath. Radial mixing took place in the oil bath to make the oil temperature uniform. The radial flow pattern moves away from the impeller, towards the sides of the vessel. The flow impacts the side and moves in either an upward or downward direction to fill the top and bottom of the impeller. This paddle type also made a big wave with turbulent oil. The thickness of the boundary layer of unmoving fluid (x_0) was still large. There was a temperature difference of 6°C at steady state.

A maximum speed of 366 rpm was applied for stirrer type 2. This gave extreme turbulence in the oil bath, even when the revolution speed was low (300 rpm). The oil splashed out from the oil bath as a big wave was produced. A radial mixing pattern occurred but no axial mixing. Therefore, the temperature between oil and pan's surface was still high (5˚C).

The stirrer type 3 is known as the Rushton turbine design and it was used at 1000 rpm. This paddle created radial mixing, a simple swirling motion, producing little agitation and a vortex so the oil moved at a high velocity across the surface of the pan and a uniform temperature occurred. The movement of oil was turbulent because of these two mixing types and the high speed of the stirrer (1000 rpm). Nevertheless, the heat transfer coefficient was not high enough as there was still a high temperature difference of 3°C between the oil and pan surface. This was attributed to the small head area of the stirrer, resulting in non ideal total mixing.

The stirrer type 4 generated only axial mixing, leading to a uniform oil temperature, but the turbulent movement was not extreme enough to increase the heat transfer coefficient, even though the rotation speed was very high (1550 rpm). This may be because the contact area across the paddle was small. The difference temperature was found as 3.5°C.

The stirrer type 5 was applied at 1180 rpm. Both radial and axial mixing occurred. The axial mixing made the oil temperature uniform and the radial mixing of the oil induced a high turbulent velocity across the surface of the pan. In addition, the very high speed, and extreme turbulence created surface renewal in this system. Therefore, the heat transfer coefficient was very high which caused very fast heat transfer from the oil to the stainless steel pan sheet. The temperature difference was reduced to 2°C.

After putting the pastry samples on the pan, all samples showed a temperature drop. Paddle 5 demonstrated the fastest response of temperature compared to the other types of stirrers. It gave the smallest temperature gap between the sample surfaces and the oil and the temperature recovered back to the original temperature more quickly.

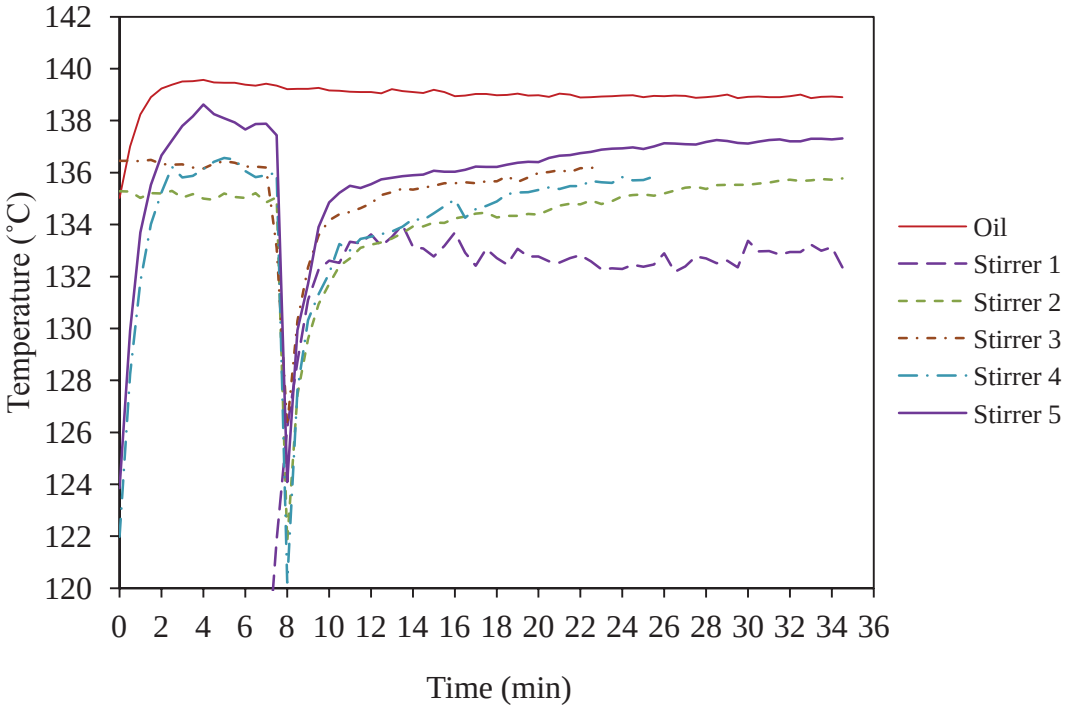

Figure 3.21 Temperature profile of the oil and the surface of the pan using different types of stirrer

The findings for the different stirrer types and stirring speed investigation are summarised in Table 3.2. It can be concluded that stirrer types 3 and 5 provided good results with smaller temperature differences. However, stirrer type 5 had the best performance because this paddle created very fast movement (turbulence) of oil across the surface of pan resulting in a small temperature difference between the oil and the

pan (θ) of 2˚C. This result was the best approximation to an isothermal process. Stirrer type 5 was therefore selected as the stirrer for use in achieving an isothermal pastry temperature.

Table 3.2 Summary of the study on the effect of the stirrer type

Stirrer types	Maximum revolution of stirrer (rpm)	Mixing type	Observations
1	300	Radial	Temperature difference was so high (6˚C)
2	366	Radial	Temperature difference was high (4˚C)
3	1000	Radial	Temperature difference was low (3˚C)
4	1550	Axial	Temperature difference was high (3.5˚C)
5	1180	Axial and radial	Temperature difference was low (2˚C)

3.5 The best method for measuring the surface temperature

After the cooking system was designed, the method for measuring temperature was the next step to be investigated. For best results the exact temperature of the pastry during cooking was needed. Figure 3.22 shows the pastry baking system. For this test the pastry samples also had a weight on top to prevent the formation of water vapour bubbles. This weight was an aluminium block, weight 600 gram. It was separated from the pastry by 3 mm of cardboard, which acted as an insulator between the pastry and the aluminium weight. The temperatures were taken at four positions (see Figure 3.22). The four positions of the cooking system where the temperature was data logged were (1) oil, (2) pan, (3) pastry surface and (4) the top surface of the pastry (Figure 3.22).

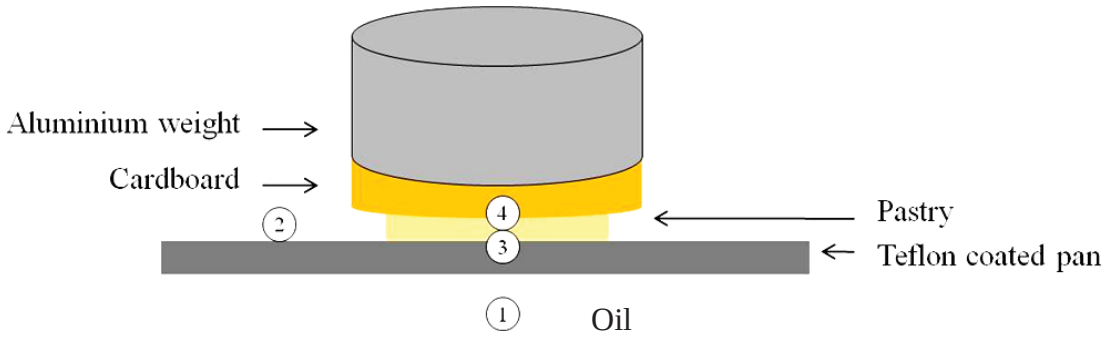

Figure 3.22 Schematic diagram of the pastry baking system

The temperatures at these four positions were measured using different thermocouple types. The temperatures of (1) oil and (2) pan were measured using a small thermocouple type K (chromel (+) and alumel (-), accuracy <250ºC ±1.5ºC). The temperatures of (3) pastry/pan interface and (4) top surface of pastry were measured by three different thermocouples to compare and select the best thermocouple type for this measurement because the temperature of pastry sample is very important for understanding the browning kinetics. Ideally thermocouples would provide a highly precise and accurate temperature measurement and have only a small impact on the browning reaction. The three different thermocouple probes for measuring the temperature of pastry sample were:

- Probe 1: a fine thermocouple type J (20 gauge, accuracy ±0.5˚C); the wire has a diameter of 0.056 mm. The response time of this probe was 0.15 second. This fine probe was covered by a rectangle of aluminium tape 50×50 mm to prevent the head of the probe penetrating the pastry surface as shown in Figure 3.23 (a). This cover may help to make a uniform heat transfer between the aluminium tape and the pastry that may reduce the distribution of brown colour across the pastry surface of due to difference of heat histories.
- Probe 2: a fine thermocouple probe type J (20 gauge, accuracy ±0.5˚C) was covered by a smaller 20×20 mm of rectangle aluminium tape as shown in Figure 3.23 (b).
- Probe 3: a surface self-adhesive thermocouple type J (SA1XL, OMEGA), with the bare sensing element of nominal 2.54×10^{-2} mm thickness. The dimensions of the probe were patch length 25.4 mm, patch width 9.5 mm and strip length 25.4 mm with 12.7 mm bare wire. The probe had a response time of 0.1 second (Figure 3.23 (c)).

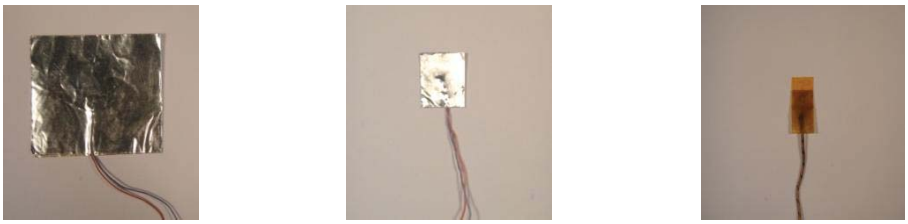

(a) probe 1 (b) probe 2 (b) probe 3

Figure 3.23 Three different probes investigated for temperature measurement in this study at the pastry/pan interface: (a) probe 1: a fine probe with 50×50 mm aluminium tape covering, (b) probe 2: a fine probe with 20×20 mm aluminium tape covering and (c) probe 3: a surface thermocouple

3.5.1 Thermocouple probes calibration

As it was important to measure accurate temperature data for all positions in the cooking system, all thermocouple probes were calibrated before use. The thermocouple calibration procedure followed these steps.

1. All probes were put in an ice/water mixture (0ºC) and then into boiling water (100ºC) and the data were collected using the data logger connected to a computer.
2. All measured temperature data of each probe were averaged and plotted against the reference temperatures of 0ºC and 100ºC for ice and boiling water, respectively.

From the calibration temperature data, the slope and intercept values in Equation 3.3 were calculated and presented in Table 3.3. These values were used for calculating the actual temperature using the following formula;

$$T_{actual} = (T_{measured} \times slope) + intercept \quad (3.3)$$

Table 3.3 Probe calibration data

Probes	Slope	Intercept
K type probe (oil temperature)	1.02	-0.07
K type probe (pan temperature)	1.02	-0.31
Fine probe (pastry temperature)	0.96	1.02
Surface thermocouple probe (pastry temperature)	1.00	0.33
Surface thermocouple probe (top of pastry temperature)	1.00	0.43

3.5.2 Investigating the best thermocouple probes

All the probes above were tested in a real experiment with the pastry sample being baked on the hot pan. Two K type probes were installed into the cooking system, one probe was placed in the oil to measure the temperature of the oil and the other was placed on the middle of the pan to measure the temperature of the pan and the probe was covered by aluminium tape to permanently attach it to the pan surface. The fine probe with a larger and smaller size of aluminium tape covering and surface thermocouples were placed at the surface of the pastry sample and connected to the data logger (Measurement Computing^{TM}: USB DAQ data acquisition) and linked to a

computer to collect the data. There were three experimental runs for exploring the efficiency and accuracy of the measurement using the three different thermocouple probe types.

The cooking pan system was turned on to heat up the oil, and the temperature of the oil was controlled by a PID controller (model CAL 3200). The system was run at the set point temperature of 160°C, for 60 minutes. The temperature data of the oil, pan and pastry surface were recorded and saved into the computer. It was noted that the temperature of oil and pan were less important for this experimental study than selecting the best thermocouple for measuring the pastry/pan interface temperature. Therefore the oil and pan temperature profiles were not included in this plot (Figure 3.24). Only the profiles of pastry/pan interface temperatures, which were measured by the different types of thermocouples were compared. Three replicates were carried out for each type of thermocouple probe study. The plots of the temperature of the pastry during baking using these three different thermocouple probes for three experimental replicates are shown in Figure 3.24.

It was found that the temperature of the pastry surface obtained using all three thermocouple probes were close in replicates 1 and 3. However, the temperature values measured by the surface thermocouple (probe 3) were higher than that of probes 1 and 2 for replicates 1 and 2 and this temperature was close to the set point temperature (160°C) for all replications. It was clearly seen in replicate 2 that the surface thermocouple (probe 3) showed a higher potential for temperature measurement than the other two probes. A big difference temperature between the pastry and the set point temperature were found for the measurements taken using the other two probes.

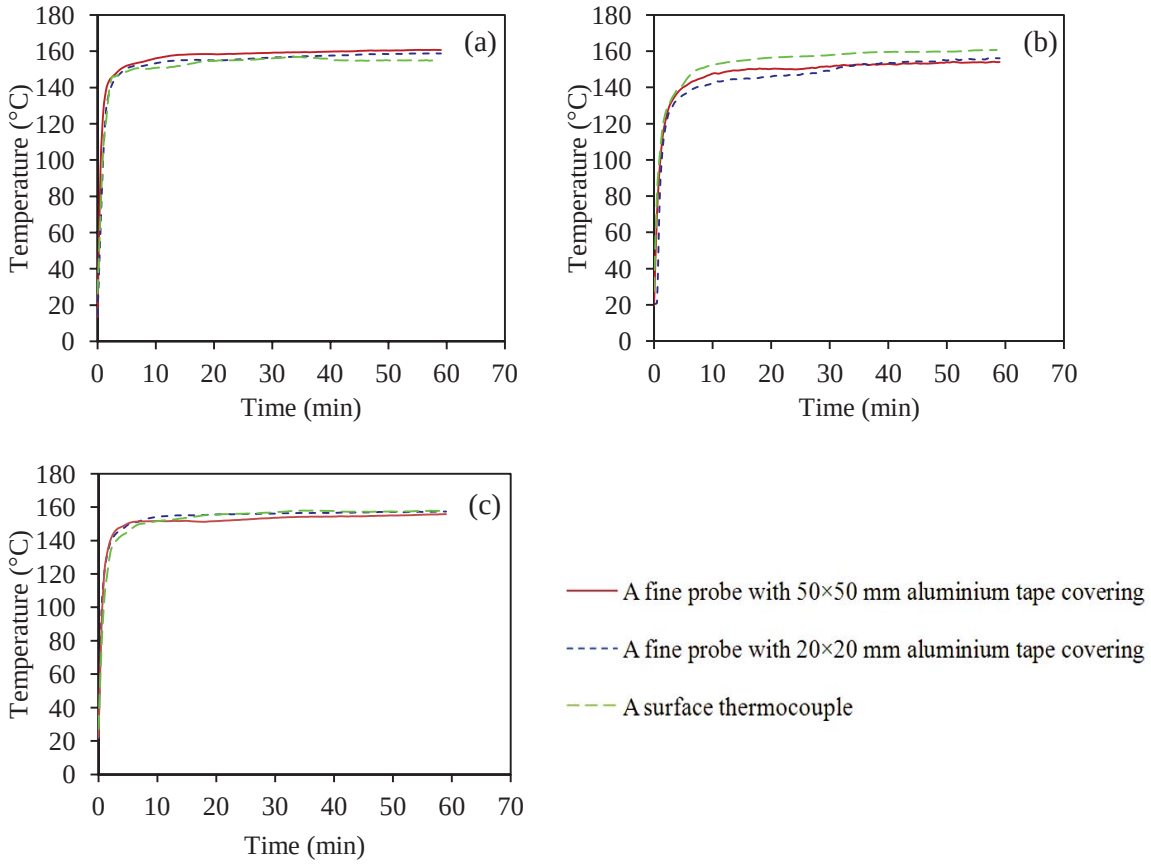

Figure 3.24 The temperature profile of pastry surface using three different types of the probes for three replicates: (a) replicate 1, (b) replicate 2 and (c) replicate 3

At the end of the process, photos of the baked pastry samples were taken and the colours of the pastry samples were measured using the image analysis system (see section 3.3). The browning property of the pastries from the three experiments were compared and presented in term of the average lightness parameter (L^*) as shown in Figure 3.25.

The brown colour on the pastry surface of all experiments was even when observed by eye (Figure 3.25). The result shows that the brown colour of the pastry surface in the experiment used probe 3 for measuring temperature was darker than that of probes 2 and 1, respectively. This was also confirmed by the value for lightness (L^*) of the pastry which was the lowest when probe 3 was used and highest when probe 1 was used. This was possibly because the large aluminium tape acted as an insulator reducing the heat transfer from the pan to the pastry in the experiment that used probe 1. The pastry in experiment used probe 2 had a smaller patch of aluminium tape interfering with the heat

transfer from pan to pastry too, as the mark of thermocouple insulator can be seen on the pastry surface when probe 2 was used. However, the surface thermocouple (probe 3) had an insignificant affect on the heat transfer because the thickness of the surface thermocouple was very thin and was made of a good conduction material. There was no mark on the pastry surface. The brown colour on the pastry surface was even, which was good for colour measurement.

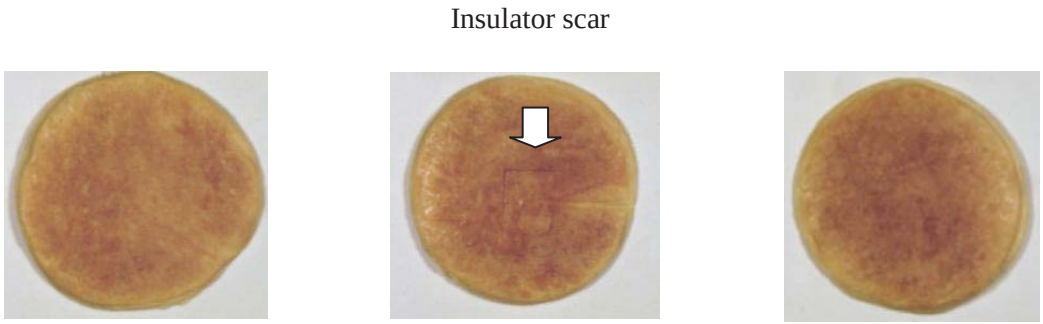

*L**= 75.76±3.43 (a) probe 1

*L** = 75.55±5.84 (b) probe 2

*L** = 74.47±2.32 (c) probe 3

Figure 3.25 Three samples of pastry after baking at 160ºC for 60 minutes: (a) probe 1: a fine probe with 50×50 mm aluminium tape covering, (b) probe 2: a fine probe with 20×20 mm aluminium tape covering and (c) probe 3: the surface thermocouple

This experimental study was carried out with three replicates, the mean values of lightness and their standard error (S.E.) were calculated and plotted to compare in Figure 3.26. The mean lightness value and the standard error (S.E.) of the baked pastry in experiment used probes 1, 2 and 3 for temperature measurement are 75.76±3.43, 75.55±5.84 and 74.47±2.32 respectively. The baked pastry sample in the experiment that used probe 3 for temperature measurement was the darkest and showed the lowest standard error (S.E.). A low standard error means good measurement reproducibility. The lightest sample was found in the experiment that used probe 1 for temperature measurement, which can be determined by a higher value of the lightness. The pastry in the experiment of probe 2 showed the highest value for standard error (Figure 3.26). This means that there was low precision in the temperature measurement among three replications when measuring the pastry temperature using thermocouple probes 1 and 2.

As a result it can be concluded that the surface thermocouple probe (probe 3) was the most appropriate to use to measure the surface temperature of the pastry because it provided both precision and accuracy in measurement.

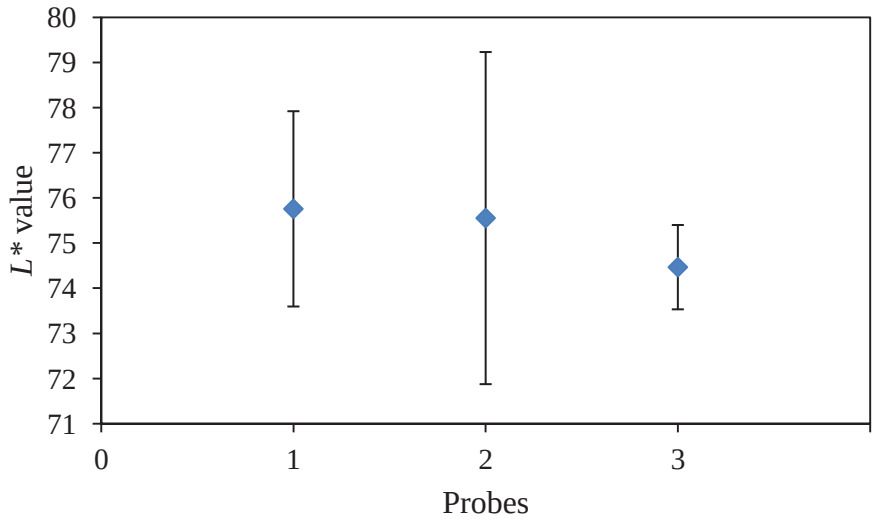

Figure 3.26 The average lightness value and the standard error (S.E.) of three pastry samples after cooking with three different types of thermocouple:
Probe 1: a fine probe with 50×50 mm aluminium tape covering
Probe 2: a fine probe with 20×20 mm aluminium tape covering
Probe 3: a surface thermocouple

Not only the intensity but the distribution of brown colour was also considered for evaluating the best type thermocouple for the measuring methodology. The distribution of brown colour across the pastry surface implies how even the brown colour was. The comparison of the standard deviations (S.D.) measured by the image analysis is presented in Figure 3.27. From the result, the standard deviation value referring to the distribution of brown colour on pastry after baking was high in probe 2. It means that the brown colour on the pastry surface in the experiment that used probe 2 for temperature measurement was less even. The low value of the standard deviation of the brown colour on pastry surface in the experiment that probe 3 was used for temperature measurement indicated that the surface thermocouple had only a small influence on the distribution of colour on the pastry surface.

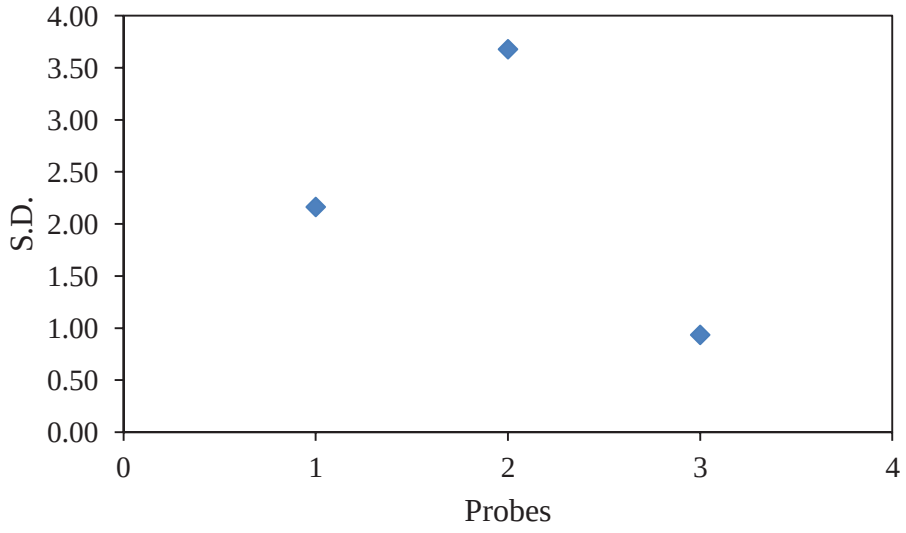

Figure 3.27 The standard deviation (S.D.) of average *L** value three pastry samples measured by image analysis after cooking using three different probes for temperature measurement:
Probe 1: a fine probe with 50×50 mm aluminium tape covering
Probe 2: a fine probe with 20×20 mm aluminium tape covering
Probe 3: a surface thermocouple

From all results of temperature profile and the colour measurement, it was concluded that the surface thermocouple offered the most accurate and precise temperature measurement. In addition, the browning reaction on the pastry sample was less affected by the surface thermocouple. Therefore the surface thermocouple was chosen to use in this study for the pastry surface temperature measurement.

3.5.3 The experimental design and the position of the thermocouple probes for the cooking system

From the preliminary study on the methodology for measuring the system temperature, the conclusion was that the surface thermocouple probe was the best type for measuring the pastry temperature. Therefore the surface thermocouple was used in measuring the pastry temperature on both surface sides of the pastry. Details of the probes used for all parts of the system are listed below.

1. Temperature of positions (1) oil and (2) pan were measured by using a small thermocouple type K (thickness of 0.3 mm). Therefore two probes of K type were used for these measurements.

2. Temperature of the positions of (3) the pastry/pan interface and (4) the top surface of the pastry were measured by using a surface self-adhesive thermocouple type J (SA1XL, OMEGA), with the bare sensing element of nominal 0.0254 mm of thickness. There were four pastry samples baking on the pan at four positions, thus this measurement set used eight probes.

All thermocouple probes were calibrated prior to use. The thermocouple probe calibration method was the comparison between measurements of the thermocouple with a standard reference thermometer over the range of temperatures. The steps of fine calibration are detailed below.

1. The thermocouple probes and reference glass thermometer were put in an oil bath, which was heated up to temperatures of 30, 50, 70, 90, 100, 110, 120, 130, 140, 150, 160 and 170ºC.
2. The temperature of the oil was measured by the reference thermometer and thermocouples, and then all temperature profiles were recorded using data logger (Agilent 34970A data acquisition). This data logger model was used instead of the DAQ data acquisition model in the preliminary experimental study because the Agilent 34970A data acquisition has 40 channels, so was able to measure all 10 thermocouples simultaneously.
3. All measured temperature data was plotted against the actual temperature (measured by the reference thermometer).
4. The slope, intercept and R^2 values of the linear plots were calculated to use for adjusting the measured data for each of the thermocouple probes.

The adjustment values in Table 3.4, were used to calculate the true system temperatures from each of the 10 probes by applying Equation 3.3.

Table 3.4 Adjustment values for calibrating the thermocouple probe

The probes to measure the temperature of	Slope	Intercept	R^2
Oil	0.98	0.48	0.99
Pan	0.99	0.08	0.99
Pastry at position 1	0.98	0.68	0.99
Pastry at position 2	0.99	0.52	0.99
Pastry at position 3	0.98	0.44	0.99
Pastry at position 4	0.98	0.92	0.99
Top surface of pastry at position 1	0.98	0.92	0.99
Top surface of pastry at position 2	0.99	0.41	0.99
Top surface of pastry at position 3	0.98	0.82	0.99
Top surface of pastry at position 4	0.98	1.04	0.99

3.6 Conclusion

To study the browning kinetics under isothermal conditions, not only a constant temperature of cooking is needed but an even brown colour development across the food sample surface due to the reaction is also important. Pastry circles were the best model food found for this study because they showed an even colour of browning across their surfaces and the samples had fewer variables in their chemical and physical properties. To measure the colour of browning development, an image analysis method was selected since this new technology is versatile in providing rapid, easy, accurate, low cost, fast and non destructive assessment. The rate of the Maillard browning reaction is affected by the temperature of the sample; therefore good temperature control of the cooking system was required. A baking pan heated by oil was chosen to provide a cooking system that could quickly heat the pastry samples up to and hold them at a pre-determined temperature. It was found that the temperature values of the baking system were best measured by using the surface thermocouple probe. Thus model food, cooking system and image analysis protocol allows subsequent experimental data collection of browning rates at a range of temperature from 100-200°C.

Chapter 4

PRELIMINARY TRIALS

4.1 Introduction

The model food, cooking system, and image analysis system, were designed and developed in Chapter 3 for studying Maillard browning kinetics under near isothermal conditions. This chapter describes the preliminary study to test these systems. This isothermal cooking system was designed to provide a constant baking temperature and even browning colour on the model food (pastry) surface. The colour change on the pastry surface during cooking is determined in terms of the *L*a*b** colour space using non-destructive imaging to measure the appropriate colour parameters representing the browning reaction. These results of colour changes are required in order to develop an isothermal kinetics model for describing the browning reaction in the food. The browning kinetics in many kinds of foods, especially bread based products, have been mostly found to follow the first order kinetic as discussed in section 2.7. Therefore, the first order kinetic model is developed in this chapter to explain the colour change on the pastry surface during baking.

As was discussed in Chapter 2, the cooking conditions of temperature and moisture content are the two most significant factors that must be reasonably accounted for in a kinetic model. The kinetic model for describing the colour change due to browning reaction included the temperature and water content factors (water activity or moisture content) into the model in some studies of bakery products (Savoye *et al*., 1992; Broyart *et al*., 1998; Hadiyanto *et al*., 2007 and Purlis & Salvodori, 2009). However, some studies determined that the moisture content is important only as a factor affecting the heat transfer. For example moisture evaporation was included in a heat transfer model for developing a non-isothermal kinetic model of bread baking (Zanoni *et al*., 1995 and

Zhang & Datta, 2006). Water's influence on the rate of enzymatic browning reactions in food was unclear. It was not elucidated whether both temperature and moisture content should be factors included into the kinetic model for the Maillard browning reaction. To determine and justify the moisture content effect, the last part of this chapter investigates the effect of moisture content on the kinetics of colour change of pastry baking.

4.2 Typical trial

A trial was carried out at 160°C to demonstrate repeatability of the developed system. This initial data would also be used to develop a kinetic model for browning.

4.2.1 Method

Commercial frozen pastry ("Edmonds" brand), was selected as the model food for this study because the pastry includes both sugar and protein which are the key reactants for the browning reaction and provides a smooth surface and even colour when the browning takes place (section 3.2.6). The frozen pastry was purchased from a local supermarket and stored frozen at -18°C in a domestic freezer. After thawing by leaving the pastry at the room temperature (20°C) for 10 minutes, the pastry with a thickness of 2 mm, was cut using a 50 mm diameter circular cookie cutter.

The pastry samples were cooked on a hot pan at a temperature of 160°C for 60 minutes at four different positions on the pan. The temperature of the pastry surface was measured and recorded using surface self-adhesive type J thermocouple probes (SA1XL, OMEGA) and a data logger (Agilent 34970A). During baking, pastry samples were removed randomly from one of the four different baking positions after 5, 10, 15, 20, 25, 30, 35, 40, 45, 50, 55 and 60 minutes. The removed samples were quickly cooled down on a stainless steel tray sitting on ice to stop the browning reactions. All samples were photographed for analysis using the image system described in section 3.3. The colour development on the pastry surface was analyzed to calculate $L^*a^*b^*$ colour values.

4.2.2 Results

The temperature histories of the oil, pan and pastry surface during the cooking process were recorded and an example plotted is shown in Figure 4.1. There was about 2°C

difference in temperature between the oil and the pan at steady state. This shows the potential errors that can occur if it is assumed that the surface is at the same temperature as the heating medium as was discussed in section 2.7. The pastry samples were placed on the hot pan after the temperature of the pan was constant. After placing the samples, their temperature rapidly increased and took 8 minutes to come up to be the same temperature as the pan temperature. After this short period, the pastry/pan interface surface temperatures showed a constant profile throughout the process. The constant temperature period was much longer than the short initial heating period, therefore, it was assumed that this system closely approximated an isothermal condition.

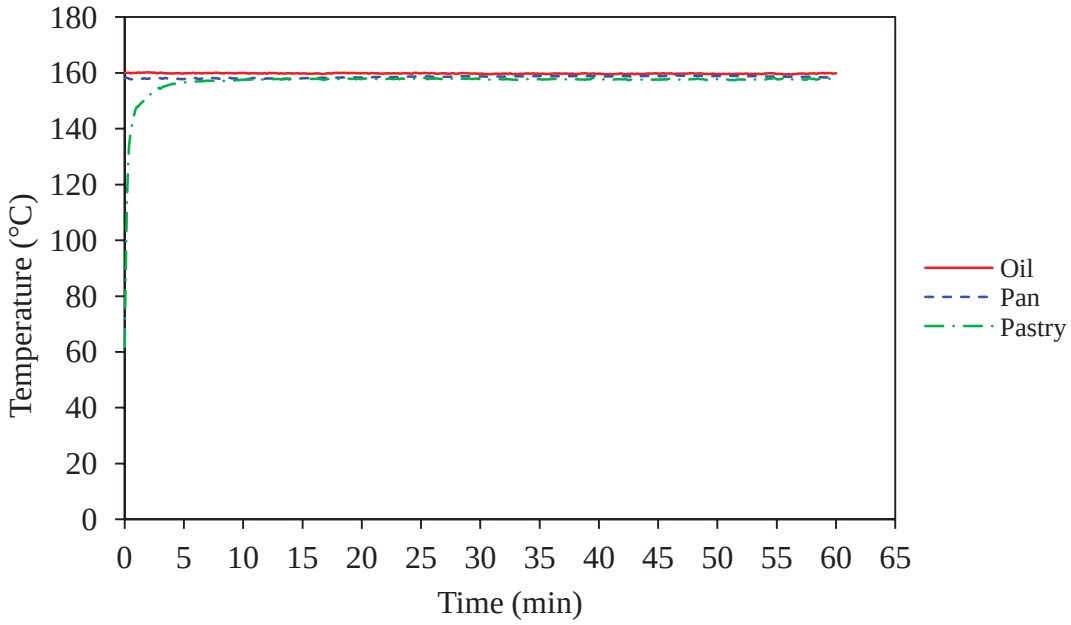

Figure 4.1 Temperature profiles of the oil, pan and pastry measured for an experiment baking at 160°C

A first assessment of the development of browning at the pastry surface during baking can be done by visual inspection of images captured using the image analysis method (Figure 4.2). Figure 4.2 shows the brown colour development (due to the Maillard browning reaction) on the pastry surface from 0 min (not baked) up to 60 min. The intensity of the colour increased with increasing time. The images show a likely even brown colour on the sample surface so the colour can be analyzed and calculated as an average value of $L^*a^*b^*$ colour space.

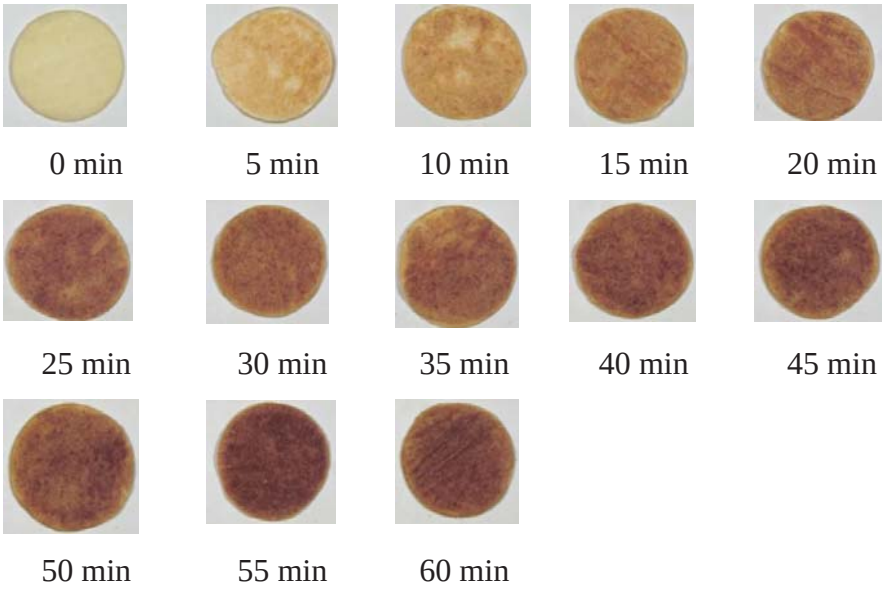

Figure 4.2 Images showing browning development on the pastry surface during baking at 160°C for up to 60 minutes

Figure 4.3 shows the colour values of *L**, *a** and *b** of the pastry. The error bars show the measured average standard deviation according to the colour distribution on the pastry surface analyzed by the image analysis method. The values of *L**, *a** and *b** represent the lightness, redness and yellowness values, respectively. The definition and interpretation of *L**, *a** and *b** values were described in section 3.3. The profiles of colour values were plotted against the baking time. It was found that the lightness value (*L**) continuously decreased with baking time. The value of lightness decreased from 90 at the beginning of the baking to a final lightness value of 61 at the end of the process. The redness value (*a**) increased from -3 to 11, but there was no trend for the yellowness index value (*b**). Based on this kinetic models to describe the changes in *L** and *a** could be developed. However because the yellowness index had no trend it is not useful for describing browning rate.

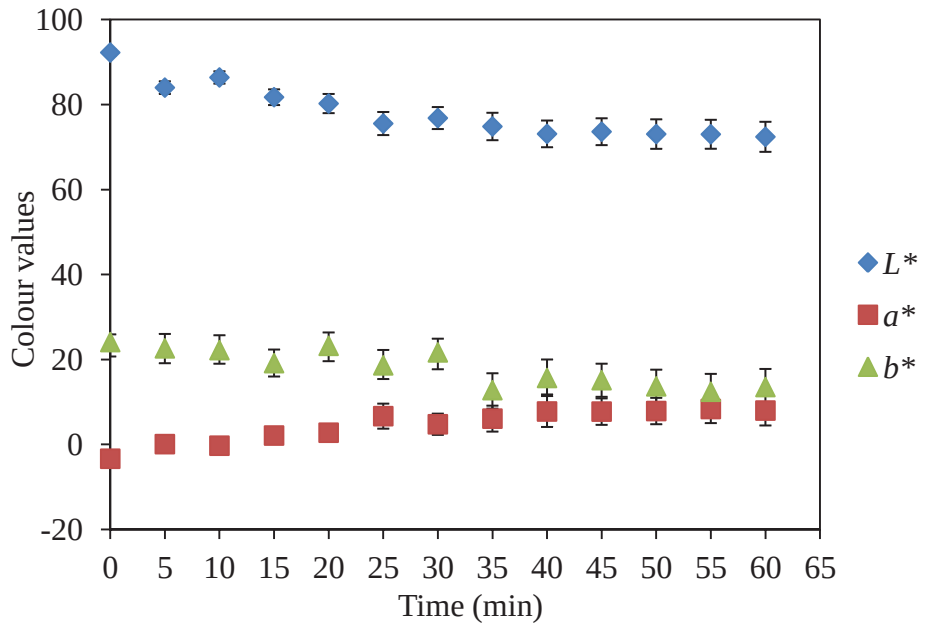

Figure 4.3 Colour values (*L**, *a** and *b**) of the pastry surface after baking at 160°C for up to 60 minutes, the error bars show the standard deviation according to the colour distribution on the pastry surface analyzed by the image analysis method

Because the temperature throughout the baking process was reasonably constant, an isothermal model to predict the colour change in *L** and *a** could be developed.

4.3 Isothermal model development

Even though the temperature changed in the first 8 minutes (Figure 4.1), the heating was much faster than the browning rate and the temperature was constant for the majority of the experiment. Therefore as a first approximation, the assumption of isothermal conditions was justified.

Many other researchers found first order kinetics apply: for example, bread and dough baking (Zanoni *et al.*, 1995; Zuckerman & Miltz, 1997 and Pulis & Salvadori, 2009), cracker baking (Broyart *et al.*, 1998) and potato frying (Krokida *et al.*, 2001). After prolonged heating, a steady state colour (L^*_∞) was reached, which was also observed by Demir *et al.* (2002) who developed the browning kinetics for hazelnut roasting at 120°C for long time periods and assuming isothermal conditions.

Based on these previous studies, first order kinetics were used to describe the lightness-time (L^*) and redness-time (a^*) curves in the pastry samples. The rate of change of L^* with respect to time is given by:

$$\frac{dL^*}{dt} = -k\left(L^* - L^*_{\infty}\right) \tag{4.1}$$

where the parameter k is a first order rate constant (min^{-1}) and L^*_{∞} is the final steady state L^* value. With isothermal conditions k is constant and this can be integrated to give an equation for L^* as a function of time.

$$\int_{L^*_0}^{L^*} \frac{dL^*}{\left(L^* - L^*_{\infty}\right)} = -k\int_0^t dt \tag{4.2}$$

$$\ln\left(\frac{L^* - L^*_{\infty}}{L^*_0 - L^*_{\infty}}\right) = -kt \tag{4.3}$$

where L^*_0 is the initial L^* value at $t = 0$. Equation (4.3) can be rearranged and expressed as:

$$L^* = L^*_{\infty} + \left(L^*_0 - L^*_{\infty}\right)\exp(-k_{L^*}t) \tag{4.4}$$

Equation 4.5 for the change in a^* with time in isothermal conditions can be developed in a similar way.

$$a^* = a^*_{\infty} + \left(a^*_0 - a^*_{\infty}\right)\exp(-k_{a^*}t) \tag{4.5}$$

The parameters L^*_0, L^*_{∞} and k_{L^*} in Equation 4.4 and a^*_0, a^*_{∞} and k_{a^*} in Equation 4.5 were fitted to the lightness and redness data by nonlinear regression using the CurveExpert software program (version 1.40, Danial Hyams).

The kinetic parameters of L^*_0, L^*_{∞} and k and a^*_0, a^*_{∞} and k for lightness and redness colour value obtained from the fitting are presented in Table 4.1. The goodness of fits (R^2) were also computed which is 0.95 for both of the lightness and redness profiles. The estimated initial and final values were 91.33 and 70.80 for L^* and -3.24 and 10.01 for a^*. These values were close to the values obtained from the experimental study, which were 92.24 and 72.40 for L^* and -3.37 and 7.97 for a^* for initial and final colour

values, respectively. This confirmed that the first order kinetic model provided a good fit.

The kinetic rate constants of the reaction were 0.045 and 0.037 min^{-1} for lightness and redness changes, respectively (Table 4.1). It can be concluded from the similarity of the kinetic rate constant that they are both measuring changes in the same underlying kinetic process (Maillard browning).

Table 4.1 Predicted kinetic parameters from isothermal 1'st order model fit

Kinetic parameters	***L****	***a****
Initial colour value	91.33	-3.24
Final colour value	70.80	10.01
k (min^{-1})	0.045	0.037
R^2	0.95	0.95

The model profile with the experimental data points of L^* and a^* values of pastry baked at 160°C are shown in Figures 4.4 and 4.5, respectively. From the fitted graph of the lightness (Figures 4.4), it can be seen that the fitted line is close to the experimental data. This shows that the changing of the lightness value followed a first order kinetic model. The lightness value can be used as a measure of the Maillard browning reaction. In addition, it was also found in Figure 4.4 that the decreasing of the lightness value was very fast at the initial period of the process (0 to 25 minutes) and slowed down during the last period of the process from 30 minutes on.

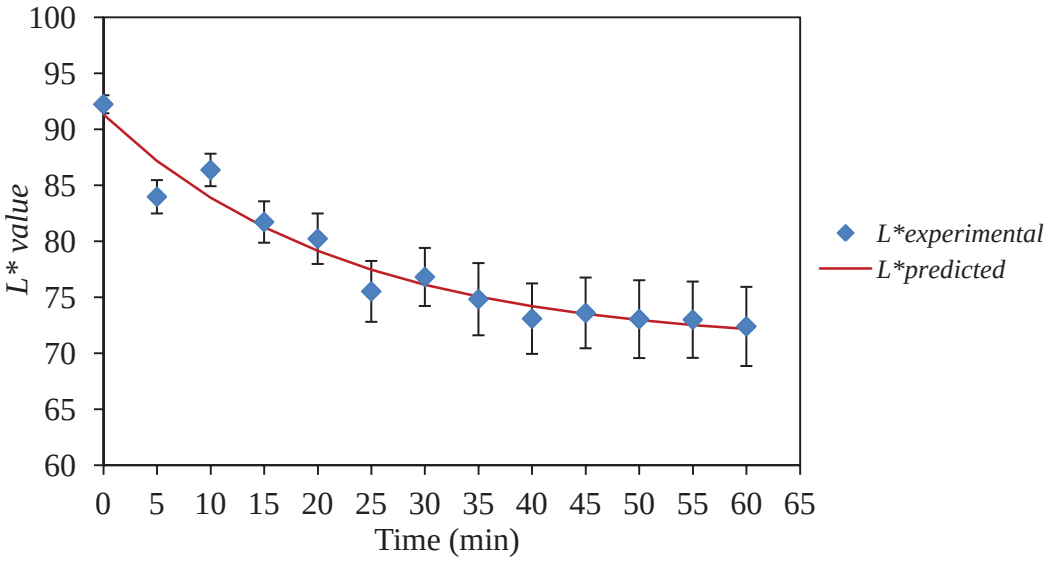

Figure 4.4 Fitted profile for the first order kinetic model compared with the experimental lightness values (L^*) data for pastry baked at 160°C

The same observation as the lightness-time curve fitting was also found in the redness-time curve fitting (Figure 4.5). A good fit was obtained when applying the first order kinetic model to the changing of the redness values with cooking time. From Figure 4.5, a fast rate of increase of the redness value was found at the beginning and tended to slow at the end of the process. This was in agreement with the observation in the lightness profile.

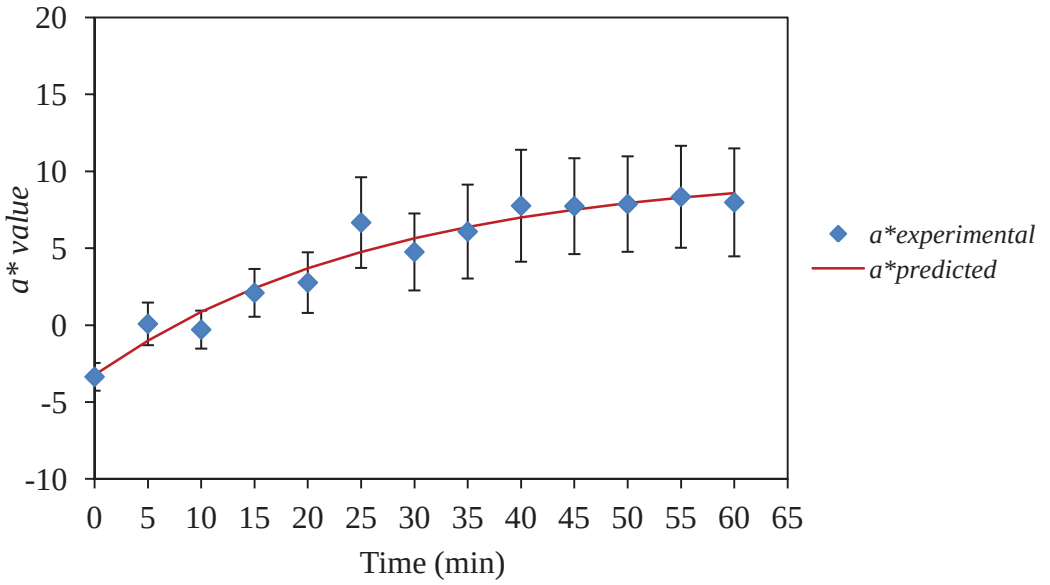

Figure 4.5 Fitted profile for the first order kinetic model compared with the experimental redness values (a^*) data for pastry baked at 160°C

These observations can be explained in that there is a higher reaction rate at the start because there is a higher concentration of reactants, compared to the later stage. The reactant concentration decreases as the process progresses.

The moisture content in the pastry sample decreased during the process due to water evaporation and this may affect the decrease in the rate of the reaction during the final stages of process. This was in agreement with the findings in the study of browning kinetics of cracker baking (Broyart *et al*., 1998). The literature also reported that the rate of reaction increases with an increase of water activity (a_w) up to a point but then decreases as water activity increases further (Labuza *et al*., 1980). The browning reaction decrease at low a_w is due to a higher viscosity, which increases the diffusion resistance of the reactants and slows down the browning reaction rate (Labuza *et al*., 1980). At high water activity lower reaction rates are explained in the literature by the dilution of reactants at higher moisture content (Shierwin & Labuza, 2003).

For these reasons, the study of the effect of the water content in the model food sample on the Maillard browning kinetic was investigated in the next section.

4.4 The effect of water content of the pastry on the browning kinetics

The result of the preliminary study showed that the reaction rate of the Maillard browning decreased during the last stage of the process. This could be due to water evaporation resulting in a decrease of the water content. However, it was unclear in the observations and the literature whether the moisture content or water activity in the food has any influence on the non-enzymatic browning reaction.

As was discussed in section 2.3.2 on the water's influence on the rate of non-enzymatic browning reaction in food is illustrated in Figure 2.2. A maximum browning rate has been reported in many foods between water activities (a_w) 0.6 and 0.7 (Lea & Hannan, 1949). This was also reported by Labuza & Baiser (1992) who stated that the maximum rate of the Maillard reaction was observed at the medium value of water activity and the reaction starts to occur at a water activity (a_w) of 0.2-0.3 for most foods and the rate increases with increasing water activity (a_w) up to the maximum rate at the medium water activity and then decreases at higher water activities (a_w) due to the browning reactants being diluted (Eichner & Karel, 1972; Labuza *et al*., 1980; Toribio *et al*., 1984; Cuzzoni *et al*., 1988; Shierwin & Labuza, 2003; Vaikousi *et al*., 2008 and

Jiménez *et al*., 2012). In addition, high water content may have an inhibitory effect due to the water produced during the formation of 5-HMF step of the Maillard reaction mechanism (Resnik & Chirife, 1979; Martins *et al*., 2001 and Ameur *et al*., 2006).

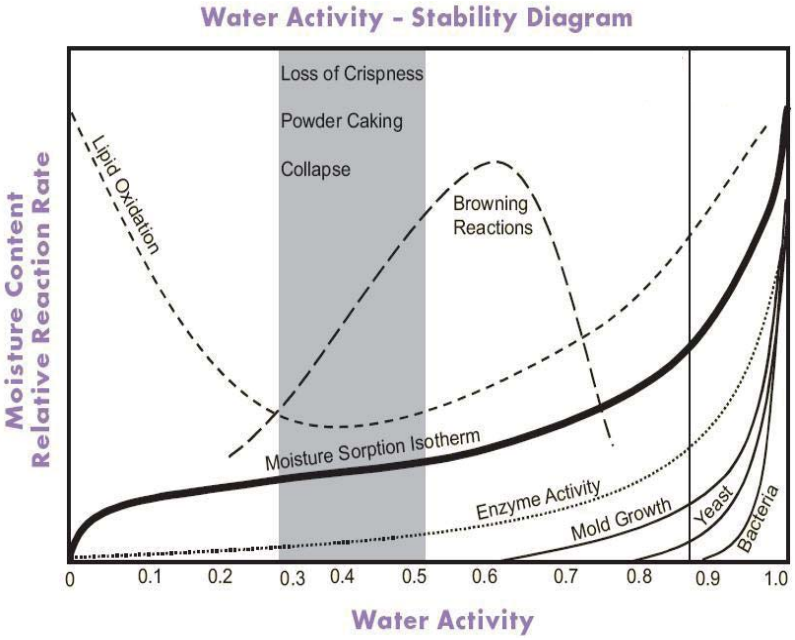

Figure 2.2 The influence of moisture content and water activity (a_w) on chemical reaction of food (adapted from Labuza, 1977).

The decreasing rate of browning reaction at very high water activity due to the concentration of the reactants being diluted was supported by the study findings of Vaikousi *et al*. (2008). They investigated the effect of the water activity (in the range of 0.74-0.99) on the kinetics of the non-enzymatic browning in apple juice concentrate under isothermal treatment at 60, 70, 80 and 90°C. The results showed that, the water activity had no direct effect on the kinetics of the reaction but the higher water activities were due to dilution of the juice concentrate. The amount of water influenced the initial reactant concentration. Higher water activity diluted the reactant concentration of the juice, so the browning reaction rate decreased. Decreasing water activity increased the browning rate constants due to high concentration of reactants.

Conversely, for some solid food systems such as cracker baking at high air temperature (180-330°C), the decreasing water activity factor during the baking process decreased the non-enzymatic browning rate (Broyart *et al*., 1998). In the baking process, the moisture content is high at the beginning and decreases during the process so the Maillard browning reaction was reported to start when the water activity decreased to

less than 0.4-0.7 (Shibukawa *et al*., 1989; Broyart *et al*., 1998; Wählby & Skjöldebrand, 2002; Ait Ameur *et al*., 2006, 2007; Gökmen *et al*., 2008b and Purlis & Salvadori, 2009). After this initiation point, the browning reaction increased when the water activity of the samples decreased and the temperature increased during the process (Savoye *et al*., 1992; Ait Ameur *et al*., 2006, 2207 and Gökmen *et al*., 2008b and Purlis & Salvadori, 2009).

The water activity was found to have no effect on the kinetics of browning in the baking of biscuits (Mundt & Wedzicha, 2007). The rate of browning at 105-135ºC was compared for varying water activities (a_w = 0.04-0.40) by baking in saturated air throughout the process, so the hot biscuit surface was in equilibrium with steam (at atmospheric pressure). For example, the air is saturated with water vapour (*RH* = 100%) at 100ºC but drops to *RH* <40% at temperatures >130ºC. By controlling the air relative humidity in this way there was no change in water activities of the samples surface during the process. The results showed that the different water activity of the food sample had no effect on the rate of browning.

It can be concluded from the literature review above that the effect of moisture or water activity in the food on the non-enzymatic browning has a lot of variation between the different observations. Therefore, experiments were carried out with the aim to investigate the effect of water content on the non enzymatic browning kinetics in the model pastry system undergoing high temperature cooking. The initial moisture content of the pastry samples was varied before baking to determine its effect on the overall rate of colour change. The sorption isotherm of pastry drying was also investigated in this study.

4.4.1 Preparing pastry with different moisture contents

Commercial frozen pastry samples were thawed by leaving them at room temperature (20ºC) for 5 minutes. After thawing, the pastry was cut into circular shapes using a cookie cutter with a diameter of 50 mm. All samples were weighed using a four digit balance (Sartorius CPA22 4S) and the data was recorded as an initial weight before drying. The initial water activity of the raw pastry was 0.97, measured by using a dew-point measuring instrument at 20ºC (a water activity meter model AquaLab Water Activity Meter 4TE). And then, all pastries were left in the desiccators which contained

silica gel with a water activity (a_w) of 0.45±0.001 S.E. for 0, 9, 20, 40 and 65 hrs for reducing the water content in the pastry After that, all samples were put in an aluminium pouch bag for 24 hrs to ensure that the moisture content of the pastry was in equilibrium. To measure a relative humidity (RH) in the aluminium pouch bag, a relative humidity probe (I-button) was put in the bag to record the relative humidity every 10 minutes. The recorded relative humidity value was loaded using the OneWireViewer software program and saved in an Excel file for further analysis.

In addition, water activity (a_w) and moisture content (%MC) were also determined by using a water activity meter (AquaLab Water Activity Meter 4TE) and the AOAC moisture content method (Horwitz & Latimer, 2005), respectively.

The methodology of AOAC moisture content measurement is described following these steps. An empty aluminium dish and lid were dried in the oven at 105°C for 3 hours and transferred to desiccators to cool. The empty dish and lid were weighed and the data recorded. Three grams of sample were weighted and put into the dish and spread uniformly. The dish was then placed in the oven to dry for 3 hours at 105°C. After drying, the dish with lid was transferred into the desiccators to cool. Later, the dish and its dried sample were reweighed and the data recorded. Finally, the moisture content was calculated by employing Equation 4.6.

$$\text{Moisture content (\%MC: wt\% of d.b.)} = [(W1-W2)/W2] \times 100 \qquad (4.6)$$

where W1: weight (g) of sample before drying and
W2: weight (g) of sample after drying

4.4.2 The RH probe calibration

Prior to measuring the relative humidity (%RH) of the air above the pastry in the aluminium pouch, the relative humidity probe was calibrated by placing it over standard saturated salt solutions which have known relative humidity values (Rahman, 1995 and Reid, 2007). Two saturated salt solutions were used: potassium chloride (KCl) and magnesium chloride ($MgCl_2$). These two solutions were prepared and then the solutions were put in a tightly closed container. After that the I-button relative humidity probes were placed in the container and left overnight at 20°C to allow the system to equilibrate. The data of the relative humidity of the environment in the container was

recorded using the I-button relative humidity probes and the data was downloaded later by using the OneWireViewer software program.

At equilibrium the relative humidity of the air above the saturated salt solutions are known as 85.11%±0.29RH and 33.07%±0.28RH for KCl and $MgCl_2$, respectively (Greenspan, 1977). These values were used as the reference values for the calibration. A calibration graph was drawn between the measured values (recorded by the relative humidity probe) and the actual values (saturated salt solution reference), and then the intercept and slope of the equation were obtained as shown in Table 4.2. The values of slope and intercept in Table 4.2 were used to calculate the actual relative humidity value in the aluminium pouches by following Equation 4.6.

$$RH_{actual} = RH_{measured} \times \text{slope} + \text{intercept} \quad (4.6)$$

Table 4.2 Adjustment values for calibrating the relative humidity probes

Adjust value	Probe 1	Probe 2	Probe 3	Probe 4	Probe 5
slope	1.03	1.04	1.02	1.02	1.02
intercept	-2.75	-2.95	-1.85	-2.78	-2.57

The adjusted values were used in the analysis.

4.4.3 Sorption Isotherm

In food dehydration, the sorption properties of food are very important. For the study of the effect of moisture content of the pastry on the browning kinetics, dehydration is involved in the sample preparation step. Therefore, knowledge of the sorption behaviour was required in the quantitative approach to predict the moisture content and water activity of the sample. Researchers commonly use the concept of water activity in the food industry. The definition of water activity is stated in Equation 4.7 (Al-Muhtaseb *et al.*, 2002).

$$a_w = p / p_0 = \% \frac{relative \quad humidity}{100} \quad (4.7)$$

where p is the partial pressure of water in the food at equilibrium (atm) and p_0 is the vapour pressure of pure water at the same temperature (atm). From Equation 4.7, it can be observed that the relative humidity is related to the water activity (a_w) of the sample

at the equilibrium condition. Therefore, the water activity of the pastry sample for this study can be converted from the relative humidity of air inside the aluminium pouch bag in contact with the pastry by applying Equation 4.7.

A sorption isotherm is a relationship between percent moisture content on a dry basis (%MC: wt% of d.b.) and water activity (a_w). Moisture sorption isotherms of most foods are nonlinear, normally sigmoid shaped. The types of sorption isotherms are generally classified into five types as shown in Figure 4.6 (Basu *et al*., 2006). Type 1 is Langmuir or similar isotherms that present a convex upwards curves, obtained assuming water monomolecular adsorption at the internal surface of the material. Type 2 is sigmoid shaped adsorption isotherms, which have concave upwards curves. This type of sorption isotherm takes into account the existence of multilayers at the internal surface of the material. Type 3 is known as the Flory-Huggins isotherm, which describes a solvent or plasticizer such as glycerol above the glass transition temperature or the solubility of sugars in water. Type 4 isotherm accounts for adsorption by a swellable hydrophilic solid. Type 5 is the Brunauer-Emmett-Teller (BET) multilayer sorption isotherm which is related to type 2 and 3 isotherms and observed for adsorption of water vapour on charcoal. Many biological materials, including food products are most commonly reported to follow the type 2 or sigmoid shape sorption isotherm (Brunauer *et al*., 1940; and Basu *et al*., 2007).

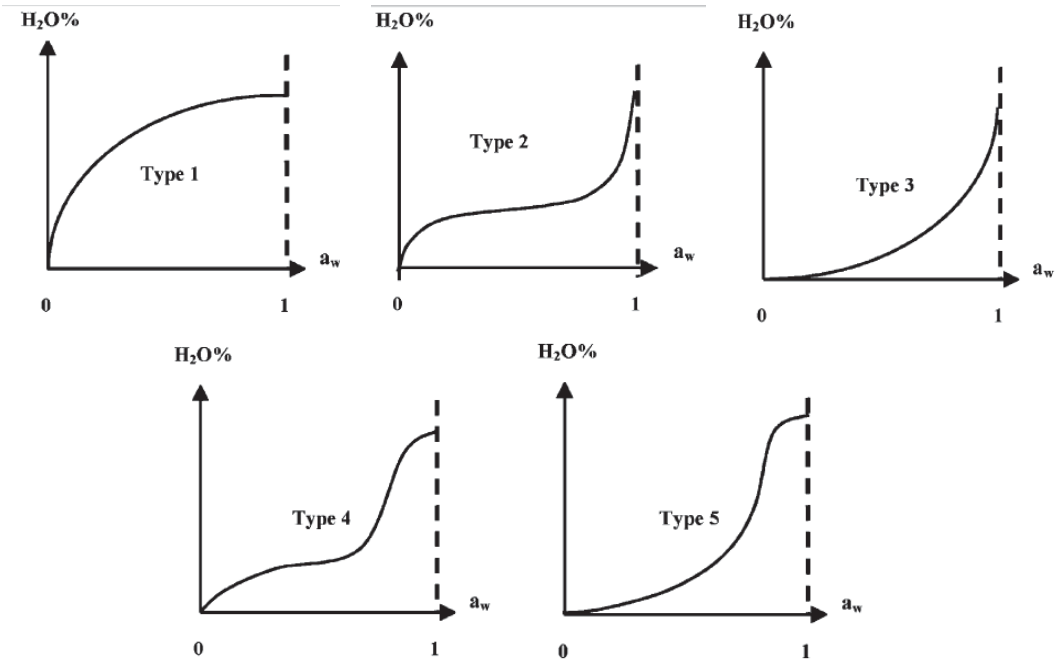

Figure 4.6 Five types of isotherms (reprinted from Basu *et al*., 2007)

To measure water sorption isotherms, there are many methods available such as gravimetric, manometric and hygrometric method. For this study, the gravimetric method was used to measure the sorption isotherm for pastry. The gravimetric method involves the measurement of weight changes which can be continuously or discontinuously determined (Al-Muhtaseb *et al.*, 2002).

4.4.4 Mathematical description of moisture sorption isotherms

According to Labuza (1975) water is associated with the food matrix by different mechanisms in different water activity regions, so there is no sorption isotherm model that can fit data over the whole range of relative humidity for all types of foods (Labuza, 1975). As a consequence, there are many mathematical models used to describe water sorption isotherms of food materials. Examples of models, commonly used in the literature, are the Brunauer-Emmett-Teller (BET), the Guggenheim-Anderson-deBoer (GAB), Halsey equation, Oswin equation, Smith equation and Henderson equation which are discussed below (Timmermann *et al*., 2001).

The Brunauer-Emmett-Teller (BET) sorption isotherm is normally applied for the estimation of the monolayer moisture content of foods over the lower water activity range (0.05-0.35). The BET equation is useful in identifying the optimum moisture content for drying and storage stability of foods.

The Guggenheim-Anderson-deBoer (GAB) is an improved version of the BET model. It has been suggested to be the most versatile sorption model available in the literature. This model is used in a wide range of water activities from 0.05-0.95.

The Halsey equation is a good model to present sorption isotherms in different types of food with a range of water activities (0.1-0.9).

The Smith equation describes the final curved portion of water sorption isotherm of high molecular weight biopolymers. This model could be used in the water activity range from 0.3-0.9.

The Henderson equation is one of the most widely used models in many foods, but its applicability has been limited compared to the Halsey equation (Basu *et al*., 2007).

The Oswin equation is a mathematical series expansion for a sigmoid-shaped curve. It is normally applied in the water activity range from 0.05-0.90.

These model equations of moisture sorption isotherms and their application for a range of water activities and food material are summarized in Table 4.3.

Table 4.3 Summary of moisture sorption isotherm models used to fit experimental data (Modified from Al-Muhtaseb *et al*., 2002)

Model	Equation*	a_w range	Food material
BET	$\frac{MC}{M0} = \frac{Ca_w}{(1-a_w)(1-a_w+Ca_w)}$	0.05-0.35	Protein, Chicken, Peanut flakes, Potato, Lentil seed, Onion, Pineapple, Rice, Turkey, Tomato, Potato starch, Wheat starch
GAB	$MC = \frac{M_0 CKa_w}{(1-Ka_w)(1-Ka_w+CKa_w}$	0.05-0.95	Protein, Starch, Casein, Potato starch, Fish, Starchy food, Raisins, Figs and apricot, Protein and starch food, Potato, Red pepper, Macadamia nuts, Pasta products, Carrot, tomato, onion and green pepper, Yogurt powder, Potato, Pineapple, Rice, Turkey, Chicken, Tomato, Wheat starch, Chestnut, Hazelnut, Cured beef
Halsey	$a_w = \exp\left(-A/RT\theta^r\right)$	0.05-0.80	Starchy food, Proteins, Meats and Fruits, Milk, Potato, Raisin, Yogurt powder, Lentil seeds Hazel nut, Chestnut, Cured beef, Cocoa beans
Oswin	$MC = A\left[\frac{a_w}{1-a_w}\right]^B$	0.05-0.90	Proteins, Meats, Fruits, Starch food, Potato, Lentil seed, Onion, Hazelnut, Chestnut, Cured beef
Smith	$MC = Y + Z\log(1-a_w)$	0.30-0.90	Wheat, Corn starch, Soy flour, Beef, Casein, Pineapple, Hazelnut, Chestnut, Cocoa beans
Henderson	$MC = \left[\frac{\ln(1-a_w)}{-A}\right]^{1/B}$	0.05-0.80	Different food product, Starchy food, Protein, Meats, Fruits, Potato, Lentil seeds, Onion, Pineapple, Chestnut, Cocoa beans

*Note: the symbol in the equations are defined as: *MC* is the moisture content (kg·kg^{-1} dry solid), M_0 is the monolayer moisture content (kg·kg^{-1} dry solid), a_w is the water activity, *C* and *K* are dimensionless parameters related to the net heat of sorption, *A* and *r* are constants (dimensionless parameters), $\theta = MC/M_0$, *R* is the universal constant (8.314 kJ mol^{-1} K^{-1}), *T* is the absolute temperature (K), *Y* is the quantity of water in the first sorbed fraction and *Z* is the quantity of water in the multilayer moisture fraction (dimensionless parameters)

It was found in the literature that BET and GAB models were most widely applied in food systems. Especially, the GAB model is found to be suitable for analysing fruits, vegetables, meat, and starchy food including pasta products. Therefore for this study on pastry, the GAB model was used.

All experimental data of the water activity (a_w) and the moisture content (%MC) were plotted and fitted to the GAB model as expressed in Equation 4.8 (Van Den Berg, 1985 and Timmermann *et al*., 2001). The GAB model was applied using non-linear regression (MATLAB® version 6.5 The Mathworks Inc, Natick, Mass. U.S.A) software to fit the prediction equation. The GAB sorption model is usually presented in the form:

$$MC = \frac{M_0 CKa_w}{(1-Ka_w)(1-Ka_w+CKa_w)} \tag{4.8}$$

where MC : the moisture content (wt% of d.b.)

a_w : the water activity

M_0: the moisture content corresponding to the 'monomolecular layer' on the whole free surface of the material

and K and C : the free sorption dimension parameters characterizing sorption properties of the material and these two parameters depend on temperature by Arrhenius-type equations (Van den Berg, 1985 and Timmermann *et al*., 2001).

The initial values of M_0, K and C were guessed and simultaneously fitted to all data of a_w and %MC from the experimental result by non-linear fit function *nlinfit* in MATLAB® and the confidence interval for the non-linear regression prediction was applied with function *nlpredci* in MATLAB®. The MATLAB® code for this fitting is shown in Appendix A2. The fitted prediction curve of moisture sorption isotherm for pastry is shown in Figure 4.7.

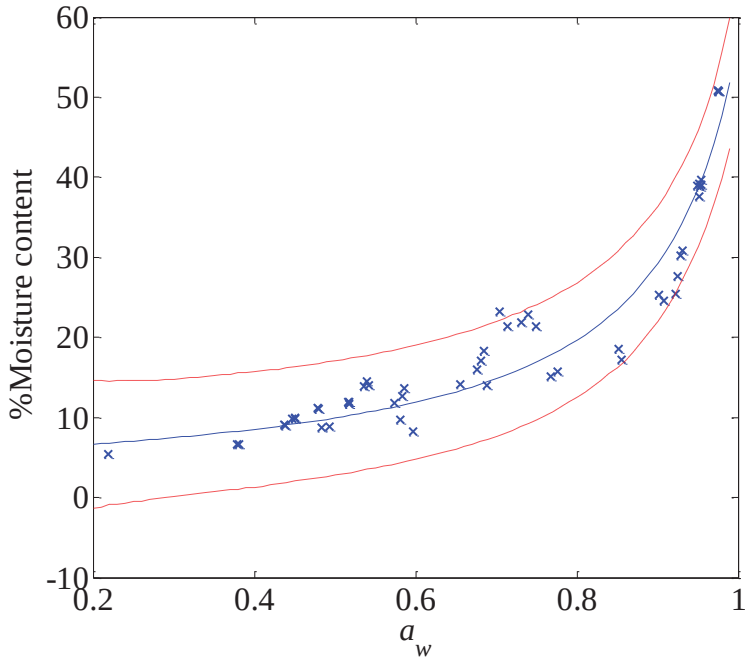

Figure 4.7 The data plot and the predicted isotherm for pastry fitting with GAB model with the 95% confidence interval

The parameters values for the GAB model for pastry obtained from the fitted curve are listed in Table 4.4.

Table 4.4 Estimated parameters of the GAB equation for pastry

Parameters	**Values**
M_0 (%)	5.16
K (dimensionless)	0.91
C (dimensionless)	8.26×10^{9}

A goodness of fit and an indication of the precision of the estimation of the estimate for the model applied were determined by the goodness of fit (R^2) which is a measure of the proportion of variability attributed to the model and the standard error of the estimate (S), respectively.

For this study, the goodness of fit (R^2) and the standard error of the estimate (S) for the GAB isotherm model fitted were obtained as 92.29% and 3.42, respectively. This result shows that the GAB isotherm model was a good fit with the experimental data of the water activity (a_w) and the moisture content (%MC). Therefore this model can be used

to reverse calculate between the water activity (a_w) and the moisture content (%MC) of the pastry sample when one of these two values was known.

The sorption isotherm curve of pastry is of benefit in considering the drying process of pastry. From the graph, the high water activity region of pastry has a high slope so a lot of water needs to be removed during the initial stages of the drying process, hence higher energy was required. Conversely, drying the pastry with low water activity needs to remove less water, so lower energy overall is required.

4.4.5 Calculation for moisture content

The moisture contents of the pastry sample changes during the drying process in the desiccators. The moisture content (%MC) was estimated by using Equation 4.8 when the value of the water activity (a_w) of the sample was known. The water activity (a_w) was calculated by converting the data of the equilibrium relative humidity (ERH) of the air surrounding the food in the aluminium pouch bag. The relationship between water activity (a_w) and relative humidity (ERH) is expressed in Equation 4.7. There were five experimental sets with drying times of 0, 9, 20, 40 and 65 hours. The equilibrium relative humidity of the air in the pouch bags were measured and converted to the water activity (a_w) values and those are reported in Table 4.5. Finally, the moisture content (%MC) of the pastry sample was estimated from the water activity (a_w) of the pastry by applying Equation 4.8. All values are shown in Table 4.5.

Table 4.5 Data for equilibrium relative humidity (ERH), water activity (a_w) and the moisture content of pastry calculated from the water activity (a_w)

Time (hrs)	RH	a_w	%MC (wt% of d.b.)
0	97	0.97	44.55
9	93	0.93	33.89
20	85	0.85	22.92
40	58	0.58	10.95
65	48	0.48	9.18

4.4.6 Moisture content of pastry samples for subsequent browning studies

The pastries with five different levels of initial moisture content (%MC) at 44.55, 33.89, 22.92, 10.95 and 9.18 wt% of d.b. were baked on a hot temperature controlled pan at 160°C for 60 minutes, with two replications. During the baking process, the pastry samples were removed from the hot pan to measure the brown colour development on the pastry surface by image processing (see section 3.3) every five minutes up until 60 minutes of processing. The brown colour on the pastry surface was analyzed and shown in terms of the *L*a*b** colour space to follow the browning kinetics, as detailed in section 3.3.

As was discussed in the results of the previous trial study (section 4.2.2), the Maillard browning reaction could be followed by the lightness and redness colour value. The lightness and redness values of all pastry samples for every baking condition were plotted against time. Then the lightness-time and redness-time curves were fitted with the first order kinetic model (Equation 4.4) by using the CurveExpert software program to obtain the initial lightness/ redness, final lightness/ redness and kinetic rate constants. The effect of water content (a_w) on the browning kinetics was determined by using statistical analysis (ANOVA) to determine if there was a significant difference between the kinetic rate values.

4.4.7 Results and discussion

The lightness (*L**) of the pastry surface is shown in Figure 4.8. It can be seen from the graph that the lightness of the surface colour for all initial moisture content (%MC) levels decreased as process time increased. It was found that the lightness values of the highest initial moisture content pastry (%MC = 44.55 wt% of d.b.) for both experimental replicates were higher than other samples. The reaction rate of the higher initial moisture content sample was lower than that of the lower initial moisture content sample potentially because of high dilution of the browning reactants (Labuza *et al*., 1980; Toribio *et al*., 1984; Cuzzoni *et al*., 1988 and Vaikousi *et al*., 2008). However, the decreasing trend of the lightness as a function of initial moisture content of the pastry is not clear as can be seen from the lightness profile of the other pastry samples with different levels of the initial moisture content. Therefore, it cannot be confidently concluded that the initial moisture content had an influence on the browning kinetics.

The effect of the initial moisture content on the non-enzymatic browning reaction was statistically tested by comparing the kinetic rate constant obtained from the kinetic model fitting.

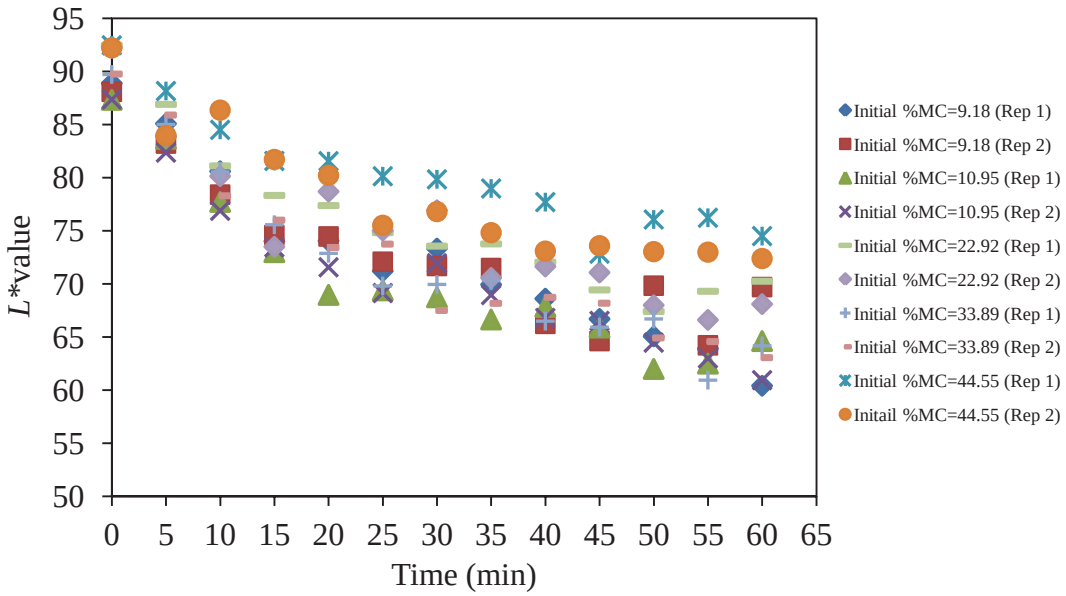

Figure 4.8 The lightness-time curve of pastry baked at 160°C for 60 minutes starting with different initial moisture content

The L^*_0, L^*_∞ and k parameters were obtained from the fitting and are presented in Table 4.6. From Table 4.6, it can be concluded that the experimental data was fitted well by the first order kinetic model because the goodness of fit (R^2) were high (0.91-0.97). The estimated initial lightness values were in the range between 88 and 92 approximately. The variation of the initial lightness was found to correlate with the amount of the initial moisture content of the pastry sample. The initial lightness values were higher at the higher of the initial moisture content of the pastry sample. There was no trend for the final lightness values, which fluctuated in the range between 56 and 74. The kinetic rate constant varied in the range from 0.028 to 0.054 min^{-1} with no clear trend with respect to initial moisture content.

Table 4.6 Predicted kinetic parameters obtained from isothermal model fitting for the lightness change for samples cooked at different moisture contents

Initial %MC (wt% of d.b.)	Replications	L^*_0	L^*_∞	k_{L^*} (min^{-1})	R^2
9.18	Rep 1	88.20	56.99	0.028	0.96
	Rep 2	88.06	65.95	0.053	0.92
10.95	Rep 1	88.05	62.66	0.054	0.97
	Rep 2	86.40	60.44	0.038	0.96
22.92	Rep 1	87.60	57.29	0.054	0.93
	Rep 2	87.47	56.91	0.047	0.96
33.89	Rep 1	89.88	61.45	0.042	0.97
	Rep 2	89.85	62.42	0.044	0.97
44.55	Rep 1	91.86	73.83	0.045	0.94
	Rep 2	91.33	70.80	0.045	0.95

The effect of the initial moisture content of the pastry on the browning kinetics can be investigated by comparing the kinetic rate parameter (k_{L^*}) among all samples by statistical analysis. The MINITAB® software (version 16; Minitab Inc., State College, PA)) was used in this study. The ANOVA (analysis of variance) is given in Table 4.7. The P-value was greater than 0.05, which indicates that the kinetic rate constant (k_{L^*}) was not significantly different at the 95% level of confidence. Therefore it can be concluded that the initial moisture content of the pastry had an insignificant effect on the browning kinetics of the pastry.

Table 4.7 ANOVA results for effect of initial moisture content on the kinetic rate constant (k) of the lightness change for pastry baking

Variance	DF	SS	MS	F	P
Factor	4	1.08×10^4	2.70×10^5	0.28	0.882^{ns}
Error	5	4.88×10^4	9.76×10^5		
Total	9	5.96×10^4			
R-sq	18.08%				

ns = Not significant at P = 0.05 level.

The effect of initial moisture content on the initial and final lightness of the pastry sample was also investigated and the statistical values are shown in Table 4.8. The initial moisture content had the most influence on the initial lightness (P<0.005), whereas the final lightness was moderately effected by initial moisture content (P<0.05).

Table 4.8 ANOVA results for the effect of initial moisture content on the initial and final lightness (L^*_0 and L^*_∞) for pastry baking

	Effect of initial moisture content on L^*_0					**Effect of initial moisture content on L^*_∞**				
Variance	**DF**	**SS**	**MS**	**F**	**P**	**DF**	**SS**	**MS**	**F**	**P**
Factor	4	26.90	6.73	21.95	0.002***	4	254.15	63.54	6.65	0.031*
Error	5	1.52	0.31			5	47.74	9.55		
Total	9	28.42				9	301.89			
R-sq	94.61%					84.19%				

*, *** = Significant at P<0.05 and P<0.005.

The mean values and standard errors of the initial, final lightness and the kinetic rate constant of the browning kinetics of pastry baking are shown in Table 4.9. The differences among mean values of all data were also tested using MINITAB software program using Tukey's multiple comparison test method at 95% confidence intervals. A significant difference in an initial lightness among pastry sample study is indicated by the superscript letters a, b and c over the mean values. Table 4.9 shows that there were significant difference between the initial and final lightness (L^*_0 and L^*_∞) for samples at different initial moisture content, although they are not an obvious function of moisture content. There was no difference among the kinetic rate constants (k_{L^*}).

Table 4.9 Mean and standard error of the initial, final lightness and kinetic rate constant values (L^*_0, L^*_∞ and k_{L^*}) for pastry baking

Initial %MC	**L^*_0**			**L^*_∞**			**k_{L^*}**		
(wt% of d.b.)	**N**	**Mean**	**S.E.**	**N**	**Mean**	**S.E.**	**N**	**Mean**	**S.E.**
9.18	2	88.13^{bc}	0.099	2	61.47^{ab}	6.34	2	0.04^{a}	0.018
10.95	2	87.22^{c}	1.167	2	61.55^{ab}	1.57	2	0.05^{a}	0.012
22.92	2	87.54^{c}	0.092	2	57.10^{b}	2.69	2	0.05^{a}	0.005
33.89	2	89.86^{ab}	0.021	2	61.94^{ab}	0.69	2	0.04^{a}	0.001
44.55	2	91.60^{a}	0.375	2	72.32^{a}	2.14	2	0.04^{a}	0.001

Note: the letters a, b and c are within column comparitors meaning that samples that do not share a letter are significantly different at the 95% confidence level, using the Tukey's method.

It can be concluded that the initial moisture content of the pastry sample had a significant influence on the initial and final lightness value but had no significant effect on the kinetic rate constant at the 95% level of confidence.

The redness value was the other colour parameter used to describe the browning reaction. Therefore the changing of redness value on the pastry surface during baking was also observed to see the effect of the initial moisture content of the sample on the browning kinetic. The redness value development during processing time was plotted and is shown in Figure 4.9. The redness values of all samples with different levels of initial moisture content increased with the processing time. The same finding as in the lightness values was found; the redness profile of the highest initial moisture content (%MC = 44.55 wt% of d.b.) was lower than that of each other samples (Figure 4.9). The browning reaction rate of the highest initial moisture content samples was slower than that of each of the other samples potentially due to higher water content needing more evaporation time for reducing the water content for the initiation of browning formation. However this trend was not evident in the changing of the redness values. Therefore the effect of the initial moisture content on the browning kinetic rate of the pastry in terms of the redness value was also tested using the statistical method.

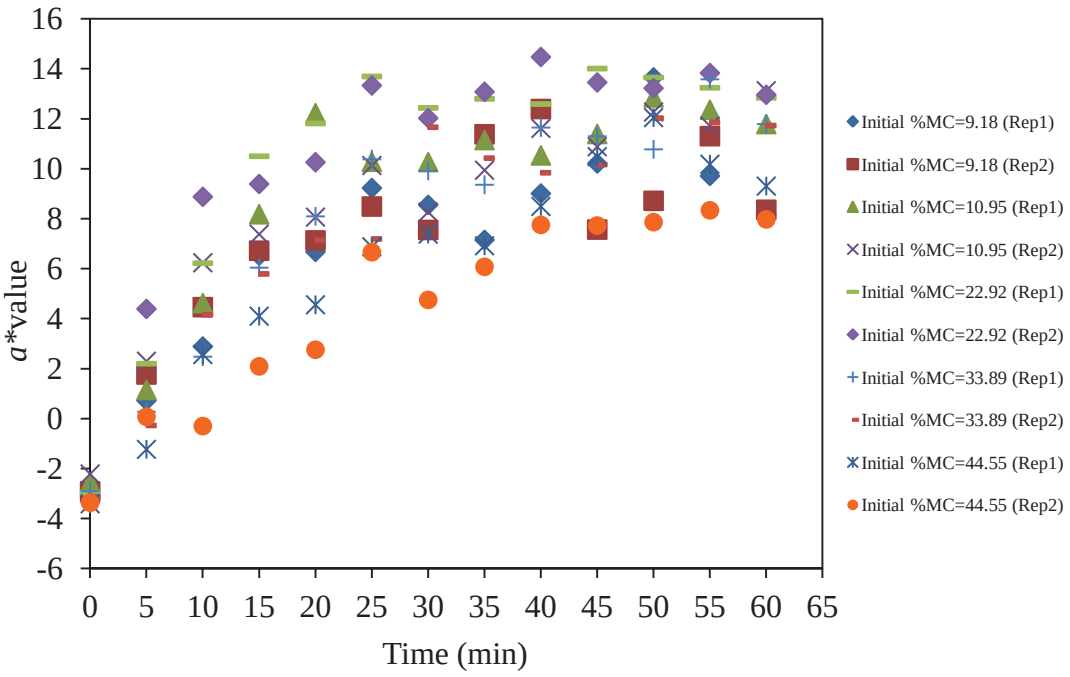

Figure 4.9 The redness-time curve of the pastry baked at 160°C for 60 minutes starting with different initial moisture content

The browning kinetic rate was obtained from the first order kinetic model fitted using the CurveExpert software. The obtained a^*_0, a^*_∞ and k_{a^*} parameters are presented in Table 4.6. The goodness of fit values (R^2) of the kinetic fitting of the redness-time curves were high (0.86-0.98). It can be seen that the redness changing followed first order kinetics. The estimated initial and final redness values were varied in the range of -1.72 and -3.56 and 9.89 and 13.62, respectively without any trend relating with the amount of water in the pastry sample. The kinetic rate constant varied in the range from 0.037 to 0.110 min^{-1}.

Table 4.10 Predicted kinetic parameters obtained from isothermal model fitting for the redness change for samples cooked at different moisture contents

Initial %MC (wt% of d.b.)	Replications	a^*_0	a^*_∞	k_{a^*} (min^{-1})	R^2
8.77	Rep 1	-3.02	10.39	0.069	0.89
	Rep 2	-2.92	9.89	0.088	0.88
14.30	Rep 1	-3.19	12.16	0.086	0.95
	Rep 2	-1.72	12.16	0.066	0.96
17.89	Rep 1	-3.56	13.62	0.980	0.98
	Rep 2	-3.04	13.46	0.110	0.98
30.55	Rep 1	-3.39	12.83	0.057	0.97
	Rep 2	-3.40	12.28	0.058	0.97
50.62	Rep 1	-3.51	11.81	0.042	0.96
	Rep 2	-3.24	10.01	0.037	0.95

The MINITAB software was used to test the effect of initial moisture content of the pastry on the kinetic rate of the changing of redness values by comparing the kinetic rate parameter (k_{a^*}) among all samples using statistical analysis. The ANOVA (analysis of variance) is given in Table 4.11. The P-value was lower than 0.01 indicating that the kinetic rate constant (k_{a^*}) was significantly different at $p<0.01$. Therefore the initial moisture content of the pastry did have a significant effect on the kinetics of the redness change due to the browning reaction of pastry.

Table 4.11 ANOVA results for effect of initial moisture content on the kinetic rate constant (k_{a^*}) of the redness change for pastry baking

Variance	DF	SS	MS	F	P
Factor	4	8.68×10^3	1.24×10^3	13.07	0.007**
Error	5	4.96×10^3	9.49×10^5		
Total	9	5.44×10^3			
R-sq	91.27%				

** = Significant at P<0.01.

The results of statistical test for the effect of initial moisture content on the initial and final redness of the pastry sample are shown in the table of ANOVA (Table 4.12). The initial redness was not significantly affected by initial moisture content at P=0.39, whereas the final redness was moderately affected by initial moisture content (P<0.05).

Table 4.12 ANOVA results for effect of initial moisture content on the initial and final redness (a^*_0 and a^*_∞) for pastry baking

	Effect of initial moisture content on a^*_0					**Effect of initial moisture content on a^*_∞**				
Variance	**DF**	**SS**	**MS**	**F**	**P**	**DF**	**SS**	**MS**	**F**	**P**
Factor	4	1.27	0.32	1.26	0.39	4	14.52	3.63	9.53	0.015*
Error	5	1.26	0.25			5	1.90	0.38		
Total	9	2.53				9	16.42			
R-sq	50.28%					88.41%				

* = Significant at P<0.05.

The summary of the mean values and standard errors of the initial, final redness and the kinetic rate constant values for the browning kinetics in pastry baking are shown in Table 4.13. Tukey's method at 95% confidence interval in the MINITAB software was also used to analyse the difference among the mean values of initial, final lightness and the kinetic rate constant values. The result showed that the initial redness values were not different but the final redness and the kinetic rate constant values were significantly different at the 95% confidence level. The difference in final redness and kinetic rate constant among pastry samples is indicated by the superscript letters a, b and c over the mean values. All statistic analysis results for the study of initial moisture content of the pastry on the browning kinetics are presented in Appendix A3.

Table 4.13 Mean and standard error of the initial, final redness and kinetic rate constant values (a^*_0, a^*_∞ and k_{a^*}) for pastry baking

Initial	a^*_0			a^*_∞			k_{a^*}		
%MC	N	Mean	S.E.	N	Mean	S.E.	N	Mean	S.E.
9.18	2	-2.97[a]	0.071	2	10.14[b]	0.354	2	0.08[ab]	0.014
10.95	2	-2.46[a]	1.039	2	12.16[ab]	0.000	2	0.08[ab]	0.014
22.92	2	-3.30[a]	0.367	2	13.54[a]	0.113	2	0.11[a]	7.07×10^3
33.89	2	-3.39[a]	0.007	2	12.56[ab]	0.389	2	0.06[bc]	0.00
44.55	2	-3.37[a]	0.191	2	10.91[b]	1.271	2	0.39[c]	4.95×10^3

Note: the letters a, b and c mean that samples that do not share a letter are significantly different at the 95% confidence level, using the Tukey's method.

It was surmised that the initial moisture content had an influence on the initial lightness, final lightness, final redness and kinetic rate constant for the redness change values in pastry baking. However, the initial moisture content had no effect on the initial redness and kinetic rate constant for the lightness change values. The changing of the redness was highly dependent on the amount of the water in the sample. This result was also found in other food products in which redness is dominant, such as blackberry juice heat treatment (Jiménez *et al*., 2012). It was reported that the effect of the water activity was found to impact the kinetic rate of the browning reaction as indicated by the redness value in blackberry juice during heat treatment. The kinetic rate increased with decreasing water activity (Jiménez *et al*., 2012).

However, there was no trend in the kinetic rate values change for the lightness data in this study of pastry baking. In addition, most of the studies on the browning kinetics of baking products preferred to use the lightness value as the key indicator for browning kinetic study. This is because the lightness (L^*) value is a good descriptor of the browning progress since it represents the intensity of images, and is decoupled from colour changes denoted by the a^* and b^* values (Gonzalez & Woods, 2008). The changes in lightness values during pastry baking were greater than that of the redness. Based on this it was concluded that the effect of the initial moisture content was insignificant for the browning kinetic of the pastry baking when using lightness as the measure of browning.

4.5 The effect of water evaporation on the temperature profile

The effect of initial moisture content on the kinetic rate was found to have an insignificant influence on the kinetic rate of the lightness (L^*) change. However the initial moisture content may affect the heat transfer in the pastry sample because of evaporation. The temperature of the bottom surface of the pastry where it is in contact with the hot pan and at the top surface were measured and plotted against time (Figures 4.10 and 4.11).

The temperature profile of the bottom surface of the pastry increased very quickly in the first 8 minutes of processing. After that the profiles were constant at around 158°C throughout the process (Figure 4.10). Because the heat up time of 8 minutes was deemed to be short compared to the total experimental time of 60 minutes, the assumption of it being an isothermal process was appropriate. The delay of temperature increase due to the evaporation of the water was not found at the bottom surface of the pastry. Hence, the browning reaction at the bottom surface of the pastry was not affected by the water content in the pastry sample.

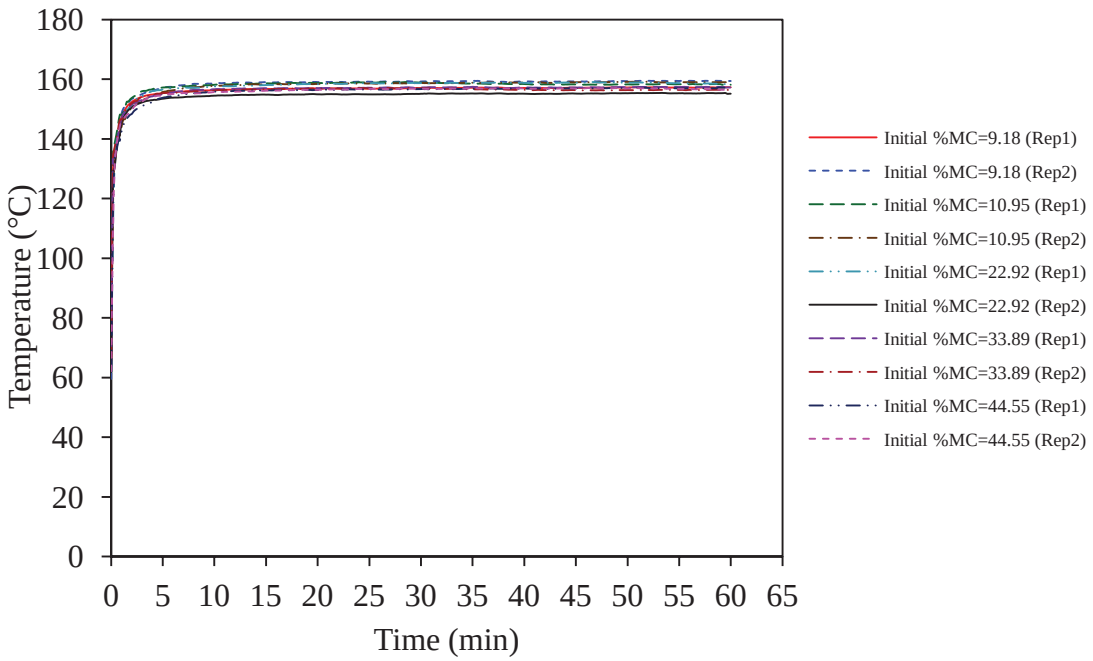

Figure 4.10 Temperature profile at the bottom surface of the pastry during baking at 160°C for 60 minutes for samples with different initial moisture contents

Temperature profiles of the top surface of pastry are shown in Figure 4.11. It is seen that the temperature profiles of all samples increased rapidly at the beginning of the process to the boiling temperature and then rose less quickly as latent heat for water evaporation was needed. This profile was also found in the frying of tofu (Baik & Mittal, 2003). Longer times for evaporating are seen in the samples with higher initial moisture content (%MC = 22.92, 33.89 and 44.55 wt% of d.b.); in contrast to the samples with lower initial moisture content (%MC = 9.18 and 10.95 wt% of d.b.) needed shorter evaporation times. This can be explained by the sorption isotherm curve of the pastry (Figure 4.7). To dry the pastry with higher initial moisture content, more heat was required to remove the water. It can be concluded that the initial moisture content of the pastry sample had an influence on the heat transfer in the pastry baking due to the water evaporation at the top surface of the pastry.

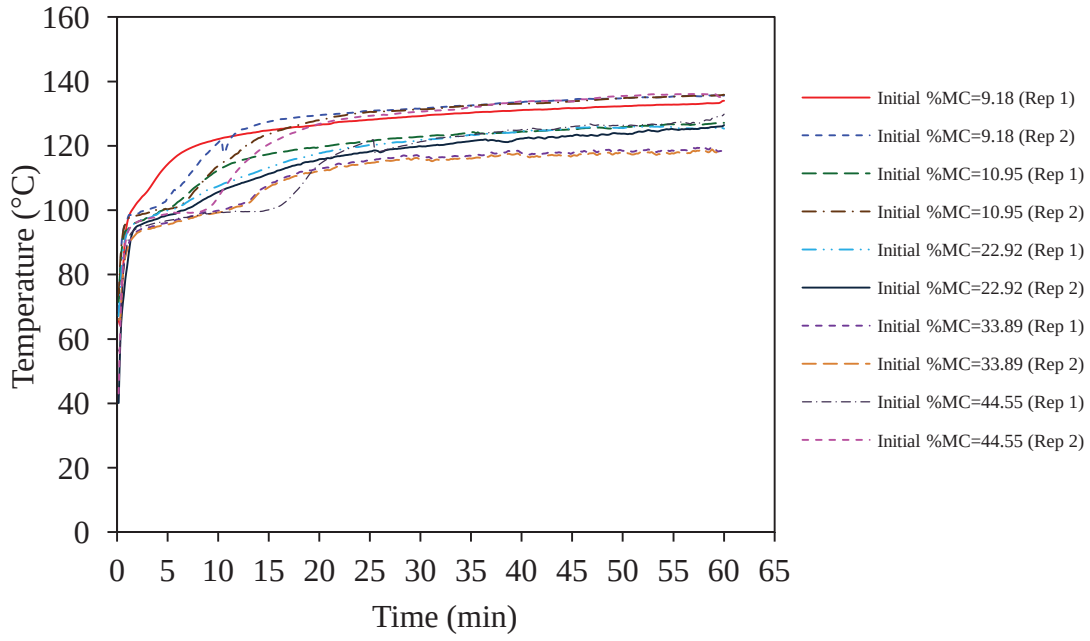

Figure 4.11 Temperature profile at the top surface of pastry during baking at 160°C for 60 minutes for all samples with different initial moisture contents

The lightness and redness values of the pastry at the top surface were measured and are plotted in Figures 4.12 and 4.13. The lightness values of all pastry samples slightly decreased during the earlier stage over 0 to 15 minutes of the baking process. The same occurred in the redness values, which changed little in this time period. This was because the water content in the pastry sample was being evaporated, maintaining the

top surface at 100°C. The browning reaction did not occur at this stage. After this stage the temperature increased and then the browning reaction started to take place as can be seen from the decreasing of the lightness and increasing of the redness profiles. However, the reaction rate was quite slow because the temperature at the top surface was not as high. It can be concluded that the browning reaction at the top surface of the pastry was affected by the heat transfer due to the water evaporation.

As the temperatures of all pastry samples at the top surface were not stable, this condition cannot be assumed to be isothermal. The first order kinetic model developed in section 4.3 cannot be applied to fit with these lightness and redness profiles. Nevertheless these results show that evaporation could be the reason why studies report an apparent effect of reducing browning rate at higher moisture content samples.

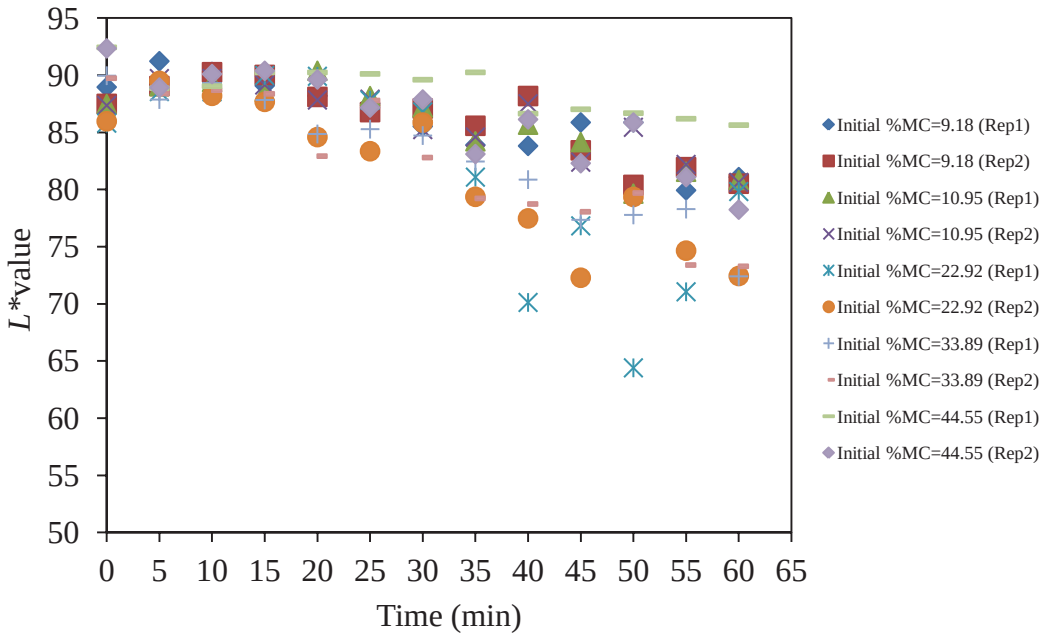

Figure 4.12 Lightness profile at the top surface of pastry during baking at 160°C for 60 minutes for samples with different initial moisture contents

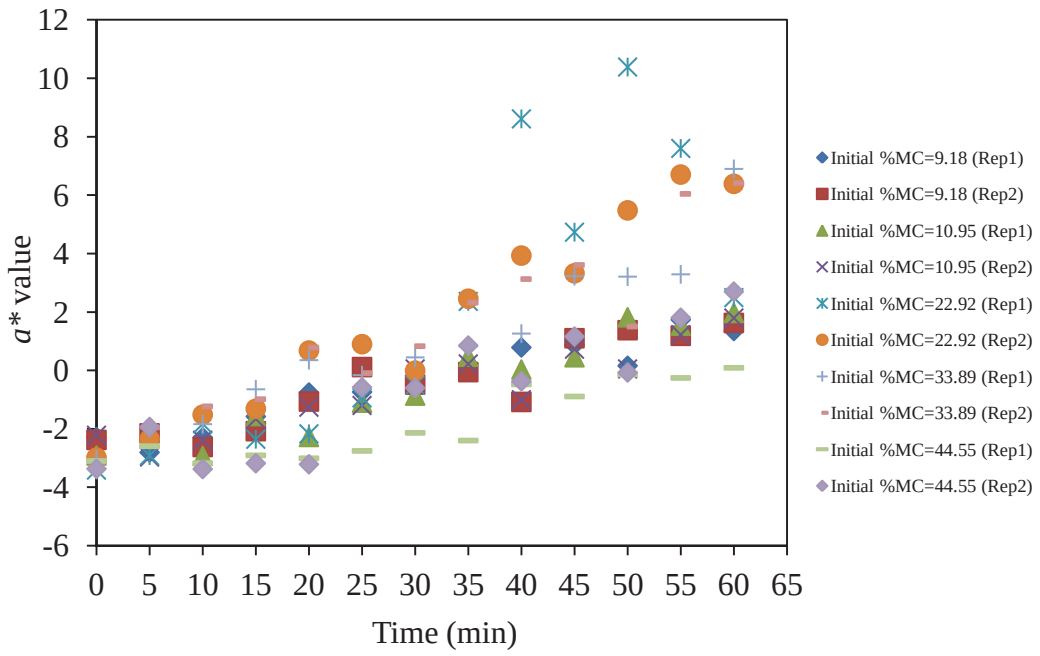

Figure 4.13 Redness profile at the top surface of pastry during baking at 160°C for 60 minutes for samples with different initial moisture contents

4.6 Conclusion

The finding of the preliminary studies showed that the Maillard browning reaction happening on the pastry surface during high temperature baking can be monitored by the colour measurement, which was represented by the values of lightness and redness. The lightness value was found to decrease with time as the sample became darker and the redness values increased over time. The change of these two colour values with time at the bottom surface of the pastry under the assumed isothermal condition followed first order kinetics. The reaction rate was faster during the early stages and slower during the later stages of the cooking period. This was due to a higher amount of the active reactants at the initial stage of cooking. The water content of the sample was expected to affect the reaction rate and this effect was therefore studied.

Using a ANOVA statistics test showed that the initial moisture content had no significant influence on the kinetic rate constant of the lightness (k_{L*}) for the browning reaction but it did affect the initial lightness ($L*_0$) and moderately affected the final lightness ($L*_\infty$). However, the initial moisture content had an effect on the kinetic rate constant of the redness data (k_{a*}). As the redness colour value was of less interest in

determining the browning kinetics of baked products, the effect of water content on the redness was not considered.

No significant effect of the initial water content on the lightness change was observed because the heat transfer rates to the pastry surface at the bottom area were very fast causing the water evaporation to occur so quickly the temperature profile was not affected. As a result there was no significant delay in the pastry surface reaching the pan temperature. However a lower heat transfer rate was found on the top surface of the pastry baking, which meant the water evaporation did affect the temperature profile of the top surface of the pastry. This was due to higher heat requirement for evaporation in the moist sample. In some heating systems however (e.g. baking), it is likely that a delay in temperature rise would occur due to evaporation. This effect could potentially explain the apparent slower browning rate at higher water content reported in some studies.

Therefore it was concluded that the browning reaction across the bottom surface of the pastry during baking took place under close to isothermal condition. The isothermal kinetic model was acceptable to describe the browning reaction of the pastry baking. The kinetic rate of the reaction depends on the cooking temperature not the water content consequently the water content would not be included in the kinetic model in future parts of this research.

Chapter 5

KINETIC MODEL DEVELOPMENT

5.1 Introduction

Chapter 4 showed that the Maillard browning reaction kinetics of pastry baking was well-represented by a first order reaction model. An assumed isothermal method was used to identify the kinetic parameters and the effect of the water content of the sample on the reaction rate. The results showed that the rate of the reaction was not significantly dependent on the water content of the sample. However the water content had an influence on the rate of heating due to the water evaporation, most evident at the top surface of the pastry sample during baking. Because of the rapid heat transfer at the bottom surface the evaporation phenomenon was not observed in the temperature profile where the browning reaction was measured.

Although there was a short heating period when the pastry samples were first added to the pan, the assumption of isothermal conditions at the bottom surface was acceptable. As such a study was carried out to evaluate the kinetics of pastry browning in the range of temperature baking 120°C to 170°C.

5.2 Browning rates in pastry as a function of baking temperature

The influence of temperature and time on browning kinetics has been confirmed by many studies for many foods and in many different cooking processes. In each case the process parameters of temperature and time both affected the rate or extent of the browning reaction.

Therefore, the temperature dependence of browning during pastry baking needs to be well understood. Six temperatures (120, 130, 140, 150, 160 and 170°C) for isothermal baking condition were used to study the temperature influence on the kinetic reactions. A uniform food (pastry), a constant condition cooking system (baking pan) and a browning evaluating method (image analysis) were all developed in Chapter 3 and were used in this study.

5.2.1 Method

As in the typical study in section 4.2, the commercial frozen savoury pastry brand of "Edmonds" was used as the model food for this study. The frozen pastry was thawed and cut into circular shapes using a cookie cutter. Round pastry samples with a diameter of 50 mm and the thickness of 2 mm were cooked on a hot pan with 5 replicates with 10°C temperature intervals from 120°C and 170°C for 60 minutes. Samples were removed randomly from one of four different baking positions after 5, 10, 15, 20, 25, 30, 35, 40, 45, 50, 55 and 60 minutes. Once removed, the samples were quickly cooled down in a stainless steel tray placed on ice to stop the browning reactions. All samples were photographed for image analysis using the system described in section 3.3.

5.2.2 Results and discussion

Figure 5.1 shows the plots of temperature history of the oil, pan and pastry surface during the cooking process at the lowest and highest temperature trials (120°C to 170°C). There was about a 2°C difference in temperature between the oil and the pan at steady state for all temperature levels. After the temperature of the pan was constant, the pastry samples were placed on the hot pan. The pastry surface temperature was measured using self-adhesive surface thermocouple probes and the data was collected by a data logger. After placing the samples, their temperature rapidly increased and took 8 minutes to come up to be the same temperature as the pan. After this short period, the pastry/pan interface surface temperatures showed a constant profile throughout the process. The constant temperature region was a very long compared with the short initial heating period. It was therefore assumed that this system approximated an isothermal condition.

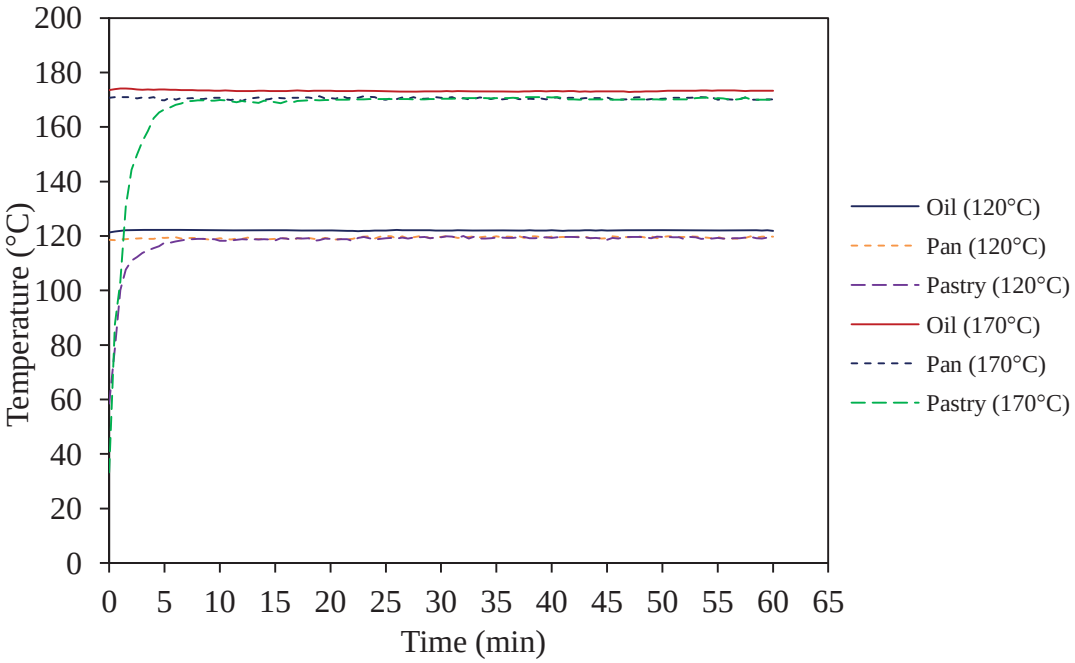

Figure 5.1 Temperature profile of oil, surface of pan and pastry for two different cooking conditions (120°C and 170°C)

Figure 5.2 shows photos of pastry cooked at six difference temperatures (120 to 170°C) for a variety of times from 0 min (not baked) up to 60 min. It can be seen that the intensity of colour of the pastry's surface increases with time and increasing temperature, as was expected. The initiation of browning was evident after 5 minutes of baking for all temperature conditions.

At the same temperature condition the pastry became darker when the baking time increased. By considering samples baked for the same time at different temperatures, it can be seen that the pastry sample was darker under higher temperature conditions. The darkest sample was found in pastry baked at 170ºC for 60 minutes, which was the highest temperature and the longest time of baking condition. The same results were reported in cookie baking (Shibukawa *et al*., 1989), hazelnut roasting (Demir *et al*., 2002), bread baking (Purlis & Salvadori, 2007, 2009) and fish grilling (Matsuda *et al*., 2013)

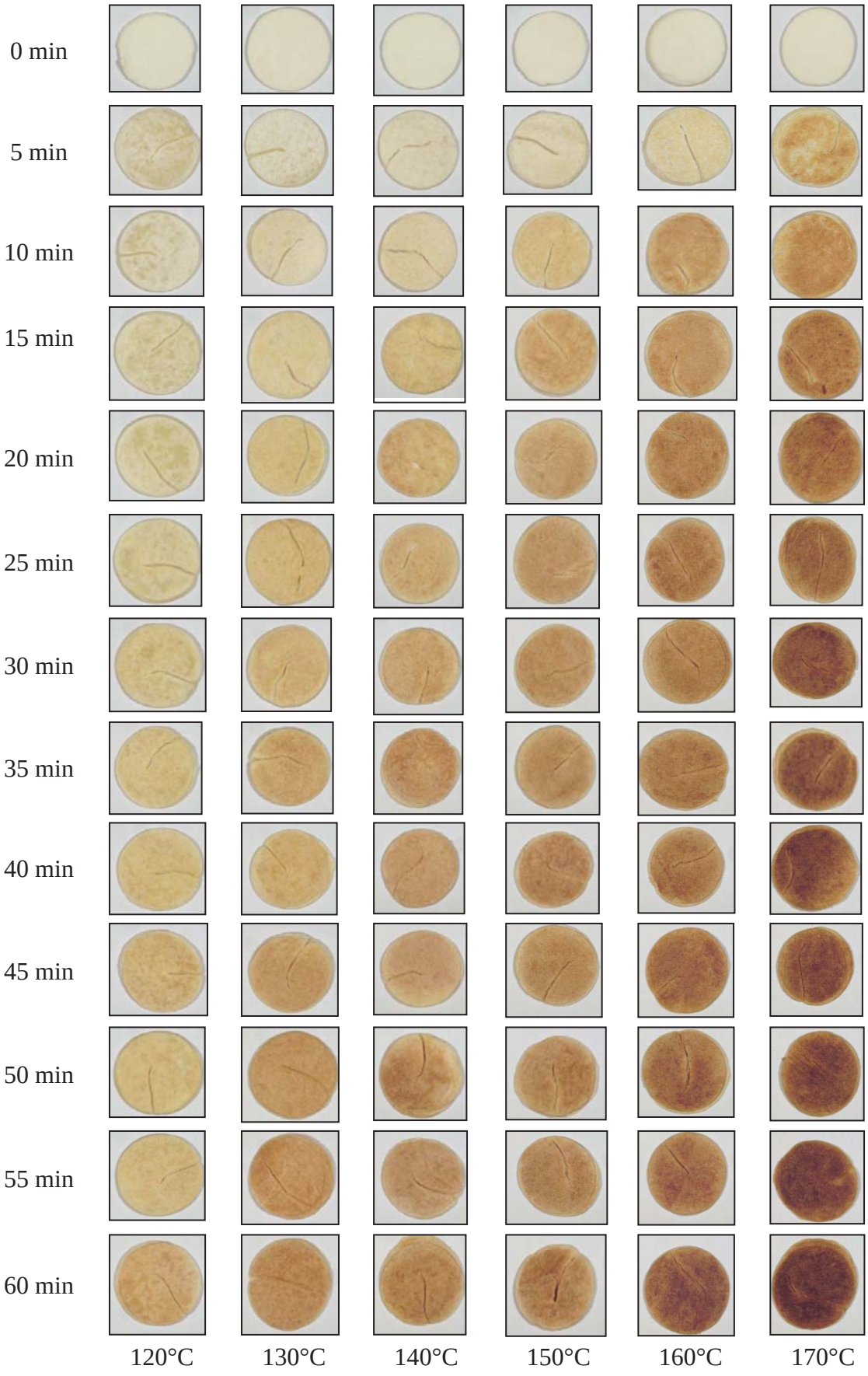

Figure 5.2 Image gallery of pastry samples cooked at six different cooking temperatures

The intensity of colour of the pastry's surface was determined by evaluating the colour parameters of *L*a*b** (CIE food colour system). Each sample has a distribution of colour. Thus there will be difference between the means of different samples. The average and standard error (S.E.) values of *L*a*b** were calculated from five replications. These are plotted against time and shown in Figures 5.3, 5.4 and 5.5 for *L**, *a** and *b**, respectively.

The lightness-time curve in Figure 5.3 shows a decreasing trend for all cooking conditions. During the first ten minutes of the study at low temperatures (120 and 130°C) the lightness rapidly dropped and increased again after fifteen minutes. This was due to the slow evaporation of water in the sample. This phenomenon was not evident at the high temperature conditions because the water evaporation occurred quickly. The slow evaporation resulted in the water moving to the sample surface, so this gave a light reflection over the surface when the photo of the sample was taken. After that the lightness of the pastry surface continuously decreased with time for all experimental baking conditions. Shibukawa *et al*. (1989) used a similar explanation for an increase in *L** at the start of biscuit baking. This behaviour was found in bread baking, but the explanation was that at the initial stage of baking the wrinkle at the dough surface of bread occurred and after that the surface of bread turned smooth (Broyart *et al*., 1998 and Purlis & Salvadori, 2007).

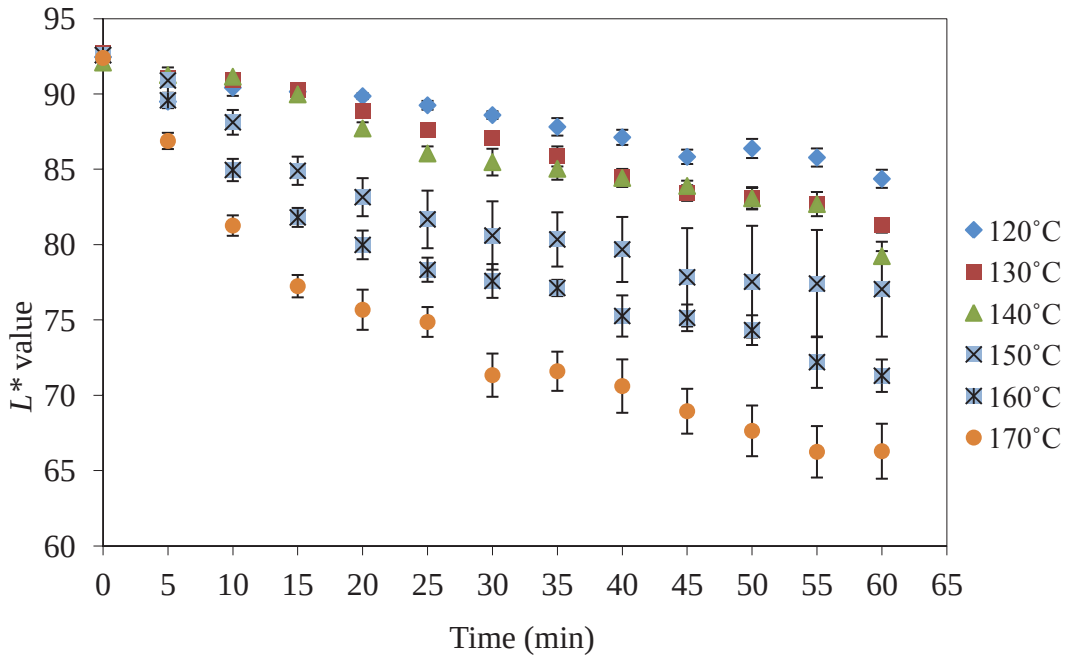

Figure 5.3 Variation of lightness (*L**) at pastry surface as a function of baking time

It can be seen from Figure 5.4 that the redness values (a^*) of the pastry surface increased with both increasing cooking temperature and time during the cooking process for all experimental conditions. It can be assumed that this redness was due to the Maillard reaction. Even so, the variation is small, especially at the lower temperature baking conditions. The same result was discovered by Ilo & Berghofer (1990) who studied the kinetics of colour change during extrusion cooking of maize grits.

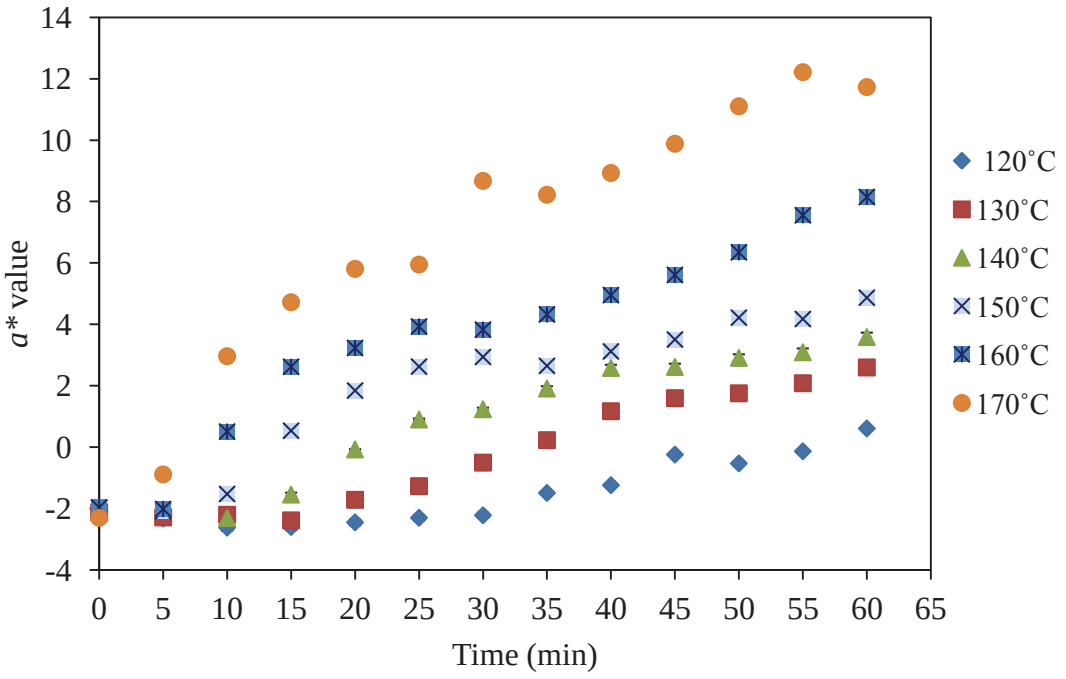

Figure 5.4 Variation of redness (a^*) at pastry surface as a function of baking time

There is no trend in the yellowness values (b^*) for all cooking temperature conditions. The graph shows a random pattern (Figure 5.5). It cannot be concluded that the cooking conditions (time and temperature) have an influence on the yellowness value (b^*) for pastry cooking. Therefore the data of yellowness was not fitted with any kinetic model.

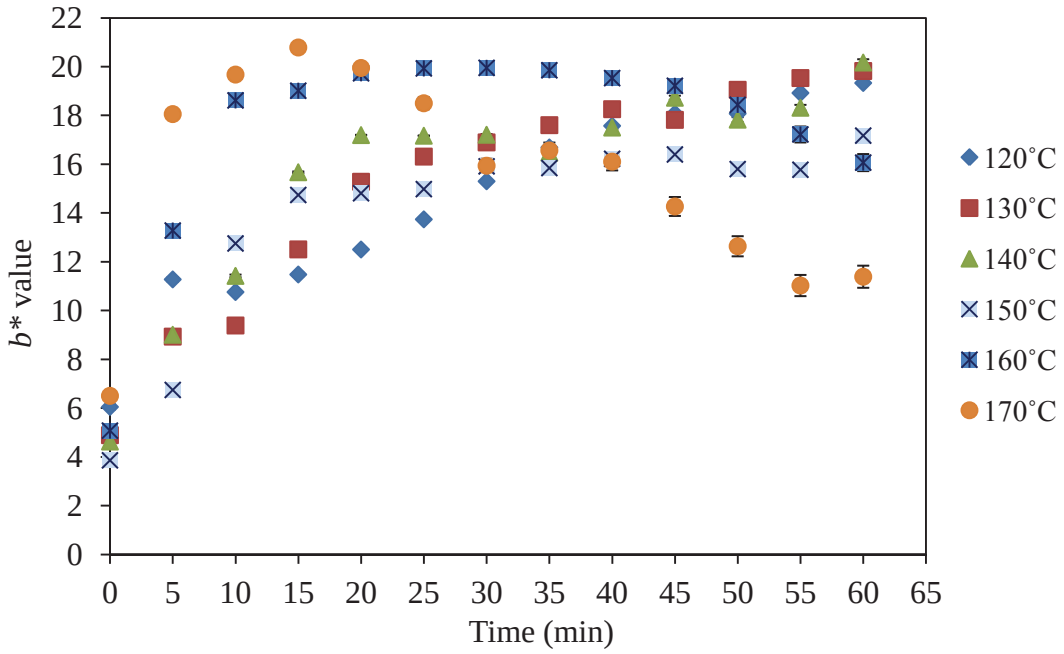

Figure 5.5 Variation of yellowness (b^*) at pastry surface as a function of baking time

5.2.3 Kinetic model fitting

The kinetic model for describing the variations of the lightness and redness-time curves due to browning reaction was developed in section 4.3. It was demonstrated that the development of browning in pastry during baking can be well described by the first order kinetics. Under isothermal conditions the first order rate equation (4.1) can be integrated and rearranged to predict the colour values of L^* for lightness and a^* for redness as a function of time (Equation 4.4).

$$L^*_{predicted} = L^*_{\infty} + (L^*_0 - L^*_{\infty})\exp(-kt) \tag{4.4}$$

The relationship of the browning reaction rate constant (k) to temperature was quantified by the Arrhenius equation (Equation 5.1).

$$k = k_0 \exp\left(-\frac{E_a}{RT}\right) \tag{5.1}$$

where k_0 is the Arrhenius constant (min^{-1}), E_a is the activation energy ($kJ \cdot mol^{-1}$), R is the universal gas constant (8.3145 $J \cdot mol^{-1} \cdot K^{-1}$) and T is absolute temperature (K). A reference temperature (T_{ref}) was introduced to rescale the parameters (Haralampu *et al*, 1985; Nunes *et al*., 1993 and Figueira *et al*., 2011). This alteration results in

replacement of the Arrhenius constant (k_0) with the rate constant at the reference temperature (k_{ref}). This allows more direct comparison of kinetic parameters in relevant conditions for different systems (Figueira *et al*., 2011). The Equation 5.1 can be therefore rewritten as:

$$k = k_{ref} \exp\left(-\frac{E_a}{R}\left(\frac{1}{T} - \frac{1}{T_{ref}} \right) \right) \tag{5.2}$$

The best reference temperature for kinetic reaction was suggested to be the middle of the temperature range for the experimental study condition (Lima *et al*., 2010), so the temperature of 150ºC was chosen for this study. The parameters L^*_0, L^*_∞, k_{150} and E_a in Equations 4.4 and 5.2 were fitted to all the data of the lightness values simultaneously by minimizing the residual sum of squared errors by non-linear regression with a Levenberg-Marquardt algorithm function *lsqcurvefit* using MATLAB® (version 6.5 The Mathworks Inc, Natick, Mass. U.S.A). The MATLAB® code for this fitting is presented in Appendix A4.

The fitted profile is compared with the experimental data points of L^* values of pastry baked at six different temperatures in Figure 5.6. The model profiles show a good fit between the experimental data and the predicted values. The goodness of fit (R^2) was calculated as 0.92. The initial lightness value (L^*_0) of the pastry surface in the experiment was measured as 92.58. It can be concluded that colour change was successfully modelled as a first order process, the temperature effect in rate constant being predicted by the Arrhenius equation.

The kinetics parameters (k_{150} and E_a) were found to be 0.017 min^{-1} and 65.93 $kJ \cdot mol^{-1}$, respectively. In general the activation energies for non-enzymatic browning in foods are between 37.0 and 167 $kJ \cdot mol^{-1}$ (Villota & Hawkes, 2007). This calculated activation energy for L^* value in this work is similar to the values reported in bread based food products (45.3 and 70.81 $kJ \cdot mol^{-1}$) (Zanoni *et al*., 1995; Zuckerman & Miltz, 1997; Broyart *et al*., 1998 and Zhang & Datta, 2006). It is also worth nothing that it was possible to fit the model well with a common L^*_∞. This suggests that the steady state browning colour is not a function of temperature.

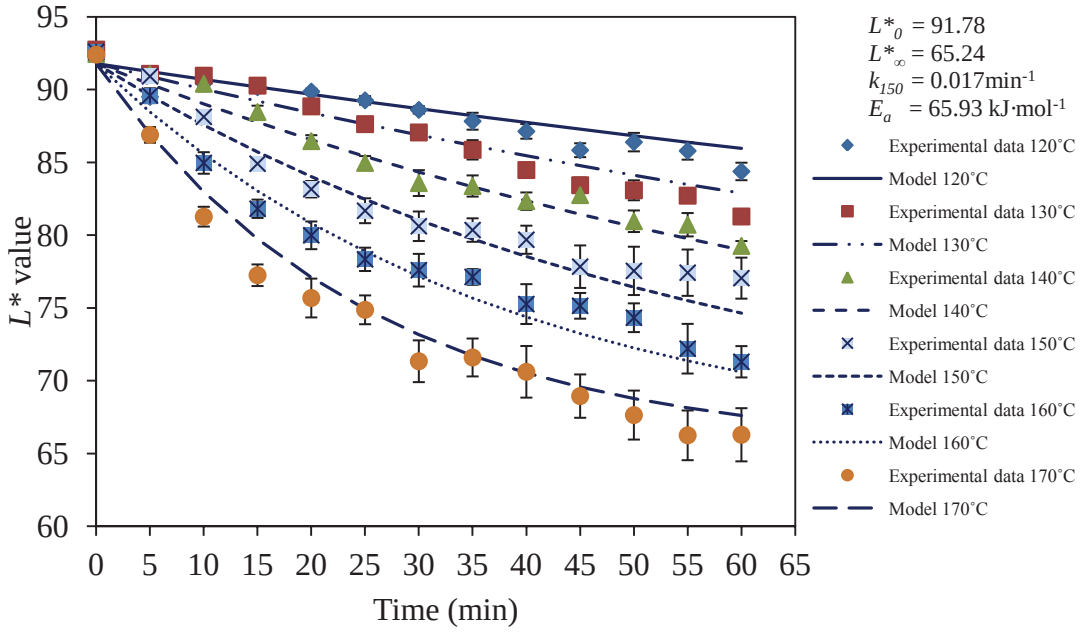

Figure 5.6 Fitted profile of the first order kinetic model compared with the experimental lightness values (L^*) measured using the image analysis for pastry baked at six different temperatures

The kinetics were also fitted with the lightness-time curve data obtained from the spectrophotometer to observe the kinetic change of the browning colour on pastry surface during baking (Figure 5.7). The graph shows that the model can fit well with the experimental data of lightness profiles. The estimated kinetic parameters were obtained as L^*_0 = 84.22, L^*_∞ = 46.09, k_{150} = 0.015 min^{-1} and E_a = 65.12 kJ·mol^{-1}. The goodness of fit (R^2) for this fitting was 0.89. These estimated kinetic parameter values were very similar to the kinetic parameters from the fit using the image analysis method. This result demonstrated that both colour measurement methods (image system and spectrophotometer) were able to be used for measuring the colour change of food sample during cooking.

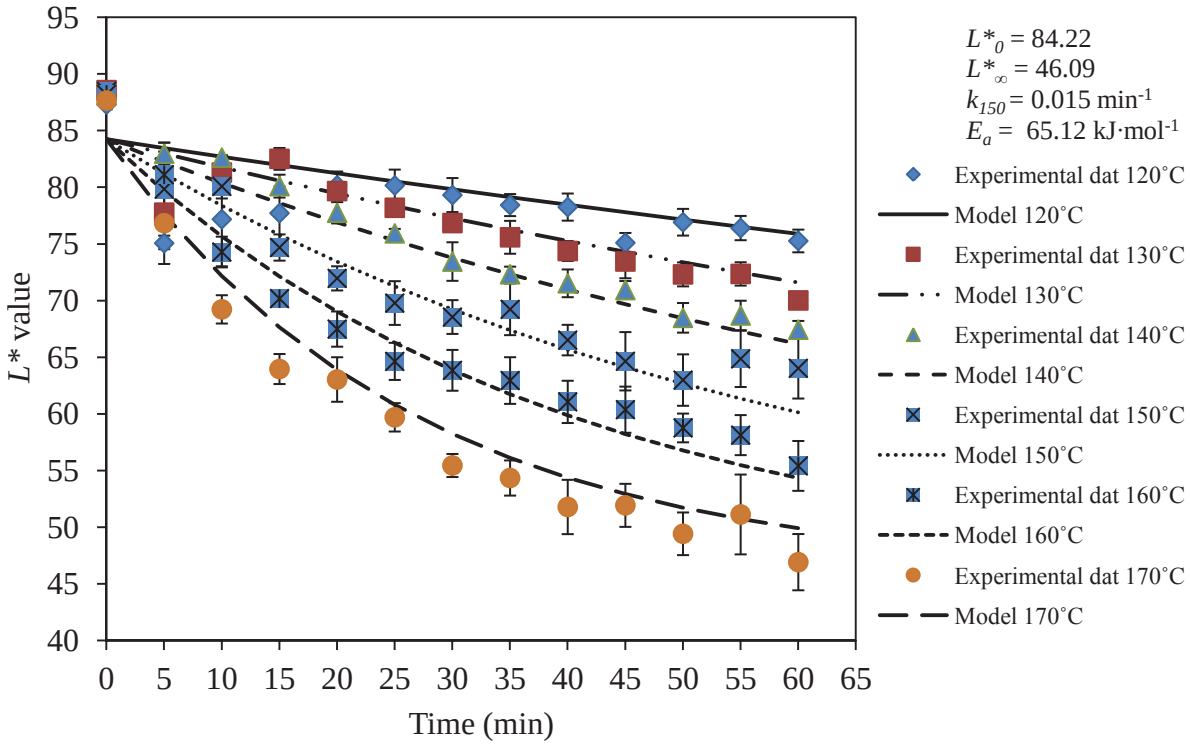

Figure 5.7 Fitted profile of the first order kinetic model compared with the experimental lightness values (L^*) measured using the spectrophotometer for pastry baked at six different temperatures

These results showed that the kinetics are the same for spectrophotometer and image data as expected for 1'st order kinetics. From Figure 3.11, it can be seen that L^*_{sp} is a linear function of L^*_{im} and can be represented the equation below.

$$L^*_{sp} = mL^*_{im} + C \tag{5.3}$$

Where m is the calibration slope and C is a systematic offset (intercept), the kinetic equation is;

$$\frac{dL^*_{sp}}{dt} = -k\left(L^*_{sp0} - L^*_{sp\infty}\right) \tag{5.4}$$

by substituting (5.3) into (5.4) giving;

$$\frac{d}{dt}\left(mL^*_{im} + C\right) = -k\left(mL^*_{im} + C - \left(mL^*_{im\infty} + C\right)\right) \tag{5.5}$$

$$m\frac{dL^*_{im}}{dt} = -km\left(L^*_{im}\ L^*_{im\infty}\right) \tag{5.6}$$

$$\frac{dL^*_{im}}{dt} = -k\left(L^*_{im} - L^*_{im\infty}\right) \tag{5.7}$$

For this reason the value of k should not be altered by the difference in L^* measurement by the two methods.

Figure 5.8 shows a similar first order model can explain the kinetics of change in the colour parameter a^*. They were fitted using the same model as for L^* (Equations 4.4 and 5.1). The goodness of fit (R^2) was found to be 0.90. The kinetic rate constant at the reference temperature of 150°C (k_{150}) and the activation energy (E_a) for the redness change was found to be 0.012 min^{-1} and 70.0 $kJ{\cdot}mol^{-1}$, respectively. These estimated kinetic parameters are of similar magnitude as that found for lightness (L^*) (65.93 $kJ{\cdot}mol^{-1}$ and 0.017 min^{-1}) suggesting both physical colour parameters reflect changes in browning product formation (melanoidins). Ilo & Berghofer (1999) reported similar comparative activation energy for a change in L^* (65 $kJ{\cdot}mol^{-1}$) and a^* (74 $kJ{\cdot}mol^{-1}$) and kinetic rate constant at the reference temperature of 150°C (k_{150}) for a change in L^* (0.19 min^{-1}) and a^* (0.15 min^{-1}) during extrusion of maize grits. These kinetic parameters are also similar which would be expected if they are measures of the same reaction.

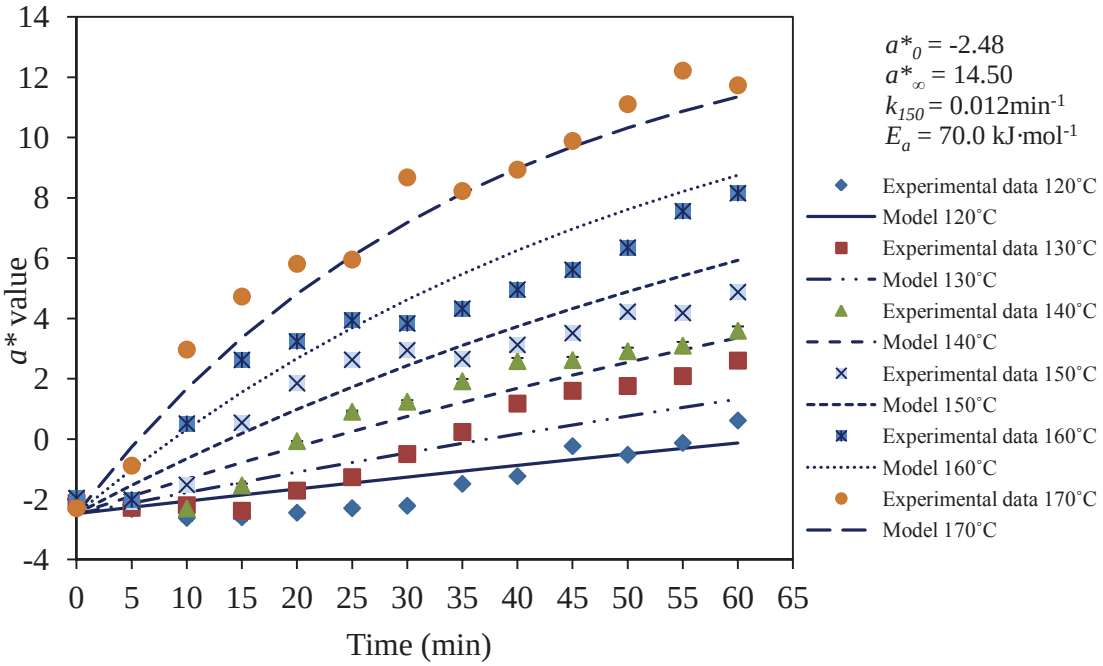

Figure 5.8 Fitted profile of the first order kinetic model compared with the experimental redness values (a^*) measured using the image analysis for pastry baking at six different temperatures

The redness values (a^*) obtained from the spectrophotometer was also fitted with the first order kinetic model using the same method as described before as shown in Figure 5.9. The goodness of fit for this graph was obtained as 0.91. The kinetic parameters of initial, final redness, kinetic rate constant and activation energy (a^*_0, a^*_∞, k_{150} and E_a) were estimated to be -1.69, 14.64, 0.05 min^{-1} and 66.95 $kJ \cdot mol^{-1}$, respectively. The activation energy from this fit is very similar to the value for the lightness change, however the rate constant at 150ºC was nearly double. The differences in kinetics between these values and those derived from the image analysis a^* measurement mean that a^* kinetics were not investigated in the remainder of the research.

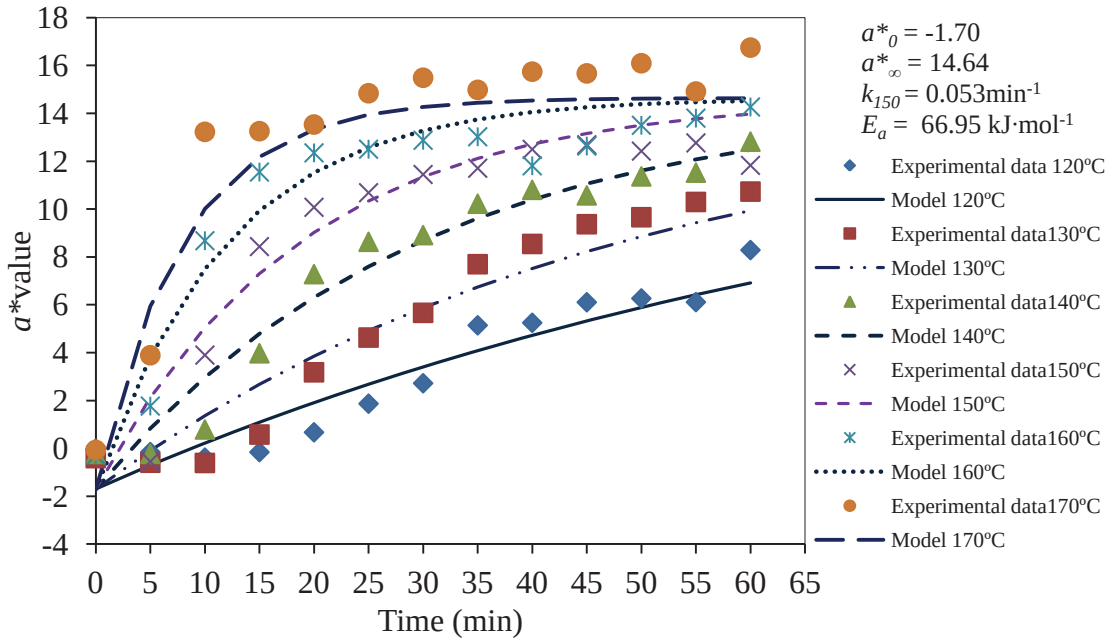

Figure 5.9 Fitted profile of the first order kinetic model compared with the experimental redness values (a^*) measured using the spectrophotometer for pastry baked at six different temperatures

This study showed that the effect of both cooking temperature and time was significant for the pastry surface. Colour change due to the browning reaction was analysed as first order kinetics and the browning reaction kinetics for pastry cooking sensitivity to temperature was described well by the Arrhenius equation. The browning development can be monitored by image analysis. The L^* parameter was the most suitable parameter to follow the browning on the pastry surface cooked under isothermal conditions because this parameter had the highest response during baking. In addition, the kinetic fit of the lightness change was better than that of the redness change, as denoted by the goodness of fit. Therefore the L^* parameter was used to indicate the browning reaction in this study. From the kinetic fitting, the kinetic parameters (L^*_0, L^*_∞, k_{150} and E_a) were obtained. These kinetic values were used to predict the browning of the pastry during baking as a function of the local temperature at the pastry surface in the next section.

5.3 Non-isothermal kinetic model development

The cooking temperature profile in a real food process follows a non-isothermal profile, so analysing the trial solution with an isothermal assumption as in section 5.2 was unlikely to achieve a perfect prediction. It was reported in the literature that it may not

work to apply conventional isothermal kinetic concepts as browning is highly temperature dependent (Purlis, 2010). Potential errors would be expected if the time-temperature history is neglected when the kinetic parameters are estimated. From this fact, using a non-isothermal kinetic approach is a more applicable method for the model of the colour development at the pastry surface during baking where the thermal history can be taken into account (Purlis & Salvadori, 2009 and Purlis, 2010).

It was found in this study, that the beginning of the process of pastry baking showed an unsteady state in the temperature profile. Water evaporation at the top surface of the pastry baking was also evident causing non-isothermal conditions.

The extent to which assuming isothermal conditions had on the kinetic parameters can be assessed by predicting the colour change using these values together with the actual temperature history using a non-isothermal model. Therefore the objective of this section was to develop and test a non-isothermal kinetic model to predict the lightness change of pastry baking using time-temperature history for each experimental sample.

5.3.1 Mathematical model formulation

To develop the mathematical model formulation for browning under non-isothermal conditions, the measured data file of time-temperature history was imported as an input data to the model.

The browning development on the pastry surface indicated by the lightness value (L^*) was predicted using first order kinetics (Equation 4.1).

$$\frac{dL^*}{dt} = -k\left(L^*_0 - L^*_\infty\right) \tag{4.1}$$

The assumptions for this kinetic model were:

- The browning rate constant (k) was related to the pastry surface temperature only. It was not correlated with moisture content of the pastry sample.
- The rate constant effect of temperature is predicted by the Arrhenius-relationship (Equation 5.8).

$$k = k_{ref} \exp\left(-\frac{E_a}{R}\left(\frac{1}{T} - \frac{1}{T_{ref}} \right) \right) \quad (5.8)$$

- T is the temperature (K) of the pastry surface, which varies with time during baking or it is a function of time T = f(t). The recorded data of time-temperature was saved in a data sheet file of Excel to be called as an input data for model solution step.
- The final lightness value (L^*_∞) was constant at the same value where the Maillard browning reaction was complete for all cooking conditions, because then there will be no further change of the lightness.

5.3.2 Model solution

The numerical solution for this kinetic model was solved using MATLAB® with the function ode45 used to solve the model. At each time step the temperature was calculated by interpolation between the experimental temperature data that were imported directly into MATLAB® for each experiment. The code is presented in Appendix A5. The estimated kinetic parameter values of L^*_0, L^*_∞, k_{150} and E_a obtained from the isothermal fit in section 5.2 were used as the initial system input to the model for this solution and are listed in Table 5.1.

Table 5.1 Kinetic parameters fitted using isothermal model in section 5.2

Parameters	Values
L^*_0 (Initial lightness)	91.78
L^*_∞ (Final lightness)	65.24
k_{150} (Kinetic rate constant at 150ºC) (min^{-1})	0.017
E_a (Activation energy) ($kJ \cdot mol^{-1}$)	65.93

Time-temperature data histories of the pastry surface at the baking temperature of 120, 130, 140, 150, 160 and 170ºC for 60 minutes for 5 replications in an Excel file were called into the non-isothermal model to predict the lightness profile for all of the experimental study conditions from 120 to 170°C. The predicted lightness curve was plotted in comparison with the experimental data for each experimental condition. An example of the time-temperature graphs and a comparison of the lightness prediction

with the experimental lightness profile at 150°C cooking condition is shown in Figure 5.10.

From the graph, it can be seen that the lightness trend decreases during processing time in both of experimental and predicted values. However, the predicted lightness profile does not fit well with the experimental lightness data. The lightness values for the prediction were higher than that of the experimental data values. It can be also seen that at the start of heating the predicted lightness profile was curved due to the non-isothermal condition at this stage. This suggests that the temperature dependence of the reaction (E_a) is too high.

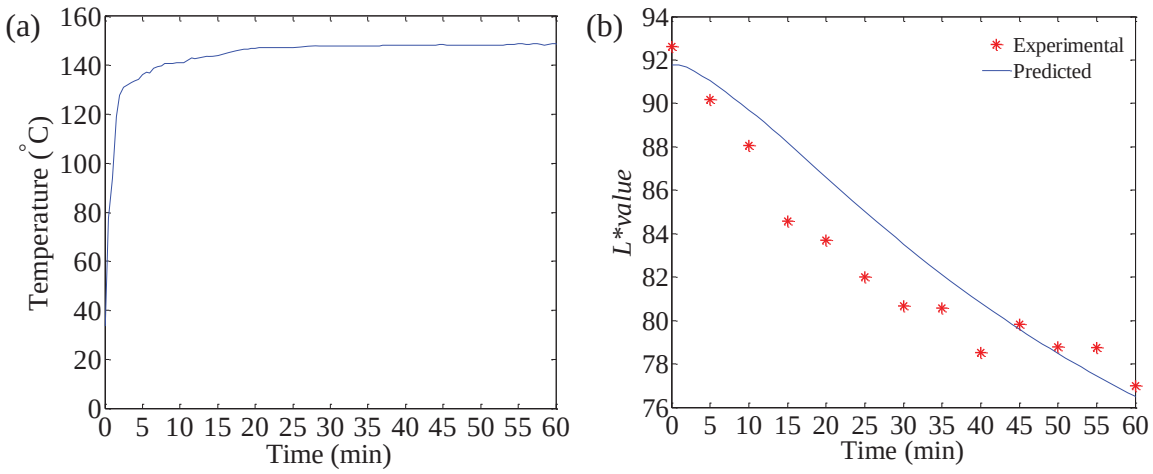

Figure 5.10 Example plots of the input temperature history and the prediction using the non-isothermal model: (a) experimental data for the temperature history of pastry surface at 150°C and (b) the lightness prediction and experimental data for pastry baking at 150°C for 60 minutes

The applicability of this model solution with the kinetic parameters obtained from the isothermal solution for predicting lightness of pastry surface was tested for all cooking conditions. A comparison of lightness, as predicted by the model, and the experimental data for all conditions, is shown in Figure 5.11.

The figure was plotted for individual groups of cooking conditions to show clearly whether the model performed well for lightness prediction under different conditions or not. The comparison revealed that, overall; the model over-predicted the lightness values by about eight units. This shows an unsatisfactory fit between the predicted and

experimental values. In addition, the calculated goodness of fit was low (R^2 = 0.88). The over-prediction of the lightness value was due to the input kinetic parameters provided for the model.

This leads to the conclusion that, using kinetic parameter values from the isothermal assumption were inapplicable for predicting the lightness development under temperature dependent conditions of non-enzymatic browning reaction. Therefore, better estimated kinetic parameters were needed to better characterise the browning kinetics. This will be developed in the next section.

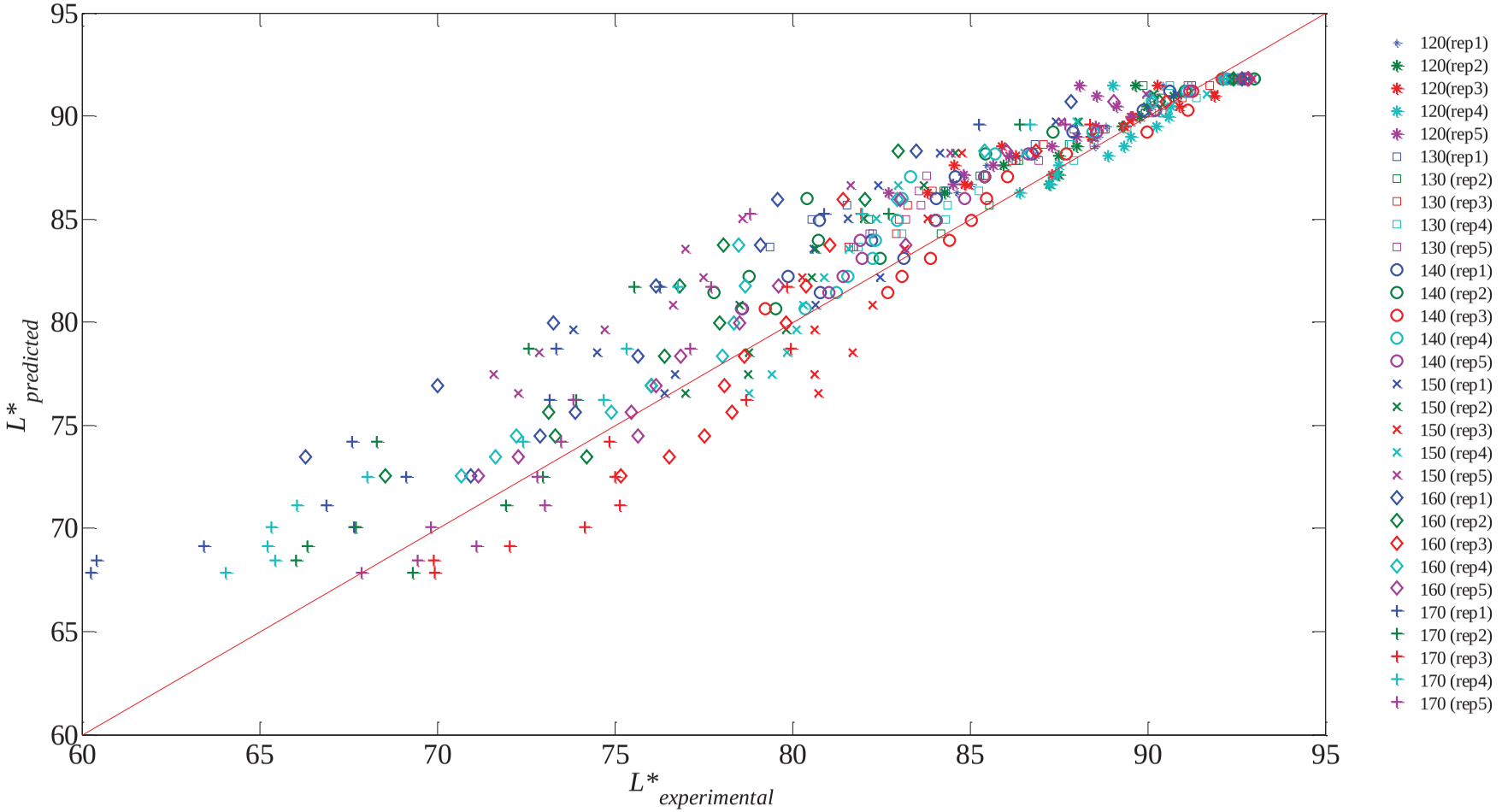

Figure 5.11 Plot of experimental data versus predicted lightness for all experimental conditions

5.4 Kinetic parameter estimation using non-isothermal kinetic model

Even though the prediction method in the section 5.3 used the actual temperature of each experimental condition into the model to solve and predict individual values of lightness for each condition, the prediction was unsatisfactory. This was because this non-isothermal solution used the kinetic parameters from the isothermal solution to predict the lightness change. Therefore, the objective of this section was to use the non-isothermal kinetic model to estimate the best values of the kinetic parameters, which best predict the lightness change of pastry baking using the time-temperature history for each experimental sample.

The MATLAB® code for estimating the kinetic parameters using the non-isothermal method was written to be able to achieve the best kinetic parameter estimation and lightness change prediction (Appendix A6). The MATLAB® function *lsqnonlin* was used to optimise the kinetic parameters using the non-isothermal model described in section 5.2.3 above, starting with initial parameter guesses as those from isothermal model fit (Table 5.1). The residuals between all experiments and their predicted L^* values were calculated by solving the nonlinear model using ode45 and the experimentally measured temperature data. The nonlinear solver then reran this function with redefined input parameters until an optimised solution was obtained.

The experimental data for temperature history and lightness profile for five different temperature conditions with five replications trials were used for the solution. The best estimated kinetic parameters were optimized and exported to an Excel file, including the lightness prediction values developing with time for each temperature sample of all experimental conditions. The list of optimized kinetic parameters is illustrated in Table 5.2.

The new kinetic parameters from the optimizing method are different from the values from the isothermal model fitting parameters (Table 5.2). The estimated initial lightness value (L^*_0) had only a small change from 91.78 to 91.21; the final lightness (L^*_∞) changed from 65.24 to 67.83. The kinetic rate constant at 150ºC (k_{150}) and the activation energy (E_a) increased considerably from 0.017 to 0.025 min^{-1} and 65.93 to71.9 $kJ \cdot mol^{-1}$, respectively. The new estimated activation energy was in the range of the activation energy for non-enzymatic browning in foods (37 and 167 $kJ \cdot mol^{-1}$) (Villota & Hawkes,

2007), but slightly higher than that of the bread based food product (45.3 and 70 kJ·mol^{-1}) (Zanoni *et al*., 1995; Zuckerman & Miltz, 1997; Broyart *et al*., 1998 and Zhang & Datta, 2006).

Table 5.2 Optimized kinetic parameters of pastry baking fitted using actual recorded surface temperature as model inputs

Parameters	**Values (section 5.23)**	**Values (revised)**
L^*_0 (Initial lightness)	91.78	91.21
L^*_∞ (Final lightness)	65.24	67.54
k_{150} (Kinetic rate constant at 150ºC) (min^{-1})	0.017	0.025
E_a (Activation energy) (kJ·mol^{-1})	65.93	71.9
R^2 (Goodness of fit)	0.88	0.92

The output of numerical solution of the lightness prediction for all experimental samples of pastry baking using the optimization of kinetic parameters is demonstrated in Figure 5.12.

The model predicted the lightness for all study experiments moderately well. The goodness of fit (R^2) was calculated as 0.92, which was greater than that of the fit using the isothermal kinetic parameters (section 5.3). The new kinetic parameters provided a better prediction than using the kinetic values from the isothermal method. However, bad predictions were found at low values of the lightness for the high temperature baking conditions. The over and under prediction was by up to 5 units. This may be because the sample started to combust at high temperatures and long time. The complicated chemical mechanism of the Maillard browning reaction may be another factor affecting this observation.

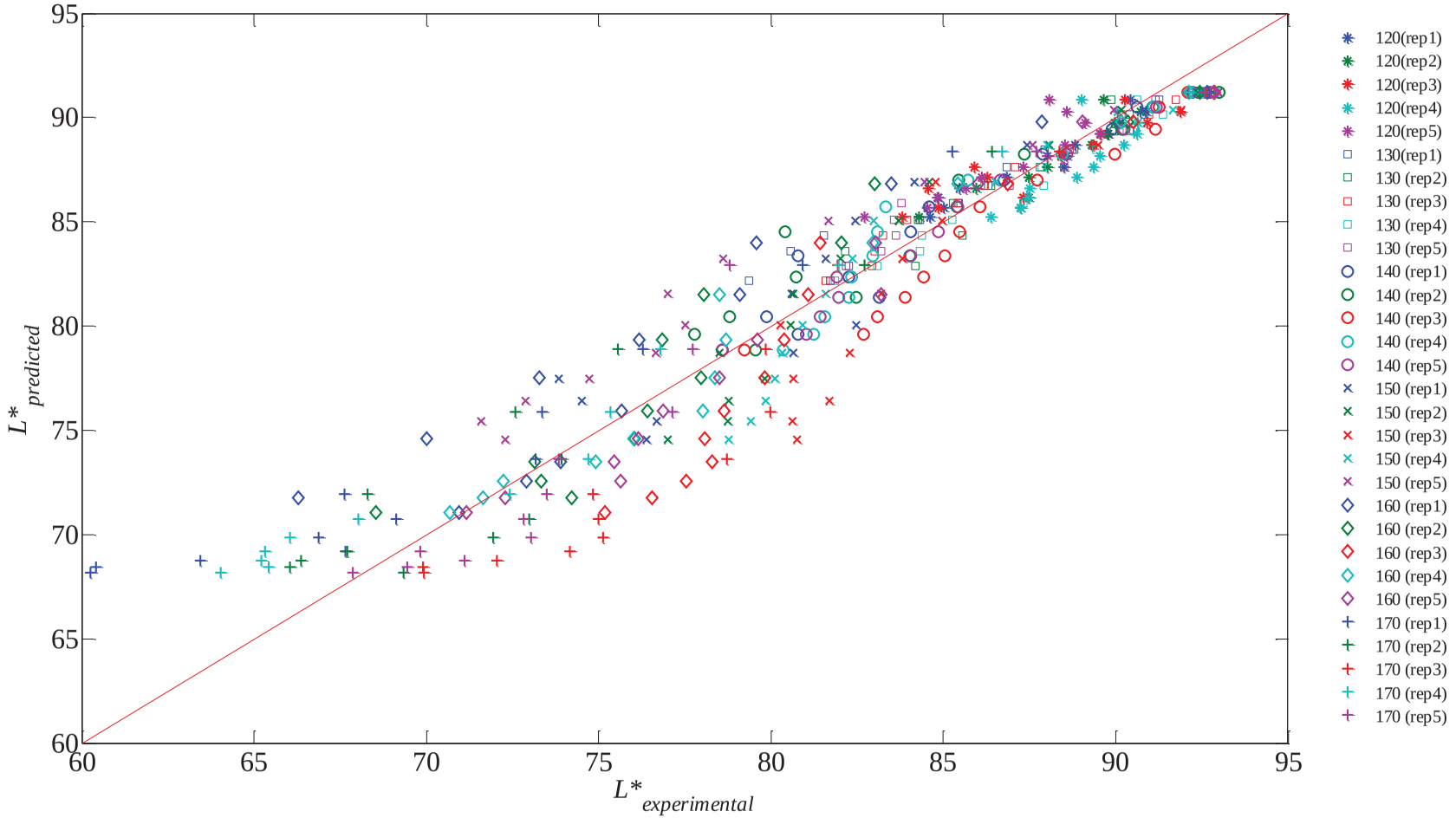

Figure 5.12 Plot of experimental data for all experimental condition versus lightness predicted using the kinetic parameters fitted by non-linear regression

5.5 Conclusion

This chapter has outlined the development of a non-isothermal kinetic model to explain the browning on the pastry baking. The best estimated kinetic parameters were obtained by optimising the kinetic parameters value using the non isothermal model ode45 and *lsqnonlin* functions to get the best fit. The validation and application of the model are illustrated and discussed in the next chapter.

Chapter 6

MATHEMATICAL MODEL VALIDATION

6.1 Introduction

A model for browning kinetics of pastry during high temperature baking under non-isothermal conditions was developed in Chapter 5. The model showed good results in predicting the browning formation on the pastry surface during baking. For further validation of the model, it was applied to predict lightness values observed in independent experiments in this chapter. Generally, baking is operated under variable non-isothermal heating conditions, therefore data for validating the model was collected by using varying time-temperature protocols.

The time-temperature histories for non-isothermal pastry baking conditions were designed to provide a range of dynamic temperature scenarios for generating the different patterns of browning colour formation. As the heating pan was used in the former studies for baking the pastry, this well controlled baking instrument was used in this study to provide the baking scenarios.

In addition, pastry is normally baked in the oven, so the experimental data for browning formation obtained under oven baking conditions were investigated for validating the developed model. The oven extends application of the model to convection heat transfer condition for pastry baking.

6.2 Experimental validation of browning model in temperature variable pan baking conditions

To test the performance of the mathematical model, validation was performed by comparing the model's output with data obtained from a series of experiments in which

non-isothermal cooking conditions were experienced. The cooking condition with conduction heat transfer was studied using the hot pan cooking system (section 3.4) because with this cooking system it was possible to develop different heating pattern scenarios. The experimental design for investigating the data to validate the browning kinetic model in the non-isothermal cooking system was created and is discussed in this chapter.

6.2.1 Method

Pastry samples were used in the validation study with the same preparation method as used in the kinetic study and baked on the same hot pan (section 5.2). Experiments were carried out at various cooking temperatures under non-isothermal conditions. Non-isothermal cooking scenarios were created for eleven patterns of temperature profiles. The temperature of the pan was controlled by manually turning on and off the oil heating element. The surface of the pan was divided into four sections, so four replicate pastry samples could be used in each experiment. The extent of browning was only measured at the completion of the experiment.

The temperature histories of the pastry for both of bottom and top surface at the four baking positions on the pan were measured using surface-thermocouples and logged throughout the process. These are presented in Figures 6.1-6.11 for cooking experiments 1 to 11, respectively. All figures show the temperature profiles at the bottom and top surface of the pastry. The symbols of P1, P2, P3 and P4 in the figures correspond to the temperature profile of the pastry at positions 1, 2, 3 and 4 in the pan, respectively.

Each experimental scenario was designed to have a different pattern of temperature profile and different cooking times. The descriptions of each experimental scenario are discussed. For experiment 1, the pan was heated up for the first 10 minutes to a maximum temperature of 130°C, and the system was held at this temperature for 10 minutes. Then the cooking system was turned off to let the temperature slowly drop until a total processing time of 180 minutes elapsed (Figure 6.1).

Experiments 2 and 3 were run with the same set point temperature as the experiment 1 (130°C) but they were different in terms of processing time. Experiments 2 and 3 took 8

minutes to increase the cooking temperature up to 130°C, and were held at this temperature for 5 minutes; then the cooking system was turned off. After stopping the cooking system, the temperature of the system slowly decreased, and then the samples were removed after 14 minutes for experiment 2 and 60 minutes for the experiment 3.

Experiments 4 and 5 had two periods of heating (Figures 6.4 and 6.5), with a maximum temperature of 130ºC for experiment 4 and 150°C for experiment 5. The temperatures of these experiments were increased to the set temperature in the first period taking 8 minutes. The systems were held at this temperature for 5 minutes; then the temperatures were decreased for 60 minutes, and the process was repeated by re-heating up to the set point temperature, holding at this temperature for 5 minutes and decreasing for 60 minutes. The total processing times for both experiments were 146 minutes.

Experiment 6 was carried out at lower temperatures (Figure 6.6). The system reached its maximum temperature of 118°C. The system was held at this temperature for 120 minutes, and the system was turned off to let the temperature decrease for 120 minutes.

Experiment 7 was a contrast to experiment 6; this experiment was heated to a high temperature for a short time. The temperature of the system was increased up to a maximum temperature of 165°C and the system was held at this temperature for 10 minutes (Figure 6.7).

Experiments 8 and 9 followed a stair pattern. The temperatures of systems were divided into 3 stages (Figures 6.8 and 6.9). The set point temperatures were 120°C, 140°C and 160°C for the first, second and third stages. The systems were held at each set point temperature for 10 minutes in each stage. For experiment 8, the pastry sample was removed from the cooking system at the end of each stage and one more sample was carried on at 160°C for 20 minutes. However, all four samples in experiment 9 were removed at the end of the process after 50 minutes.

The last two experiments were carried out with the same temperature profile (Figures 6.10 and 6.11), but the maximum temperature was different. Both systems were initially heated up to 150°C and held at this temperature for 30 minutes after that the temperature was increased again to 160°C or 170°C for experiments 10 and 11, respectively. The systems were then held at these temperatures for 60 minutes, and the samples were removed at the end of the process.

Samples were removed at the end of the process for all experiments except experiment 8. After samples were removed at the end of each stage, the brown colour of all pastry samples was analysed using the image system explained in section 3.3.

In all samples it was observed from Figures 6.1-6.11 that the temperature profile of the top surfaces reached a maximum of 100°C due to the evaporation of the water content of the pastry sample. Experiments 1-6 were run with lower temperatures and over long times and experiments 6-9 were run with high temperature but short time, so the maximum temperature at the top surface temperature was 100°C and stayed constant due to water evaporation. On the other hand, experiments 10 and 11 were carried out at high temperature so the evaporation was completed in the first period and after all the water had completely evaporated, the temperature increased until the completion of the experiments. Note that the temperature profiles at the top surface of the pastry for experiment 11 were recorded for only two of the four-samples (positions 2 and 4). This was because the thermocouples for the other two samples malfunctioned.

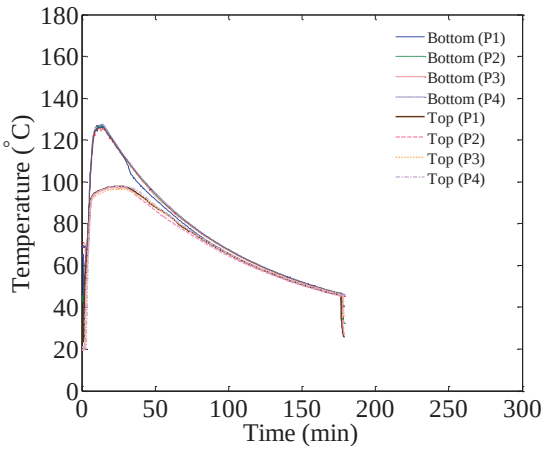

Figure 6.1 Temperature profile of pastry baked under non-isothermal conduction: Experiment 1

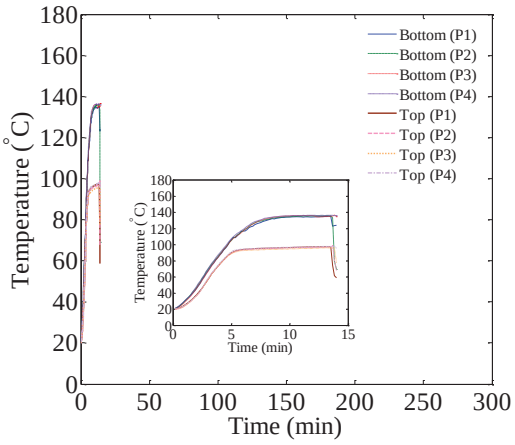

Figure 6.2 Temperature profile of pastry baked under non-isothermal conduction: Experiment 2

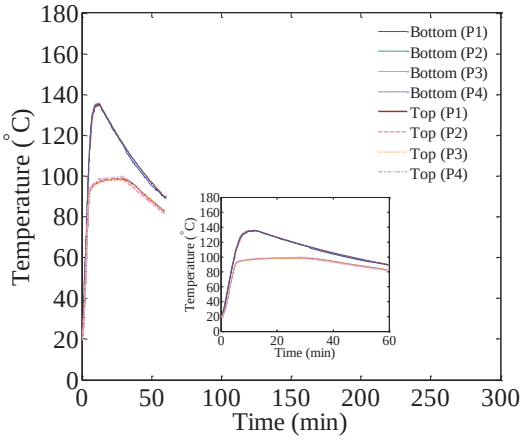

Figure 6.3 Temperature profile of pastry baked under non-isothermal conduction: Experiment 3

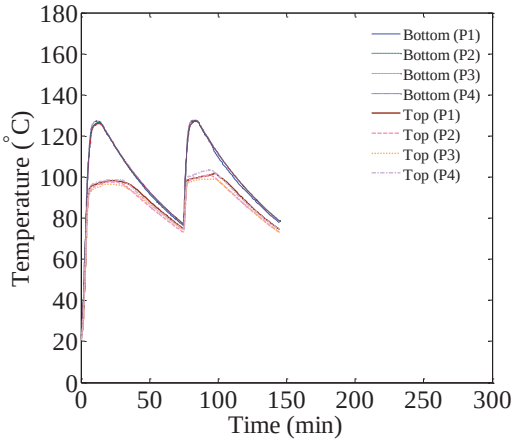

Figure 6.4 Temperature profile of pastry baked under non-isothermal conduction: Experiment 4

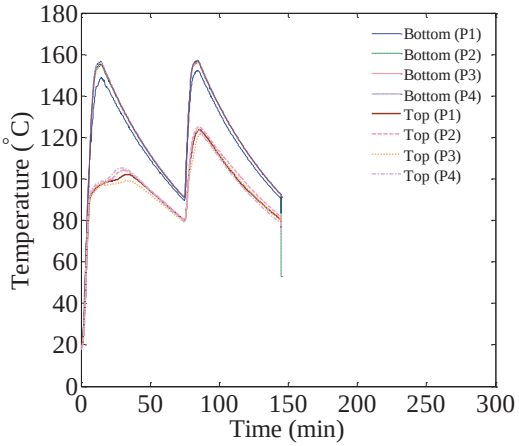

Figure 6.5 Temperature profile of pastry baked under non-isothermal conduction: Experiment 5

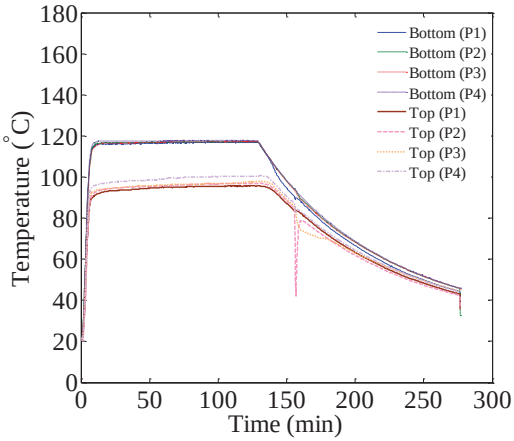

Figure 6.6 Temperature profile of pastry baked under non-isothermal conduction: Experiment 6

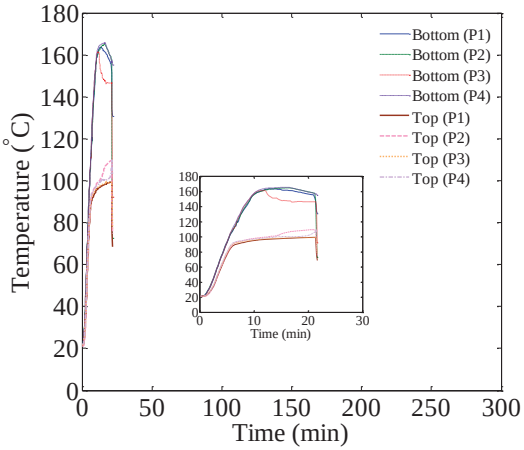

Figure 6.7 Temperature profile of pastry baked under non-isothermal conduction: Experiment 7

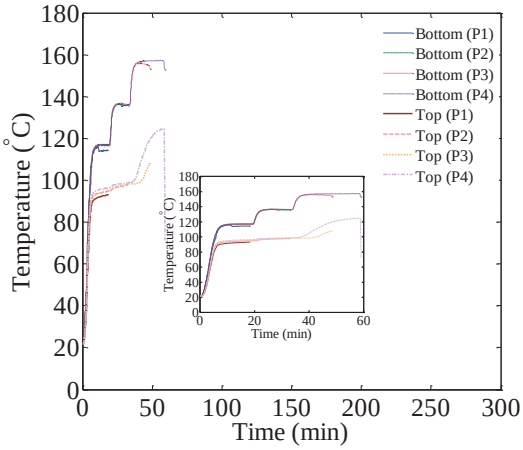

Figure 6.8 Temperature profile of pastry baked under non-isothermal conduction: Experiment 8

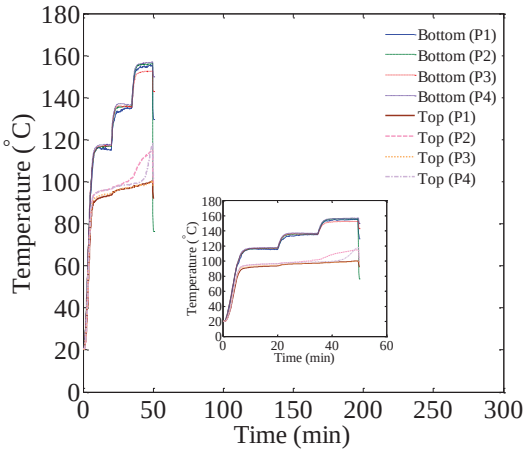

Figure 6.9 Temperature profile of pastry baked under non-isothermal conduction: Experiment 9

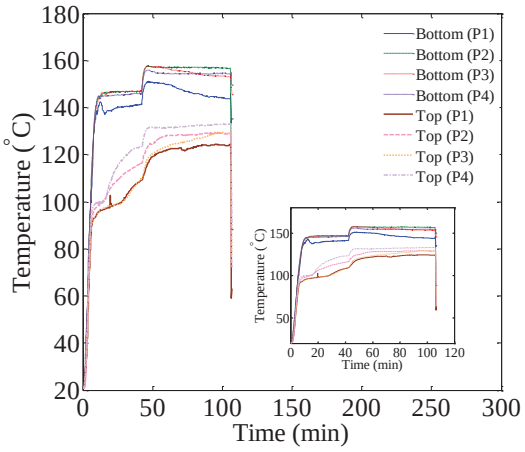

Figure 6.10 Temperature profile of pastry baked under non-isothermal conduction: Experiment 10

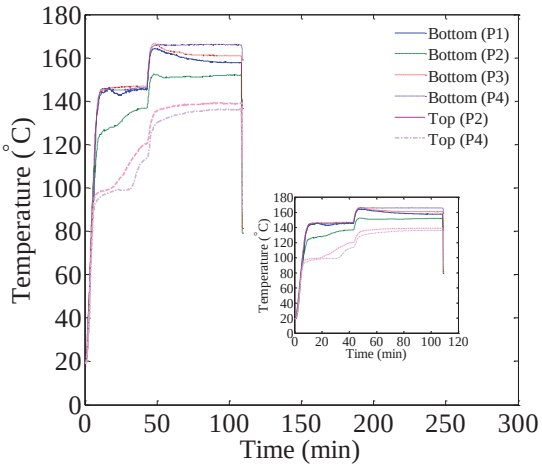

Figure 6.11 Temperature profile of pastry baked under non-isothermal conduction: Experiment 11

6.2.2 Experimental results

Each experiment had four replications, which are the four pastry samples placed in four positions in the pan and left there until the end of the processing time. The four cooked pastries were removed from the pan and cooking stopped by indirectly cooling the samples in an ice tray. Then all pastry samples were analysed by the image system to determine the colour values in *L*a*b** colour space on both the bottom and top surfaces of the pastry. However, as previous results showed that browning development is best characterized by the lightness value (*L**), the lightness of the pastry was analysed and are shown in Table 6.1.

The results show that the extent of browning in experiments 1, 2, 3, 4 and 8 (stages 1 and 2) were low. They gave high values of lightness (83-90) because these experiments were run at low temperature. In contrast, high browning extents were found in the high temperature conditions, which were experiments 5, 6, 7, 8 (stages 3 and 4), 9, 10 and 11. In experiment 11, the process was held at a high temperature for a long time and this condition produced a high level of browning colour development.

For the browning at the top surface where the evaporation occurred, the maximum temperature was 100°C. The measured lightness values were very high (between 77.74 and 90.79) (Table 6.1). It has been reported that the minimum temperature required for the Maillard browning reaction for high temperature cooking was 120°C (Purlis & Salvadori, 2009 and Purlis, 2010), so the colour change at the top surface can be not claimed to be caused by the Maillard browning reaction except in experiments 10 and 11, in which the temperature went over 120°C. The colour change that was observed at the top surface may be due to evaporation reducing the moisture content as was discussed in section 4.4.

Table 6.1 Experimental lightness values of the pastry surface after cooking with eleven non-isothermal heating scenarios

Experimental scenarios		**The experimental lightness (*L**) of cooked pastry**		**Experimental scenarios**		**The experimental lightness (*L**) of cooked pastry**	
		Bottom	**Top**			**Bottom**	**Top**
Experiment 1	P1	85.50	84.18	Experiment 7	P1	80.73	90.79
	P2	85.92	84.62		P2	79.06	90.41
	P3	85.52	84.11		P3	80.04	91.05
	P4	84.84	84.13		P4	80.43	90.65
Experiment 2	P1	90.84	89.98	Experiment 8	P1	90.95	89.31
	P2	90.84	90.30		P2	88.78	90.68
	P3	90.66	89.67		P3	80.26	89.98
	P4	90.94	89.39		P4	77.44	87.64
Experiment 3	P1	86.23	84.46	Experiment 9	P1	80.40	89.10
	P2	86.99	85.38		P2	79.70	89.41
	P3	85.72	84.63		P3	80.48	88.99
	P4	87.15	87.24		P4	79.72	90.16

Table 6.1 Experimental lightness values of the pastry surface after cooking with eleven non-isothermal heating scenarios (cont'd)

Experimental scenarios		The experimental lightness (L^*) of cooked pastry		Experimental scenarios		The experimental lightness (L^*) of cooked pastry	
		Bottom	Top			Bottom	Top
Experiment 4	P1	83.23	84.20	Experiment 10	P1	72.28	82.92
	P2	83.60	85.27		P2	72.24	83.45
	P3	83.30	83.19		P3	70.80	82.29
	P4	83.29	83.46		P4	75.20	82.41
Experiment 5	P1	73.42	86.14	Experiment 11	P1	65.60	*
	P2	73.69	86.25		P2	67.24	79.97
	P3	72.82	86.15		P3	65.71	*
	P4	74.81	87.26		P4	66.70	81.14
Experiment 6	P1	79.72	78.55				
	P2	79.79	78.45				
	P3	79.55	77.74				
	P4	77.00	79.88				

*value missing due to thermocouple probe malfunction

6.2.3 Model predictions for the non-isothermal browning kinetic of the pastry under pan baking

To assess the accuracy of the predictive models, eleven simulations were run under the different conditions measured from the experiments. The mathematical model developed for non-isothermal cooking condition in section 5.4 was used to predict the browning kinetics. The model employed the temperature profile at the bottom surface of all samples and used the kinetic parameters estimated in section 5.4 as input data into the model. The estimated kinetic parameters L^*_0, L^*_∞, k_{150} and E_a were 91.21, 67.54, 0.025 min^{-1} and 71.95 $kJ \cdot mol^{-1}$ respectively. The top surfaces of the pastry were not predicted because the Maillard browning reaction did not occur due to the low temperature. The MATLAB® ode solver was used to solve the model. The code for this solution is presented in Appendix A5.

The profiles for the predicted lightness (L^*) changes during the processing time for all experiments are presented in Figures 6.12-6.24. The predicted lightness is shown as the

line compared with one point of the experimental lightness measured at the end of each baking process. The predicted lightness profiles varied due to the different time-temperature histories. The model predicted the experimental lightness values well for all experimental scenarios, which demonstrate that the model showed good performance in predicting the browning kinetics of the pastry baking in each case.

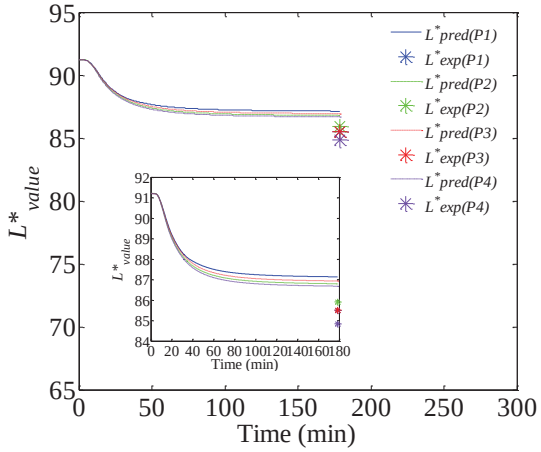

Figure 6.12 Predicted L^* profile at the bottom surface of the pastry baked under non-isothermal conditions: Experiment 1

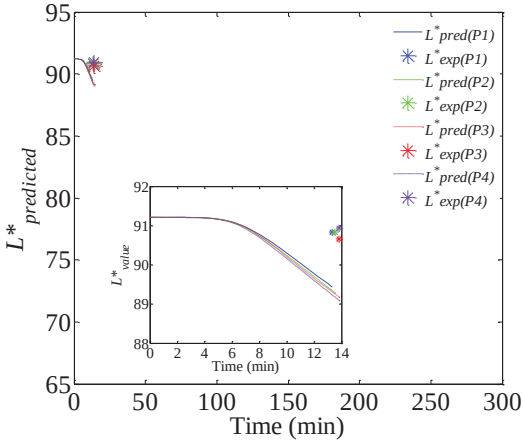

Figure 6.13 Predicted L^* profile at the bottom surface of the pastry baked under non-isothermal conditions: Experiment 2

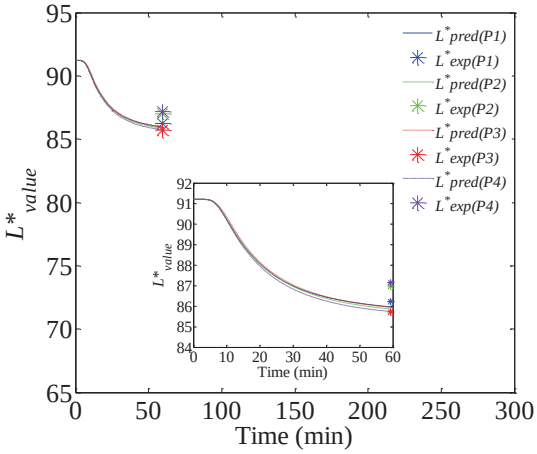

Figure 6.14 Predicted L^* profile at the bottom surface of the pastry baked under non-isothermal conditions: Experiment 3

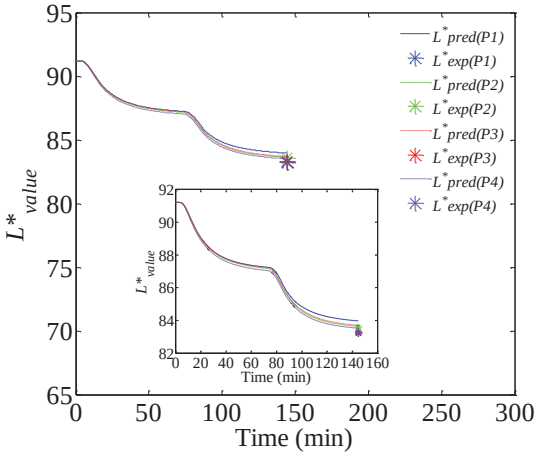

Figure 6.15 Predicted L^* profile at the bottom surface of the pastry baked under non-isothermal conditions: Experiment 4

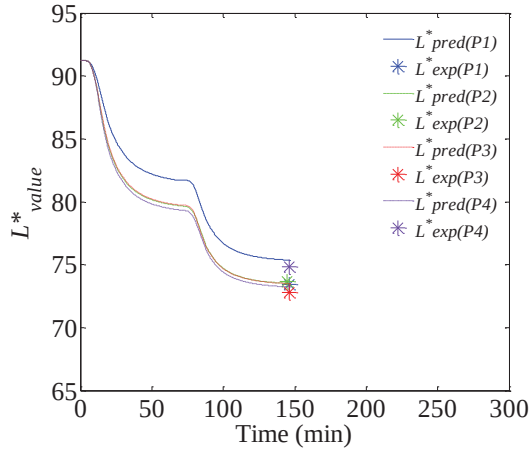

Figure 6.16 Predicted L^* profile at the bottom surface of the pastry baked under non-isothermal conditions: Experiment 5

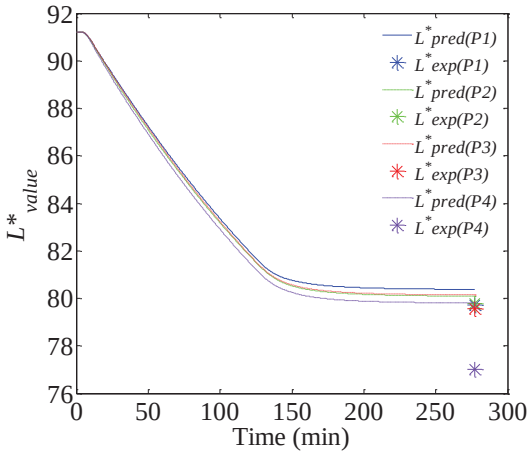

Figure 6.17 Predicted L^* profile at the bottom surface of the pastry baked under non-isothermal conditions: Experiment 6

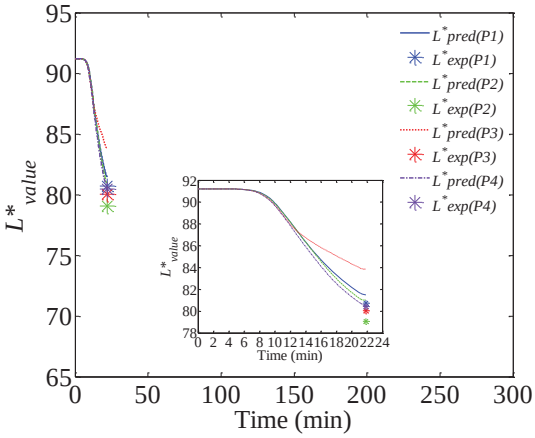

Figure 6.18 Predicted L^* profile at the bottom surface of the pastry baked under non-isothermal conditions: Experiment 7

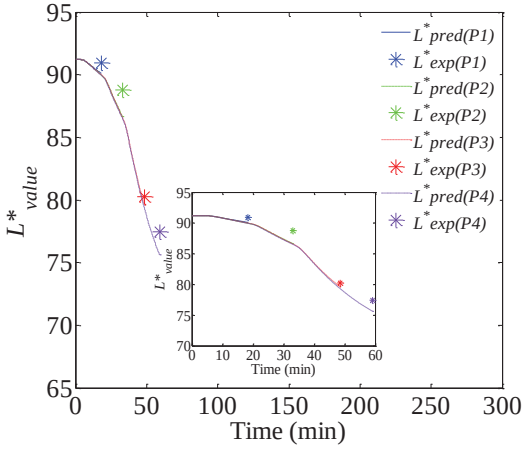

Figure 6.19 Predicted L^* profile at the bottom surface of the pastry baked under non-isothermal conditions: Experiment 8

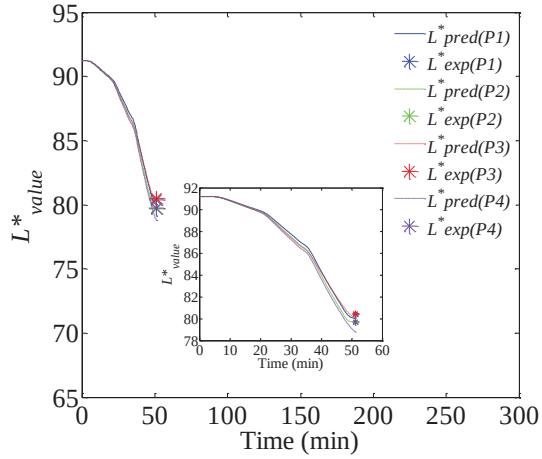

Figure 6.20 Predicted L^* profile at the bottom surface of the pastry baked under non-isothermal conditions: Experiment 9

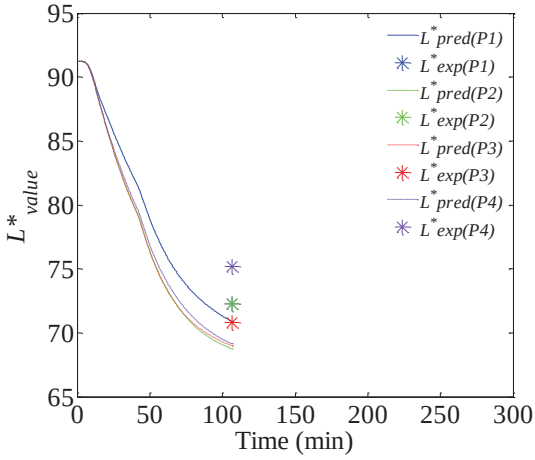

Figure 6.21 Predicted L^* profile at the bottom surface of the pastry baked under non-isothermal conditions: Experiment 10

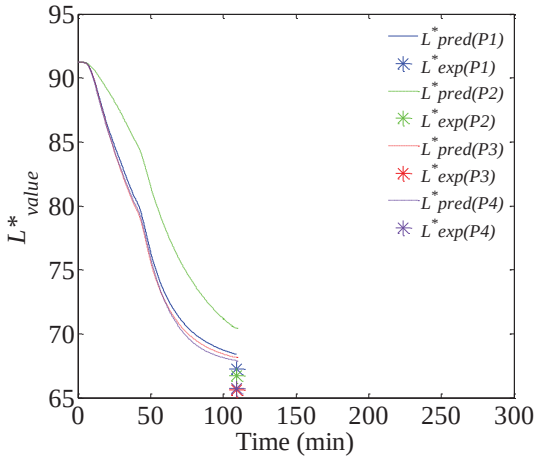

Figure 6.22 Predicted *L** profile at the bottom surface of the pastry baked under non-isothermal conditions: Experiment 11

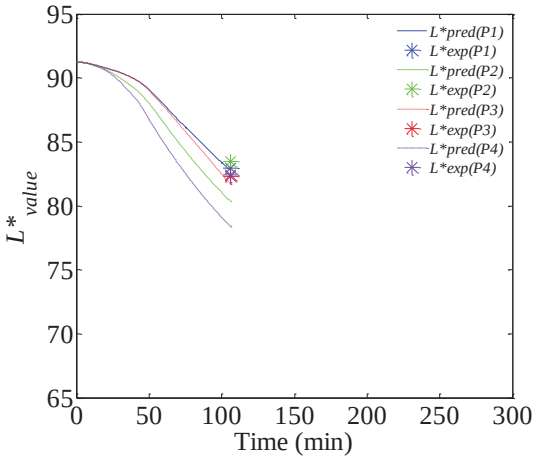

Figure 6.23 Predicted *L** profile at the top surface of the pastry baked under non-isothermal conditions: Experiment 10

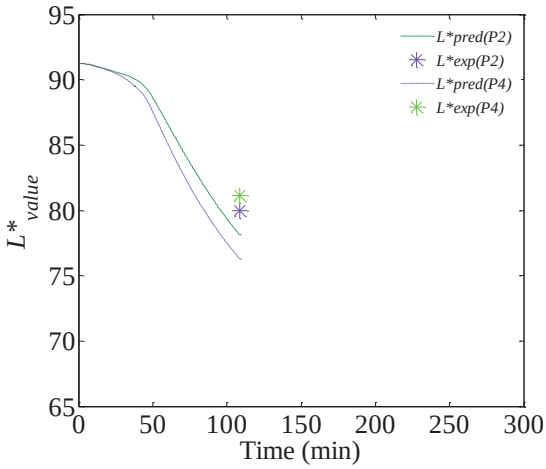

Figure 6.24 Predicted *L** profile at the top surface of the pastry baked under non-isothermal conditions: Experiment 11

6.2.4 Comparison of the predicted and measured lightness values

The predicted brown colour values were compared with the brown colour measured in the experiment in order to prove the performance of the model. The lightness (*L**) reduction, indicating the browning reaction on pastry surface at the bottom for all experimental data and at the top surface from experiments 10 and 11 are compared with the predicted data in Figure 6.25. The solid line accounts for perfect prediction. It was found that the data are scattered either side of the perfect prediction line. This means that the model predictions were close to the experimental data.

A small variation was found among the predictions for replicated experiments, and some experimental sets showed over and under prediction of around 3 and 5 units,

respectively. For example, over-predicted lightness was found in experiment 11 (bottom) and under-predicted lightness was found in experiments 10 (bottom) and 11 (top). This was because of variation of the material sample. Overall the prediction was adequate at predicting the lightness change of samples subjected to dynamic heating protocols within the confidence of the prediction.

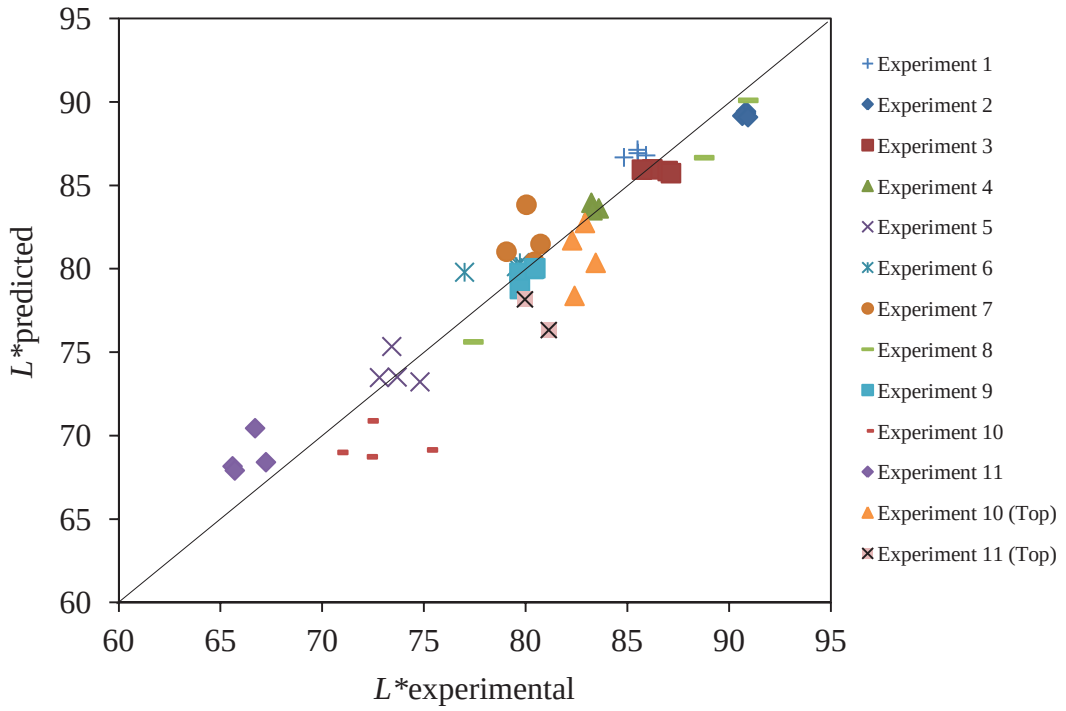

Figure 6.25 Comparison between experimental and predicted lightness for pastry baked under non-isothermal conditions

6.3 The goodness of the model prediction

The model's usefulness for predicting the browning colour change at high temperatures was assessed. The brown colour at the end of the process predicted by the model was compared to the brown colour of the pastry surface at the end process measured in the experimental study. The goodness of the model prediction was assessed by the absolute relative error, defined as:

$$e_{abs}(\%) = \frac{100}{n}\sum_{i}^{n}\left(\frac{\left|L^{*}_{experimental} - L^{*}_{predicted}\right|}{L^{*}_{experimental}}\right)_{i} \qquad (6.1)$$

where n is the number of output values taken into account.

The calculated absolute relative error was 1.93% (n = 50) for all predictions. The absolute relative error is a measure of accuracy of a method for constructing fitted time series values in statistics, specifically in trend estimation. It usually expresses accuracy as a percentage. The percentage for absolute relative error of the prediction of browning colour change in bread baking was found to be 3.61% (n = 34) (Purlis & Salvadori, 2009). Therefore, it can be seen that the prediction of the developed model in this study is very good.

6.4 Model predictions for the non-isothermal browning kinetic of the pastry under oven baking conditions

The non-isothermal model was shown to predict the non-enzymatic browning of pastry baking well under conduction heat transfer using pan baking. In real life, the pastry is generally baked in an oven, where convective heat and mass transfer occurs. Therefore, to test the potential of the developed kinetic model in predicting the browning change of pastry baking under convection heat transfer, a hot air dryer was used in this section to further validate the model.

6.4.1 Method

The pastry samples were prepared using the same method as indicated in section 5.2.1 The pastry samples were baked in a hot air dryer (located at School of Engineering and Advanced Technology, Massey University, Turitea, New Zealand). With this dryer, the convective heat transfer was significant.

Eight experiments were carried out. In each experiment, the sample was placed in the dryer at time zero and then the dryer was turned on. The dryer was run for 60 minutes for experiments 1, 2, 3, 4 and 5 (long time condition) and for 40 minutes for experiments 6, 7 and 8 (short time condition). The dryer temperature was set at 160°C. The surface thermocouple probe used in the previous study was unsuitable because the probe could not be placed so as to be touching on the pastry surface during the whole process because the pastry expanded in the oven. An infrared thermometer (Model QM7226/ DT-8838, ε = 0.95) was therefore used to measure the temperature of the pastry surface. When measuring the temperature of the pastry surface in the dryer, the dryer door needed to be opened because the infrared thermometer was not able to measure the temperature of the object through the glass or any other material.

In order to use the infrared thermometers, the emissivity property (energy-emitted) of the object needs to be known because the infrared thermometer measures the object's temperature by measuring the infrared energy that is emitted from the object. The temperature of the object directly relates to the infrared energy emitting from that object. Therefore, knowing the emissivity of the pastry samples was necessary for IR temperature measurement.

6.4.1.1 Measuring the pastry emissivity

The emissivity of a material (usually written ε or e) is the relative ability of its surface to emit energy by radiation. It is the ratio of energy radiated by a particular material to energy radiated by a black body at the same temperature. A true black body would have an emissivity equal to one ($\varepsilon = 1$) while any real object has $\varepsilon < 1$.

The emissivity of pastry was measured using the following method: a frozen pastry sample was left at ambient temperature (20°C) for 30 minutes. During this period, the pastry temperature was measured using a calibrated glass thermometer (which was used as a reference thermometer) and at the same time the pastry was also measured using the infrared thermometer. The temperature on both the glass thermometer and the infrared thermometer were read every 1 minute for 30 minutes. The data on the pastry temperature measured by both the glass and the infrared thermometer were compared.

The emissivity was calculated using this relationship:

$$I = \varepsilon \sigma T_s^4 \tag{6.2}$$

Where I is the radiation intensity for emitted radiation ($W \cdot m^{-2}$), ε is the emissivity of the object, σ is the Stefan–Boltzmann constant ($W \cdot m^{-2} \cdot K^{-4}$), and T_s is the temperature of the object (K). From Equation 6.2, the temperature of the object was called $T_{measured}$. Equation 6.2 was rearranged to Equation 6.3.

$$T_{measured} = \left(\frac{I}{\varepsilon \sigma} \right)^{1/4} \tag{6.3}$$

In this case, the emissivity of the infrared thermometer was set at 0.95 (default setting); the measured temperature was incorrect due to the initial emissivity being incorect.

Therefore, the true temperature was related to the true emissivity of the sample and calculated using the following the Equation 6.4.

$$T_{true} = \left(\frac{I}{\varepsilon\sigma}\right)^{1/4} \times \left(\frac{0.95}{\varepsilon_{true}}\right)^{1/4} \tag{6.4}$$

Substituting Equation 6.4 with Equation 6.3, so the equation for calculating the true temperature was obtained (Equation 6.5).

$$T_{true} = T_{measured} \times \left(\frac{0.95}{\varepsilon_{true}}\right)^{1/4} \tag{6.5}$$

T_{true} is the real temperature, which was obtained using the glass thermometer. $T_{measured}$ is the temperature that was obtained from the infrared thermometer. Then the emissivity of the sample was calculated using this equation:

$$\varepsilon_{true} = \frac{0.95}{\left(\frac{T_{true}}{T_{measured}}\right)^4} \tag{6.6}$$

To calculate the emissivity of pastry, the value of the true and the measured temperatures that were measured using the glass and the infrared thermometers were substituted into Equation 6.6 as follows:

$$\varepsilon_{true} = \frac{0.95}{\left(\frac{293.17}{296.66}\right)^4} \tag{6.7}$$

The emissivity of pastry was calculated to be 0.99. This value was used to calibrate and calculate the real temperature of the pastry surface during the experiments using Equation (6.5). During the eight experiments, the measured temperature of the pastry surfaces were recorded and then corrected to obtain the real temperature.

6.4.1.2 The results of the calibrated temperature of the pastry

The calibrated temperature profiles of the pastry surface during baking in the dryer are shown in Figure 6.26. It can be seen that the temperature profiles of the pastry surface of all eight experiments follow the same pattern. They were similar in so far as all experiments took approximately eight minutes to increase the temperature of the pastry surface to reach over 100°C. After that, the temperature of all pastry samples continued to increase until the end of the process. The temperatures of all samples fluctuated because the oven door was opened during baking to allow measurement. Opening the door meant conditions were non-isothermal.

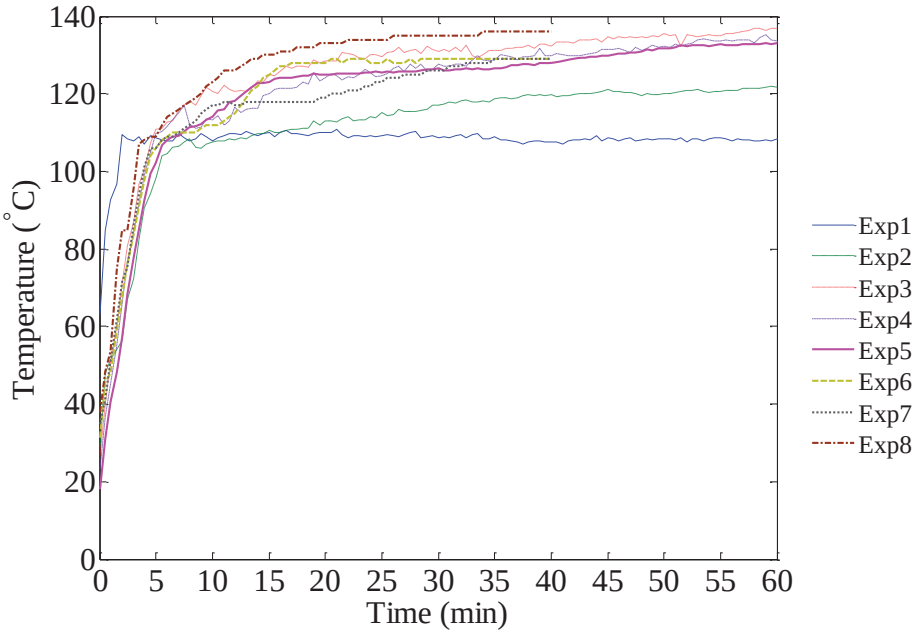

Figure 6.26 Temperature profiles of the pastry surface in the convection oven cooking process

6.4.2 Model predictions for non-isothermal browning of pastry cooked under the convection heat transfer

All temperature profiles for the pastry samples' surfaces were imported to the non-isothermal model developed in the section 5.4. The kinetic parameters estimated in section 5.4 were used as input data for the model to predict the lightness of the pastry surface thus indicating the browning kinetic. The kinetic parameters of L^*_0, L^*_∞, k_{150} and E_a used were 91.21, 67.54, 0.025 min^{-1} and 71.95 $kJ \cdot mol^{-1}$ respectively. The

prediction was solved using the ode function of the MATLAB® program and the same code as sections 5.32 and 6.2.3 was used (Appendix A5).

The predicted lightness profiles of the pastry surface for all eight experiments are shown in Figure 6.27. The predicted lightness values of all eight experiments were plotted against time to see the browning development during the baking process. The lightness of the pastry surface decreased from the initial lightness of 91 to the final value of between 81 and 87. The final lightness also depended on the temperature, at high temperatures the final lightness was lower than at low temperatures.

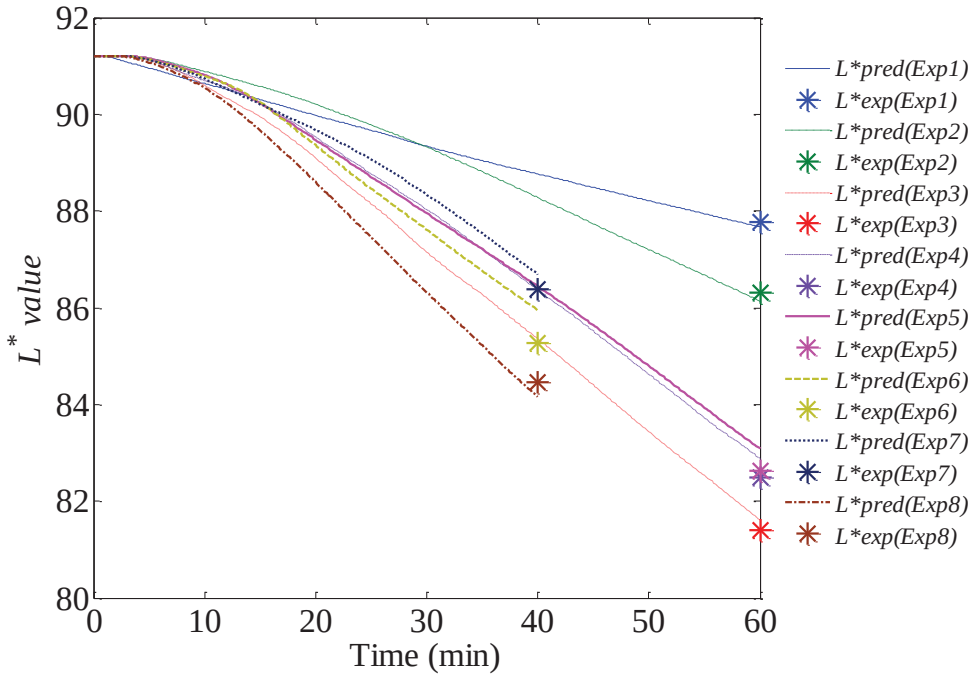

Figure 6.27 Predicted *L**values of the pastry baking in the convection oven cooking process

6.4.3 Comparison of the predicted and measured lightness values

The final lightness of the pastry samples in each experiment was measured using the image analysis system outlined in section 3.3. Then the experimental lightness values were compared to the predicted lightness value to assess the potential of the model. The experimental and predicted lightness values are compared in Figure 6.28. The comparison shows that the developed model performed well in predicting the lightness change in convective heat transfer cooking conditions.

As can be seen in Figure 6.28, all predictions are very close to the perfect prediction line. The model performance was computed comparing experimental and predicted values using Equation 6.1. The estimation error (e_{abs} [%]) of this model in browning kinetic prediction on pastry baking for convective heat transfer condition was very small at 0.38% (n = 8). It can be concluded that the developed model worked very well for predicting the browning kinetics of pastry baked in convective heat transfer conditions.

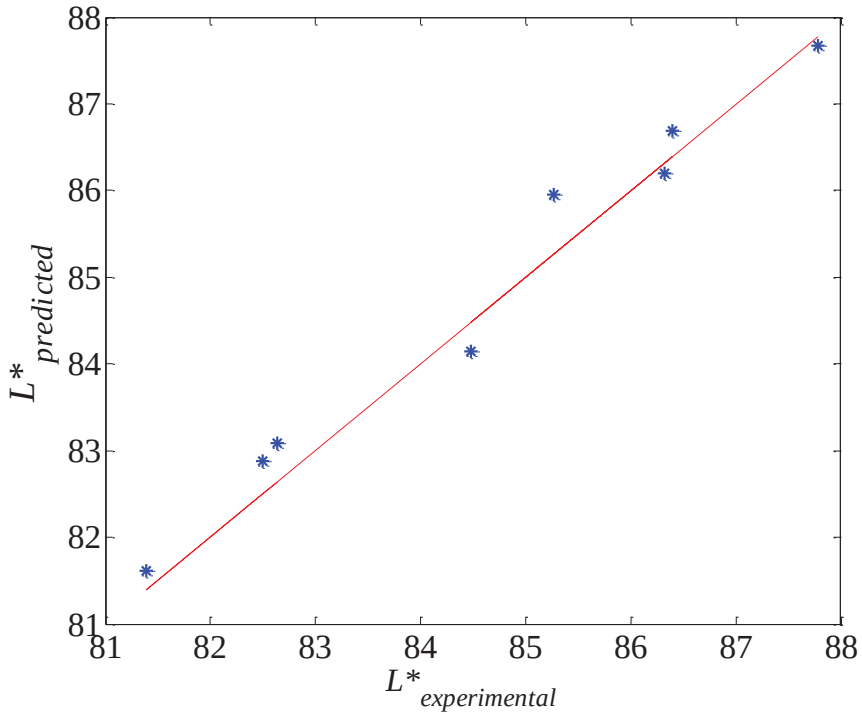

Figure 6.28 Comparison between experimental and predicted lightness of the pastry baked under non-isothermal convection heating

6.5 Conclusion

The non-isothermal kinetic model developed in this study can be used to predict the browning development of pastry baked under non-isothermal cooking conditions in both conduction and convection heat transfer situations. The conduction heat transfer cooking condition was studied using a hot pan baking system, while for the convective heat transfer cooking, a dryer oven was used. The cooking scenarios were designed to have different profiles of temperature history over a wide range of the real cooking processes to test the model.

The histories of the pastry where the temperature exceeded 120°C (minimum temperature for Maillard browning) of the bottom surface (all experiments) and the top surface (experiments 10 and 11) for the pan-baked pastry and at the top surface for the oven-baked pastry were introduced into the model to predict the colour change during baking. The results of the model, in most experimental scenarios, agreed well with the experimentally measured lightness values (browning indicator) of the sample surfaces.

The accuracy of the prediction was considered as the absolute relative error (e_{abs} %) to show the degree of the prediction. The calculated absolute relative errors were 1.93% (n = 50) for the pan-baked pastry and 0.38% (n = 8) for the oven-baked pastry. These small values show the good prediction of the model.

This leads to the conclusion that the model developed can therefore be utilised as a tool to predict the non-enzymatic browning kinetic of pastry samples for any processing conditions or methods, if the time-temperature profile of the surface of the pastry sample is known. The models and experimental methodologies developed in this work may potentially be applicable for other food systems. This will be the focus of the next chapter.

Chapter 7

MATHEMATICAL MODEL APPLICATIONS

7.1 Introduction

Chapter 6 showed that the model was good at predicting browning development on pastry samples cooked under non-isothermal conditions with different heating scenarios and with different types of cooking systems. The Maillard browning reaction occurs in many foods, so the developed model would have wide utility if it could be extended to apply to other food types. The application of the model to these foods could be used to optimise processing conditions to control the extent of browning.

This chapter investigates whether the developed model can be adapted for another food to test this. In Chapter 6 it was shown that the model worked well in predicting the browning in pastry baking. Therefore it could be expected that the model could be applied for bread or bakery products. For this reason a processed potato product was selected to study in this chapter since its chemical and physical properties are different from pastry.

This chapter therefore describes the application of the non-isothermal browning kinetic model to predicting the browning of a processed potato product.

7.2 Method

The methodology for the study of the browning kinetic in processed potato products was similar to the study of pastry. Circular frozen medellion potatoes (“Watties” brand) with a diameter of 70 mm and a thickness of 12 mm were purchased from the

supermarket. The ingredients of the medellian potatoes consisted of potatoes (87%), canola oil (7%), seasoning mix (maize starch, maltodextrin, soy flour, rice flour, salt, flavour enhancer [635], spice, spice extract), glucose, mineral salt (450), traces of wheat, milk and egg. Prior to the study, the frozen processed potato products were left at room temperature (20°C) to thaw.

The processed potato products were then baked in four different positions on the hot pan (section 3.4). As the bottom surface temperature profile needed to be collected, a surface self-adhesive thermocouple type J (SA1XL, OMEGA) was placed under each processed potato product sample. The temperature of each sample was logged using a data logger (Agilent 34970A data acquisition) connected to a computer (section 3.5).

There were five levels of cooking temperature: 120, 130, 140, 150, and 160°C. The experiments were carried out for 5, 10, 15, 20, 25, 30, 35, 40, 45, 50, 55 and 60 minutes. Each sample was removed at the end of the process time and rapidly cooled down on a stainless steel tray cooled indirectly with ice to stop the cooking process. For the temperature of 150°C, the cooking time was extended to 200 minutes to see the extent of browning after a long time. All of the baked processed potato product samples were photographed so their colour could be analysed using the image processing method outlined in section 3.3.

7.3 Results and discussion

7.3.1 Temperature data

During the process, the surface temperatures of each processed potato product sample under all temperature conditions were recorded. Figure 7.1 shows an example of the temperature profiles of processed potato product baked at a pan temperature of 160°C for 5, 10, 15, 20, 25, 30, 35, 40, 45, 50, 55 and 60 minutes.

Figure 7.1 shows that the temperature of each processed potato product sample surface increased very quickly because the processed potato products were placed on the hot pan after the temperature of the pan was stable at the set point temperature. The temperature of each sample increased slightly through the study and approached the set point temperature. Nevertheless, the maximum temperature of each sample did not reach the set point temperature because the processed potato product sample surfaces

were uneven and there were many air spaces between the rough surface of the processed potato product and the pan. The temperature of the processed potato product samples' surfaces was not as high as the pastry sample surfaces for the same oil temperature condition because the contact between the pastry and the pan was more complete. There were fewer air spaces on the surface of the pastry samples compared to the processed potato product sample even though both types had aluminium weights, placed on top of them.

Interestingly, it can be seen from the figure that there was variations in the temperature profiles between samples baked at the same temperature conditions and the same experimental run. This was because of differences in the sample surfaces, such as the roughness, making placement of the probe more variable. Consequently, individual temperature profiles relating to individual lightness value readings were used for model fitting in this study rather than using one temperature profile of 60 minutes only, like the previous study for pastry baking.

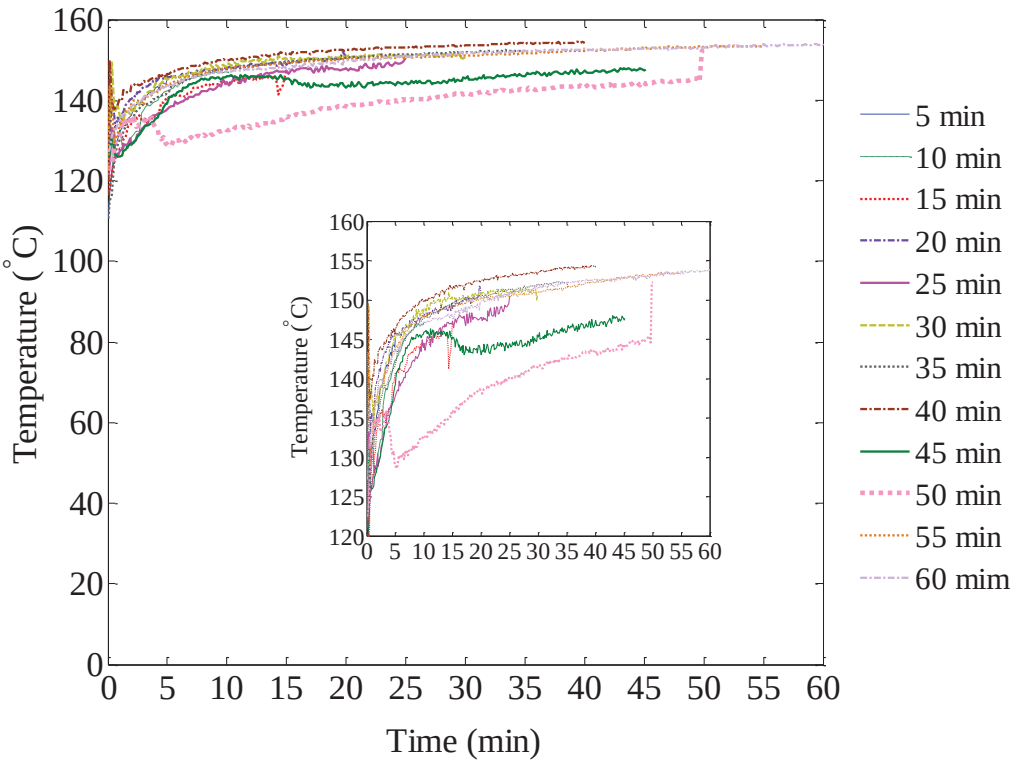

Figure 7.1 An example of temperature profile of processed potato product surface baked at 160ºC (the insert figure is the same data with a magnified temperature scale)

7.3.2 Lightness data

At the end of each experimental cooking time (5, 10, 15, 20, 25, 30, 35, 40, 45, 50, 55 and 60 minutes), the processed potato product sample was removed to take a photo for colour analysis. The photos of the processed potato product samples baked at five different temperature conditions for 60 minutes are shown in Figure 7.2. Similar results to the pastry baking were obtained in terms of the brown colour developed during the process.

However, it was seen that the brown colour on the processed potato product surfaces was uneven because the surface of the processed potato product was rough. Darker colours were found at the edges and the blisters due to higher heat transfer at these areas. The overall colour of the processed potato product became darker as the process continued. Under high temperature conditions, the processed potato product was darker than at low temperature conditions.

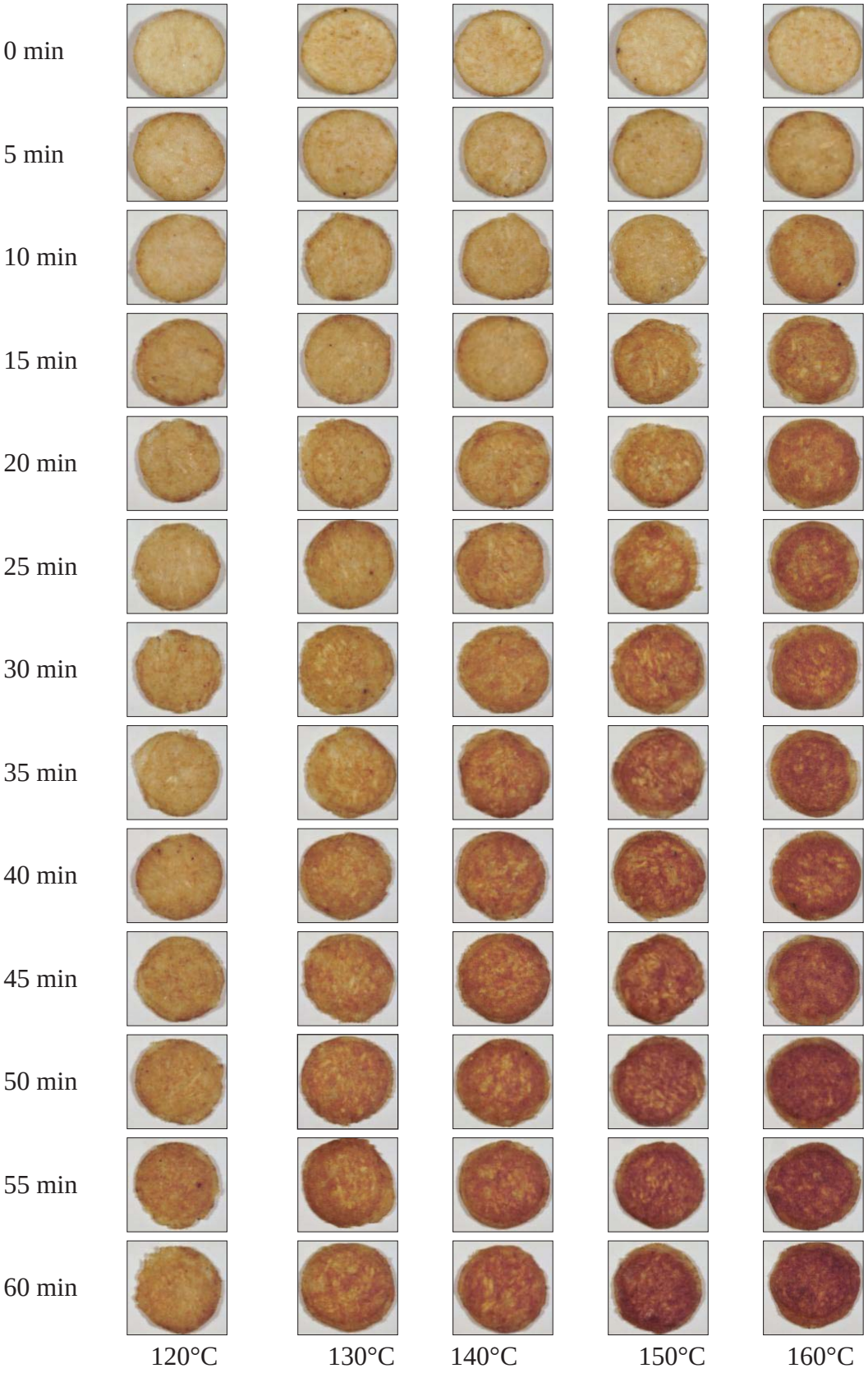

Figure 7.2 Image galleries of processed potato product samples during cooked at five different temperatures for 60 minutes

To evaluate the end lightness of the processed potato product samples, the temperature condition of 150°C was extended beyond 60 minutes to 200 minutes. The photos after baking from this experiment are presented in Figure 7.3. The brown colours on the processed potato product samples were very dark due to the long baking time. The intensity of the colour of the processed potato product increased as the cooking time increased. The darkest colour was found in the sample cooked at 150°C for 200 minutes. The lightness values of the processed potato product surfaces during the process were determined to see the browning development.

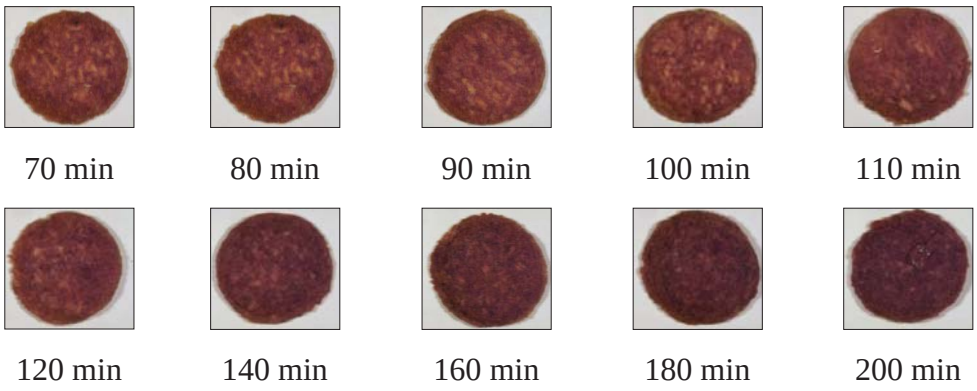

Figure 7.3 Image galleries of processed potato product samples baked at 150°C for 70 to 200 minutes

The lightness profiles of all experiments are plotted and are shown in Figure 7.4. The lightness of the processed potato product samples decreased as cooking time progressed and the rate of decrease depended on the cooking temperature. The final lightness was found to be 51. The browning development in the processed potato product samples was similar to the browning development in the pastry samples. Therefore, the method of fitting the first order browning reaction kinetics to the processed potato product samples could be applied as for the pastry samples. All the temperature and lightness profiles of the processed potato product samples were used to fit the non-isothermal model and obtain the kinetic parameters.

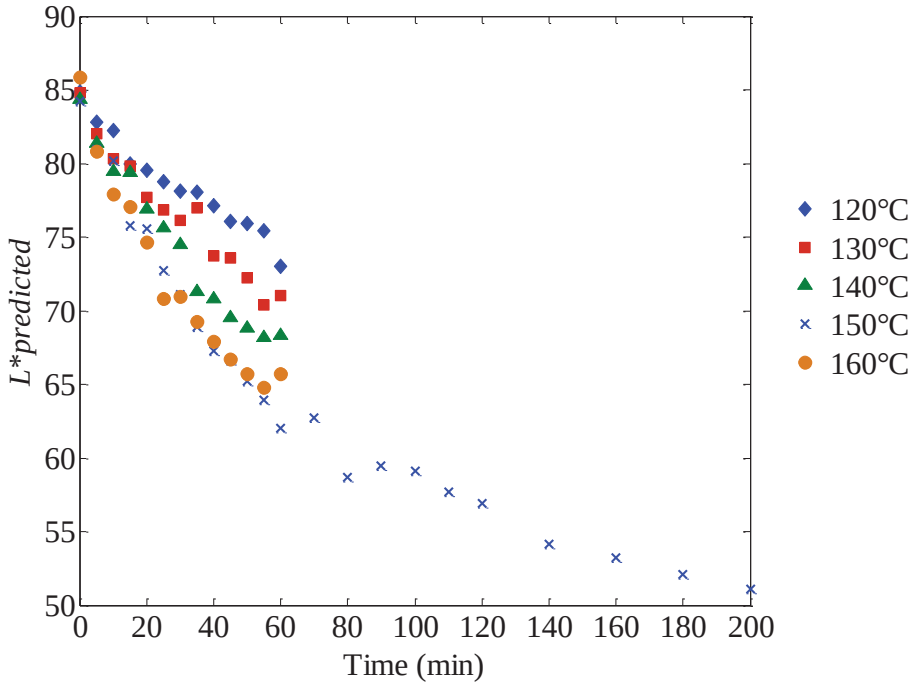

Figure 7.4 Lightness profile of processed potato product surface baked at five different conditions

7.4 Non-isothermal model fitting

With the same method of fitting as in the pastry baking study, the non-isothermal model developed in Chapter 5, section 5.4 (Equations 4.1 and 5.2) were used. For this study the experiments were run for 5, 10, 15, 20, 25, 30, 35, 40, 45, 50, 55 and 60 for each temperature condition and 200 minutes for the condition of 150°C, so the temperatures were recorded for these cooking times and the lightness values were determined at the end of each cooking time. Thus there were 60 temperature profiles and 60 lightness values from 60 minutes baking at 120, 130, 140, 150 and 160°C and 10 more data for temperature and lightness values from the extra time of the baking condition of 150°C where the cooking time was carried on until 200 minutes.

The numerical solution was solved using MATLAB® (version 6.5 The Mathworks Inc, Natick, Mass. U.S.A) to get the best fit by using the functions of ode45 and *lsqnonlin*. The code is presented in Appendix A7. The initial guesses for the kinetic parameter values for L^*_0, L^*_∞, k_{150} and E_a are listed in Table 7.1. The fitting of the solution was highly sensitive to the initial guess. Therefore optimization simulations were started from a range of sensible initial guesses to achieve the best fit with the highest R^2.

Table 7.1 List of initial guess kinetic parameters used to fit non-isothermal kinetics model to processed potato product

Parameters	Values
L^*_0 (Initial lightness)	82.91
L^*_∞ (Final lightness)	47.75
k_{150} (Kinetic rate constant at 150ºC) (min^{-1})	0.025
E_a (Activation energy) ($kJ \cdot mol^{-1}$)	51

After solving, the model provided the lightness predicted profile of each experimental temperature condition. The predicted lightness curve was plotted so it could be compared with the experimental data for each experimental condition. The examples of experimental time-temperature plot and the experimental lightness compared with predicted lightness profile at 140°C for 55 minutes cooking condition are shown in Figure. 7.5 as an example. It can be seen that the temperature of the processed potato product continuously increased until the end of the process at 55 minutes (Figure 7.5 (a)).

Figure 7.5 (b) shows the comparison between the experimental data and the predicted lightness developed of the processed potato product sample surface. A star symbol represents the experimental data for the lightness and a continuous line represents the predicted lightness of the processed potato product. As the lightness data from the experiment was obtained at the end of the process, there is only one lightness value for each experiment. The graph shows that the predicted lightness decreases during processing.

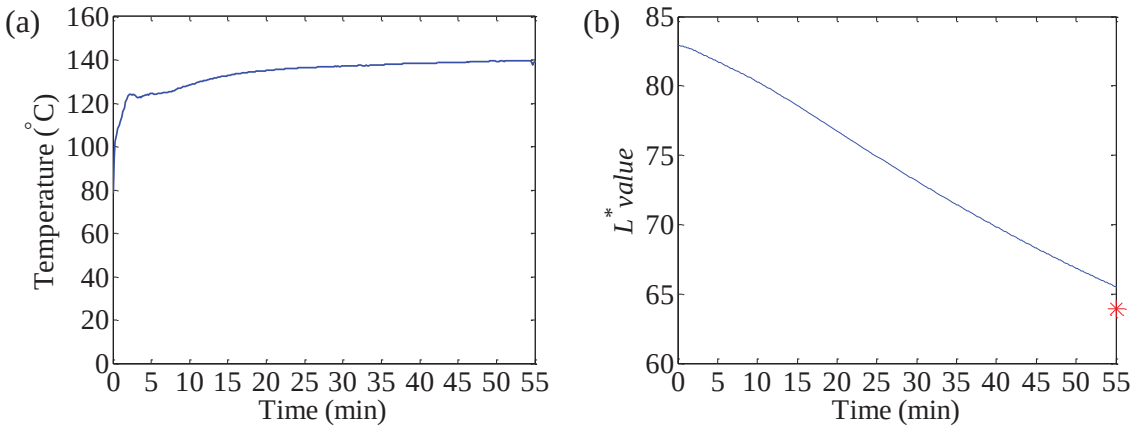

Figure 7.5 Temperature and lightness profiles of the processed potato product surface cooked at a temperature of 140°C: (a) temperature history of processed potato product surface baking at 140°C for 55 minutes and (b) experimental (*) and predicted (solid line) lightness profile for 55 minutes

The overall fitting between the predicted and experimental lightness for all of the experiments is shown in Figure 7.6. This reveals that overall, the model made good predictions, as all the prediction plots are scattered close to the perfect line of prediction. The model over-predicted and under-predicted the lightness values by a maximum value of about 4 at both the high and the low values of lightness. This shows a satisfactory relationship between the predicted and experimental values. The calculated goodness of fit is high (R^2 = 0.97). From this result, it can be concluded that the model can be used to predict the lightness development in processed potato product baking.

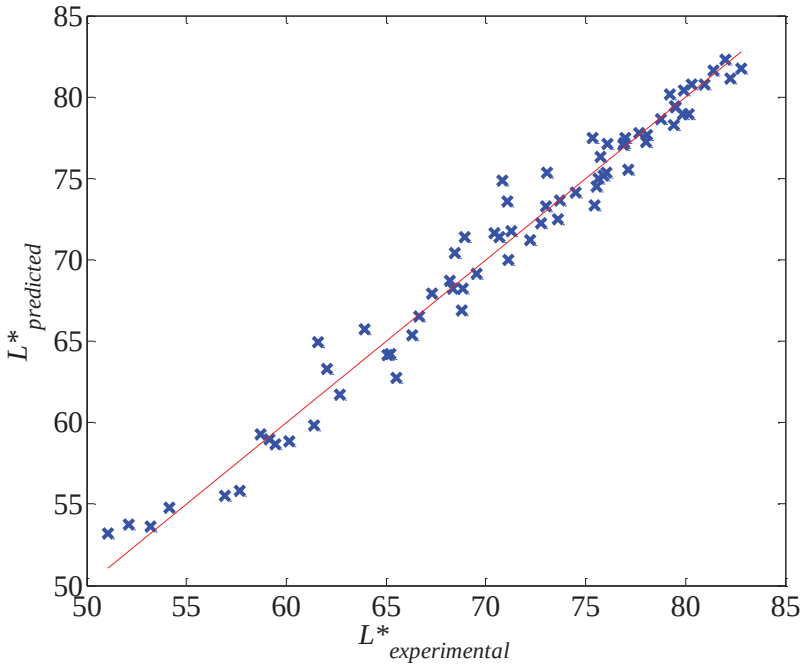

Figure 7.6 Plot of experimental data versus predicted lightness for all experimental conditions

From the best fit, the kinetic parameters that were obtained are shown in Table 7.2. The initial and final lightness values were 82.49 and 52.49, respectively. The reference temperature for this study was selected at 150°C, the same reference temperature as in the pastry study. The kinetic rate constant at the reference temperature (k_{150}) and activation energy (E_a) were 0.026 min^{-1} and 51.7 $kJ \cdot mol^{-1}$, respectively.

The activation energy for the browning reaction of processed potato product baking in this study was lower than that of potato cooking reported for other cooking processes, such as the potato frying, which were cooked at high temperatures. The activation energies of potato frying were 89.9 $kJ \cdot mol^{-1}$ (Nourian & Ramaswamy, 2003) and 95.0 $kJ \cdot mol^{-1}$ (Sahin, 2000) for the temperature range between 160 and 190°C and 150 and 180°C, respectively. This comparison shows that the browning reaction of processed potato product baking was less sensitive to the temperature than that of potato frying as can be seen from lower activation energy for processed potato product baking. This may be because the study of potato frying assumed the potato temperature to be the same as the oil temperature in modelling the kinetics (Sahin, 2000 and Nourian & Ramaswamy, 2003). In fact, the sample temperature might be lower than the heating medium

temperature especially when water is being evaporated from the surface, so the colour change was not interpreted using the real temperature of the sample.

Table 7.2 List of optimised the kinetic parameters for processed potato product baking

Parameters	Values
L^*_0 (Initial lightness)	82.49
L^*_∞ (Final lightness)	52.49
k_{150} (Kinetic rate constant at 150ºC) (min^{-1})	0.026
E_a (Activation energy) ($kJ \cdot mol^{-1}$)	51.7
R^2 (Goodness of fit)	0.97

7.5 Comparison of the kinetic rates of pastry and processed potato product baking

The kinetic parameters of processed potato product baking were compared with that of pastry baking to compare the rate of the browning reaction of these two foods (Table 7.3). The initial lightness values of both food samples were different due to the different components of the individual foods.

The kinetic rate constant at 150ºC and the activation energy values were compared. It was found that the kinetic parameters obtained from both studies were the same suggesting that the rate of browning reaction of the pastry and processed potato product were the same at 150ºC. The activation energy for the non-enzymatic browning reaction of these two food samples were 71.95 and 51.7 $kJ \cdot mol^{-1}$ for the pastry and processed potato product, respectively. These are in the range of the activation energy for non-enzymatic browning in foods (37.0 and 167 $kJ \cdot mol^{-1}$) (Villota & Hawkes, 1992). The Maillard reaction in pastry baking was more temperature-sensitive than that in the processed potato product baking as can be seen from higher value of activation energy for the pastry baking.

Table 7.3 Comparison between the kinetic parameters of the pastry and processed potato product baking

Parameters	Pastry	Processed potato product
L^*_0 (Initial lightness)	91.2	82.5
L^*_∞ (Final lightness)	67.5	52.5
k_{150} (Kinetic rate constant at 150ºC) (min^{-1})	0.025	0.026
E_a (Activation energy) ($kJ \cdot mol^{-1}$)	72.0	51.7
R^2 (Goodness of fit)	0.92	0.97

The rate of the reaction of processed potato product and pastry baking can be compared by determining the time required to reach 50% total of the reaction, which was calculated from Equation 7.1.

$$t_{0.5} = \frac{-\ln(1-0.5)}{k_{150}\exp\left(\frac{-E_a}{R}\left(\frac{1}{T}-\frac{1}{T_{150}}\right)\right)} \tag{7.1}$$

The comparison of the rate of the browning reaction in pastry and processed potato product baking is shown in Figure 7.7. It can be seen that the reaction rate of browning reaction in pastry and processed potato product baking was similar. However, different rates were found at lower and higher cooking temperatures. The browning reaction of processed potato product baking was faster than that of the pastry baking at lower temperature between 100 and 145°C, but at temperature higher than 145°C, the pastry browned faster than the processed potato product.

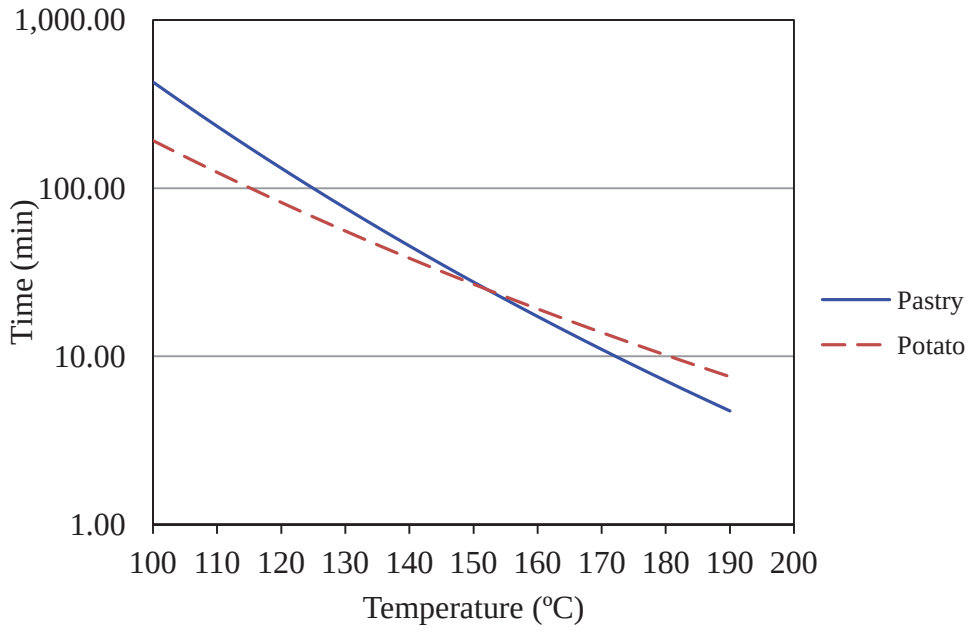

Figure 7.7 Time required to reach 50% total browning reaction for pastry and processed potato product baking at different temperatures

7.6 Model validation

As done for pastry in section 6.3, the kinetic parameters obtained from section 7.5 in this study were used to predict the browning kinetic under non-isothermal cooking conditions for processed potato product baking to validate the developed model. The processed potato product was baked under high temperature conditions, with five different temperature scenarios. The same baking pan as for pastry baking was used and the features of the hot pan are detailed in section 3.4. The temperature of the hot pan was controlled by turning it on and off manually. Each experiment included four replications from four sections on the hot pan. The temperature of the processed potato product bottom surface was measured and logged only at the bottom surface because the browning reaction did not occur at the top. The temperature profiles of all experimental runs are shown in Figures 7.8-7.12.

Five experimental scenarios were used. Experiment 1 had an up and down pattern, the maximum temperature was set as 160°C, but the maximum temperature of the processed potato product surface did not reach the set point temperature. This may be because heat was lost due to an uneven surface of the processed potato product. This experiment was run for 110 minutes; the processing time was divided into two periods,

and the first period was run for 55 minutes. The processed potato product reached the maximum temperature within 10 minutes. The system was then turned off and the temperature cooled to 100°C over the next 45 minutes. The second period was repeated using the same method as the first period, so the total time was 110 minutes (Figure 7.8).

Experiment 2 was a stair pattern; the process was divided into three stages, and each stage took 30 minutes. During the first stage, the temperature increased to close to the set point temperature of 120°C and continued at this temperature for 30 minutes. The second and third stages were the same as the first stage, but the set point temperatures were 140 and 160°C, respectively. Therefore, the total time for this experiment was 90 minutes (Figure 7.9).

Experiment 3 had one period, but the experiment was carried out for a long time (80 minutes). The system was heated to increase the processed potato product temperature to close to the set point temperature of 160°C, and the system was left at this temperature for 10 minutes. The system was then turned off to let the processed potato product cool for 60 minutes (Figure 7.10).

The same pattern as in the first scenario was repeated in experiment 4, but this experiment was divided into three periods. Each period was 60 minutes, the temperature set point of the first, second and third periods were 130, 150 and 170°C, respectively. The temperature was kept at its set point temperature for 15 minutes and the temperature was then decreased for 35 minutes (Figure 7.11).

The last experiment was carried out for 90 minutes, with the set point temperatures of 140 and 160°C for the first and second periods. The temperature of the processed potato product was held at the set point temperature for 20 minutes for each period. At the first period, after the temperature was held at the set point temperature for 20 minutes, the temperature was left to decrease for 30 minutes (Figure 7.12).

As can be seen from Figures 7.8-7.12 the temperature profiles of the four replicates for the same experimental scenario showed very good repeatability. The measured temperature profiles were close together in each experiment.

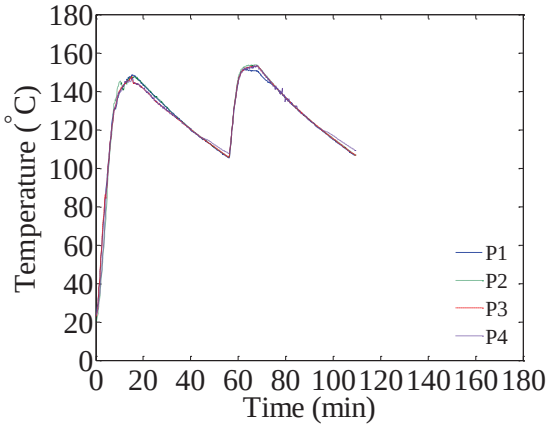

Figure 7.8 Temperature profile at the bottom surface of the processed potato product baked under non-isothermal conditions: Experiment 1

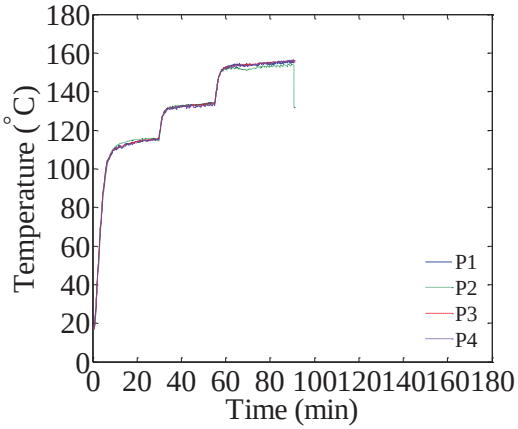

Figure 7.9 Temperature profile at the bottom surface of the processed potato product baked under non-isothermal conditions: Experiment 2

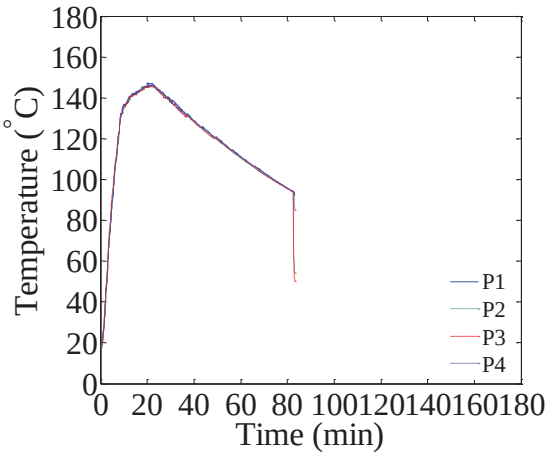

Figure 7.10 Temperature profile at the bottom surface of the processed potato product baked under non-isothermal conditions: Experiment 3

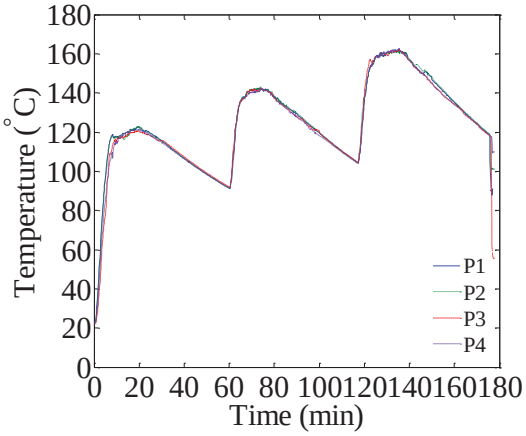

Figure 7.11 Temperature profile at the bottom surface of the processed potato product baked under non-isothermal conditions: Experiment 4

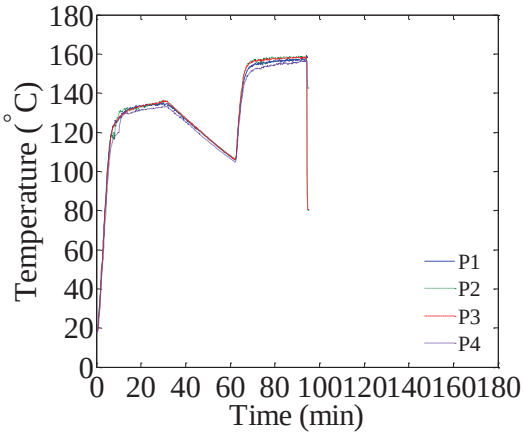

Figure 7.12 Temperature profile at the bottom surface of the processed potato product baked under non-isothermal conditions: Experiment 5

At the end of the process the processed potato product samples from the four sections of baking pan were removed and the colour was measured using image analysis. All lightness values are presented in Table 7.4. The temperature data from all experiments was used in the non-isothermal model in order to predict the lightness.

The predicted lightness values are presented as continuous lines of lightness reduction with increasing processing time (Figures 7.13-7.17). All predicted lightness profiles from the model predictions are presented in the pattern following the history of the temperature of the processed potato product. The graphs show the predictions for all four replications in one experiment, it was seen that there was high repeatability for the predicted lightness of the four replicates. This was because the predicted lightness values were calculated from the measured experimental temperature histories, which showed a high degree of consistency between replicates. The predicted lightness values of the processed potato product baked at high temperatures of baking were lower than those baked at low temperatures.

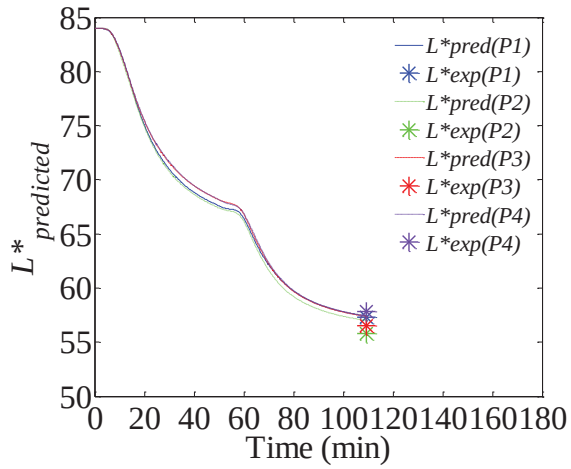

Figure 7.13 Predicted L^* profile of the processed potato product baked under non-isothermal conditions: Experiment 1

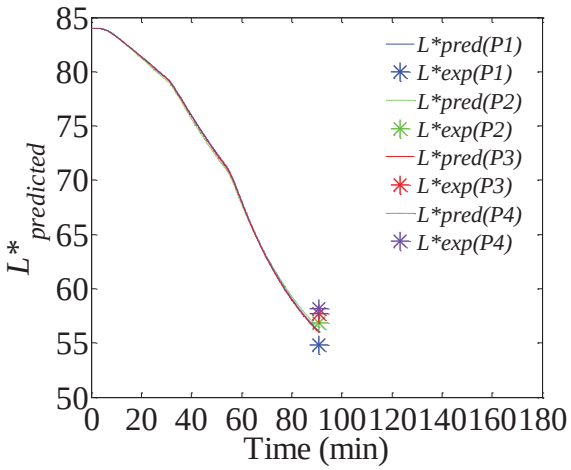

Figure 7.14 Predicted L^* profile of the processed potato product baked under non-isothermal conditions: Experiment 2

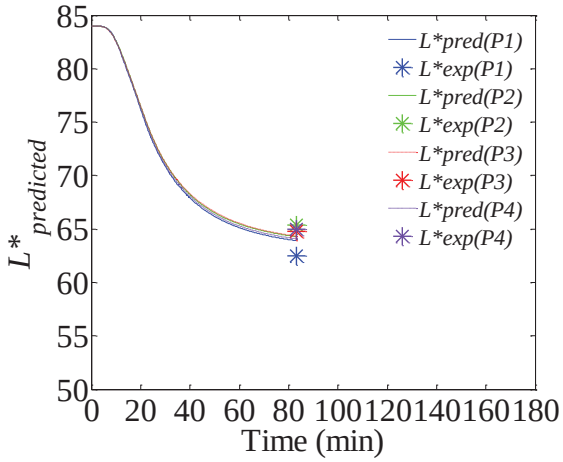

Figure 7.15 Predicted L^* profile of the processed potato product baked under non-isothermal conditions: Experiment 3

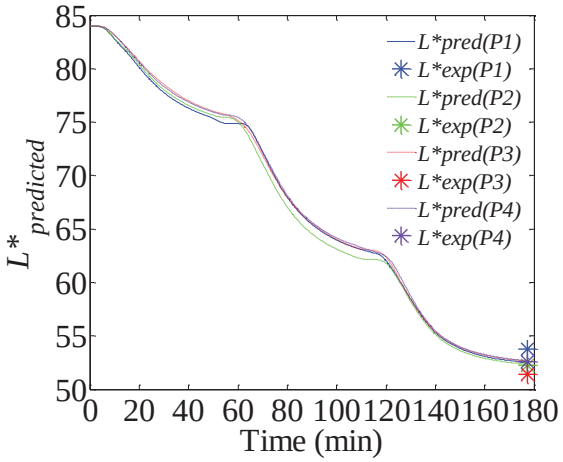

Figure 7.16 Predicted L^* profile of the processed potato product baked under non-isothermal conditions: Experiment 4

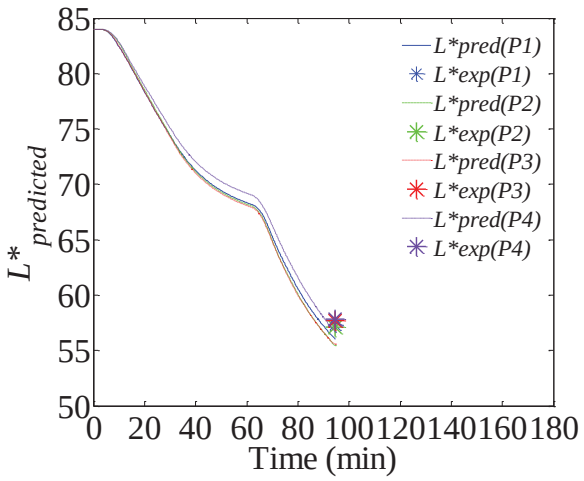

Figure 7.17 Predicted L^* profile of the processed potato product baked under non-isothermal conditions: Experiment 5

The predicted lightness values were compared with the experimental lightness evaluated at the end of the cooking period for the five experimental scenarios, as shown in Table 7.4 and Figure 7.18. The mean absolute relative error (e_{abs}[%]) was calculated using Equation (6.1) to show the goodness of the model prediction. The calculated e_{abs} was 1.95% (n = 20), confirming that the model performed well for the processed potato product baking.

The processed potato product samples at four different baking positions on the hot pan are presented using the symbols of P1, P2, P3 and P4 for position 1, 2, 3 and 4, respectively. From the table, it was found that the predicted lightness values were close to the experimental values, the largest different between the experimental and the predicted lightness values was 2 units.

Table 7.4 Comparison between the experimental lightness values of the processed potato product surface at the end of cooking and the predicted lightness values for five non-isothermal heating scenarios

Experimental scenarios		The lightness (L^*) of baked potato product		Experimental scenarios		The lightness (L^*) of baked potato product	
		Experimental	Predicted			Experimental	Predicted
Experiment 1	P1	57.31	57.43	Experiment 4	P1	53.80	52.49
	P2	55.83	57.02		P2	52.28	52.38
	P3	56.52	57.40		P3	51.40	52.62
	P4	57.85	57.40		P4	52.61	52.68
Experiment 2	P1	54.84	56.06	Experiment 5	P1	57.34	56.03
	P2	56.83	56.44		P2	57.08	55.46
	P3	57.71	55.99		P3	57.69	55.58
	P4	58.13	56.08		P4	58.86	56.74
Experiment 3	P1	62.47	63.91				
	P2	65.34	64.30				
	P3	64.79	64.33				
	P4	64.97	64.09				

Figure 7.18 shows a prediction plot, it was observed that the predictions are scattered closely around on the perfect prediction line. There is a small variation among the same experimental run which was due to the variation of the sample quality. As can be seen in Figures 7.2 and 7.3, the surface of processed potato product samples were very rough resulting in an uneven browning colour. This uneven surface could contribute to the variation in replicate measurements.

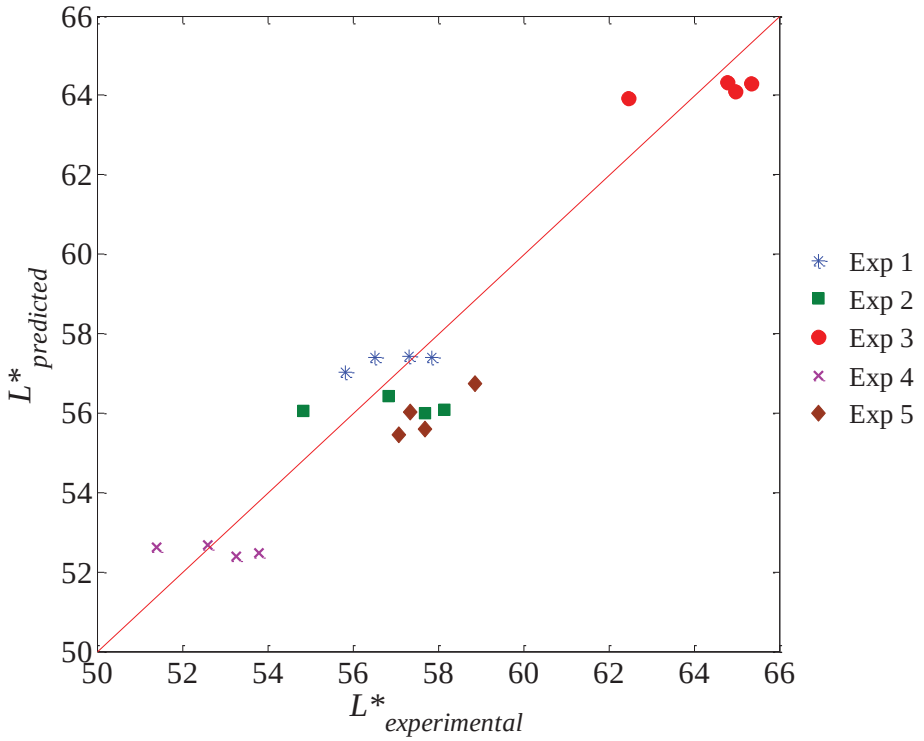

Figure 7.18 Comparison between experimental and predicted lightness of the processed potato product during baking

7.7 Conclusion

This chapter demonstrated the application of the non-isothermal model to predicting the browning for another food product. The browning kinetic model for processed potato product baking was developed using the same method as for pastry baking. The model was solved by applying all temperature histories to predict the lightness values for each experiment to achieve the best fit. The estimated kinetic parameters of the browning change for processed potato product baking were compared with that of the pastry baking to explore the kinetics of the reaction. It was discovered that the estimated kinetic parameters of the browning reaction for processed potato product baking were different from those of pastry baking. From the comparison of the kinetic parameters, it was found that the browning reaction in pastry baking was more temperature-sensitive than that in processed potato product baking. The rate of reaction at 150ºC baking of these two samples baking was similar which can be seen from k_{150} values, however the rates were different when baking at lower and higher than 150ºC. The reaction rate in processed potato product baking was faster at lower temperature and slower at higher temperature. This was likely as the compositions of the processed potato product and

pastry are different, so the kinetics of the browning reaction for these two food samples were different even when they were cooked with the same method.

The developed model was then validated with other non-isothermal cooking patterns by using five different temperature profiles. The lightness profiles of each cooking scenario were predicted using the developed model, the actual temperature profiles and the estimated kinetic parameters. The results showed that the developed model predicted the lightness of processed potato product under non-isothermal baking process well. These results suggest that the browning kinetic model developed using the non-isothermal condition method may applicable to describe the Maillard browning reaction in a range of foods, however differences in the reaction kinetic parameters for the different kinds are expected. For this reason, the kinetic parameters must be re-estimated for different foods.

The model was demonstrated to work well for predicting the browning under the cooking condition ranges for which the model had been developed. Many experiments were needed to collect the data required, which were in the temperature range of interest. From these findings, it is proposed that the non-isothermal kinetic model may potentially be fitted to one experiment if the experimental conditions are designed to cover the range of temperatures over which the browning reactions happen. The one experiment method for non-isothermal model development would take less time and cost. The potential design of a system to allow this will be studied in the next chapter.

Chapter 8

MODEL FITTING USING ONE EXPERIMENT

8.1 Introduction

The previous chapters found that estimating the kinetic parameters using the direct contact pan method has the disadvantage of being time consuming and has the high cost of doing many experiments. It was suggested that the kinetic model can be potentially fitted with the best kinetic parameters from one non-isothermal experiment as long as the surface temperature can be recorded together with colour. This method has advantages over the previous method because it is simple, and takes less time.

This chapter aims to design an experimental study for one experiment that can be used to determine the non-isothermal kinetic parameters for the browning reaction. Ideally, the conditions of the experiment should be similar to the real world application and cover the range over which the reaction occurs. In real life, most foods, in which browning is important are baked using an oven. An oven was therefore used for baking the pastry for this study by designing the oven and measurement system to measure the browning development and the temperature history at the pastry surface through an infrared window.

8.2 Instrument setting and calibration

A baking oven was used as the cooking system for this study because this system would be adapted to enable both the colour and the temperature of the sample to be measured at the same time. The continuous measurement of colour of the sample in this cooking system without removing the sample from the environment was a key improvement. To

achieve this real time assessment, the cooking system needed to capture both the temperature data and colour change during the course of the experiment. The experimental system consisted of the oven for baking, the infrared thermal camera (FLIR E60, duel IR, light sensors; Wilsonville, Oregon, USA) and the lighting system.

8.2.1 The baking oven

The baking oven (Breville BOV800; Breville Pty Ltd., Botany, NSW, Australia) was selected. The dimensions of the oven interior were 470 mm wide, 320 mm deep and 275 mm high. This oven was adapted for use in the study. The inside area of the oven was painted matt white with a very high temperature paint to provide good internal reflection and uniform diffuse lighting. A circular hole was cut into the top of the oven to install a special glass IR window (FLIR model IRW 4C; Wilsonville, Oregon, USA) with a diameter of 100 mm for photo acquisition and temperature measurement using the infrared thermal camera (FLIR E60; Wilsonville, Oregon, USA). This camera was able to capture both a regular colour image, and a thermal infrared image calibrated to the surface temperature. The oven was placed on a table 455 mm from the floor and the camera was held by a tripod perpendicularly 210 mm above the oven. The photo and diagram of the oven cooking system are shown in Figures 8.1 and 8.2.

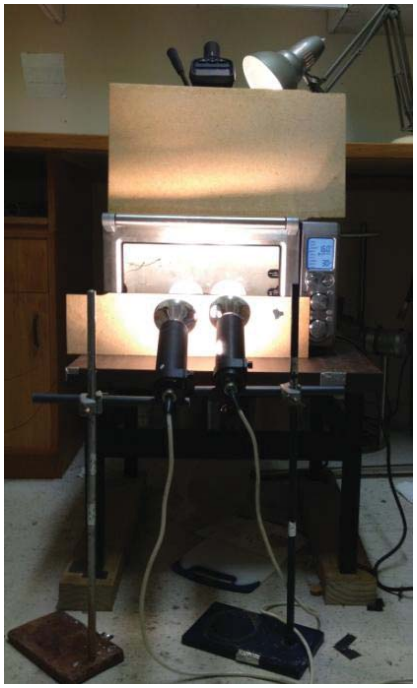

Figure 8.1 Oven cooking system setup showing lighting

8.2.2 Lighting setup

To monitor the colour change of the sample surface inside the oven during the process, an image of the sample was captured using the camera. To obtain a good quality of photo, providing uniform lighting was an important factor. The main limitation was that the light bulb cannot be put inside the oven because of the high temperature. The best way to apply the light was found when the light was placed outside the oven and directed through the front glass door of the oven. The diffuse reflection or the inner surface of the oven helped to improve the uniformity of lighting within the oven.

Figure 8.2 shows the diagram of the lighting set up. Two light bulbs (PHILLIP 100 W with a beam angle of 80°, colour temperature of 2700 K and colour rendering index (CRI) of 80) were placed at the front of the oven and one light bulb (OSRAM 60 W with a beam angle of 80° and colour temperature of 2700 K) was located above the oven. The two light bulbs at the front of the oven were held by clamp stands so they were 560 mm from the floor. The right bulb was 150 mm from the oven and the left side was 120 mm away. These two light bulbs were the main light source for the sample. The light bulb above the oven was put 1100 mm from the floor and 140 mm from the oven top.

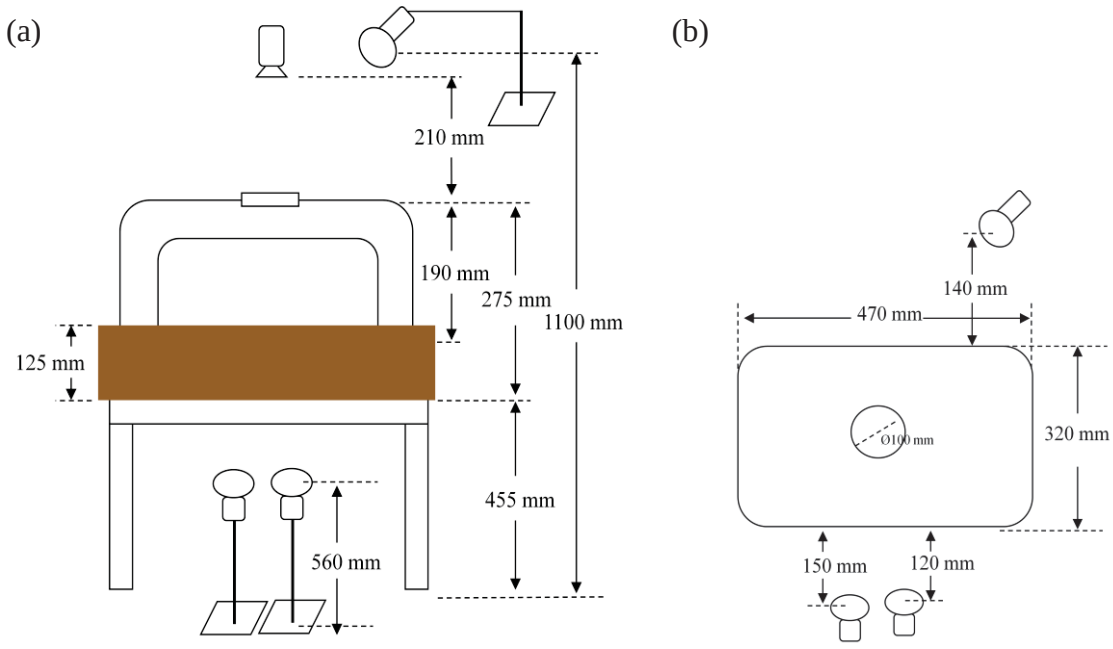

Figure 8.2 Cooking and lighting system diagram: (a) front view of oven and lighting system (b) top view of oven and lighting system

To get high quality images of the pastry rising during the cooking process, providing light directly to the sample surface created a problem for image analysis because specular reflection produced highlights as shown in Figure 8.3.

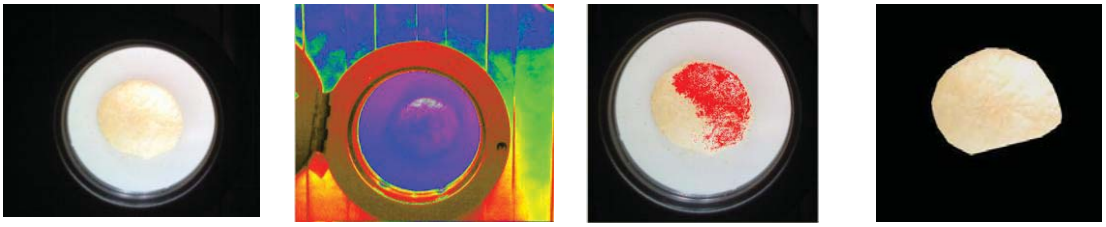

(a) (b) (c) (d)

Figure 8.3 Image of cooked pastry under direct lighting conditions: (a) pastry with direct lighting, (b) false colour image showing highlights, (c) check showing saturated pixels after calibration and (d) segmented image used for colour measurement

Therefore direct light on the pastry surface needed to be avoided. The solution was to place a wood sheet of 125 mm height in front of the oven to block the direct light (Figure 8.4). Consequently, the light passed over the wooden guard to the white painted wall and roof of the oven and then reflected to the pastry and the tile base.

Figure 8.4 A wooden guard placed at the front door of the oven

It was also important for the lighting of the sample to be uniform for correct calibration of the sample colour. The VIPS program was used to check the evenness of the lighting by analysing the range of pixel values in the tile background under the sample. The program also checks that the image is not saturated as this would distort the colour measurement. The VIPS code is listed in Appendix A1.2. Figure 8.5 shows an image with a good even light and the same image after segmentation.

(a) (b) (c)

Figure 8.5 Good even light images: (a) normal image with a good even light (b) showing only a few pixels saturated pixels (coloured red) and (c) sample after segmenting sample from background

Another feature of the camera that caused problems with image capture was the auto-exposure. With the sample being only a small fraction of the image through the viewing port, when the sample darkened, the exposure increased to compensate (Figure 8.6). This caused the background to saturate. Since the tile background is used for colour calibration, saturation presents inaccurate calibration.

(a) (b)

Figure 8.6 Image series of pastry samples with self adjustment of the camera during the cooking process: (a) a light brown pastry sample with the reference white background and (b) a dark brown pastry sample with saturated background

To solve this problem the average light level was increased so that changes in the sample had less effect on the overall light level. This was accomplished by placing a sheet of white cardboard on top of the oven around the viewing port (Figure 8.7).

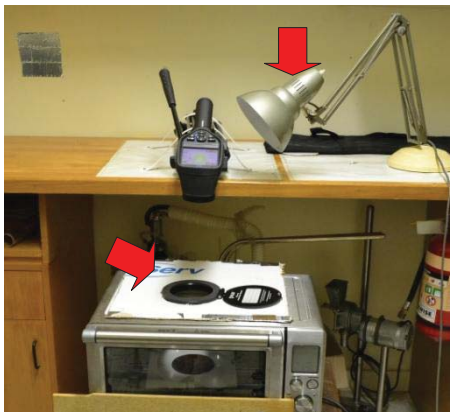

Figure 8.7 The light bulb above the oven and the white cardboard on the oven to overcome self adjustment issue

After providing the cardboard above the oven, good images were obtained as shown in Figure 8.8.

(a) (b)

Figure 8.8 Image series of pastry samples taken during the cooking process: (a) a light brown pastry sample with the reference white tile background and (b) a dark brown pastry sample with unsaturated reference white tile background

8.2.3 Temperature measurement method

The infrared camera (FLIR E60; Wilsonville, Oregon, USA) was used to measure the temperature of the sample surface during the cooking process. The camera had several advantages. Firstly the camera can take both IR and visible images for analyzing the temperature and the colour at the same time. Secondly, the sample did not need to be removed from the oven to measure the colour. Thirdly, the infrared camera provided more accurate temperature measurement than the thermocouple probe because the infrared camera can measure the complete pastry surface and not just at one point. In

addition, there was trouble in placing the thermocouple probe on the pastry surface; this caused an error in temperature measurement, which the infrared camera thermometer solved, once calibrated.

Prior to using the infrared camera to measure the temperature of the object, the infrared camera needed to be calibrated. This involved several steps. The sample was placed inside the oven and the IR camera accesses the object through the IR window, on the top of the oven (Figure 8.2). Therefore, to obtain accurate colour and temperature properties of the pastry, calibration had to take into account the transmission value of the IR window.

8.2.3.1 Estimation of the transmission value of the IR window

This section describes a simple procedure for estimating transmission losses in IR windows. Using this method, it was possible to achieve temperature measurements that are accurate enough for applications.

1. Materials

1) Aluminium block
2) Electrical tape
3) Aluminium foil mounted on cardboard or other flat study surface
4) IR camera and IR window being calibrated
5) A calibrated thermocouple probe and data logger
6) A relative humidity meter and thermometer (TH 210, 5%-95% RH, -20-70ºC, EIRELEC LTD)

2. Methodology

The reference object was prepared by placing electrical tape on the outside surface of an aluminium block so that the tape did not overlap. The interval parameters of the IR camera were set as shown in Table 8.1.

Table 8.1 List of the parameters values set into the IR camera during calibration

Parameters	Values
Emissivity	1.00
Object distance	1 m
Relative humidity (%) (measured by RH meter)	50*
Atmospheric temperature (ºC) (measured by thermometer)	23*
External IR window compensation	off

*The values of relative humidity and atmospheric temperature of the environment were measured using RH meter and thermometer before setting in the IR camera.

The reflected temperature was measured using a flat aluminium foil surface by positioning the foil perpendicular to camera's line of sight and at a distance of 60 mm. This step was to calculate the temperature effects from the thermographer and camera's reflections in the window by measuring the temperature of the foil and inputting this number into the IR camera's setting menu in the parameter of reflected temperature (Figure 8.9).

Figure 8.9 Measurement the reflected temperature the foil

In this study the measured reflection temperature was 26.0ºC (Figure 8.10).

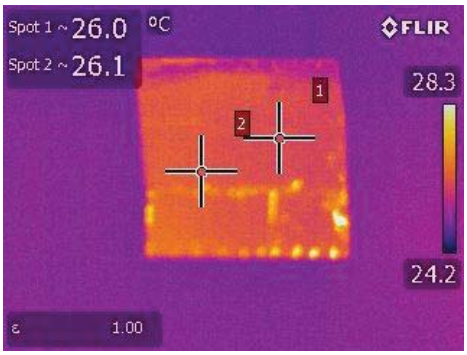

Figure 8.10 Temperature of the foil measured by the IR camera to check the reflection effect

The aluminium block was then placed into the oven and heated up to a set point temperature of 160ºC. The temperature of the aluminium block was measured by both the calibrated thermocouple probe and the IR camera. The temperature was read at 125ºC by the calibrated thermocouple probe. After that, the camera was aimed directly at the hot reference aluminium block and the apparent temperature was measured through the window. The emissivity setting on the IR camera was then adjusted until the temperature reading through the window equalled the true temperature as measured by the thermocouple probe (Figure 8.11).

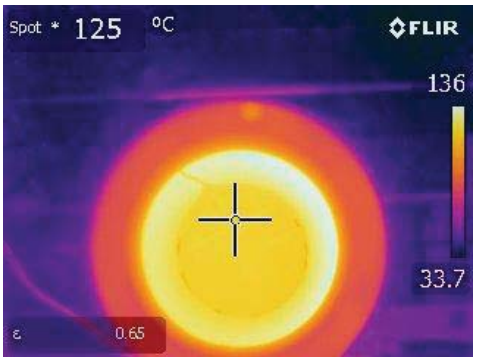

Figure 8.11 The emissivity adjustment to find the transmission value of the IR window by measuring the temperature of the reference object (aluminium block) using the IR camera

The emissivity was found to be 0.65. This emissivity value is then converted to be 65% for the transmission value of the window. After that, the external IR window compensation mode on the camera was turned on and the values of parameters of the IR camera were reset (see in Table 8.2).

Table 8.2 Values of parameters setting in the IR camera after calibration

Parameters	Values
Emissivity	1.00
Object distance (m)	1
Relative humidity (%) (measured by RH meter)	50
Atmospheric temperature (ºC) (measured by thermometer)	23
Reflected temperature (ºC)	26
External IR window compensation	on
Transmission (%)	65
External temperature (ºC) (measured by thermometer)	30

After resetting all parameters, the temperature of the reference object was re-measured again through the window and this value compared with the true temperature read from the calibrated thermocouple probe, which was 112ºC. The image of temperature reading from the IR camera is shown in Figure 8.12.

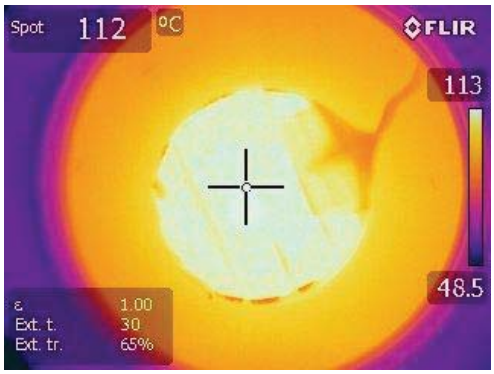

Figure 8.12 The temperature of the reference object after calibration measured by the IR camera through the IR window

8.2.3.2 Thermal camera calibration before using in each experiment

Prior to using the infrared camera for each experimental study, the infrared camera was calibrated. After turning on the infrared camera, all functions of the camera were set at the default, such as the IR window option was turned off, the emissivity value was set as 1, and the distance of the object was 1 m. The important parameters that needed to be re-measured before every experiment were the temperature and relative humidity of the atmosphere of the experimental room for this case. This was because the room

environment was not the same at the different times of the experimental study, and these values influenced the IR camera measuring accuracy. The temperature and the relative humidity of the room were measured using a RH meter; these values were recorded and used to re-set the IR camera.

After setting the values of atmospheric temperature and relative humidity into the IR camera, the reflected temperature was measured using the same method as described in section 8.2.3.1. Then, the reflected temperature value was put into the camera mode. The IR window mode was turned on to set the transmission value and the environment temperature, which were 65% and 30°C, respectively for every experimental run.

After the infrared camera was calibrated, the camera would be used in the cooking process for measuring the temperature and the colour of the pastry sample by taking photos. Figure 8.13 shows two photos obtained from the camera: IR image and digital images, respectively. The IR image was used for temperature analysis and the normal digital image was used for colour analysis.

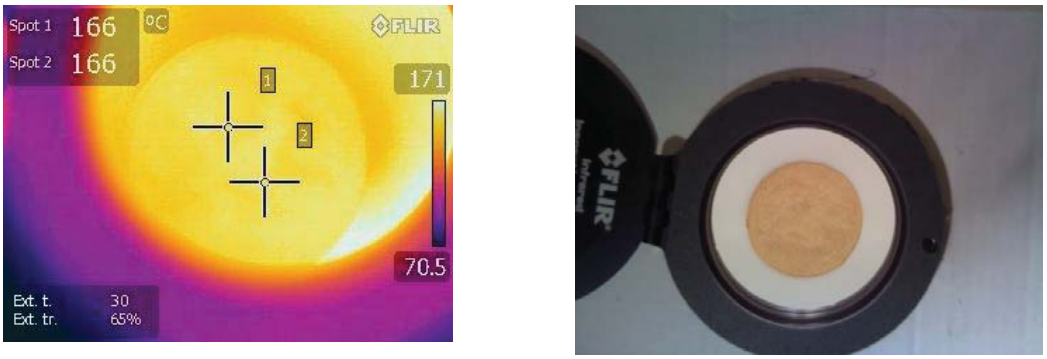

(a) (b)

Figure 8.13 Pictures captured by the FLIR infrared camera: (a) an infrared image and (b) a regular colour image

The IR images were imported into specially developed software for temperature analysis. This software was created by the FLIR company (Wilsonville, Oregon, USA). When an image was analyzed the circle and box were dragged to cover the pastry area, and then the FLIR program calculated the maximum, minimum and average temperature within the circle and the box areas as shown in Figure 8.14 (a). All temperature data was listed (Figure 8.14 (b)). The average temperatures of a circle and squares of each sample were chosen to represent the temperature of pastry surface and

applied in the fitting of the kinetic model. The decision to use the average was made by firstly comparing the temperatures at various points. As there was little difference, the average measured temperature in the circle was considered the most representative for the sample surface.

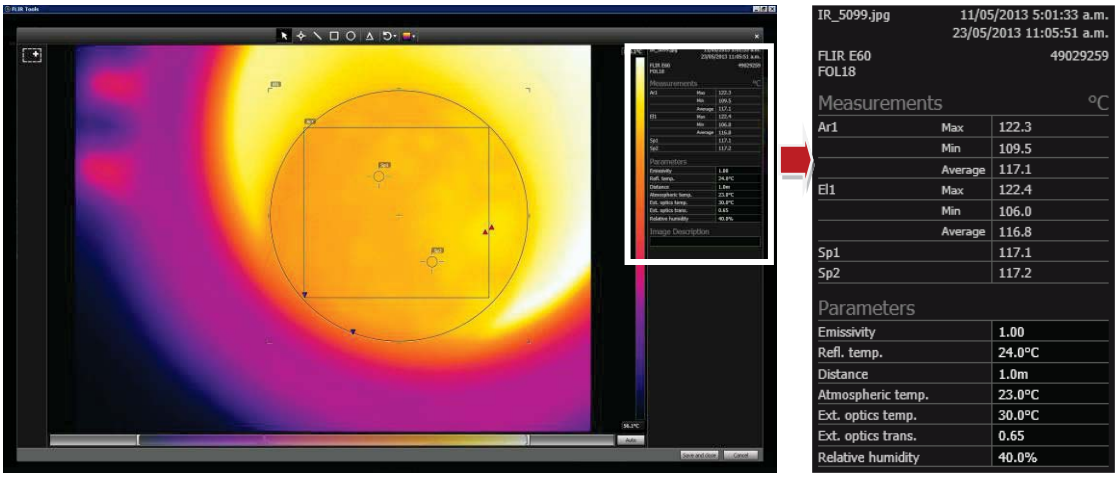

Figure 8.14 Application of the FLIR software program to analyze the IR image of the pastry sample during the baking process (captured by the FLIR camera)

8.3 Experimental design

The objective of this study was to achieve the best non-isothermal experiment that would allow calculation of the best kinetic parameters. Dolan (2003) stated the best kinetic parameters can be estimated from one experiment by using a non-isothermal method that benefits in reducing the experimental effort. In addition, designing a dynamic cooking condition for experimental study to be closer to commercial processing conditions is recommended to allow estimation of the relavant kinetic parameters and overcoming the thermal lag problems (Cunla & Oliveira, 2000 cited by Dolan, 2003). Therefore, the cooking conditions of this method need to be designed by varying the temperature over the range of the commercial cooking conditions and reactions occurring. Based on the findings of the previous study (Chapter 5), the cooking conditions of those experiments were varied from 120°C to 170°C. Therefore, the cooking conditions for this study were designed to cover that temperature range for the Maillard reaction. Two experimental temperature profiles were trialed. The first profile was designed to be a continuous increase of temperature. The oven was heated from room temperature (20°C) to the set point temperature (230°C); this took 30 minutes.

The second condition was carried out by increasing the temperature from room temperature (20°C) to 140°C and holding it at this temperature for 20 minutes. Then the temperature was increased to 160°C and held at this temperature for 15 minutes. This was repeated for 180°C, 200°C and 220ºC for 10, 8 and 5 minutes, respectively. The total time for this experimental set was 80 minutes. Each experiment was repeated three times to see the consistency of data and model fitting. In addition, the second profile had an extra replicate, which was continued on for 70 minutes at 200°C to observe the final lightness value at the end of the reaction. Therefore, this experiment took a total of 130 minutes.

For this study, raw pastry (see section 3.2.6) was used as the model food sample. The commercial pastry was cut using a cookie cutter with a diameter of 120 mm (to fill the field of view of the thermal camera). The pastry was put into the oven at time 0 and then the oven was turned on. Therefore, the pastry temperature started from room temperature (20°C) and was heated to be close to the set point temperature as explained in section 8.3. Note that the experiments were carried out in a dark room and only the light from the lighting system was present.

During the cooking process, images of pastry sample were captured every 30 seconds in an IR file for temperature analysis using the FLIR software and a JPEG file with the resolution of 2048×1536 for colour analysis using the VIPS software.

8.4 Results and discussion

The temperature profiles of the pastry surface for all experiments were plotted and are shown in Figure 8.15. It can be observed from the Figure 8.15 that, the actual temperature of pastry surface that was read by the thermal camera did not reach the set point oven temperature. The difference in temperature between the oven and the pastry surface was around 10ºC. Moreover, it was observed that the system took at least five minutes for the pastry temperature to achieve the next set point temperature. This was because the convection heat transfer to the sample caused a time lag in the temperature at surface of the pastry sample compared to the oven temperature.

Figure 8.15 shows two separate groups of temperature profiles, corresponding to the fast and the step-wise heating experiment. For the fast heating rate experiment, the temperature of the pastry started from a low temperature which was close to room

temperature, and the temperature increased continuously after the oven was turned on. The rate of increase in temperature was very fast in the first 15 minutes and slower for the last 15-30 minutes. The temperature increased from 20-30 °C to 210°C from the beginning to the end of the process. The fast rate of temperature increase was due to the large temperature gradient between the pastry and the oven; however this gradient was reduced in the later stages of heating.

The temperature profile for the second experimental condition used a step-wise heating profile, with different times at each step. This was based on the hypothesis that the Maillard reaction needs a longer time for the reaction at lower temperatures to achieve the same colour change. Therefore at low temperature, the cooking process was run for a long time and the holding time was reduced at higher temperatures. The temperature range covered the range over which the Maillard reaction takes place.

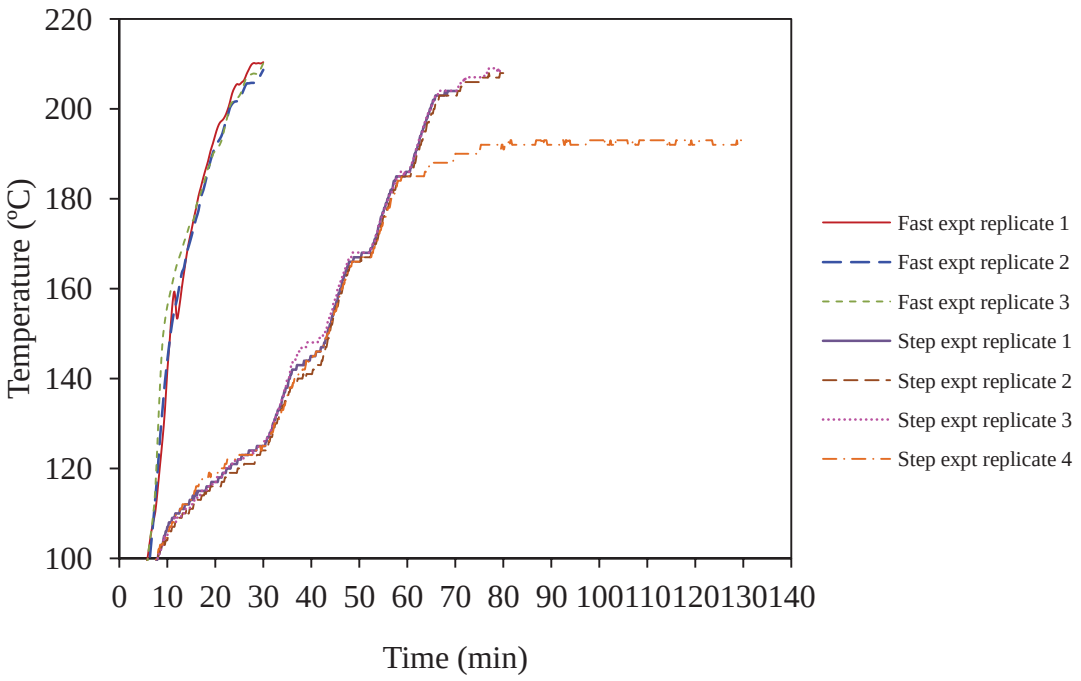

Figure 8.15 Temperature profiles at the top surface of pastry samples for the fast and step-wise heating conditions

The lightness profile of the pastry surface is presented in Figure 8.16. It can be seen that there are two different groups of lightness profiles which were obtained from the two different experimental conditions. The lightness value of the raw pastry at the start of

the experiments was about 93, and then when the heating had been going for 5 minutes, the lightness decreased to around 87 and then increased again to about 94 at 10 minutes.

After this peak, the profile continuously decreased again until the end of process in the fast heating rate experiment. For the step-wise heating experimental condition after the initial dip, the peak value of lightness was stable for first 35 minutes of cooking and then decreased continuously throughout until the end of the process. This profile can be explained as being due to the Maillard reaction starting to take place at the point where the temperature reached about 120°C (Figure 8.15).

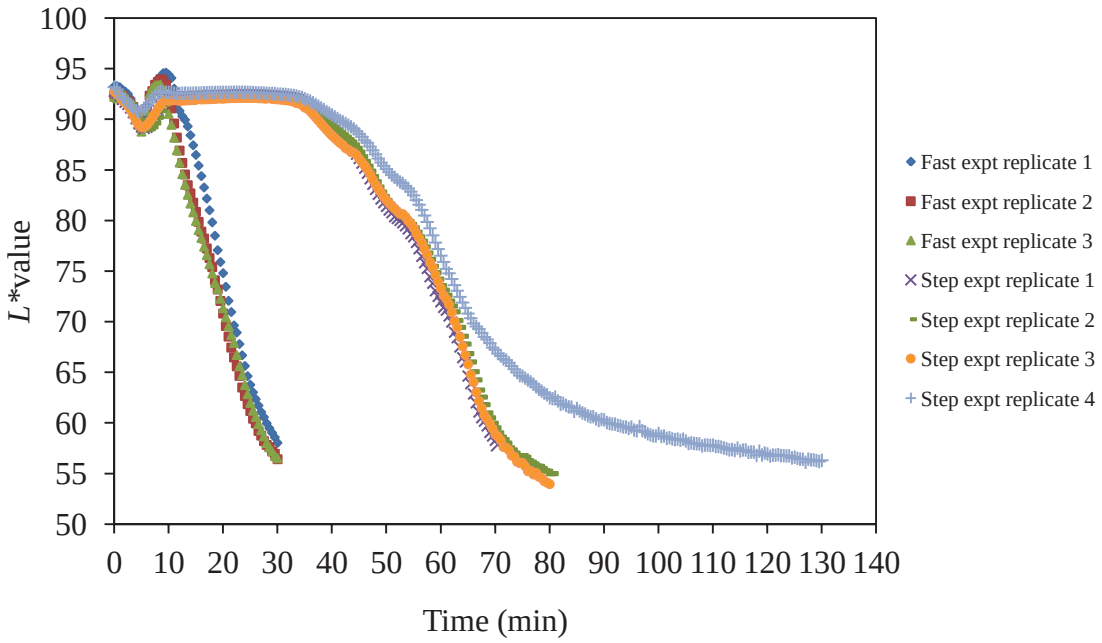

Figure 8.16 Lightness (L^*) profile at the surface of pastry samples during the baking process

The results showing the initial drop then increase in the lightness profile that happened during the initial period of the process can be divided into three stages. The three stages were the drop, increase and final decrease in the lightness profile.

8.4.1 Stage 1

The decreasing of lightness value over the first few minutes was due to the drying process that happens during this stage. The temperature profiles show that temperature came up to 100°C in 5 minutes. To confirm this hypothesis, pastry with four different levels of moisture content were compared. Four 120 mm diameter samples of pastry

were left in the desiccators for 0, 12, 24, 36 and 71 hours to dry. After drying, all pastries were removed from the desiccators and photographed under the controlled lighting system using the thermal camera (the same condition as for the pastry baking study). The colour of these four pastries was analyzed using the VIPS software program. The algorithm for image analysis is presented in Appendix A1.2. The colour value data of these four pastries are presented in Table 8.3 and the plot of lightness values and the moisture content values of the pastry are shown in Figure 8.17.

Table 8.3 The pre-baking *L**, *a** and *b** colour values of pastry samples with different moisture content

Samples	a_w	**%MC (wt% of d.b.)**	***L****	***a****	***b****
Normal sample	0.96	41.30	93.07±0.49	-1.04±0.93	9.43±1.05
12 hrs drying	0.92	31.97	91.22±0.75	-1.38±1.13	13.63±2.63
24 hrs drying	0.87	24.93	90.26±0.83	-1.23±2.58	14.82±2.58
36 hrs drying	0.84	22.02	89.58±0.88	-1.17±1.09	16.42±2.43
71 hrs drying	0.66	12.95	90.55±1.27	-1.11±1.11	15.39±3.66

It can be seen from Figure 8.17 that as the moisture content of the pastry decreased from 41.30 to 22.02 wt% of d.b. the lightness decreased from 93 to 89. The pastry became darker when the pastry was dry. However, it was found that when the moisture content reduced to a very low value, about 12 wt% of d.b., the colour of the pastry started to get brighter again. The value of lightness was measured as 90.55. Therefore it can be concluded that the moisture content of the pastry affected its colour. This agreed with the results of the study of the effects of the moisture content of the pastry on the browning kinetic of pastry baking in section 4.4 where the moisture content had an effect on the initial lightness of the pastry.

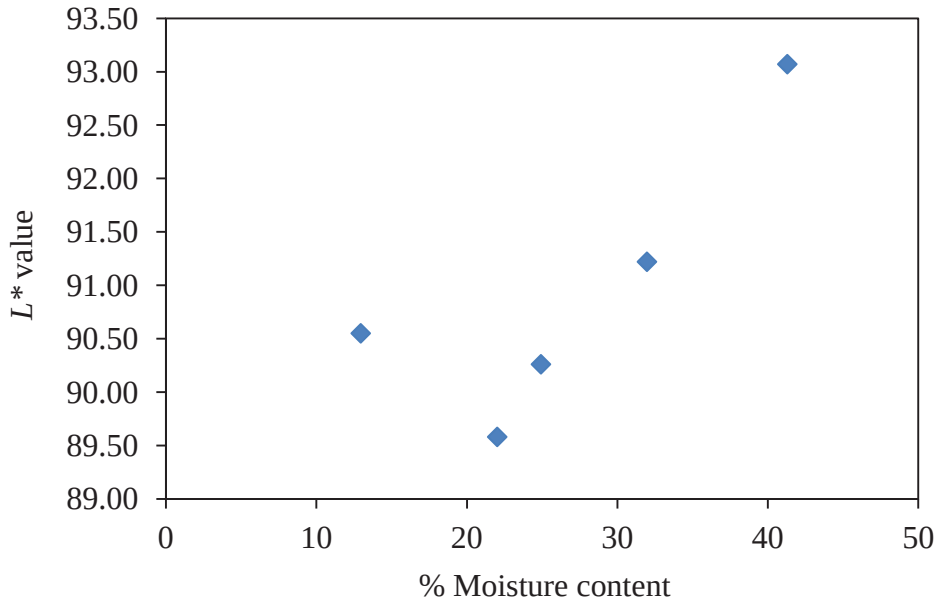

Figure 8.17 The lightness values of the pastry at different moisture contents

This hypothesis was also tested by an additional experiment with a low moisture content pastry. Using the same temperature profile as the fast heating rate experimental, the lightness was measured every 30 seconds during the process for 30 minutes. The lightness profile was plotted against the processing time and is shown in Figure 8.18.

It can be seen from Figure 8.18 that the lightness value at the beginning of the process starts at a lower value (89) than that of the moist pastry sample, which had a lightness value of around 93. As the process started with a low moisture content of the pastry with a lower value of lightness, the decrease of the lightness due to moisture evaporation in the first stage was not found in this study. The lightness value stayed constant at a low value for 5 minutes and then started to increase again during 5-8 minutes of the cooking process. The increasing of lightness value after this cooking time can be assumed as the second stage, and is discussed in the next section.

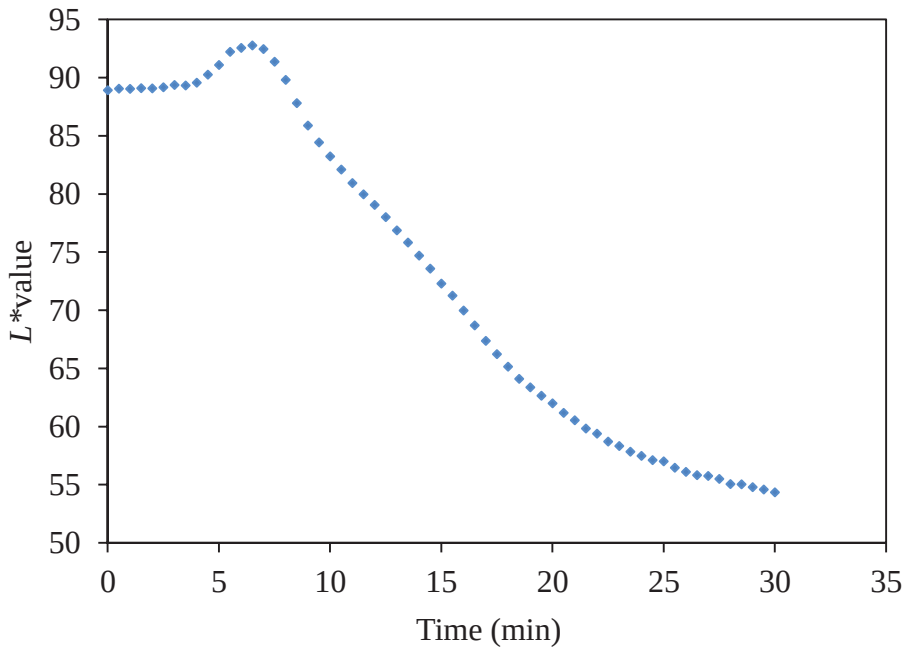

Figure 8.18 The lightness profile of the low moisture content pastry sample during baking in the oven

8.4.2 Stage 2

The second stage happened when the temperature of the pastry's surface was between 100 and 120ºC (Figures 8.16 and 8.18). It was found in the experiment that the pastry rose and the fat separation phenomenon took place at this stage. This caused the surface of pastry sample to become brighter and the lightness value to increase (Figure 8.19). This has been found in other research studies, for example in cookie baking (Shibukawa *et al.*, 1989) and cracker baking (Broyart *et al.*, 1998). The explanation for this has been reported as the dough was rising up due to the pressure of water evaporation inside the sample. The rising of the sample surface resulted in the increasing of lightness value. This explanation was also found in the study of cracker baking by Savoye *et al.*, 1992 and Broyart *et al.*, 1998. They explained this phenomenon saying that the rising of the cracker surface during the initial stage of the baking process made the product surface appear to be lighter due to more reflection. This is also in agreement with the report of Pulis & Salvadori, 2007, 2009 and Pulis, 2010, who stated that the lightening at the beginning of the process was due to the physical changes of the bread dough during baking. Some studies reported that the increase of the L^* value at the early stage of heating was due to the drying of the surface of the dough sample (Shibukawa *et al.*, 1989).

This matter can be clearly seen in Figure 8.19. A difference in colour was observed between the raised area and the non-raised area, a lighter colour is seen on the risen area with the rest of the dough looking darker. The lightness increased until the pastry was completely risen. The lightness started to decrease again after the surface temperature reached 120°C, the point at which the Maillard reaction begins.

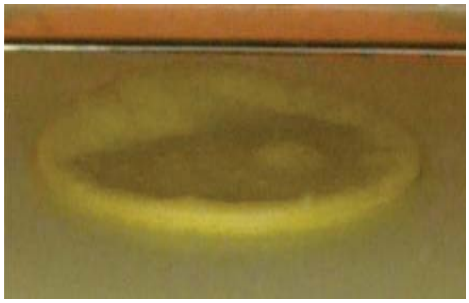

Figure 8.19 The risen area of the pastry sample at 8 minutes baking time

Figure 8.20 shows the change of the pastry in terms of colour and physical properties with the lightness profile. It can be clearly seen that the surface of the pastry was changing during the processing time. For the first stage there was no rising of the surface and the colour was darker. This correlated with the decrease in the lightness profile. The rising of the pastry surface started to appear at 6 minutes, resulting in an increase of the lightness value again. The highest peak of pastry was found at the highest lightness value after 10 minutes of cooking. After this point, the browning reaction began to take place. It can be seen from Figure 8.20 that the lightness value declined again and the profile shows that the colour of pastry surface continued to become darker until the end of the process.

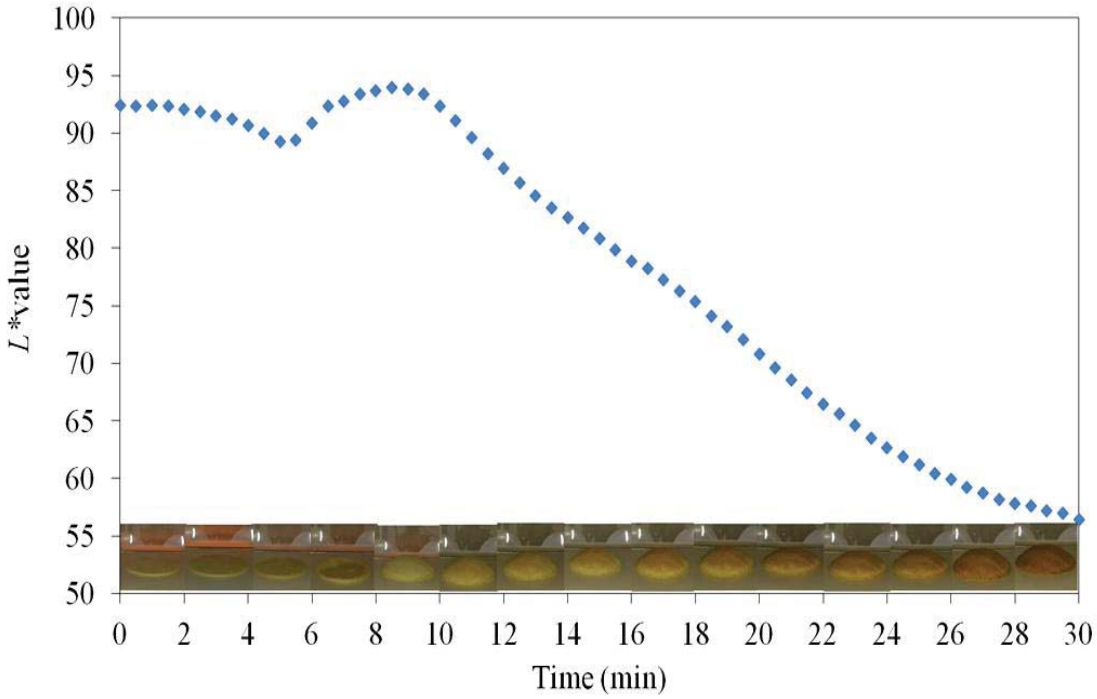

Figure 8.20 Colour and physical changes in the pastry surface at different times of baking

8.4.3 Stage 3

The third stage of this study was regarded as the time when the browning reaction occurred. The lightness value decreased from the point where the temperature of pastry surface was at about 120°C. The Maillard reaction onset temperature has been reported as 120ºC (Shibukawa *et al.*, 1989; Pulis & Salvodari, 2009) or 110ºC (Broyart *et al.*, 1998; Wahlby & Skjoldebrand, 2002 and Mondal & Datta, 2008).

The experiment for investigating and confirming the onset temperature of the Maillard browning reaction was studied by baking the pastry in the oven. The condition for this study was the same as the fast heating rate experiment but the temperature of oven was held at 120°C for 10 minutes and then increased continuously for 24 minutes. The temperature profile of pastry surface of this study is shown in Figure 8.21.

At the early stage of the process, the temperature of the oven rapidly increased until 90°C, and then the temperature slowly increased up to 120°C. The temperature of the oven was held at 120°C until the pastry had been in for 20 minutes of baking (Figure 8.21). As can be seen in Figure 8.22 after this 20 minutes period, the lightness value of

the pastry started to decrease. It can be concluded from Figures 8.21and 8.22 that the Maillard browning reaction in this study for the pastry baking started at 120°C.

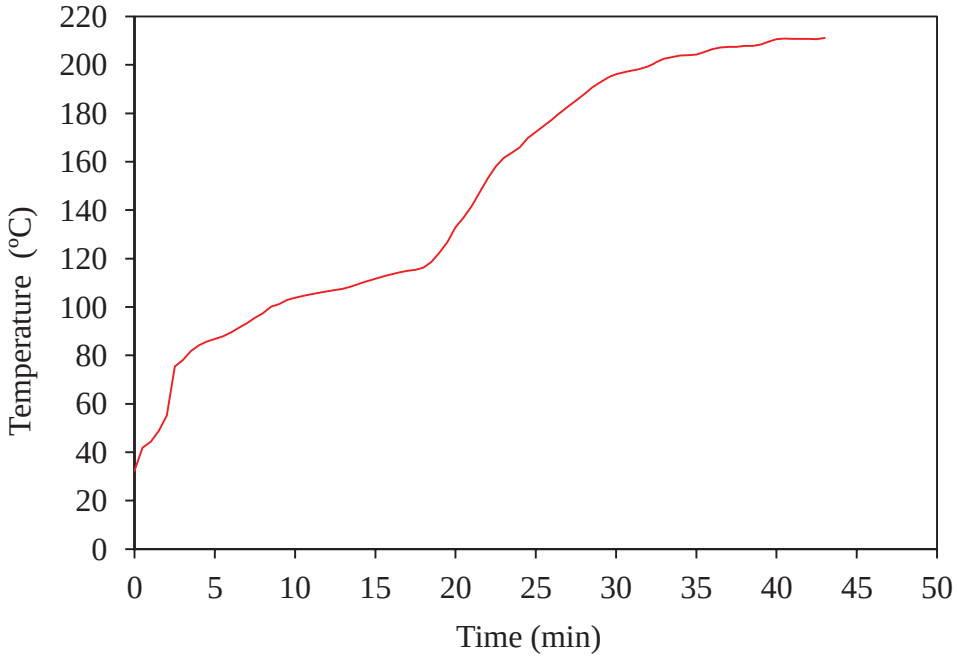

Figure 8.21 Temperature profile of pastry baked at the holding temperature of 120°C for 10 minutes followed by a continuous temperature rise

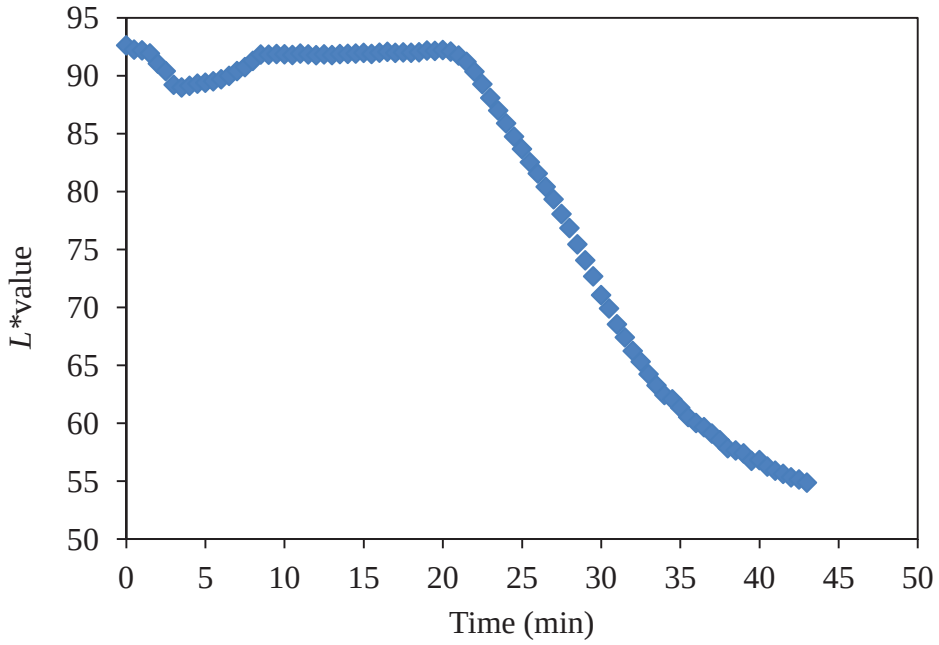

Figure 8.22 Lightness profile of pastry baked at the holding temperature of 120°C for 10 minutes followed by a continuous temperature rise

8.5 The experimental result used for kinetic model fitting

As measurable Maillard browning rates occured at 120°C, the lightness data and time-temperature history used for fitting the kinetic model was started from where the temperature of pastry surface reached 120°C. The resulting profiles of temperature and lightness are shown in Figures 8.23 and 8.24, respectively. The moisture evaporation and the rising stages area were not included in the model fitting since the Maillard browning reaction did not occur during those periods.

From Figure 8.23, the temperature of all experiments started at 120°C. The lightness decreased from the initial value of 94 and 93 for the fast and step-wise heating experiments, respectively (Figure 8.24). The lightness profiles of pastry sample baking in the fast heating rate experiments decreased faster and steeper than that of the pastry baking in step-wise heating experiments.

In both experiments the temperatures were increased up to a maximum of around 210°C, except in replicate four of the step-wise heating experiment. The lightness values of the fast heating rate experiment ended at around 56 but the final lightness values of the step-wise heating experiment were around 54. Lower values of lightness for the step-wise heating experiment were due to the pastry being baked for a longer time at the highest temperature of 210°C than that for the fast heating rate experiment. The temperature profile of replicate four of the step-wise heating experiment was slightly lower than that of others, so the lightness value profile from this experiment was slightly higher than that of the other experiments (Figures 8.23 and 8.24). At the last stage of replicate four for the step-wise heating experiment, the lightness value was slightly decreased because the process was held at the stable temperature of 190°C for 50 minutes. The final lightness was measured as 56.

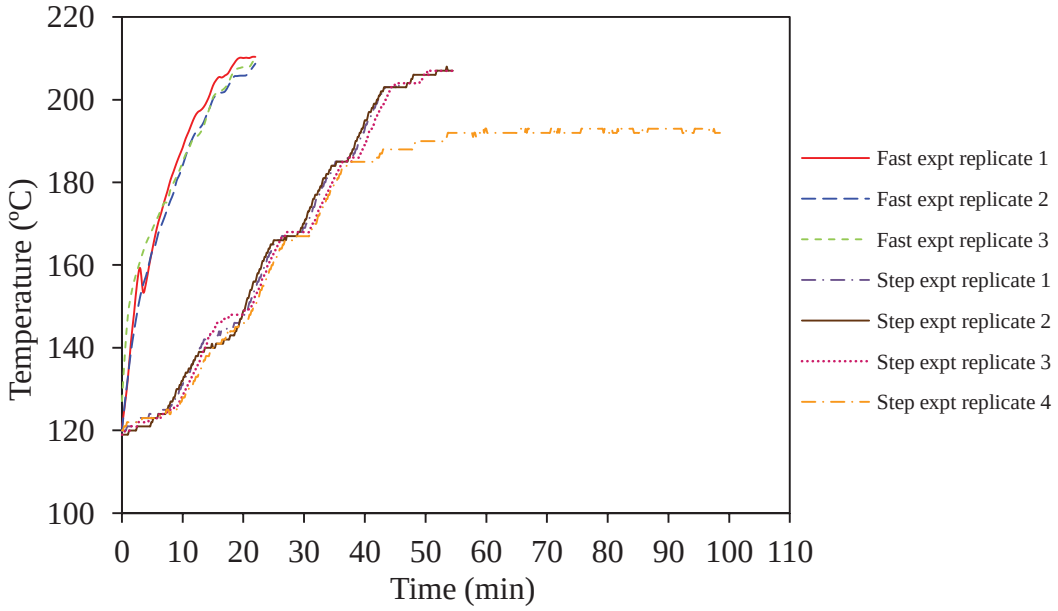

Figure 8.23 Temperature profiles of pastry baked in the range of the Maillard browning reaction for fast and step-wise heating experiments

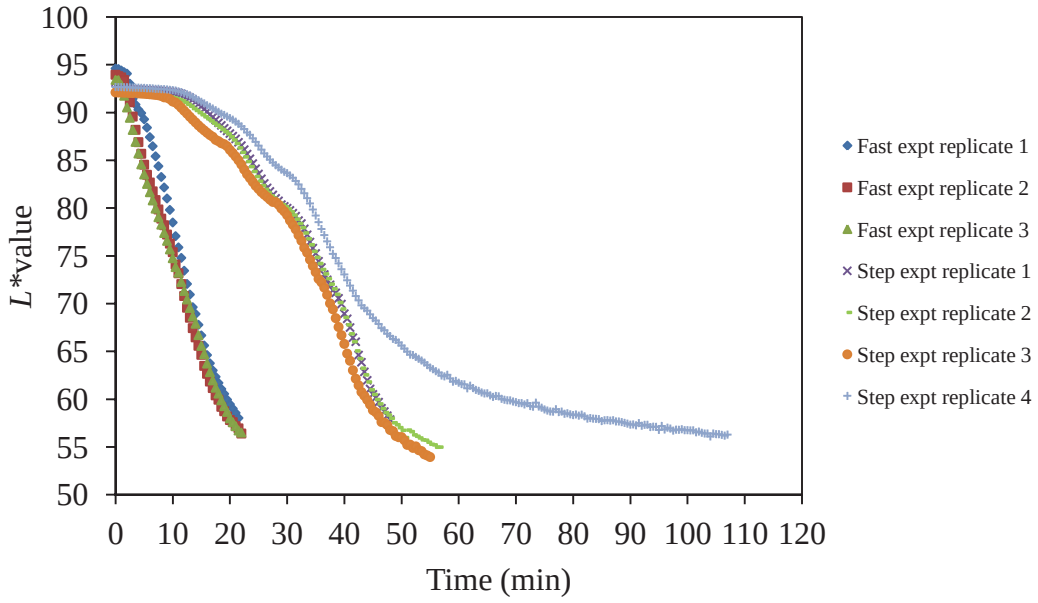

Figure 8.24 Lightness profiles of pastry baked in the range of the Maillard browning reaction for fast and step-wise heating experiments

8.6 Kinetic model fitting

All of the temperature and lightness data were recorded in Excel data sheet files. These data sheet files were used to fit the model using the *lsqnonlin* function in MATLAB®.

The kinetic model was fitted using the non-isothermal model that was developed in section 5.4 and the kinetic parameters were estimated from the model fitting. The code for this solution was the same code as using in section 5.4 (Appendix A6). The estimated kinetic parameters for each experiment are listed in Table 8.4 and compared with the values obtained from the pan experiment (section 5.4).

It was found that the kinetic parameters of each experimental set were different. The activation energy (E_a) obtained from the pan experiment was the highest and the value obtained from the step-wise heating experiment was higher than that of the fast heating rate experiment. This means that the Maillard reaction for the pan experiment was more temperature-sensitive than the step-wise and fast heating rate experiments. The kinetic rate constant at 150°C (k_{150}) obtained from the fast heating rate experiment was the highest and the value obtained from the pan was higher than that of the step-wise heating experiment. The rate of browning reaction for the pastry baking was the fastest using the oven baking at 150ºC for the fast heating rate experiment as can be seen from the highest value of k_{150}. Conversely, the slowest browning reaction rate was of oven-baked pastry calculated using the step-wise heating experiment.

Considering the estimated kinetic parameters obtained from each experiment within the same experimental set, it was found that both values of activation energy (E_a) and kinetic rate constant at 150°C (k_{150}) were similar for the four replicates for the step-wise heating experiments. They were in the range between 58.68 and 71.18 kJ·mol^{-1} and between 0.011 and 0.014 min^{-1} for activation energy (E_a) and the kinetic rate constant at 150°C (k_{150}) values, respectively. However, the estimated kinetic parameters obtained from the fast heating rate experiment were obviously different among the three replicates, the activation energy values (E_a) were between 14.56 and 53.93 kJ·mol^{-1} and the kinetic rate constant at 150ºC (k_{150}) were between 0.029 and 0.046 min^{-1}. The goodness of fit for all experiments was calculated and the results showed that the pan experiment presented the lowest value whereas the other experiments gave very high values. This was because the empirical model was separately fitted with each set of experimental data for the fast and the step-wise heating experiments, while the model for pan experiment was an overall fit using numerous experimental data.

Table 8.4 Estimated kinetic parameters from the single experiment browning kinetic model fitting

Kinetic parameters		E_a (kJ·mol^{-1})	k_{150} (min^{-1})	L^*_0	L^*_∞	R^2
Pan experiment		71.95	0.025	91.21	67.54	0.920
Fast heating rate experiment	Replicate 1	53.93	0.029	94.70	54.31	0.999
	Replicate 2	26.81	0.046	94.50	48.16	0.998
	Replicate 3	14.56	0.033	93.93	33.96	0.998
Step-wise heating experiment	Replicate 1	58.68	0.011	93.47	41.78	0.997
	Replicate 2	66.34	0.014	92.58	52.16	0.997
	Replicate 3	71.18	0.011	92.19	51.14	0.998
	Replicate 4	67.79	0.012	93.37	56.92	0.998

8.7 Comparison of the kinetic rates between the different experiments

To compare the rates of the Maillard reaction for all experiments, the kinetic parameters were used to calculate the time requirement to reach 50% of the total reaction under isothermal conditions using Equation 7.1 as done in section 7.5 to compare the kinetics of pastry and processed potato product samples and the graph is shown in Figure 8.25. Three separate trends for reaction rate can be seen. The first group was the fastest reaction rates which were of the fast heating rate experimental condition replicates 2 and 3. The second group in the middle of the graph, consisted of the pan experiment and the fast heating rate experiment replicate 1 and the last group were all of the step-wise heating experiments.

From this graph, it can be seen that the kinetic model fits from different experimental sets gave different rates. The step-wise heating experiments showed similar rates among them and gave the slowest reaction rate compared with the other experiments. The fastest rates of the browning reaction of pastry baking were found in the fast heating rate experiment replicates 2 and 3, especially at low temperatures. As can be determined from the time require to reach 50% completion of reaction in the pastry baking for the fast heating rate experiment replicates 2 and 3 were shorter than that for the other experiments when baking pastry at low temperatures of between 120 and 150ºC. However, during temperatures higher than 170ºC, to reach 50% Maillard

reaction extent, the baking with the pan and fast heating rate experiment replicates 1 required smaller times than the other experimental conditions.

It can be concluded from these findings that the pastry baking under different cooking conditions generated different browning reaction kinetics. Consequently, the developed kinetic models were inapplicable to predict the browning development of pastry baking under different baking conditions since their reaction kinetics were different.

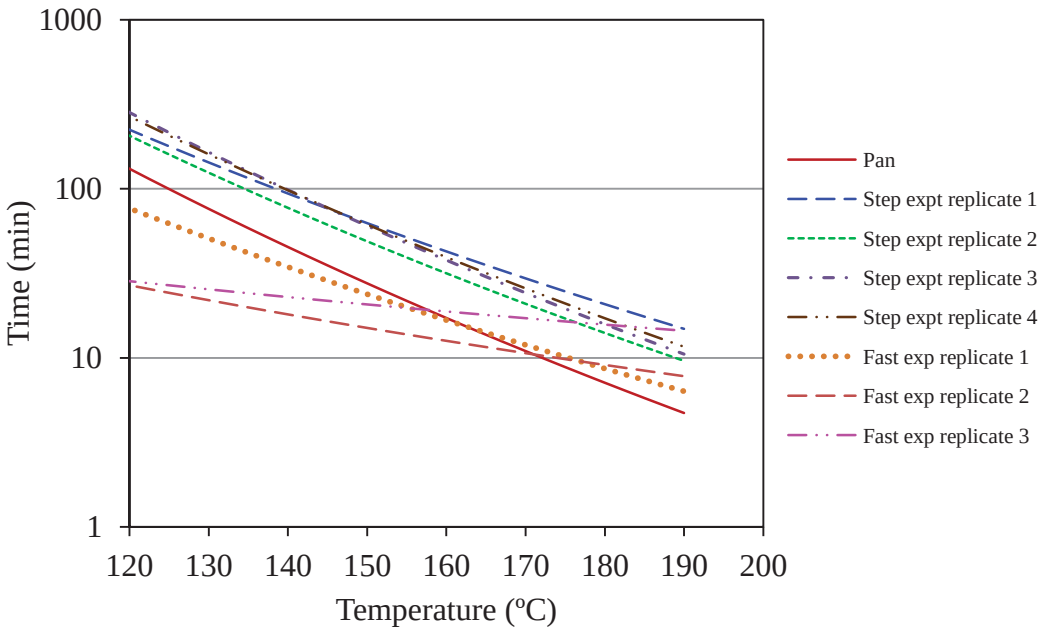

Figure 8.25 The time required for the Maillard reaction to achieve 50% of the reaction at different temperature

8.8 Potential causes of observed browning kinetics differences

The different cooking conditions resulted in different kinetics for the reaction. The possible causes of the different results in kinetic reactions may be potential errors in the experimental measurements of the temperature and colour and the complexity of the mechanism of the Maillard reaction. All three potential factors are therefore explored and discussed in this section.

8.8.1 Temperature measurement

The temperature profile was the significant input parameter in the model fitting for evaluating the kinetic parameters. Potential errors in the input temperature data could be a possible cause of the different kinetics results. It was shown that the thermal camera

was calibrated in section 8.2.3 for each run. Therefore, the measured temperatures of the pastry surface were probably accurate and it is difficult to see how an independent check could be made.

The average temperature across the pastry surface was used as the input temperature profile for fitting the model in this study. However, there was a temperature distribution on the pastry surface that may impact on the kinetic fit. To test this hypothesis, the kinetics were re-fitted by importing the temperature profiles at ten different points on the pastry surface to see the effect of the temperature distribution on the kinetic fit. Ten different points on the pastry surface were defined as:

- P1 and P2 were the point at positions 1 and 2 on the pastry surface, manually read by the experimenter
- SP1 and SP2 were the point at positions 1 and 2 on the pastry surface, read using the FLIR software
- Max (Box), Min (Box) and Average (Box) were the maximum, minimum and average temperature in the box area on the pastry surface, measured using the FLIR software
- Max (Circle), Min (Circle) and Average (Circle) were the maximum, minimum and average temperature in the circle area on the pastry surface measured using the FLIR software. Average (Circle) was the usual method used

Table 8.5 shows an example of the estimated kinetic parameters obtained from all ten temperature data measured on the pastry surface for the fast heating rate experiment replicate 2 and the step-wise heating experiment replicate 3. Note that, other kinetic fitting results are presented in Appendix A8. It was found from Table 8.5 that the estimated kinetic parameters from different points on the pastry surface for the same experimental replicates were similar for the same replicate. Thus the temperature distribution had little effect on the kinetic parameters estimation and the average temperature (circle) can be used as the input temperature data for model fitting.

Table 8.5 The values of estimated kinetic parameters fitting using temperature data at different points on the pastry sample

Kinetic parameters		E_a (kJ·mol^{-1})	k_{150} (min^{-1})	L^*_0	L^*_∞	R^2
Fast heating rate experiment replicate 2	P1	30.83	4.25	94.28	48.85	0.998
	P2	31.79	4.29	94.32	49.37	0.998
	SP1	31.34	4.25	94.28	49.03	0.998
	SP2	31.96	4.28	94.30	49.40	0.998
	Max(Box)	27.98	3.96	94.67	47.51	0.998
	Min(Box)	23.48	6.79	94.77	50.15	0.998
	Average(Box)	28.04	4.48	94.43	48.32	0.998
	Max (Circle)	26.79	3.86	94.75	46.50	0.998
	Min(Circle)	21.38	7.06	94.88	50.20	0.998
	Average(Circle)*	26.81	4.60	94.50	48.16	0.998
Step-wise heating experiment replicate 3	P1	71.31	1.22	92.20	51.34	0.998
	P2	72.61	1.16	92.29	51.30	0.998
	SP1	71.03	1.14	92.20	51.12	0.998
	SP2	72.54	1.17	92.30	51.39	0.998
	Max(Box)	71.94	2.09	92.45	64.11	0.843
	Min(Box)	66.22	1.45	92.16	50.84	0.998
	Average(Box)	71.31	1.20	92.21	51.32	0.998
	Max (Circle)	73.79	1.06	92.32	51.48	0.998
	Min(Circle)	65.86	1.56	92.16	50.61	0.997
	Average(Circle)*	71.19	1.14	92.19	51.14	0.998

*Method used originally for all fitting

8.8.2 Colour measurement

The lightness profile was another data input which was used for fitting the model, so this factor may affect the different results of the kinetics. The lightness was measured using image analysis. The lighting conditions and analysis process were very well controlled, so the measured lightness values were reasonable assumed to be consistent.

However, with the different baking conditions between the pan and the oven and between the oven cooking for the fast and step-wise heating conditions, the development of brown colour on the pastry surface and the changes in the physical properties of the pastry did not occur in the same way.

Compared with the pastry baking in the pan experiment, the samples were topped with an aluminium weight, so the pastry did not rise in the pan experiment. The pastry from the pan cooking was assumed to be opaque. In contrast, cooking pastry by oven baking produced water evaporation which made the pastry surface rise. It was found that the transparency of the raised area on the pastry surface as was discussed in section 8.4.2 resulted in a lower intensity of brown colour, and the lightness values of the pastry baking in the oven were higher than that of the pastry baking on the pan.

The colour was highly impacted by the transparency of the object. This transparency effect was also reported in the study of Talens *et al.* (2002), who investigated the changes in optical and mechanical properties during osmodehydro freezing of kiwifruit and found that the kiwifruit samples that had a transparent area from freezing damage to these cells created a darker colour. This evidence showed the transparency affected an increase in the colour intensity for the fresh fruit. The transparency reduced the colour intensity for bread-based products, as was observed in this study.

Moreover, the rising of the pastry surface may influence the concentration of the brown colour. This phenomenon of the rising up of the pastry surface causing a lighter pastry colour was discussed in section 8.4.2. This can explain how the surface of the pastry was changed with different rising patterns during the oven cooking process. This may have affected the different shade of brown colour even when they were baked under the same temperature and time conditions. It can be concluded that the same amount of Maillard browning reaction may not create the same value of brown colour because many factors were affecting the colour appearance such as physical property changes.

8.8.3 Maillard reaction mechanism

It was discussed in Chapter 2 that it was notoriously difficult to develop the mathematical model describing the Maillard browning reaction because the reaction mechanism of this reaction is very complex and various factors involved in food processing influence the mechanism. Therefore, the chemical mechanism of the

Maillard browning reaction was a potential cause of the different kinetics that were observed in this study. Most researchers applied the kinetic approach for modelling browning by simplifying the complex mechanism of browning and assuming the colour formation as the browning indicator (Zanoni *et al*., 1995).

However, this approach may not be useful in this case, as was reported in section 8.6 that different browning reaction kinetics were found for different cooking conditions. Consequently, the actual mechanisms of the reaction need to be determined to describe the different kinetic fits obtained from the different baking conditions used in this study. It was recommended in the literature that understanding the actual mechanism and transport phenomena occurring in the product during processing is the best approach to model the browning development (Purlis, 2010).

The Maillard reaction mechanism was re-written as a simple scheme for easy understanding (Figure 8.27). The reaction starts from the reaction between the amino acid and a reducing sugar. A condensation product N-substituted glycosilamine is produced and further rearranged to form the Amadori rearrangement product (ARP). There are three distinct pathways of the ARP degradation to form the final product of brown nitrogenuous polymers and co-polymers, known as melanoidins, depending on pH and temperature of the system (Figure 8.27).

At pH 7 or below, it mainly goes through hydroxymethylfurfural (HMF) formation. This intermediate compound is significant in the Maillard browning reaction (Martins *et al*., 2001 and Eskin, 2005). HMF was reported as the indicator in the Maillard reaction evaluation for some food processes such as the drying of pasta (Resmini & Pellegrino, 1994 and Anese *et al*., 1999), baby cereals (Fernádez-Artigas *et al*., 1999) and breakfast cereals (García-Villanova *et al*., 1993). This is because the HMF compound is not present in the raw sample until the reaction takes place during the heat treatment process (Ameur *et al*., 2006). However, determining HMF is a complex chemical method and cannot be applied in process monitoring. This method was not used for this present research study. Instead, the colour index of lightness value was used. Ramírez-Jiménez *et al*. (2000) reported that both of HMF and colour are useful indicators for Maillard browning evaluation, but HMF is more sensitive than colour. Therefore HMF is more useful in samples without distinct colour (Ramírez-Jiménez *et al*., 2000).

At pH above 7 the reductones and a variety of fission products are formed. High temperature also has an influence on the fission product pathway. This may create a fast rate of the reaction. This is a possible explanation why a fast reaction rate was found in the fast heating rate experimental condition where high temperatures were active over the majority of the colour change. In addition, some fission products e.g. pentose may react with amine to give orange dye products, influencing the colour of the food (Hodge, 1953; deMan, 1999 and Eskin, 2005). This colour product may have affected the total colour of the pastry under the high temperature conditions. The intensity of the colour of the sample may be high due to other pigment colours.

For the reductone pathway, the reductone compounds take part in further reactions by condensing with free amino groups, resulting in aldimine reaction product formation, which is a reversible reaction. Another reaction, from the reductone compounds is the Strecker degradation; this reaction produces some product compounds such as aroma and volatile compounds (Hodge, 1953; Benzing-Purdie *et al*., 1985; deMan, 1999 and Eskin, 2005). It can be assumed that less brown colour pigment of melanoidins was produced when this pathway was significant in the cooking system. Therefore, the intensity of brown colour on the pastry surface was lower, because of the low temperature conditions operating at the initial stage for the step-wise heating experiment. Moreover, this reaction pathway may slow the rate of reaction because of the reversible reaction.

It can be concluded that the different baking conditions may produce a different amount of Melanoidin due to differences in the reaction pathways. In addition, some reports (e.g. Eskin, 2005) stated that Melanoidin was not the best indicator for this browning reaction because some compounds may react with others to form other pigment colours, and these may affect to the appearance colour. Therefore, identifying the intermediates produced in the reaction and defining the reaction pathway route are important in kinetic modelling for the Maillard reaction (Van Boekel, 1998; Martins *et al*., 2001 and Eskin, 2005).

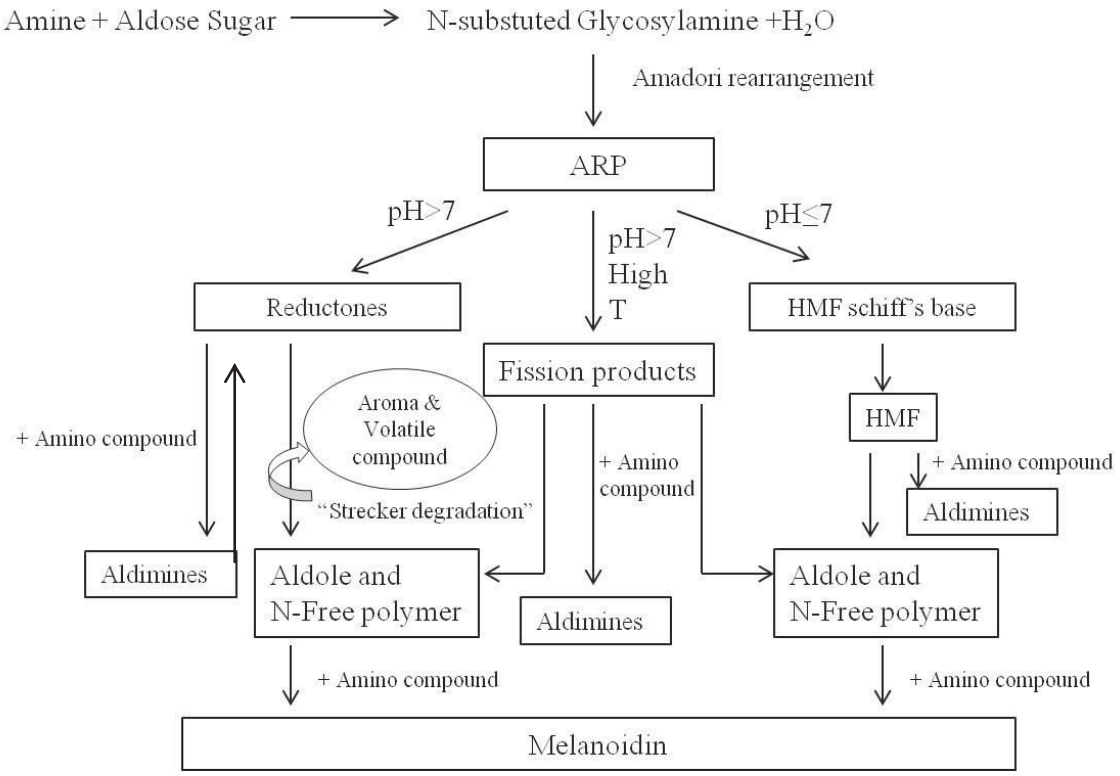

Figure 8.26 A reaction scheme for the Maillard mechanism (modified from Hodge 1953)

Furthermore, it was reported that the Maillard reaction was not the only one that occurs. There were other reactions that also take place in high temperature food processes, for example pyrolysis and combustion. These two reactions, pyrolysis and combustion, may have an influence on the colour development of the food sample during the cooking process, especially the final development of colour value. The minimum temperature for pyrolysis is reported at 200°C (Antal & Grønli, 2003 and Neves *et al*., 2011), while the Maillard reaction occurs in the range between 120°C and 180°C (Purlis & Salvadori, 2009 and Purlis, 2010). As the temperature range for this study was between 120°C and 220°C, both of the Maillard and pyrolysis reactions were implicated. At temperatures lower than 180°C, the Maillard reaction was dominant. In contrast, the pyrolysis takes effect when the temperature rises to a temperature higher than 200°C.

The effect of the different reactions on the colour change can obviously be seen from the plot of redness (a^*) and yellowness (b^*) values of pastry baking for the fast and step-wise heating experimental studies in Figures 8.27 and 8.28. It was found that evaporation and the pastry rising effects were reflected in the changing of the redness

(*a**) and yellowness (*b**) during the first ten minutes of the cooking process. These were in agreement with the result of lightness profile which was discussed in section 8.4.

Considering the last period of the process, a sudden decrease of the redness (*a**) and yellowness (*b**) values was found. These critical points were found at 20 and 65 minutes of baking time for the fast and step-wise heating experimental conditions, respectively. They were at the temperature of 200°C for both experimental sets (see the temperature profile in Figure 8.15). However, there was no decrease of redness values for the last experiment of replicate four of the step-wise heating experimental study. This may be because the operating temperature for this experimental replicate did not quite reach 200°C.

It can be concluded from this finding that other reactions, such as pyrolysis, took place at high temperatures of 200°C or greater. The pyrolysis reaction was assumed to have an influence on the overall colour of the pastry sample for the last period of baking at very high temperature baking conditions. This highly impacted on the lightness value because there was no critical point for the lightness profile in the last period of the process. The lightness value continuously decreased until the end of process. This means that the lightness value was changed due to both of the Maillard and pyrolysis reactions. Therefore the final lightness value for the Maillard browning kinetic model was affected when fitting the browning kinetics for this study.

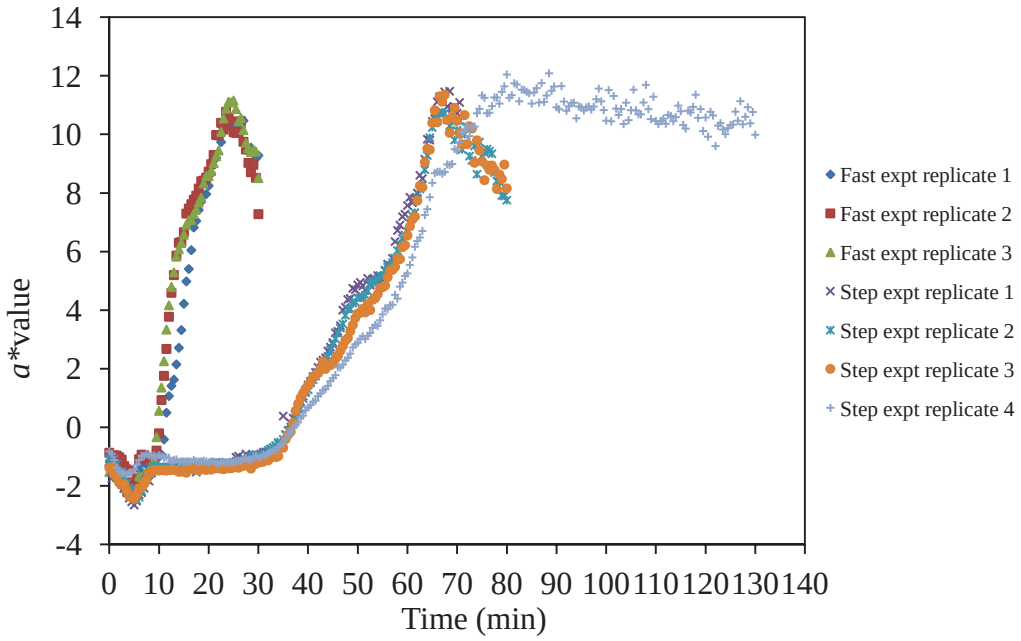

Figure 8.27 Redness (*a**) profile at the surface of pastry during the baking process

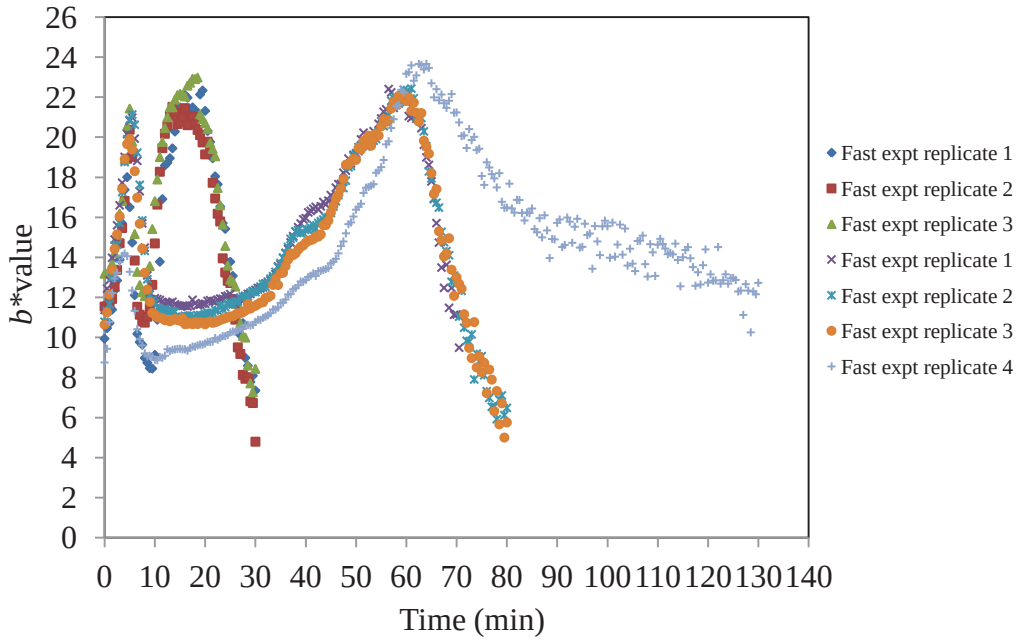

Figure 8.28 Yellowness (b^*) profile at the surface of pastry during the baking process

8.9 Conclusion

It was found from this study that the high temperature baking process resulted in a colour change of the pastry samples due to the Maillard browning reaction. During the baking process, not only was the colour of the samples changed but the physical property of the samples also changed, such as the pastry surface rose up. This affected the colour evaluation according to the transparency effect, which decreased the apparent intensity of the sample colour. Therefore, the colour change profiles of each experiment were different, which lead to a difference in kinetic parameters fitted.

There were many routes to form the brown pigment colour, which are highly dependent on the system conditions, such as pH and temperature. At the high temperature condition, the reaction rate is faster and the intensity of sample colour was higher, because the brown colour pigment was produced more by the fission route than the alternatives, which are dominant under lower temperature conditions. Many compounds e.g. aroma, volatile compounds and some intermediates are generated in the Maillard reaction during cooking under lower temperature conditions, which results in brown colour formation. It was concluded that these different reactions led to the different reaction kinetic parameters found is these experiments for the different temperature profiles used.

Additionally, other reactions such as the pyrolysis reaction were found to be active at temperatures above 200°C. These affected the final value of the lightness. Therefore, the estimated final lightness value for this study was low because the change of lightness value was not formed entirely due to the Maillard reaction. It was the outcome of the Maillard and pyrolysis reactions.

The kinetic model was successfully developed from one experimental method using the oven baking and thermal camera for measuring the temperature and brown colour at the same time. However, the kinetics of browning reaction for the food was found to be sensitive to the different cooking conditions such as time and temperature, so the browning on the foods may be developed with different kinetics. The fast and slow heating rate kinetics were observed from this study. As a result, the practical kinetic models should combine these two kinetics for predicting the browning development in the case that these two kinetics are both significant.

Chapter 9

GENERAL DISCUSSION AND CONCLUSIONS

The Maillard reaction strongly affects food quality especially its colour because of the brown pigment (melanoidin) that is produced. This brown pigment has significant effect on the perception of quality of food since colour is a key factor in influencing customer acceptance. In addition this reaction also produces volatile compounds which relate to aroma and taste in foods. Consequently, trying to predict or optimise browning from the Maillard reaction in high temperature food processing is necessary. Kinetic modelling has been used for this purpose and the first order kinetic is mostly used.

The present study also applied the first order kinetic model to predict the browning development during baking of pastry and a processed potato product. The results showed a good prediction and confirmed that the first order kinetic model worked well in these model foods. From the findings it was found that the browning kinetics of these two foods were different, most likely due to the differences in their compositions. The rate of the reaction is highly related to the temperature history at the food sample surface where the browning takes place. Hence achieving accurate temperature measurements of the food surface is necessary to develop an accurate kinetic model.

Measuring the real temperature of the food surface is difficult, so the pastry and an adapted deep fryer baking pan system were developed as a model food and cooking prototype that could provide even brown colour development on the food surface. The temperature at food surface was measured by the calibrated thermocouple probe connected with a data logger to record the temperature. The colour on the food sample was assessed using the imaging method by removing the sample from the cooking

system during the cooking. This cooking system had a limitation that the colour measurement could not be recorded continuously. The samples needed to be removed from the cooking process for offline measurement of the colour by an image analysis system. As a result it is impractical to apply this method in industry. A modified oven baking system was therefore developed to solve this problem.

The oven was adapted by placing an infrared window on its top to allow continuous measurement of the surface temperature and colour change of the food sample during the cooking process. A calibrated thermal camera was used which could measure both temperature and take colour images at the same time, so the colour value can be linked to its actual temperature. This gave accurate experimental data that could be used to fit the model, so the accurate kinetics of the browning reaction occurring in the food could be achieved.

For this study, the browning model for pastry baking was then obtained from the measured temperature and lightness values. It was found from the results in this study that the Maillard browning reaction happened with different kinetics depending on the heating rate condition. For example, the fast rate of heating gave a fast kinetic rate. This was attributed to one mechanism of the Maillard pathway being dominant. In contrast, another mechanism pathway was significant when the slow step-wise heating rate was applied.

In real cooking systems, the different kinetic rates could happen due to the different mechanisms of the reaction. For this reason, developing applicable browning models for use in predicting the browning in the food processes, the expected cooking conditions of that food should be known. Then, the experimental condition for cooking food should be designed to be close to the real cooking condition using the developed cooking system and the thermal camera to investigate the real temperature and colour data for model fitting. As a result, the experimental data used for kinetic fitting can be obtained from one experimental run.

However, some cooking process cannot be defined or specified. Many cases for cooking conditions should be introduced to investigate all of the potential kinetics which may occur for that food. Therefore a more powerful model formulation, which is more versatile, may be needed to predict the actual browning reaction. Such a model may

consist of at least two kinetic equations. For example in this study, based on the hypothesised different mechanisms the model may be written as Equation 9.1. Two terms in the equation explain two different reaction mechanisms, the first term may explain the reaction at lower temperatures and the rate at higher temperature may be described by the second term. The kinetic rate constants would be different as indicated by different subscripts (k_1 and k_2). Each rate constant would also vary differently with respect to temperature having a different activation energy. This model supposes to have more advantage over the single term model if suitable data for fitting it is available and the mechanism is valid.

$$\frac{dL^*}{dt} = -k_1\left(L^* - L^*_\infty\right) - k_2\left(L^* - L^*_\infty\right) \tag{9.1}$$

Further work to identify appropriate kinetic models could allow prediction over a wider range of conditions. Although this would make the model more useful fitting of the simple first order model for conditions relevant to its intended application provides very good prediction as shown in this work.

From the findings of this research, the obtained knowledge could be applied for monitoring and predicting the browning reaction that happen in other foods and cooking systems. The key important issue for developing the browning kinetic model for whatever foods under any cooking systems was that the time-temperature histories of the food surface need to be known since the browning kinetic at the food surface was highly affected by the temperature. For further study, understanding on how to define kinetic models that apply for a wider range of condition is suggested. This will lead to development of a versatile browning kinetic model for food industry application. It is also recommended that to optimise the cooking process for the commercial or industrial application, a heat transfer model might be developed and applied to predict the temperature of the food surface and then the browning reaction could be predicted.

REFERENCES

Abdullah, M. Z., Guan, L. C., Lim, K. C., & Karim, A. A. (2004). The applications of computer vision system and tomographic radar imaging for assessing physical properties of food. *Journal of Food Engineering, 61*(1), 125-135.

Abramovi, H., & Klofutar, C. (1998). The temperature dependence of dynamic viscosity for some vegetable oils. *Acta Chi . Slov, 45*(1), 69-77.

Acevedo, N. C., Schebor, C., & Buera, P. (2008). Non-enzymatic browning kinetics analysed through water-solids interactions and water mobility in dehydrated potato. *Food Chemistry, 108*(3), 900-906.

Adhikari, H., & Tappel, A. (1973). Fluorescent products in a glucose glycine browning reaction. *Journal of Food Science, 38*(3), 486-488.

Ajandouz, E. H., Desseaux, V., Tazi, S., & Puigserver, A. (2008). Effects of temperature and pH on the kinetics of caramelisation, protein cross-linking and Maillard reactions in aqueous model systems. *Food Chemistry, 107*(3), 1244-1252.

Al-Muhtaseb, A. H., McMinn, W. A. M., & Magee, T. R. A. (2002). Moisture Sorption Isotherm Characteristics of Food Products: A review. *Trans IChemE, Part C, (Food and Bioproducts Processing), 80*(2), 118-128.

Alamprese, C., Ratti, S., & Rossi, M. (2009). Effects of roasting conditions on hazelnut characteristics in a two-step process. *Journal of Food Engineering, 95*(2), 272-279.

Ames, J. M. (1990). Control of the Maillard reaction in food systems. *Trends in Food Science & Technology, 1*, 150-154.

Ames, J. M. (1998). Applications of the Maillard reaction in the food industry. *Food Chemistry, 62*(4), 431-439.

Ames, J. M. & Benjamin, C. (2003). Nonenzymatic browning. In: B. Caballero, L. Trugo, & P. Finglas (Eds), *Encyclopedia of food sciences and nutrition* (pp. 665–672). London, England: Academic Press.

Ameur, L. A., Trystram, G., & Birlouez-Aragon, I. (2006). Accumulation of 5-hydroxymethyl-2-furfural in cookies during the backing process: Validation of an extraction method. *Food Chemistry, 98*(4), 790-796.

Amiot, M., Tacchini, M., Aubert, S., & Nicolas, J. (1992). Phenolic composition and browning susceptibility of various apple cultivars at maturity. *Journal of Food Science, 57*(4), 958-962.

Anese, M., Nicoli, M. C., Massini, R., & Lerici, C. R. (1999). Effects of drying processing on the Maillard reaction in pasta. *Food Research International, 32*(3), 193-199.

Antal, M. J., & Grønli, M. (2003). The Art, Science, and Technology of Charcoal Production. *Industrial & Engineering Chemistry Research, 42*(8), 1619-1640.

Ávila, I. M. L. B., & Silva, C. L. M. (1999). Modelling kinetics of thermal degradation of colour in peach puree. *Journal of Food Engineering, 39*(2), 161-166.

Bachelor, B. G. (1985). *Lighting and viewing techniques in automated visual inspection*. Bedford, UK: IFS Publication Ltd.

Badoud, R., Fay, L., Richli, U., & Husek, P. (1991). Gas chromatographic determination of N-carboxymethyl amino acids, the periodate oxidation products of Amadori compounds. *Journal of Chromatography A, 552*, 345-351.

Baik, O., & Mittal, G. (2003). Kinetics of tofu color changes during deep-fat frying. *LWT-Food Science and Technology, 36*(1), 43-48.

Bailey, D. G., & Hodgson, R. M. (1988). VIPS- a digital image processing algorithm development environment. *Image and Vision Computing, 6*(3), 176-184.

Basu, S., Shivhare, U. S., & Mujumdar, A. S. (2006). Models for Sorption Isotherms for Foods: A Review. *Drying Technology, 24*(8), 917-930.

Batchelor, M., & Searcy, S. (1989). Computer vision determination of the stem/root joint on processing carrots. *Journal of Agricultural Engineering Research, 43*, 259-269.

Benzing-Purdie, L. M., Ripmeester, J. A., & Ratcliffe, C. I. (1985). Effects of temperature on Maillard reaction products. *Journal of Agricultural and Food Chemistry, 33*(1), 31-33.

Bolin, H. R., & Steele, R. J. (1987). Nonenzymatic Browning in Dried Apples During Storage. *Journal of Food Science*, *52*(6), 1654-1657.

Briones, V., & Aguilera, J. M. (2005). Image analysis of changes in surface color of chocolate. *Food Research International*, *38*(1), 87-94.

Brosnan, T., & Sun, D.-W. (2002). Inspection and grading of agricultural and food products by computer vision systems: A review. *Computers and Electronics in Agriculture*, *36*(2002), 193-213.

Brosnan, T., & Sun, D.-W. (2004). Improving quality inspection of food products by computer vision: A review. *Journal of Food Engineering*, *61*(1), 3-16.

Broyart, B., & Trystram, G. (2002). Modelling heat and mass transfer during the continuous baking of biscuits. *Journal of Food Engineering, 51*(1), 47-57.

Broyart, B., Trystram, G., & Duquenoy, A. (1998). Predicting colour kinetics during cracker baking. *Journal of Food Engineering*, *35*(3), 351-368.

Brunauer, S., Deming, L. S., Deming, W. E., & Teller, E. (1940). On a theory of the van der waals adsorption of gases. *Journal of the American Chemical Society*, *62*(7), 1723-1732.

Burdurlu, H. S., Koca, N., & Karadeniz, F. (2006). Degradation of vitamin C in citrus juice concentrates during storage. *Journal of Food Engineering, 74*(2), 211-216.

Burton, H. S., & McWeeny, D. J. (1963). Non-enzymatic browning reactions: Consideration of sugar stability. *Nature*, *197*(4864), 266-268.

Charissou, A., Ait-Ameur, L., & Birlouez-Aragon, I. (2007). Kinetics of formation of three indicators of the Maillard reaction in model cookies: Influence of baking temperature and type of sugar. *Journal of Agricultural and Food Chemistry, 55*(11), 4532-4539.

Cunha, L. M. & Oliveira FAR. (2000). Optimal experimental design for estimating the kinetic parameters of processes described by the first-order Arrhenius model under linearly increasing temperature profiles. *Journal of Food Engineering, 46*, 53-60.

Cuzzoni, M. T., Stoppini, G., Gazzani, G., & Mazza, P. (1988). Influence of water activity and reaction temperature of ribose-lysine and glucose-lysine Maillard systems on mutagenicity, absorbance and content of furfurals. *Food and Chemical Toxicology*, *26*(10), 815-822.

Damasceno, L. F., Fernandes, F. A. N., Magalhães, M. M. A., & Brito, E. S. (2008). Non-enzymatic browning in clarified cashew apple juice during thermal treatment: Kinetics and process control. *Food Chemistry, 106*(1), 172-179.

Danehy, J. P. (1986). Maillard reactions: nonenzymatic browning in food systems with special reference to the development of flavor. *Advances in Food Research, 30*, 77-138.

Davenel, A., Guizard, C., Labarre, T., & Sevila, F. (1988). Automatic detection of surface defects on fruit by using a vision system. *Journal of Agricultural Engineering Research, 41*(1), 1-9.

Davies, C. G. A., & Labuza, T. P. (1997). The Maillard reaction: Application to confectionery products. In G. Zeigler (Ed.), *Confectionery science* (pp. 35-66). Pennsylvania, PA: Penn State University Press.

deMan, J. M. (1999). *Principles of food chemistry* (3rd ed.). Gaithersburg, MD: Aspen Publishers.

Demir, A. D., Celayeta, J. M. F., Cronin, K., & Abodayeh, K. (2002). Modelling of the kinetics of colour change in hazelnuts during air roasting. *Journal of Food Engineering, 55*(4), 283-292.

Demirbas, A. (2008). Relationships derived from physical properties of vegetable oil and biodiesel fuels. *Fuel, 87*(8-9), 1743-1748.

Dolan, K. D. (2003). Estimation of Kinetic Parameters for Nonisothermal Food Processes. *Journal of Food Science, 68*(3), 728-741.

Dworschak, E., & Carpenter, K. (1980). Nonenzyme browning and its effect on protein nutrition. *Critical Reviews in Food Science and Nutrition, 13*(1), 1-40.

Eichner, K., & Karel, M. (1972). Influence of water content and water activity on the sugar-amino browning reaction in model systems under various conditions. *Journal of Agricultural and Food Chemistry, 20*(2), 218-223.

Ellis, G. P. (1959). The maillard reaction. *Advances in carbohydrate chemistry, 14*, 63-134.

Eskin, N. A. M., & Shahidi, F. (2005). Browning Reactions in Foods. In N. A. M. Eskin, & F. Shahidi (Eds.), *Biochemistry of foods [electronic resource]* (3rd Ed.) (pp. 245-280). San Diego, CA: Academic Press [Imprint] of Elsevier Science & Technology Books. Retrieved from http://www.sciencedirect.com/science/book/9780122423529

Fairchild, M. D. (2005). *Color appearance models* (2nd ed.). Hoboken, NJ: John Wiley & Sons.

Fayle, S.E., & Gerrard, J. A. (2002). *The Maillard Reaction*. Cambridge, UK: Royal Society of Chemistry.

Fernández-Artigas, P., Guerra-Hernández, E., & García-Villanova, B. (1999). Browning Indicators in Model Systems and Baby Cereals. *Journal of Agricultural and Food Chemistry, 47*(7), 2872-2878.

Figueira, A. C., Makinde, O., & Vieira, M. C. (2011). Process optimisation of sweet potato (*Ipomoea batatas*) puree as an ingredient in a formulation of weaning food. *The Maillard Reaction in Food Processing, Human Nutrition and Physiology, 5*(2), 25-34.

Franzen, K., Singh, R. K., & Okos, M. R. (1990). Kinetics of nonenzymatic browning in dried skim milk. *Journal of Food Engineering, 11*(3), 225-239.

Furth, A. (1988). Methods for assaying nonenzymatic glycosylation. *Analytical Biochemistry, 175*(2), 347-360.

Garcia-Villanova, B., Guerra-Hernandez, E., Martinez-Gomez, E., & Montilla, J. (1993). Liquid chromatography for the determination of 5-(hydroxymethyl)-2-furaldehyde in breakfast cereals. *Journal of Agricultural and Food Chemistry, 41*(8), 1254-1255.

Gerrard, D. E., Gao, X., & Tan, J. (1996). Beef Marbling and Color Score Determination by Image Processing. *Journal of Food Science, 61*(1), 145-148.

Giannakourou, M. C. & Taoukis, P. S. (2007). Reaction kinetics. In S. S. Sablani, M. S. Rahman, A. K. Datta, & A. S. Mujumdar (Eds.), *Handbook of food and bioprocess modeling techniques* (pp. 235-259). Boca Raton, FL: CRC Press.

Gilchrist, A., Nobbs, J., & John, L. (2010). Colorimetry, Theory. *Encyclopedia of Spectroscopy and Spectrometry* (pp. 380-385). Oxford, UK: Academic Press.

Gökmen, V., Açar, Ö. Ç., Serpen, A., & Morales, F. (2008). Effect of leavening agents and sugars on the formation of hydroxymethylfurfural in cookies during baking. *European Food Research and Technology, 226*(5), 1031-1037.

Gökmen, V., Açar, Ö. Ç., Arribas-Lorenzo, G., & Morales, F. J. (2008). Investigating the correlation between acrylamide content and browning ratio of model cookies. *Journal of Food Engineering, 87*(3), 380-385.

Goňi, S. M., & Salvadori, V. O. (2011). Kinetic modelling of colour changes during beef roasting. *Procedia Food Science, 1*, 1039-1044.

Gonzalez, R. C., & Woods, R. E. (2008). *Digital image processing* (3rd ed.). Harlow, NJ: Pearson Education, Inc.

Greenspan, L. (1977). Humidity fixed points of binary saturated aqueous solutions. *Journal of Research of the National Bureau of Standards, A. Physics and Chemistry A, 81*, 89-96.

Gunasekaran, S. (1996). Computer vision technology for food quality assurance. *Trends in Food Science & Technology, 7*(8), 245-256.

Gunasekaran, S. (2001). Non-destructive food evaluation techniques to analyse properties and quality. *Food Science and Technology (vol. 105)*. New York, NY: Marcel Decker.

Gunasekaran, S., & Ding, K. (1994). Using computer vision for food quality evaluation. *Food Technology, 48*(6), 151-154.

Hadiyanto, Asselman, A., Straten, G. V., Boom, R. M., Esveld, D. C., & Boxtel, A. J. B. V. (2007). Quality prediction of bakery products in the initial phase of process design. *Innovative Food Science & Emerging Technologies, 8*(2), 285-298.

Hamey, L. G., Watson, A. J., & Westcott, C. T. (1993). Machine inspection of biscuit bake. In *Proceedings of Digital Image Computing Techniques and Applications, 8-10 December 1993, Sydney, Australia* (pp. 124-129).

Haralampu, S. G., Saguy, I., & Karel, M. (1985). Estimation of Arrhenius model parameters using three least squares methods. *Journal of Food Processing and Preservation, 9*(3), 129-143.

Hartkopf, J., & Erbersdobler, H. (1993). Stability of furosine during ion-exchange chromatography in comparison with reversed-phase high-performance liquid chromatography. *Journal of Chromatography A, 635*(1), 151-154.

Heinemann, P., Varghese, Z., Morrow, C., Sommer III, H., & Crassweller, R. (1995). Machine vision inspection of '*Golden Delicious*' apples. *Applied Engineering in Agriculture, 11*(6), 901-906.

Hernández, J. A., Heyd, B., & Trystram, G. (2008). Prediction of brightness and surface area kinetics during coffee roasting. *Journal of Food Engineering, 89*(2), 156-163.

Heyd, B., Broyart, B., Hernandez, J. A., Valdovinos-Tijerino, B., & Trystram, G. (2007). Physical model of heat and mass transfer in a spouted bed coffee roaster. *Drying Technology, 25*(7), 1243-1248.

Hodge, J. E. (1953). Dehydrated foods, chemistry of browning reactions in model systems. *Journal of Agricultural and Food Chemistry, 1*(15), 928-943.

Hodge, J. E., Mills, F. D., & Fisher, B. E. (1972). Compounds of browned flavor derived from sugar-amine reactions. *Cereal Science Today, 17*(2), 34.

Horwitz, W., & Latimer Jr, G. W. (2005). *Official Methods of Analysis of AOAC international* (18th ed.). Association of Official Analytical Chemists, Washington, D.C., USA.

Hunt, R. W. G., & Pointer, M. R. (2011). *Measuring colour* (4th ed.). West Sussex, UK: John Wiley & Sons Ltd.

Ibanoglu, E. (2002). Kinetic study on colour changes in wheat germ due to heat. *Journal of Food Engineering, 51*(3), 209-213.

Ibarz, A., Pagan, J., & Garza, S. (2000). Kinetic models of non enzymatic browning in apple puree. *Journal of the Science of Food and Agriculture, 80*(8), 1162-1168.

Ilie, A., & Welch, G. (2005). Ensuring color consistency across multiple cameras. In *Proceedings of the Tenth IEEE International Conference on Computer Vision (ICCV'05), 17-21 Oct. 2005, Chapel Hill, NC, USA.*

Ilo, S., & Berghofer, E. (1999). Kinetics of colour changes during extrusion cooking of maize grits. *Journal of Food Engineering, 39*(1), 73-80.

Jain, A. (1989). *Fundamentals of digital image processing*. Englewood Cliffs, NJ: Prentice-Hall Inc.

Jayendra Kumar, A., Singh, R. R. B., Patel, A. A., & Patil, G. R. (2006). Kinetics of colour and texture changes in Gulabjamun balls during deep-fat frying. *LWT - Food Science and Technology, 39*(7), 827-833.

Jiménez, N., Bohuon, P., Dornier, M., Bonazzi, C., Pérez, A. M., & Vaillant, F. (2012). Effect of water activity on anthocyanin degradation and browning kinetics at high temperatures (100-140°C). *Food Research International, 47*(1), 106-115.

Kahyaoglu, T., & Kaya, S. (2006). Modeling of moisture, color and texture changes in sesame seeds during the conventional roasting. *Journal of Food Engineering, 75*(2), 167-177.

Kort, M. (1971). Reactions of free sugars with aqueous ammonia. *Advances in Carbohydrate Chemistry and Biochemistry, 25*, 311-349.

Krokida, M. K., Oreopoulou, V., Maroulis, Z. B., & Marinos-Kouris, D. (2001). Colour changes during deep fat frying. *Journal of Food Engineering, 48*(3), 219-225.

Kwok, K. C., MacDougall, D. B., & Niranjan, K. (1999). Reaction kinetics of heat-induced colour changes in soymilk. *Journal of Food Engineering, 40*(1-2), 15-20.

Labuza, T. P. (1975). Sorption phenomena in foods: Theoretical and practical aspects. In C. Rha (Ed), *Theory, Determination and Control of Physical Properties of Food Materials* (pp. 197-219). Dordrecht, Holland: Springer Netherlands.

Labuza, T. P. (1977). The properties of water in relationship to water binding in foods: A review. *Journal of Food Processing and Preservation, 1*(2), 167-190.

Labuza, T. P. (1980). The effect of water activity on reaction of kinetics of food deterioration. *Food Technology, 34*, 36-41.

Labuza, T. P. (1990). The Maillard reaction. In P. A. Finot, H. U. Aeschbacher, R. F. Hurrell, & R. Liardon (Eds.), *The Maillard Reaction in Food Processing, Human Nutrition and Physiology* (pp. 16-18). Basel, Switzerland: Birkhäuser Verlag.

Labuza, T. P., & Baisier, W. M. (1992). The kinetics of nonenzymatic browning. In H. Schwartzberg, & R. W. Hartel (Eds), *Physical Chemistry of Foods* (pp. 595-649). New York, NY: Marcel Dekker.

Labuza, T. P., Reineccius, G., Monnier, V., O'Brien, J., & Baynes, J. (1994). *Maillard reactions in chemistry, food and health*. Cambridge, UK: Royal Society of Chemistry.

Lea, C. H., & Hannan, R. S. (1949). Studies of the reaction between proteins and reducing sugars in the "dry" state: I. The effect of activity of water, of pH and of temperature on the primary reaction between casein and glucose. *Biochimica et Biophysica Acta, 3*, 313-325.

Lea, C. H., & Hannan, R. S. (1950). Studies of the reaction between proteins and reducing sugars in the 'dry' state II. Further observations on the formation of the casein-glucose complex. *Biochimica et Biophysica Acta, 4*, 518-531.

Ledl, F., & Schleicher, E. (1990). Chemical Pathway of the Maillard Reaction. In P. A. Finot, H. U. Aeschbacher, R. F. Hurrell, & R. Liardon (Eds.), *The Maillard Reaction in food processing, human nutrition and physiology* (pp. 19-42). Basel, Switzerland: Birkhäuser Verlag.

Lee, C. M., Sherr, B., & Koh, Y.-N. (1984). Evaluation of kinetic parameters for a glucose-lysine Maillard reaction. *Journal of Agricultural and Food Chemistry, 32*(2), 379-382.

Lee, J.-W., Oh, S.-H., Kim, J.-H., Byun, E.-H., Ree Kim, M., Baek, M., et al. (2007). The effect of irradiation temperature on the non-enzymatic browning reaction in cooked rice. *Radiation Physics and Chemistry, 76*(5), 886-892.

Leemans, V., Magein, H., & Destain, M. F. (1998). Defects segmentation on [`]Golden Delicious' apples by using colour machine vision. *Computers and Electronics in Agriculture, 20*(2), 117-130.

León, K., Mery, D., Pedreschi, F., & León, J. (2006). Color measurement in *L*a*b** units from RGB digital images. *Food Research International, 39*(10), 1084-1091.

Lima, J. R., Elizondo, N. J., & Bohuon, P. (2010). Kinetics of ascorbic acid degradation and colour change in ground cashew apples treated at high temperatures (100-180 °C). *International Journal of Food Science & Technology, 45*(8), 1724-1731.

Lingnert, H. (1990). Development of the Maillard reaction during food processing. In P. A. Finot, H. U. Aeschbacher, R. F. Hurrell, & R. Liardon (Eds.), *The Maillard Reaction in Food Processing, Human Nutrition and Physiology* (pp. 171-185). Basel, Switzerland: Birkhäuser Verlag.

Locht, P., Thomsen, K., & Mikkelsen, P. (1997). Full color image analysis as a tool for quality control and process development in the food industry. In *1997 ASAE Annual International Meeting, Paper No. 973006*. St. Joseph, Michigan, USA.

Lopez, A., Pique, M. T., Boatella, J., Parcerisa, J., Romero, A., Ferrá, A., et al. (1997). Influence of drying conditions on the hazelnut quality. III. Browning. *Drying Technology, 15*(3), 989-1002.

Lukac, H., Amrein, T. M., Perren, R., Conde Petit, B., Amadò, R., & Escher, F. (2007). Influence of roasting conditions on the acrylamide content and the color of roasted almonds. *Journal of Food Science, 72*(1), C033-C038.

Maga, J. A., & Katz, I. (1982). Pyrazines in foods: An update. *Critical Reviews in Food Science and Nutrition, 16*(1), 1-48.

Maillard, L. C., & Gautier, M. A. (1912). The reaction of amino acids with sugars: Mechanisms of melanoid formation. *CR Seances Academic Science III, 154*, 66-68.

Manzocco, L., Calligaris, S., Mastrocola, D., Nicoli, M. C., & Lerici, C. R. (2000). Review of non-enzymatic browning and antioxidant capacity in processed foods. *Trends in Food Science & Technology, 11*(9-10), 340-346.

Martinez, M. V., & Whitaker, J. R. (1995). The biochemistry and control of enzymatic browning. *Trends in Food Science & Technology, 6*(6), 195-200.

Martins, S., Jongen, W., & Van Boekel, M. (2001). A review of Maillard reaction in food and implications to kinetic modelling. *Trends in Food Science & Technology, 11*(9-10), 364-373.

Maskan, M. (2001). Kinetics of colour change of kiwifruits during hot air and microwave drying. *Journal of Food Engineering, 48*(2), 169-175.

Matiacevich, S. B., & Pilar Buera, M. P. (2006). A critical evaluation of fluorescence as a potential marker for the Maillard reaction. *Food Chemistry, 95*(3), 423-430.

Matsuda, H., Llave, Y., Fukuoka, M., & Sakai, N. (2013). Color changes in fish during grilling-Influences of heat transfer and heating medium on browning color. *Journal of Food Engineering, 116*(1), 130-137.

Mauron, J. (1981). The Maillard reaction in food: A critical review from the nutritional standpoint. *Progress in Food & Nutrition Science, 5*(1-6), 5-35.

McLaren, K. (1976). XIII—The development of the CIE 1976 (*L* a* b**) uniform colour space and colour difference formula. *Journal of the Society of Dyers and Colourists, 92*(9), 338-341.

Mendoza, F., & Aguilera, J. M. (2004). Application of Image Analysis for Classification of Ripening Bananas. *Journal of Food Science, 69*(9), E471-E477.

Mendoza, F., Dejmek, P., & Aguilera, J. M. (2007). Colour and image texture analysis in classification of commercial potato chips. *Food Research International, 40*(9), 1146-1154.

Meydav, S., Saguy, I., & Kopelman, I. (1977). Browning determination in citrus products. *Journal of Agricultural and Food Chemistry, 25*(3), 602-604.

Mohd Jusoh, Y. M., Chin, N. L., Yusof, Y. A., & Abdul Rahman, R. (2009). Bread crust thickness measurement using digital imaging and *L a b* colour system. *Journal of Food Engineering, 94*(3-4), 366-371.

Mondal, A., & Datta, A. K. (2008). Bread baking: A review. *Journal of Food Engineering, 86*(4), 465-474.

Moyano, P. C., Ríoseco, V. K., & González, P. A. (2002). Kinetics of crust color changes during deep-fat frying of impregnated french fries. *Journal of Food Engineering, 54*(3), 249-255.

Mundt, S., & Wedzicha, B. L. (2007). A kinetic model for browning in the baking of biscuits: Effects of water activity and temperature. *LWT - Food Science and Technology, 40*(6), 1078-1082.

Namiki, M. (1988). *Chemistry of Maillard reactions: Recent studies on the browning reaction mechanism and the development of antioxidants and mutagens* (Vol. 32). London, UK: Academic Press.

Narayanan, K. R. A., Kumar, A., & Patil, G. R. (1993). Kinetics of various deteriorative changes during storage of UHT soy beverage and development of a shelf-life prediction model. *LWT - Food Science and Technology, 26*(3), 191-197.

Nelson, P. R. (1983). Stability prediction using Arrhenius' model. *Computer Programs in Biomedicine, 16*, 55-60.

Neves, D., Thunman, H., Matos, A., Tarelho, L., & Gómez-Barea, A. (2011). Characterization and prediction of biomass pyrolysis products. *Progress in Energy and Combustion Science, 37*(5), 611-630.

Nourian, F., & Ramaswamy, H. S. (2003). Kinetics of quality change during cooking and frying of potatoes:Part II. colour. *Journal of Food Process Engineering, 26*(4), 395-411.

Nunes, R. V., Swartzel, K. R., & Ollis, D. F. (1993). Thermal evaluation of food processes: The role of a reference temperature. *Journal of Food Engineering, 20*(1), 1-15.

Nursten, H. (1986). Maillard browning reactions in dried foods. *Concentration and Drying of Foods*, 53–68.

Özdemir, M., & Devres, O. (2000). Kinetics of color changes of hazelnuts during roasting. *Journal of Food Engineering, 44*(1), 31-38.

Pagliarini, E., Vernile, M., & Peri, C. (1990). Kinetic study on color changes in milk due to heat. *Journal of Food Science, 55*(6), 1766-1767.

Papadakis, S. E., Abdul-Malek, S., Kamdem, R. E., & Yam, K. L. (2000). A versatile and inexpensive technique for measuring color of foods. *Food Technology, 54*(12), 48-51.

Paschos, G. (2001). Perceptually uniform color spaces for color texture analysis: An empirical evaluation. *IEEE Transactions on Image Processing, 10*(6), 932-937.

Pedreschi, F., Bustos, O., Mery, D., Moyano, P., Kaack, K., & Granby, K. (2007). Color kinetics and acrylamide formation in NaCl soaked potato chips. *Journal of Food Engineering, 79*(3), 989-997.

Pedreschi, F., León, J., Mery, D., & Moyano, P. (2006). Development of a computer vision system to measure the color of potato chips. *Food Research International, 39*(10), 1092-1098.

Pedreschi, F., León, J., Mery, D., Moyano, P., Pedreschi, R., Kaack, K., et al. (2007). Color development and acrylamide content of pre-dried potato chips. *Journal of Food Engineering, 79*(3), 786-793.

Purlis, E. (2010). Browning development in bakery products: A review. *Journal of Food Engineering, 99*(3), 239-249.

Purlis, E., & Salvadori, V. O. (2007). Bread browning kinetics during baking. *Journal of Food Engineering, 80*(4), 1107-1115.

Purlis, E., & Salvadori, V. O. (2009). Modelling the browning of bread during baking. *Food Research International, 42*(7), 865-870.

Quevedo, R., Díaz, O., Ronceros, B., Pedreschi, F., & Aguilera, J. M. (2009). Description of the kinetic enzymatic browning in banana (Musa cavendish) slices using non-uniform color information from digital images. *Food Research International, 42*(9), 1309-1314.

Rahman S. (1995). Water activity and sorption properties of food. *Food Properties Handbook* (pp. 1-46). Boca Raton, FL: CRC Press.

Ramirez-Jimenez, A., Guerra-Hernandez, E., & Garcia-Villanova, B. (2000). Browning indicators in bread. *Journal of Agricultural and Food Chemistry, 48*(9), 4176-4181.

Rapusas, R. S., & Driscoll, R. H. (1995). Kinetics of non-enzymatic browning in onion slices during isothermal heating. *Journal of Food Engineering, 24*(3), 417-429.

Reid, D. S. (2007). Water activity: Fundamentals and relationaships. In G. V. Barbosa-Cánovas, A. J. Fontana, Jr., S. J. Shmidt, & T. P. Labuza (Eds), *Water activity in foods: Fundamentals and applications* (pp. 15-28). Oxford, UK: Blackwell Publishing Ltd.

Resmini, P., Pellegrino, L., & Battelli, G. (1990). Accurate quantification of furosine in milk and dairy products by a direct HPLC method. *Italian Journal of Food Science, 2*(3), 173-183.

Resmini, P., & Pellegrino, L. (1994). Occurence of protein-bound lysylpyrrolaldehyde in dried pasta. *Cereal Chemistry, 71*(3), 254-262.

Resnik, S., & Chirife, J. (1979). Effect of moisture content and temperature on some aspects of nonenzymatic browning in dehydrated apple. *Journal of Food Science, 44*(2), 601-605.

Rhim, J. W., Jones, V. A., & Swartzel, K. R. (1988). Kinetics studies in the colour changes of skim milk. *LWT - Food Science and Technology*, *21*(6), 334-338.

Saklar, S., Katnas, S., & Ungan, S. (2001). Determination of optimum hazelnut roasting conditions. *International Journal of Food Science & Technology, 36*(3), 271-281.

Sapers, G. M., Hicks, K. B., Phillips, J. G., Garzarella, L., Pondish, D. L., Matulaitis, R. M., et al. (1989). Control of enzymatic browning in apple with ascorbic acid derivatives, polyphenol oxidase inhibitors, and complexing agents. *Journal of food science*, *54*(4), 997-1002.

Sahin, S. (2000). Effects of frying parameters on the colour development of fried potatoes. *European Food Research and Technology*, *211*(3), 165-168.

Savoye, I., Trystram, G., Duquenoy, A., Brunet, P., & Marchin, F. (1992). Heat and mass transfer dynamic modelling of an indirect biscuit baking tunnel-oven. Part I: Modelling principles. *Journal of Food Engineering, 16*(3), 173-196.

Schamberger, G. P., & Labuza, T. P. (2006). Evaluation of front-face fluorescence for assessing thermal processing of milk. *Journal of Food Science, 71*(2), C69-C74.

Schanda, J. (Ed.). (2007). *Colorimetry: Understanding the CIE system*. Hoboken, NJ: Wiley-Interscience.

Segnini, S., Dejmek, P., & Öste, R. (1999). A low cost video technique for colour measurement of potato chips. *LWT - Food Science and Technology*, *32*(4), 216-222.

Selen Burdurlu, H., & Karadeniz, F. (2003). Effect of storage on nonenzymatic browning of apple juice concentrates. *Food Chemistry, 80*(1), 91-97.

Sherwin, C. P., & Labuza, T. P. (2003). Role of moisture in Maillard browning reaction rate in intermediate moisture foods: Comparing solvent phase and matrix properties. *Journal of Food Science, 68*(2), 588-593.

Shibukawa, S., Sugiyama, K., & Yano, T. (1989). Effects of heat transfer by radiation and convection on browning of cookies at baking. *Journal of Food Science, 54*(3), 621-624.

Shin, S., & Bhowmik, S. R. (1995). Thermal kinetics of color changes in pea puree. *Journal of Food Engineering, 24*(1), 77-86.

Sonka, M., Hlavac, V., & Boyle, R. (2008). *Image processing, analysis, and machine vision*. (3rd ed.). Toronto: Thompson Learning.

Steet, J. A., & Tong, C. H. (1996). Degradation kinetics of green color and chlorophylls in peas by colorimetry and HPLC. *Journal of Food Science, 61*(5), 924-928.

Sun, D.-W. (2000). Inspecting pizza topping percentage and distribution by a computer vision method. *Journal of Food Engineering, 44*(4), 245-249.

Talens, P., Martínez-Navarrete, N., Fito, P., & Chiralt, A. (2002). Changes in optical and mechanical properties during osmodehydrofreezing of kiwi fruit. *Innovative Food Science & Emerging Technologies, 3*(2), 191-199.

Timmermans, A.J.M. (1998). Computer vision system for online sorting of pot plants based on learning techniques. *Acta Horticulturae, 421, 91-98*.

Timmermann, E. O., Chirife, J., & Iglesias, H. A. (2001). Water sorption isotherms of foods and foodstuffs: BET or GAB parameters. *Journal of Food Engineering, 48*(1), 19-31.

Tirelli, A., & Pellegrino, L. (1995). Determination of furosine in dairy products by capillary zone electrophoresis: A comparison with the HPLC method: Determinazione della furosina in prodotti lattiero-caseari attraverso elettroforesi zonale capillare: confronto con il metodo HPLC. *Italian journal of food science, 7*(4), 379-385.

Toribio, J. L., Nunes, R. V., & Lozano, J. E. (1984). Influence of water activity on the nonenzymatic browning of apple juice concentrate during storage. *Journal of Food Science, 49*(6), 1630-1631.

Vaikousi, H., Koutsoumanis, K., & Biliaderis, C. G. (2008). Kinetic modelling of non-enzymatic browning of apple juice concentrates differing in water activity under isothermal and dynamic heating conditions. *Food Chemistry, 107*(2), 785-796.

Vaikousi, H., Koutsoumanis, K., & Biliaderis, C. G. (2009). Kinetic modelling of non-enzymatic browning in honey and diluted honey systems subjected to isothermal and dynamic heating protocols. *Journal of Food Engineering, 95*(4), 541-550.

Van den Berg, C. (1985). Development of B.E.T. like models for sorption of water of foods; theory and relevance. In D. Simatos, & J. L. Multon (Eds.), *Properties of water in foods* (pp. 119–135). Dordrecht: Martinus Nijhoft Publishers.

Van Boekel, M. A. J. S. (1998). Effect of heating on Maillard reactions in milk. *Food Chemistry, 62*(4), 403-414.

Villota, R., & Hawkes, J. (2007). Reaction kinetics in food systems. In R. D. Heldman, D. B. Lund (Eds), *Handbook of food engineering* (pp. 39-144). Boca Raton, FL: CRC Press.

Vízhányó, T., & Felföldi, J. (2000). Enhancing colour differences in images of diseased mushrooms. *Computers and electronics in agriculture, 26*(2), 187-198.

Wählby, U., & Skjöldebrand, C. (2002). Reheating characteristics of crust formed on buns, and crust formation. *Journal of Food Engineering, 53*(2), 177-184.

Wang, H.-H., & Sun, D.-W. (2001). Evaluation of the functional properties of Cheddar Cheese using a computer vision method. *Journal of Food Engineering, 49*(1), 49-53.

Wang, H.-H., & Sun, D.-W. (2003). Assessment of cheese browning affected by baking conditions using computer vision. *Journal of Food Engineering, 56*(4), 339-345.

Yam, K. L., & Papadakis, S. E. (2004). A simple digital imaging method for measuring and analyzing color of food surfaces. *Journal of Food Engineering, 61*(1), 137-142.

Yang, Q. (1994). An approach to apple surface feature detection by machine vision. *Computers and Electronics in Agriculture, 11*(2-3), 249-264.

Yeo, H., & Shibamoto, T. (1991). Effects of moisture content on the Maillard browning model system upon microwave irradiation. *Journal of Agricultural and Food Chemistry, 39*(10), 1860-1862.

Zanoni, B., Peri, C., & Bruno, D. (1995). Modelling of browning kinetics of bread crust during baking. *LWT - Food Science and Technology, 28*(6), 604-609.

Zhang, J., & Datta, A. K. (2006). Mathematical modeling of bread baking process. *Journal of Food Engineering, 75*(1), 78-89.

Zhu, D., Ji, B., Eum, H. L., & Zude, M. (2009). Evaluation of the non-enzymatic browning in thermally processed apple juice by front-face fluorescence spectroscopy. *Food Chemistry, 113*(1), 272-279.

Zuckerman, H., & Miltz, J. (1997). Prediction of dough browning in the microwave oven from temperatures at the susceptor/product interface. *LWT - Food Science and Technology, 30*(5), 519-524.

Appendix A1

The algorithm for image analysis

Image analysis was used to analyse the colour change of the pastry during baking due to the browning reaction. There were two different sources of image acquisition for two parts of this study. These were a firewire camera used for capturing the pan-baked study and a mobile digital camera which was used for the oven-baked study. The images were analysed directly for the pan-baked experiments but for the oven-baked experiment, the images were saved as a digital files and loaded into the computer to analyse. In addition, there were different conditions for the lighting systems between the pan and oven baking experiments. Consequently, the algorithms for analysing the images were divided into two parts for the two applications of this study.

A1.1 The algorithm for analysing an image captured from the firewire camera

(Accompanying CD/ A1 The Algorithm for Image Analysis/ A1.1 Analyse Image from the firewire camera _Ch 3)

A1.1.1 Measuring the colour of an image (snap.vip)

```
Program
  IF %EXIST( snap_im ) = 0
    DECLARE COLOUR (960 1280) snap_im
    DECLARE COLOUR (480 640) snap_im2 (240 320) snap_im3
    DECLARE  IMAGE  (480  640)  snap_r  snap_g  snap_b  snap_mask  snap_x  snap_ll  snap_aa
snap_bb
    DECLARE REAL snap_mn snap_mn2 snap_sd
    DECLARE STRING snap_reply snap_filename
    DECLARE INTEGER snap_area
  END
  SET auto /OFF
  SET OUTPUT /OFF

  REPEAT
    FIREWIRE snap_im                ! Capture an image from firewire camera
    ZOOM snap_im snap_im2 0.5       ! And reduce resolution to manageable size
    FIRECLOSE
    DISPLAY snap_im2 (0 0)
    INQUIRE "Image OK [Y]? " /ent snap_reply
    IF %LENGTH( snap_reply ) = 0
      LET snap_reply = "Y"
    END
  UNTIL snap_reply = "Y"
```

```
  COLOUR snap_im2 snap_r snap_g snap_b
  LET snap_mask = snap_r
  OR /F snap_mask snap_g
  OR /F snap_mask snap_b              ! Get maximum or RGB components
  LET snap_x = snap_mask
  THRESH snap_mask 0 200              !  Find  points  where  the  maximum  (background
reference)
  SHRINK snap_mask 3                  ! is too large
  AND snap_g snap_mask
  AND snap_b snap_mask
  INV snap_mask
  OR snap_r snap_mask                 ! And mark those points in red.

  STAT snap_r 0 254 ,,snap_mn
  STAT snap_r snap_mn 254,, snap_mn   ! Estimate the background in the red image
  EXPAND snap_r 0 (snap_mn * 1.2)     ! And scale to make use of available dynamic range
  STAT snap_g 0 254 ,,snap_mn
  STAT snap_g snap_mn 254,, snap_mn
  EXPAND snap_g 0 (snap_mn * 1.2)     ! Same for green and blue images
  STAT snap_b 0 254,, snap_mn
  STAT snap_b snap_mn 254 ,,snap_mn
  EXPAND snap_b 0 (snap_mn * 1.2)

  COLOUR snap_r snap_g snap_b snap_im2

  AREA snap_mask 254 snap_area
  IF snap_area > 0
    DISPLAY snap_im3 (0 0)            ! Display a small image showing points that are
overexposed
    WRITE "*** Image is overexposed ***" /LINE
    BEEP
    EXIT
  END

  REPEAT
    IF %EXIST( snap_date ) = 0
      DECLARE STRING snap_date
      INQUIRE "Sample date (DDMMYY) " /ENT snap_date
    ELSE
      INQUIRE ("Sample date [" & snap_date & "] ") /ENT snap_reply
      IF %LENGTH( snap_reply ) > 4
        LET snap_date = snap_reply
      END
    END
    IF %EXIST( snap_temp ) = 0
      DECLARE INTEGER snap_temp
      INQUIRE "Enter temperature " snap_temp
    ELSE
      INQUIRE ("Sample temperature [" & %STR('snap_temp') & "] ") /ENT snap_reply
      IF %LENGTH( snap_reply ) > 0
        LET snap_temp = 'snap_reply'
      END
    END
    IF %EXIST( snap_time ) = 0
      DECLARE INTEGER snap_time
      INQUIRE "Enter process time " snap_time
    ELSE
      INQUIRE ("Process time [" & %STR('snap_time') & "] ") /ENT snap_reply
      IF %LENGTH( snap_reply ) > 0
        LET snap_time = 'snap_reply'
      END
    END
    IF %EXIST( snap_pos ) = 0
      DECLARE STRING snap_pos
      INQUIRE "Sample position " /ENT snap_pos
    ELSE
      INQUIRE ("Sample position [" & snap_pos & "] ") /ENT snap_reply
      IF %LENGTH( snap_reply ) > 0
        LET snap_pos = snap_reply
      END
    END

    LET snap_filename = snap_date & "_" & %STR('snap_temp') & "_" & %STR( 'snap_time' )
& "_" & snap_pos & ".BMP"
    IF %EXIST( 'snap_filename' /file ) = 1
```

```
      INQUIRE ("File " & snap_filename & " already exists. Continue? [N] ") /ENT
snap_reply
      IF snap_reply = "Q"
        EXIT
      END
    ELSE
      LET snap_reply = "Y"
    END
  UNTIL snap_reply = "Y"

  SAVE 'snap_filename' /BMP snap_im2 ! Save the normalised image.

  BOX AVE snap_b snap_mask 9         ! Use blue channel to create a mask of the
background
  STAT snap_b 0 254 ,, snap_mn
  STAT snap_b 0 snap_mn ,, snap_mn2
  THRESH snap_mask 0 ((snap_mn + snap_mn2) / 2)
  SHRINK snap_mask 9
  AND snap_r snap_mask               ! Remove the background from the image
  AND snap_g snap_mask
  AND snap_b snap_mask
  COLOUR snap_r snap_g snap_b snap_im2       ! Display the masked image

  DISPLAY snap_im2 (0 0)

  IF %EXIST( data.csv /FILE ) = 0
    FILE /OPEN /WRITE data.csv
    WRITE /FILE "Date,Temperature,Time,Position,R mean,R sd,G mean,G sd,B mean,B sd,L*
mean,L* sd,a* mean,a* sd,b* mean,b* sd" /LINE
  ELSE
    FILE /APPEND data.csv
  END

  WRITE /FILE snap_date, ",", snap_temp, ",", snap_time, ",", snap_pos, ","


! Calculate RGB statistics
  STATISTICS snap_r 1 ,,, snap_mn snap_sd
  WRITE "R = " snap_mn " +-" snap_sd /LINE /FILE snap_mn,",",snap_sd,","
  STATISTICS snap_g 1 ,,, snap_mn snap_sd
  WRITE "G = " snap_mn " +-" snap_sd /LINE /FILE snap_mn,",",snap_sd,","
  STATISTICS snap_b 1 ,,, snap_mn snap_sd
  WRITE "B = " snap_mn " +-" snap_sd /LINE /FILE snap_mn,",",snap_sd,","

! Get LAB components, and calculate LAB statistics
  COLOUR snap_im2 snap_ll snap_aa snap_bb /LAB
  AND snap_ll snap_mask
  STATISTICS snap_ll 1,,, snap_mn snap_sd
  WRITE "L* = " (snap_mn / 2.5) " +-" (snap_sd / 2.5) /LINE
  WRITE /FILE (snap_mn / 2.5) "," (snap_sd / 2.5) ","
  AND snap_aa snap_mask
  STATISTICS snap_aa 1,,, snap_mn snap_sd
  WRITE "a* = " ((snap_mn - 128) / 1.25) " +-" (snap_sd / 1.25) /LINE
  WRITE /FILE ((snap_mn - 128) / 1.25) "," (snap_sd / 1.25) ","
  AND snap_bb snap_mask
  STATISTICS snap_bb 1,,, snap_mn snap_sd
  WRITE "b* = " ((snap_mn - 128) / 1.25) " +-" (snap_sd / 1.25) /LINE
  WRITE /FILE ((snap_mn - 128) / 1.25) "," (snap_sd / 1.25) /LINE

  FILE /CLOSE
  SET auto /on
  SET OUTPUT /ON
End
```

A1.2 The algorithm for analysing an image captured from the digital camera

(Accompanying CD/ A1 The Algorithm for Image Analysis/ A1.2 Ananlyse Image from the digital camera_Ch 8)

A1.2.1 Login the program (login.vip)

```
PROGRAM
LOAD check.vip check
LOAD measure.vip measure
END
```

A1.2.2 Checking the saturation of an image (check.vip)

```
PROGRAM
  IF %EXIST( n_sat ) = 0
    DECLAR IMAGE (512 512) n_sat
        DECLARE COLOUR (512 512) n_clr n_clr2
  END

  SET ERROR /ERROR
  LOAD #1 aa
  ZOOM aa aa2 0.5
  COLOUR aa2 r g b

  LET d = r                          ! Multiply planes to get mask
  MULT /N d g
  MULT /N d b
FILL d 10 10 /le
  BOX AVE d e 5
  STAT e 0 255,, mn
  STAT e mn 255 ,, mn  ! Threshold to get window
  THRESH e (mn / 2)
  CHAIN CODE e cc
  LET l = {}
  AREA cc l
  EXTRE l ,,,, mp
  SELECT cc cs mp
  COG cs cog
  AREA cs ar
  LET rad = %SQRT((ar / 3.1415926))

  TEST e 0
  DRAW CIRCLE cog (rad - 9) 255 e
  DRAW CIRCLE cog (rad - 50) 255 e
  FILL e 255 (cog - (0 (%int(rad) - 30)))           ! Get a ring on outside of window

  LET d = r
  OR /F d g
  OR /F d b                          ! Find saturated pixels before scaling
  COPY d n_sat ((256 256) - cog)

  AND r e
  STAT r 1 ,,, mnr sdr
  AND g e
  STAT g 1 ,,, mng sdg
  AND b e
  STAT b 1 ,,, mnb sdb

  COPY aa2 n_clr ((256 256) - cog)
  COLOUR n_clr r g b
  MULT r (212.5 / mnr) /SAT
  MULT g (212.5 / mng) /SAT
  MULT b (212.5 / mnb) /SAT
  COLOUR r g b n_clr2         ! Save processed image for later processing

  OR /F n_sat r
  OR /F n_sat g
  OR /F n_sat b
  THRESH n_sat 255                   ! Saturated pixels after scaling
```

```
  ADD r n_sat /SAT
  SUB g n_sat /SAT
  SUB b n_sat /SAT

  LET bgx = {(mnr / sdr) (mng / sdg) (mnb / sdb)}
  WR bgx /LINE
  EXTRE bgx mn
  if mn < 22
       EXTE g /CLE 10
       EXTE b /CLE 10
       ADD r 1
       EXTE r /CLE 10
       SUB r 1
  END
  COLOUR r g b n_clr          ! Normalised image with bad pixels marked

END
```

A1.2.3 Measuring the colour of an image (measure.vip)

```
PROGRAM
  SET auto /OFF
  SET OUTPUT /OFF

  COLOUR n_clr2 r g b

  BOX AVE b mask 9            ! Use blue channel to create a mask of the background
  BOX AVE r r2 9
  LET m2 = mask
  THRESH m2 128                       ! Separate window from light patch inside
  CHAIN CODE m2 cc
  LET arl = {}
  AREA cc arl
  EXTREME arl ,,,, cn  ! Find biggest object - the light patch inside the window
  SELECT cc cs cn
  TEST m2
  AREA cs ch_a
  LET ch_r = %SQRT((ch_a / 3.1415926)) - 20
  COG cs cog
  DRAW CIRCLE cog ch_r 255 m2
  FILL m2 255 cog
  DIV mask r2
  AND mask m2                 ! Select only inside the window
  STAT mask 1 254 ,, snap_mn
  STAT mask 1 snap_mn ,, snap_mn2
  STAT mask snap_mn 254 ,, snap_mn
  THRESH mask 1 ((snap_mn + snap_mn2) / 2)
  CHAIN CODE mask cc
  CHAIN SORT cc cs
  CHAIN DRAW cs mask /fill

  SHRINK mask 5
  AND r mask                  ! Remove the background from the image
  AND g mask
  AND b mask
  COLOUR r g b n_clr   ! Display the masked image

  DISPLAY n_clr (0 0)


! Get LAB components, and calculate LAB statistics
  COLOUR n_clr snap_ll snap_aa snap_bb /LAB
  AND snap_ll mask
  STATISTICS snap_ll 1,,snap_area, snap_mn snap_sd
  WRITE "Area = " snap_area /LINE
  WRITE "L* = " (snap_mn / 2.5) " +-" (snap_sd / 2.5) /LINE
  AND snap_aa mask
  STATISTICS snap_aa 1,,, snap_mn snap_sd
  WRITE "a* = " ((snap_mn - 128) / 1.25) " +-" (snap_sd / 1.25) /LINE
  AND snap_bb mask
  STATISTICS snap_bb 1,,, snap_mn snap_sd
  WRITE "b* = " ((snap_mn - 128) / 1.25) " +-" (snap_sd / 1.25) /LINE
```

```
  if %exist( snap_ll2 ) = 1
  subtract snap_ll2 snap_ll
  STATISTICS snap_ll2 1,,snap_area, snap_mn snap_sd
  WRITE "Area = " snap_area /LINE
  WRITE "L* = " (snap_mn / 2.5) " +-" (snap_sd / 2.5) /LINE
  END

  LET snap_ll2 = snap_ll

  SET auto /on
  SET OUTPUT /ON
END
```

Appendix A2

MATLAB® code to fit experimental isotherm data to GAB model using fitting algorithm *nlinfit*

Non linear confidence intervals for the model prediction were evaluated with the MATLAB® function *nlinfit*.

A2 Sorption isotherm plot using GAB model (A2SorptionIsothermPlot.m)

(Accompanying CD/ A2 MATLAB® code for sorption isotherm plot)

```
%Read experimental data
awexp=xlsread('B2 Measured Data of Preliminary study.xlsx','Aw and
MC','b4:b57');
mcexp=xlsread('B2 Measured Data of Preliminary study.xlsx','Aw and
MC','c4:c57');

%GAB model
mdl=@(a,aw)(a(1)*a(3)*a(2)*aw)./((1-a(2)*aw).*(1-
a(2)*aw+a(3)*a(2)*aw));
a0=[5.16;0.91;8.26E+09];

%Plot experimental data of aw and %MC
plot(awexp,mcexp,'o');

%Calculation dependence variables
[beta,r,J,COVB,mse] = nlinfit(awexp,mcexp,mdl,a0);
aw_model=[0.2:0.01:0.99];
hold on

%Calculation 95% confidence interval
[ypred,delta] =
nlpredci(mdl,aw_model,beta,r,'covar',COVB,'mse',mse,'alpha',0.05);
[ypred,deltaobs] =
nlpredci(mdl,aw_model,beta,r,'covar',COVB,'mse',mse,
'predopt','observation','alpha',0.05);
plot(aw_model,ypred);
delta=[delta]';

%Plot sorption isotherm with 95% confidence interval
plot(aw_model,ypred+deltaobs','r--');
plot(aw_model,ypred-deltaobs','r--');
```

```
xlabel('aw')
ylabel('%MC')
ci = nlparci(beta,r,'covar',COVB)
R = corrcoef(aw_model,ypred);

%Calculation the goodness of fit (R2)
awexp_Av=mean(awexp);
ssER=sum((awexp-aw_model).^2);
ssTot=sum((awexp-awexp_Av).^2);
Rsq=1-ssER/ssTot;

fprintf('R^2 = %d. \n',Rsq);
```

Appendix A3

Statistic analysis of the initial moisture content effect study

A3.1 The statistic analysis of the effect of the initial moisture content on the browning kinetic considered by the lightness (*L**) change

- The effect of %MC on the initial lightness (L^*_0)

One-way ANOVA: 9.18, 10.95, 22.92, 33.89, 44.55

Source	DF	SS	MS	F	P
Factor	4	26.903	6.726	22.12	0.002
Error	5	1.520	0.304		
Total	9	28.423			

S = 0.5514 R-Sq = 94.65% R-Sq(adj) = 90.37%

Individual 95% CIs For Mean Based on Pooled StDev

Level	N	Mean	StDev	-+---------+---------+---------+--------
9.18	2	88.130	0.099	(-----*-----)
10.95	2	87.225	1.167	(-----*-----)
22.92	2	87.535	0.092	(-----*-----)
33.89	2	89.865	0.021	(------*-----)
44.55	2	91.595	0.375	(-----*------)

-+---------+---------+---------+--------

86.4 88.0 89.6 91.2

Pooled StDev = 0.551

Grouping Information Using Tukey Method

	N	Mean	Grouping
44.55	2	91.5950	A
33.89	2	89.8650	A B
9.18	2	88.1300	B C
22.92	2	87.5350	C
10.95	2	87.2250	C

Means that do not share a letter are significantly different.

Tukey 95% Simultaneous Confidence Intervals
All Pairwise Comparisons
Individual confidence level = 98.98%
9.18 subtracted from:

	Lower	Center	Upper	---------+---------+---------+---------+
10.95	-3.1159	-0.9050	1.3059	(-----*------)
22.92	-2.8059	-0.5950	1.6159	(-----*------)
33.89	-0.4759	1.7350	3.9459	(-----*-----)
44.55	1.2541	3.4650	5.6759	(-----*-----)

---------+---------+---------+---------+
-3.5 0.0 3.5 7.0

10.95 subtracted from:

	Lower	Center	Upper	---------+---------+---------+---------+
22.92	-1.9009	0.3100	2.5209	(-----*-----)
33.89	0.4291	2.6400	4.8509	(------*-----)
44.55	2.1591	4.3700	6.5809	(-----*------)

---------+---------+---------+---------+
-3.5 0.0 3.5 7.0

22.92 subtracted from:

	Lower	Center	Upper	---------+---------+---------+---------+
33.89	0.1191	2.3300	4.5409	(------*-----)
44.55	1.8491	4.0600	6.2709	(------*-----)

---------+---------+---------+---------+
-3.5 0.0 3.5 7.0

33.89 subtracted from:

	Lower	Center	Upper	---------+---------+---------+---------+
44.55	-0.4809	1.7300	3.9409	(-----*-----)

---------+---------+---------+---------+
-3.5 0.0 3.5 7.0

Residual Plots for 9.18, 10.95, 22.92, 33.89, 44.55

- *The effect of %MC on the final lightness (L^*_∞)*

One-way ANOVA: 9.18, 10.95, 22.92, 33.89, 44.55

Source	DF	SS	MS	F	P
Factor	4	254.15	63.54	6.65	0.031
Error	5	47.74	9.55		
Total	9	301.89			

S = 3.090 R-Sq = 84.19% R-Sq(adj) = 71.54%

Individual 95% CIs For Mean Based on
Pooled StDev

Level	N	Mean	StDev	------+---------+---------+---------+---
9.18	2	61.470	6.336	(-------*-------)
10.95	2	61.550	1.570	(-------*-------)
22.92	2	57.100	0.269	(-------*-------)
33.89	2	61.935	0.686	(-------*--------)
44.55	2	72.315	2.143	(-------*-------)

------+---------+---------+---------+---
56.0 63.0 70.0 77.0

Pooled StDev = 3.090

Grouping Information Using Tukey Method

N Mean Grouping

44.55 2 72.315 A

33.89 2 61.935 A B

10.95 2 61.550 A B

9.18 2 61.470 A B

22.92 2 57.100 B

Means that do not share a letter are significantly different.

Tukey 95% Simultaneous Confidence Intervals

All Pairwise Comparisons

Individual confidence level = 98.98%

9.18 subtracted from:

Lower Center Upper --------+---------+---------+---------+-

10.95 -12.308 0.080 12.468 (-------*-------)

22.92 -16.758 -4.370 8.018 (-------*-------)

33.89 -11.923 0.465 12.853 (--------*--------)

44.55 -1.543 10.845 23.233 (-------*-------)

--------+---------+---------+---------+-

-15 0 15 30

10.95 subtracted from:

Lower Center Upper --------+---------+---------+---------+-

22.92 -16.838 -4.450 7.938 (-------*-------)

33.89 -12.003 0.385 12.773 (--------*--------)

44.55 -1.623 10.765 23.153 (-------*-------)

--------+---------+---------+---------+-

-15 0 15 30

22.92 subtracted from:

Lower Center Upper --------+---------+---------+---------+-

33.89 -7.553 4.835 17.223 (-------*-------)

44.55 2.827 15.215 27.603 (-------*-------)

--------+---------+---------+---------+-

-15 0 15 30

33.89 subtracted from:

Lower Center Upper --------+---------+---------+---------+-

44.55 -2.008 10.380 22.768 (-------*-------)

--------+---------+---------+---------+-

-15 0 15 30

Residual Plots for 9.18, 10.95, 22.92, 33.89, 44.55

- The effect of %MC on the kinetic rate constant (k) for lightness change

One-way ANOVA: 9.18, 10.95, 22.92, 33.89, 44.55

Source DF SS MS F P
Factor 4 0.0001077 0.0000269 0.28 0.882
Error 5 0.0004880 0.0000976
Total 9 0.0005957
S = 0.009879 R-Sq = 18.08% R-Sq(adj) = 0.00%
Individual 95% CIs For Mean Based on
Pooled StDev
Level N Mean StDev -+---------+---------+---------+--------
9.18 2 0.040600 0.018102 (--------------*--------------)
10.95 2 0.046000 0.011597 (--------------*--------------)
22.92 2 0.050500 0.004950 (--------------*--------------)
33.89 2 0.043200 0.001131 (--------------*--------------)
44.55 2 0.044900 0.000141 (--------------*--------------)
-+---------+---------+---------+--------
0.024 0.036 0.048 0.060
Pooled StDev = 0.009879

Grouping Information Using Tukey Method

N Mean Grouping
22.92 2 0.050500 A
10.95 2 0.046000 A
44.55 2 0.044900 A
33.89 2 0.043200 A
9.18 2 0.040600 A
Means that do not share a letter are significantly different.
Tukey 95% Simultaneous Confidence Intervals
All Pairwise Comparisons
Individual confidence level = 98.98%
9.18 subtracted from:
Lower Center Upper ---------+---------+---------+---------+
10.95 -0.034207 0.005400 0.045007 (---------------*---------------)
22.92 -0.029707 0.009900 0.049507 (---------------*---------------)
33.89 -0.037007 0.002600 0.042207 (---------------*---------------)
44.55 -0.035307 0.004300 0.043907 (---------------*---------------)
---------+---------+---------+---------+
-0.025 0.000 0.025 0.050

10.95 subtracted from:

	Lower	Center	Upper
22.92	-0.035107	0.004500	0.044107
33.89	-0.042407	-0.002800	0.036807
44.55	-0.040707	-0.001100	0.038507

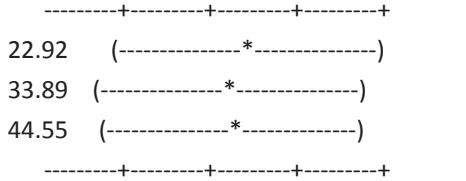

22.92 subtracted from:

	Lower	Center	Upper
33.89	-0.046907	-0.007300	0.032307
44.55	-0.045207	-0.005600	0.034007

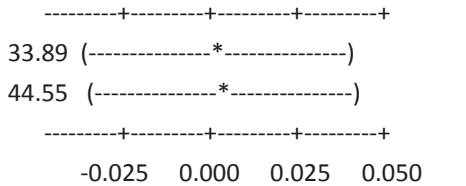

33.89 subtracted from:

	Lower	Center	Upper
44.55	-0.037907	0.001700	0.041307

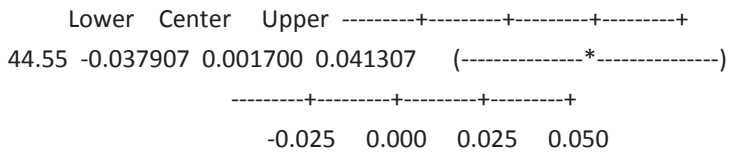

Residual Plots for 9.18, 10.95, 22.92, 33.89, 44.55

A7.2 The statistic analysis of the effect of the initial moisture content on the browning kinetic considered by the redness (*a**) change

- *The effect of %MC on the initial redness (a^*_0)*

One-way ANOVA: 9.18, 10.95, 22.92, 33.89, 44.55

Source	DF	SS	MS	F	P
Factor	4	1.271	0.318	1.26	0.393
Error	5	1.257	0.251		
Total	9	2.528			

S = 0.5014 R-Sq = 50.28% R-Sq(adj) = 10.50%

Individual 95% CIs For Mean Based on Pooled StDev

Level	N	Mean	StDev	--+---------+---------+---------+-------
9.18	2	-2.9700	0.0707	(-----------*-----------)
10.95	2	-2.4550	1.0394	(-----------*-----------)
22.92	2	-3.3000	0.3677	(-----------*-----------)
33.89	2	-3.3950	0.0071	(-----------*-----------)
44.55	2	-3.3750	0.1909	(-----------*-----------)

--+---------+---------+---------+-------

-4.20 -3.50 -2.80 -2.10

Pooled StDev = 0.5014

Grouping Information Using Tukey Method

	N	Mean	Grouping
10.95	2	-2.4550	A
9.18	2	-2.9700	A
22.92	2	-3.3000	A
44.55	2	-3.3750	A
33.89	2	-3.3950	A

Means that do not share a letter are significantly different.

Tukey 95% Simultaneous Confidence Intervals

All Pairwise Comparisons

Individual confidence level = 98.98%

9.18 subtracted from:

	Lower	Center	Upper	+---------+---------+---------+---------
10.95	-1.4954	0.5150	2.5254	(-----------*-----------)
22.92	-2.3404	-0.3300	1.6804	(-----------*-----------)
33.89	-2.4354	-0.4250	1.5854	(-----------*-----------)
44.55	-2.4154	-0.4050	1.6054	(-----------*-----------)

+---------+---------+---------+---------

-3.0 -1.5 0.0 1.5

10.95 subtracted from:

```
      Lower   Center   Upper    +---------+---------+---------+---------
22.92  -2.8554  -0.8450  1.1654     (------------*-------------)
33.89  -2.9504  -0.9400  1.0704    (-------------*------------)
44.55  -2.9304  -0.9200  1.0904    (-------------*------------)
                        +---------+---------+---------+---------
                      -3.0     -1.5      0.0      1.5
```

22.92 subtracted from:

```
      Lower   Center   Upper    +---------+---------+---------+---------
33.89  -2.1054  -0.0950  1.9154         (------------*-------------)
44.55  -2.0854  -0.0750  1.9354         (-------------*------------)
                        +---------+---------+---------+---------
                      -3.0     -1.5      0.0      1.5
```

33.89 subtracted from:

```
      Lower  Center   Upper    +---------+---------+---------+---------
44.55  -1.9904  0.0200  2.0304          (------------*-------------)
                        +---------+---------+---------+---------
                      -3.0     -1.5      0.0      1.5
```

Residual Plots for 9.18, 10.95, 22.92, 33.89, 44.55

- *The effect of %MC on the final redness (a^*_∞)*

One-way ANOVA: 9.18, 10.95, 22.92, 33.89, 44.55

```
Source  DF     SS    MS     F      P
Factor   4  14.518  3.630  9.53  0.015
Error    5   1.904  0.381
Total    9  16.422
S = 0.6170   R-Sq = 88.41%   R-Sq(adj) = 79.13%
                    Individual 95% CIs For Mean Based on Pooled StDev
Level   N    Mean  StDev    +---------+---------+---------+---------
9.18    2  10.140  0.354    (-------*------)
10.95   2  12.160  0.000               (------*-------)
22.92   2  13.540  0.113                      (------*-------)
33.89   2  12.555  0.389                (-------*------)
44.55   2  10.909  1.271        (-------*------)
                  +---------+---------+---------+---------
                  9.0     10.5     12.0     13.5
Pooled StDev = 0.617
```

Grouping Information Using Tukey Method

	N	Mean	Grouping
22.92	2	13.5400	A
33.89	2	12.5550	A B
10.95	2	12.1600	A B
44.55	2	10.9085	B
9.18	2	10.1400	B

Means that do not share a letter are significantly different.

Tukey 95% Simultaneous Confidence Intervals

All Pairwise Comparisons

Individual confidence level = 98.98%

9.18 subtracted from:

	Lower	Center	Upper	-------+---------+---------+---------+--
10.95	-0.4539	2.0200	4.4939	(--------*-------)
22.92	0.9261	3.4000	5.8739	(-------*--------)
33.89	-0.0589	2.4150	4.8889	(-------*-------)
44.55	-1.7054	0.7685	3.2424	(--------*-------)

-------+---------+---------+---------+--

-3.0 0.0 3.0 6.0

10.95 subtracted from:

	Lower	Center	Upper	-------+---------+---------+---------+--
22.92	-1.0939	1.3800	3.8539	(--------*-------)
33.89	-2.0789	0.3950	2.8689	(-------*--------)
44.55	-3.7254	-1.2515	1.2224	(-------*-------)

-------+---------+---------+---------+--

-3.0 0.0 3.0 6.0

22.92 subtracted from:

	Lower	Center	Upper	-------+---------+---------+---------+--
33.89	-3.4589	-0.9850	1.4889	(--------*-------)
44.55	-5.1054	-2.6315	-0.1576	(-------*-------)

-------+---------+---------+---------+--

-3.0 0.0 3.0 6.0

33.89 subtracted from:

	Lower	Center	Upper	-------+---------+---------+---------+--
44.55	-4.1204	-1.6465	0.8274	(--------*-------)

-------+---------+---------+---------+--

-3.0 0.0 3.0 6.0

Residual Plots for 9.18, 10.95, 22.92, 33.89, 44.55

- The effect of %MC on the kinetic rate constant (k) for redness change

One-way ANOVA: 9.18, 10.95, 22.92, 33.89, 44.55

Source DF SS MS F P
Factor 4 0.0049616 0.0012404 13.07 0.007
Error 5 0.0004745 0.0000949
Total 9 0.0054361

S = 0.009742 R-Sq = 91.27% R-Sq(adj) = 84.29%

Individual 95% CIs For Mean Based on Pooled StDev

Level N Mean StDev ---+---------+---------+---------+------
9.18 2 0.08000 0.01414 (-----*-----)
10.95 2 0.08000 0.01414 (-----*-----)
22.92 2 0.10500 0.00707 (-----*-----)
33.89 2 0.06000 0.00000 (-----*-----)
44.55 2 0.03850 0.00495 (-----*-----)
---+---------+---------+---------+------
0.030 0.060 0.090 0.120

Pooled StDev = 0.00974

Grouping Information Using Tukey Method

N Mean Grouping
22.92 2 0.10500 A
10.95 2 0.08000 A B
9.18 2 0.08000 A B
33.89 2 0.06000 B C
44.55 2 0.03850 C

Means that do not share a letter are significantly different.

Tukey 95% Simultaneous Confidence Intervals
All Pairwise Comparisons
Individual confidence level = 98.98%

9.18 subtracted from:

Lower Center Upper --------+---------+---------+---------+-
10.95 -0.03906 0.00000 0.03906 (------*------)
22.92 -0.01406 0.02500 0.06406 (-----*------)
33.89 -0.05906 -0.02000 0.01906 (------*-----)
44.55 -0.08056 -0.04150 -0.00244 (-----*------)
--------+---------+---------+---------+-
-0.060 0.000 0.060 0.120

10.95 subtracted from:

Lower Center Upper --------+---------+---------+---------+-
22.92 -0.01406 0.02500 0.06406 (-----*------)
33.89 -0.05906 -0.02000 0.01906 (------*-----)
44.55 -0.08056 -0.04150 -0.00244 (-----*------)
--------+---------+---------+---------+-
-0.060 0.000 0.060 0.120

22.92 subtracted from:

	Lower	Center	Upper	--------+---------+---------+---------+-
33.89	-0.08406	-0.04500	-0.00594	(-----*------)
44.55	-0.10556	-0.06650	-0.02744	(------*-----)
				--------+---------+---------+---------+-
				-0.060 0.000 0.060 0.120

33.89 subtracted from:

	Lower	Center	Upper	--------+---------+---------+---------+-
44.55	-0.06056	-0.02150	0.01756	(-----*------)
				--------+---------+---------+---------+-
				-0.060 0.000 0.060 0.120

Residual Plots for 9.18, 10.95, 22.92, 33.89, 44.55

Appendix A4

MATLAB® code for non linear fitting of isothermal model *lsqcurvefit*

(Accompanying CD/ A4 Isothermal kinetic fit)

A4.1 Function file (Lpred.m)

```
function L=Lpred(parameters,xdata);

%Define variables
Li=parameters(1);   %The initial lightness
Linf=parameters(2); %The final lightness
k150=parameters(3); %The kinetic rate constant at reference
temperature(min-1)
E=parameters(4);    %The activation energy (J.mol-1)

%Import data from the data sheet file
t=xdata(:,1);       %The data of baking time (min)
T=xdata(:,2)+273.15; %The data of temperature (˚C)

%The first order eqaution for isothermal kinetic
L=Li-(Li-Linf)*(1-exp(-k150*exp(-E/8.314.*(1/T-1/423.15)).*t));
```

A4.2 Script file (ResidualDeepfrying.m)

```
%Read the data from the data sheet file
expdata=xlsread('B3 Measured Data of Pastry Baking on the Hot
Pan.xlsx','Lexp for Isothermal Fit','B10:D399');

%Import experimental data
time=expdata(:,1);%Import the data of time from the data sheet file
temperature=expdata(:,2);%Import the data of temperature from the data
sheet file
Lstar=expdata(:,3);%Import the data of experimental lightness from the
data sheet file
params=[92 64 642254 61453];%Provide the guess values of the kinetic
parameters
```

```
Lpredicted = Lpred(params,[time temperature]);%Calculation the
lightness values

%Plot graph of the prediction and experimental values of the lightness
plot(Lpredicted,Lstar,'ob')
%Estimate the kinetic parameters
newparams=lsqcurvefit('Lpred',params,[time temperature],Lstar);
Lnew = Lpred(newparams,[time temperature]);

hold on
plot(Lnew,Lstar,'xg')

%Plot predicted lightness versus experimental lightness
ylim([60 95]);
xlabel('L^*_p_r_e_d_i_c_t_e_d');
ylabel('L^*_e_x_p_e_r_i_m_e_n_t_a_l');
legend('initial guess','fitted model','x=y');
hold on
XY=[60 95];
plot(XY, XY, 'r');

%Plot predicted and experimental lightness versus time
figure
plot(time,Lstar,'og');
hold on
plot(time,Lnew,'-b');
xlabel('Time (min)');
ylabel('L^* value');

%Show the values of the estimated kinetic parameters
Li=newparams(1)
Linf=newparams(2)
k150=newparams(3)
E=newparams(4)
```

Appendix A5

MATLAB® code to predict colour from given kinetic parameters and experimental surface history

(Accompanying CD/ A5 Non isothermal prediction)

A5.1 Function file (findT.m)

```
function T=findT(t)

%Define global variables
global texp; %time from experimental data
global Texp; %temperature data

%Temperature at the pastry surface
i=find(t<=texp);
if i(1)==1
    T=Texp(1);
else
    T=(((t-texp(i(1)-1))/(texp(i(1))-texp(i(1)-1)))*(Texp(i(1))-
Texp(i(1)-1)))+(Texp(i(1)-1));
end
```

A5.2 Function file (nonisothermal.m)

```
function dL=nonisothermal(t,L)

%Define global variables
global Linf; %Infinity Lightness
global k150; %frequency factor
global E; %Activation energy
global R; %Universal gas constant

%The non-isothermal kinetic
T=findT(t);
k=k150*exp(-E/R.*(1./(T+273.15)-1/(150+273.15)));
dL=-k*(L-Linf);
```

A5.3 Script file (scriptfile.m)

```
%Read experimental data
exptime=xlsread('B3 Measured Data of Pastry Baking on the Hot
Pan.xlsx','Texp','a5:a125');
expT=xlsread('B3 Measured Data of Pastry Baking on the Hot
Pan.xlsx','Texp','ae5:ae125');

%Define global variables
global Li; %Initial Lightness
global Linf; %Infinity Lightness
global k150; %frequency factor
global E; %Activation energy
global R; %Universal gas constant
global texp; %time from experimental data
global Texp; %temperature data

%Import experimental data
texp=xlsread('B3 Measured Data of Pastry Baking on the Hot
Pan.xlsx','Texp','a5:a125');
Texp=xlsread('B3 Measured Data of Pastry Baking on the Hot
Pan.xlsx','Texp','b5:b125');
Lexp=xlsread('B3 Measured Data of Pastry Baking on the Hot
Pan.xlsx','Lexp','b5:b17');
tt=xlsread('B3 Measured Data of Pastry Baking on the Hot
Pan.xlsx','Lexp','a5:a17');
texp=texp*60;

%System Input
E=6.5932e+004;%J/mol
k150=(1.75e-002)/60;%min-1
Li=91.7836;
Linf=65.2384;
R=8.3145; %J/molK

%ODE solving
[t,L]=ode45('nonisothermal',[0:60:3600],Li);

%Plot experimental and predicted lightness versus time
figure
plot(tt,Lexp','*r')
hold on
plot(t/60, L)
xlabel('Time (min)')
ylabel('L*value')
legend('Experimental','Predicted');

%plot temperature versus time
figure
plot(texp/60,Texp)
xlabel('Time (min)')
ylabel('Temperature (^{\circ}C)')
```

Appendix A6

MATLAB® code to repeatedly solve non-isothermal model ode's' within the *lsqnonlin* optimisation algorithm for pastry data

(Accompanying CD/ A6 Kinetic Parameter Estimation for Pastry baking)

A6.1 Function file (SOLVER.m)

```
function RES=SOLVER(params,t_T_exp,T_exp,L_exp,t_L_exp)

%number of runs
Num_runs=size(L_exp,2);

[t L]=ode45(@(t,L)
dLnonlin(t,L,params,t_T_exp,T_exp),t_L_exp,ones(1,Num_runs)*params(1))
;

RES=L_exp-L;
```

A6.2 Function file (dLnonlin.m)

```
function dL=dLnonlin(t,L,params,t_T_exp,T_exp)

%Temperature at the pastry surface
i=find(t<=t_T_exp);
if i(1)==1
    T=T_exp(1,:);
else
    T=(((t-t_T_exp(i(1)-1))/(t_T_exp(i(1))-t_T_exp(i(1)-
1)))*(T_exp(i(1),:)-T_exp(i(1)-1,:)))+(T_exp(i(1)-1,:));
end
T=T';

%Define parameters
R=8.314;
k150=params(2);
E=params(3);
Linf=params(4);
```

```
%The non-isothermal kinetic
k=k150*exp(-E/R.*(1./(T+273.15)-1/(150+273.15)));
dL=zeros(size(L));
dL=-k.*(L-Linf);
```

A6.3 Script file (FitDataScriptfile.m)

```
%Choose experimental data from excel file
filename=uigetfile('*.xlsx','Choose file with experimental data');
t_L_exp=xlsread(filename,'Lexp','A5:A17');
L_exp=xlsread(filename,'Lexp','B5:AE17');
t_T_exp=xlsread(filename,'Texp','A5:A125');
T_exp=xlsread(filename,'Texp','B5:AE125');

%number of runs
Num_runs=size(L_exp,2);

%set up best guesses of parameters
Li=91.78;
k150=0.0175;
E=65936;
Linf=65.24;
params_guess=[Li k150 E Linf];

%Calculate new parameters
RES=SOLVER(params_guess,t_T_exp,T_exp,L_exp,t_L_exp);
RESULTS=lsqnonlin(@(params)
SOLVER(params,t_T_exp,T_exp,L_exp,t_L_exp), params_guess);
[t L]=ode45(@(t,L)
dLnonlin(t,L,RESULTS,t_T_exp,T_exp),t_L_exp,ones(1,Num_runs)*RESULTS(1
));

Length=size(L,1);

%Save new parameters and the predicted L value in to Excel file
[newmatfile, newpath] = uiputfile('*.xlsx', 'Save As');
newfilename = [newpath,newmatfile];

TITLES={'Li' 'k150' 'E' 'Linf'};
xlswrite(newfilename, TITLES, 'Sheet1', 'A1')
xlswrite(newfilename, RESULTS, 'Sheet1' , 'A2')
xlswrite(newfilename, t, 'Sheet1', 'A8')
xlswrite(newfilename, {'Time (min)'}, 'Sheet1','A6')
xlswrite(newfilename, L, 'Sheet1', 'B8')
xlswrite(newfilename, {'Predicted L values at Temp....'}, 'Sheet1',
'B6')

TITLES=xlsread(filename, 'Lexp', 'B1:ZZ1');
xlswrite(newfilename, TITLES, 'Sheet1','B7')

%Plot predicted lightness versus experimental lightness
figure
plot(L_exp(:,1:5), L(:,1:5),'*');
hold on
plot(L_exp(:,6:10), L(:,6:10),'s');
plot(L_exp(:,11:15), L(:,11:15),'o');
plot(L_exp(:,16:20), L(:,16:20),'x');
plot(L_exp(:,21:25), L(:,21:25),'d');
```

```
plot(L_exp(:,26:30), L(:,26:30),'+');
ylim([60 95]);
ylabel ('L^*_p_r_e_d_i_c_t_e_d');
xlabel ('L^*_e_x_p_e_r_i_m_e_n_t_a_l')
XY=[60 95];
plot(XY, XY, 'r');
legend('120(rep1)',
'120(rep2)','120(rep3)','120(rep4)','120(rep5)','130(rep1)','130
(rep2)','130 (rep3)','130 (rep4)','130 (rep5)','140 (rep1)','140
(rep2)','140 (rep3)','140 (rep4)','140 (rep5)','150 (rep1)','150
(rep2)','150 (rep3)','150 (rep4)','150 (rep5)','160 (rep1)','160
(rep2)','160 (rep3)','160 (rep4)','160 (rep5)','170 (rep1)','170
(rep2)','170 (rep3)','170 (rep4)','170 (rep5)');

 %this is to plot 6 x experimental temperature versus time
    T_exp_1=T_exp(:,1);
    T_exp_2=T_exp(:,6);
    T_exp_3=T_exp(:,11);
    T_exp_4=T_exp(:,16);
    T_exp_5=T_exp(:,21);
    T_exp_6=T_exp(:,26);
figure
plot(t_T_exp,T_exp_1)
ylabel('Temperature (^{\circ}C)')
xlabel('Time (min)')
figure
plot(t_T_exp,T_exp_2)
ylabel('Temperature (^{\circ}C)')
xlabel('Time (min)')
figure
plot(t_T_exp,T_exp_3)
ylabel('Temperature (^{\circ}C)')
xlabel('Time (min)')
figure
plot(t_T_exp,T_exp_4)
ylabel('Temperature (^{\circ}C)')
xlabel('Time (min)')
figure
plot(t_T_exp,T_exp_5)
ylabel('Temperature (^{\circ}C)')
xlabel('Time (min)')
figure
plot(t_T_exp,T_exp_6)
ylabel('Temperature (^{\circ}C)')
xlabel('Time (min)')

%-------------------------------------------------------------------------
%this is to plot 6 x experimental lightness versus time

    L_exp_1=L_exp(:,1);
    L_exp_2=L_exp(:,6);
    L_exp_3=L_exp(:,11);
    L_exp_4=L_exp(:,16);
    L_exp_5=L_exp(:,21);
    L_exp_6=L_exp(:,26);

    L_1=L(:,1);
    L_2=L(:,6);
    L_3=L(:,11);
    L_4=L(:,16);
```

```
L_5=L(:,21);
L_6=L(:,26);

    figure
plot(t, L_exp_1, 'r*')
hold on
plot(t, L_1);
ylabel('L^*')
xlabel('Time (min)')
    figure
plot(t, L_exp_2, 'r*')
hold on
plot(t, L_2);
ylabel('L^*')
xlabel('Time (min)')
    figure
plot(t, L_exp_3, 'r*')
hold on
plot(t, L_3);
ylabel('L^*')
xlabel('Time (min)')
    figure
plot(t, L_exp_4, 'r*')
hold on
plot(t, L_4);
ylabel('L^*')
xlabel('Time (min)')
    figure
plot(t, L_exp_5, 'r*')
hold on
plot(t, L_5);
ylabel('L^*')
xlabel('Time (min)')
    figure
plot(t, L_exp_6, 'r*')
hold on
plot(t, L_6);
ylabel('L^*')
xlabel('Time (min)')
```

Appendix A7

MATLAB® code to repeatedly solve non-isothermal model ode's' within the *lsqnonlin* optimisation algorithm for processed potato product data

(Accompanying CD/ A7 Kinetic Parameter Estimation for Potato baking)

A7.1 Function file (SOLVER.m)

```
function RES=SOLVER_New(params,t_T_exp,T_exp,L_exp,t_L_exp)

%number of runs
Num_runs=size(L_exp,2);

[t L]=ode45(@(t,L)
dLnonlin(t,L,params,t_T_exp,T_exp),t_T_exp,ones(1,Num_runs)*params(1))
;

Lpred=zeros(size(L_exp));
for j=1:Num_runs
    i=find(t_T_exp>=t_L_exp(j));
    Lpred(j)=L(i(1),j);
end

RES=L_exp-Lpred;
```

A7.2 Function file (dLnonlin.m)

```
function dL=dLnonlin(t,L,params,t_T_exp,T_exp)

i=find(t<=t_T_exp);
if i(1)==1
    T=T_exp(1,:);
else
    T=(((t-t_T_exp(i(1)-1))/(t_T_exp(i(1))-t_T_exp(i(1)-
1)))*(T_exp(i(1),:)-T_exp(i(1)-1,:)))+(T_exp(i(1)-1,:));
end
T=T';
```

```
R=8.314;
k150=params(2);
E=params(3);
Linf=params(4);
k=k150*exp(-E/R.*(1./(T+273.15)-1/(150+273.15)));
dL=zeros(size(L));
dL=-k.*(L-Linf);
```

A7.3 Script file (FitDataScriptfile.m)

```
%import data
filename=uigetfile('*.xlsx','Choose file with experimental data');
t_L_exp=xlsread(filename,'Texp','B4:BS4');
L_exp=xlsread(filename,'Texp','B5:BS5');
t_T_exp=xlsread(filename,'Texp','A6:A1207');
T_exp=xlsread(filename,'Texp','B6:BS1207');

%number of runs
Num_runs=size(L_exp,2);

%add in data for missing time values. This is to allow solutions for
all
%exp using all the same time array. Predictions beyond each exp will
not be
%used.
for j=1:Num_runs
    i=find(isfinite(T_exp(:,j)));
    T_exp(i(end)+1:end,j)=T_exp(i(end),j);
end

%set up best guesses of parameters
Li=82.91;
k150=0.025;
E=51000;
Linf=47.75;
params_guess=[Li k150 E Linf];

% RES=SOLVER_New(params_guess,t_T_exp,T_exp,L_exp,t_L_exp);
options=optimset('TolFun',1e-9,'TolX',1e-9);
[RESULTS,ssER]=lsqnonlin(@(params)
SOLVER_New(params,t_T_exp,T_exp,L_exp,t_L_exp),
params_guess,[],[],options);
%
L_exp_Av=mean(L_exp);
ssTot = sum((L_exp-L_exp_Av).^2);
Rsq=1-ssER/ssTot;

%ODE solving
[t L]=ode45(@(t,L)
dLnonlin(t,L,RESULTS,t_T_exp,T_exp),t_T_exp,ones(1,Num_runs)*RESULTS(1
));

Lpred=zeros(size(L_exp));
for j=1:Num_runs
    i=find(t_T_exp>=t_L_exp(j));
    Lpred(j)=L(i(1),j);
end
%
% Plot L*predicted versus L*experimental
```

```
plot(L_exp, Lpred,'x');
hold on
plot([min(L_exp) max(L_exp)],[min(L_exp) max(L_exp)],'-k');
ylabel ('L*_p_r_e_d_i_c_t_e_d');
xlabel ('L*_e_x_p_e_r_i_m_e_n_t_a_l')

%Show the result of estimated kinetic parameters
fprintf('k150 = %d min-1. \n',RESULTS(2));
fprintf('E  = %d J/mol. \n',RESULTS(3));
fprintf('Lo = %d. \n',RESULTS(1));
fprintf('Lf = %d. \n',RESULTS(4));
fprintf('R^2 = %d. \n',Rsq);

%Plot experimental temperature versus time for all experiments
figure
plot(t_T_exp, T_exp(:,11));
xlim ([0 55]);
xlabel('Time (min)');
ylabel('Temperature (^{\circ}C)')
figure
plot(t_T_exp, T_exp(:,3*12+11));
xlim ([0 55]);
xlabel('Time (min)');
ylabel('Temperature (^{\circ}C)')

%Plot experimental lightness versus time
figure
plot(t, L(:,11));
hold on
plot(55, L_exp(11),'r*');
xlim ([0 55]);
xlabel('Time (min)');
ylabel ('L*');

figure
plot(t, L(:,3*12+11));
hold on
plot(55, L_exp(3*12+11),'r*');
xlim ([0 55]);
xlabel('Time (min)');
ylabel ('L*');
```

Appendix A8

The estimated kinetic parameters from temperature data at different points on the pastry sample

Kinetic parameters		E_a (kJ·mol^{-1})	k_{150} (min^{-1})	L^*_0	L^*_∞	R^2
	P1	50.31	0.032	94.76	53.93	0.9997
	P2	57.78	0.025	94.44	54.73	0.9995
	SP1	50.56	0.031	94.76	53.96	0.9997
Fast heating	SP2	57.78	0.025	94.43	54.74	0.9995
rate	Max(Box)	68.57	0.017	94.66	54.87	0.9998
experiment	Min(Box)	44.75	0.046	94.85	54.79	0.9996
replicate 1	Average(Box)	54.91	0.027	94.69	54.19	0.9997
	Max (Circle)	71.08	0.016	94.65	54.94	0.9997
	Min(Circle)	43.08	0.058	95.06	55.99	0.9996
	Average(Circle)	53.93	0.029	94.70	54.31	0.9997
	P1	30.83	0.043	94.28	48.85	0.9983
	P2	31.79	0.043	94.32	49.37	0.9985
	SP1	31.34	0.043	94.28	49.03	0.9984
Fast heating	SP2	31.96	0.043	94.30	49.40	0.9985
rate	Max(Box)	27.98	0.040	94.67	47.51	0.9983
experiment	Min(Box)	23.48	0.068	94.77	50.15	0.9981
replicate 2	Average(Box)	28.04	0.045	94.43	48.32	0.9983
	Max (Circle)	26.79	0.039	94.75	46.50	0.9981
	Min(Circle)	21.38	0.071	94.88	50.20	0.9984
	Average(Circle)	26.81	0.046	94.50	48.16	0.9983

The estimated kinetic parameters from temperature data at different points on the pastry sample (cont'd)

Kinetic parameters		E_a (kJ·mol^{-1})	k_{150} (min^{-1})	L^*_0	L^*_∞	R^2
	P1	14.34	0.033	93.94	33.69	0.9987
	P2	9.24	0.032	94.07	26.78	0.9986
	SP1	8.45	0.032	94.07	25.77	0.9986
Fast heating	SP2	9.15	0.032	94.07	26.55	0.9986
rate	Max(Box)	11.38	0.030	94.08	27.90	0.9986
experiment	Min(Box)	6.53	0.036	94.17	27.38	0.9986
replicate 3	Average(Box)	8.49	0.031	94.06	25.49	0.9986
	Max (Circle)	9.64	0.029	94.12	23.97	0.9986
	Min(Circle)	10.11	0.049	94.09	38.93	0.9988
	Average(Circle)	14.56	0.033	93.93	33.96	0.9987
	P1	57.92	0.011	93.45	41.23	0.9974
	P2	54.63	0.011	93.55	39.08	0.9970
	SP1	58.67	0.011	93.47	41.94	0.9972
Step-wise	SP2	55.34	0.011	93.52	39.85	0.9972
heating	Max(Box)	65.92	0.010	93.48	46.08	0.9972
experiment	Min(Box)	49.32	0.010	93.23	29.58	0.9976
replicate 1	Average(Box)	58.15	0.011	93.49	41.66	0.9971
	Max (Circle)	65.85	0.010	93.44	45.86	0.9974
	Min(Circle)	71.93	0.030	92.45	64.11	0.9515
	Average(Circle)	58.68	0.011	93.47	41.78	0.9972
	P1	57.43	0.014	92.64	52.24	0.9975
	P2	68.67	0.014	92.52	52.39	0.9978
	SP1	66.08	0.014	92.60	52.01	0.9976
Step-wise	SP2	69.25	0.014	92.50	52.45	0.9979
heating	Max(Box)	73.64	0.011	92.62	52.70	0.9981
experiment	Min(Box)	61.29	0.017	92.64	51.26	0.9970
replicate 2	Average(Box)	68.96	0.014	92.55	52.38	0.9978
	Max (Circle)	73.80	0.011	92.63	52.71	0.9981
	Min(Circle)	71.93	0.061	92.46	64.10	0.7827
	Average(Circle)	66.34	0.014	92.58	52.16	0.9977

The estimated kinetic parameters from temperature data at different points on the pastry sample (cont'd)

Kinetic parameters		E_a (kJ·mol^{-1})	k_{150} (min^{-1})	L^*_0	L^*_∞	R^2
Step-wise heating experiment replicate 3	P1	71.31	0.012	92.20	51.34	0.9980
	P2	72.61	0.012	92.29	51.30	0.9982
	SP1	71.03	0.011	92.20	51.12	0.9980
	SP2	72.54	0.012	92.30	51.39	0.9982
	Max(Box)	71.94	0.021	92.45	64.11	0.8433
	Min(Box)	66.22	0.015	92.16	50.84	0.9977
	Average(Box)	71.31	0.012	92.21	51.32	0.9981
	Max (Circle)	73.79	0.011	92.32	51.48	0.9983
	Min(Circle)	65.86	0.016	92.16	50.61	0.9974
	Average(Circle)	71.19	0.011	92.19	51.14	0.9982
Step-wise heating experiment replicate 4	P1	61.42	0.014	93.40	56.94	0.9989
	P2	69.16	0.012	93.25	56.99	0.9989
	SP1	61.43	0.014	93.39	56.97	0.9989
	SP2	68.76	0.012	93.30	56.92	0.9990
	Max(Box)	72.27	0.011	93.37	57.09	0.9987
	Min(Box)	66.63	0.014	93.11	56.95	0.9990
	Average(Box)	67.41	0.012	93.25	56.96	0.9989
	Max (Circle)	73.73	0.010	93.38	57.11	0.9988
	Min(Circle)	72.03	0.048	92.44	31.21	0.8376
	Average(Circle)	67.79	0.012	93.37	56.92	0.9989